KASHMIR JOURNAL OF GEOLOGY

Volume 10   1992

DEDICATED

TO

PROFESSOR Dr. F. A. SHAMS

LIFE SKETCH OF PROFESSOR F. A. SHAMS

Professor Dr. F(Faiz). A(Ahmad). Shams has been the seniormost Professor of Geology of the country. Born on 8th August, 1930, Professor Shams studied at Faisalabad and Multan, and at the Government College, Lahore as the Punjab University student of Chemistry (1951-53). During his last year of M.Sc. studies, he was among the two students who joined UNESCO-established new Department of Mineralogy at the Punjab University, and specialized in the field of Mineral and Rock Chemistry. In 1955, he also qualified in B.Sc. Geology examination. From 1957-1959, he studied at the Cambridge University, U.K., where he earned B.A. (Tripos Hons.) and was later awarded M.A. (Hons.). He again visited Cambridge University (1965-1966) for specialized training and research in X-Ray Crystallography. He also spent a term in the Lab. of Professor Tom F.W. Barth at Oslo, Norway, doing research work in advanced Mineralogy.

Professor Shams had an unique career at the Punjab University as the first Research Scholar, first Assistant Professor, Associate Professor and the first Professor of Geology. In 1967, he became the first Pakistani Head of the Geology Department, when the last expatriate left after 10 years of UNESCO and 5 years of post-UNESCO foreign headship. In 1979, he was appointed first (founder) Director, Institute of Geology, Punjab University, when the Department was raised to the Institute level. He had also been the Dean, Faculty of Science, Punjab University, for nine years (1981-1990), when he established so far the country's only Department of Space Science.

Professor Shams has been a leading researcher in the field of Mineralogy and Petrology, having earned international recognition as the Granite-Man, concentrating on the granitic complexes of the Himalayas. These frontline studies also enabled him to contribute heavily on the associated metamorphic rocks, resulting into the discovery of blueschist metamorphism in the Swat Himalayas, that happened to be the first in the entire Himalayan arc. Thus, he provided a sound basis for plate-tectonic modelling for the origin of the Himalayas.

Professor Shams has been an institution in participating as well as organizing geological activities in the country. Following his earliest (1957) call for mineral development, he organized first National Seminar on Mineral Development in 1970 that established a trend for mineral policy, followed by many leading events, the more important being: The first National Expedition to Northern Areas (1974), when the Karakorum Highway was opened for traffic; another Expedition, particularly to Baltistan (1983), as Centenary Celebration event of the Punjab University; the First Pakistan Geological Congress (1984); the First Field Workshop on Plate Tectonics and Crust of Pakistan (1987), that lead to the establishment of a regular UNESCO-Training Course in Plate Tectonics for South Asia. He has been the Convener, Pakistan National Committee for International Geological Correlation Programme; Member, National Committee on Geology; President, Punjab Geological Society, and the Founder-President, Pakistan Academy of Geological Sciences. He has represented Pakistan on many international geological and related bodies, and has presented research papers in many conferences, meetings and seminars.

During his later years at the Punjab University, he initiated establishment of a Section of Industrial Mineralogy at the Institute of Geology with the collaboration of University of Leicester, U.K. which is going to be the first centre of this highly specialized field in south Asia. He was also responsible for preparing and introducing Professional Degree course in development-oriented Applied Geology that received international recognition.

Professor Shams has been a prolific publisher; in addition to large number of research papers in national and international journals, he has published many books, such as the Mineral Industry in Pakistan and the monumental, Granites of Himalayas, Karakorum and Hindu Kush (1983), that has become a lasting reference text of information, He is one of the authors of the pioneer publication - The Geology of Pakistan - that has been produced by a joint Pakistan-German authorship. Professor Shams has been Editor of Geological Bulletin of Punjab University for over 20 years that helped to establish its international status.

After his retirement from University service in 1990, Professor Shams is working as Director, Centre for Integrated Mountain Research, that he had initiated in 1987; it is the only institution of its kind in Pakistan. Under the auspices of this Centre, he developed prestigious Pakistan-Germany, and Pakistan-Italy-France collaboration for many multi-disciplinary and inter-disciplinary research projects in northern Pakistan. He has initiated publication of Mountnews, a magazine devoted to mountain research in Pakistan.

The present volume of the Journal is a recognition of multifarious contributions of Professor Shams to the geological sciences and related disciplines for the progress of knowledge and the betterment of humanity.

Page

CONTENTS

PETROGENESIS OF ACID MINOR BODIES OF MANSEHRA GRANITIC COMPLEX, HAZARA HIMALAYA, NW PAKISTAN

BY

MOHAMMAD ASHRAF

Institute of Geology, Azad Jammu & Kasmir University, Muzaffarabad.

ABSTRACT:- The acid minor bodies in the Mansehra and Batgram area were emplaced in the granitic rocks and the associated metasediments. These bodies have been identified as (1) Albitites, (2) albite - aplites / pegmatites, (3) albite - (microcline) - aplite / pegmatites, (4) albite - microcline - aplites / pegmatites, (5) microcline - albite - aplites / pegmatites and (6) complex - aplites / pegmatites. The first 4 types occur as independent and composite bodies in the interior - lateral zone (1675 m above sea level), types 4 and 5 occur in the interior - marginal zone (1525 to 2750 m above sea level) and types 5 and 6 are present in both interior - marginal zone and marginal - exterior zone (over 2750 m above sea level). Field, mineralogical and chemical evidences show that the acid minor bodies are genetically related with the granitic rocks of the area. This genetic relationship is significant due to continued enrichment of soda in the granites from Mansehra granitic gneiss (a potassic facies) to Hakle tourmaline granite and Chail Sar microgranite. The Mansehra granitic complex is itself a product of partial melting of Hazara and Lower Tanol Formations when they reached to metamorphic grade of kyanite- silliminite. The enrichment of soda is due to gradual cooling and increase in vapour pressure of the complex (in tightly closed environments) more than 10 Kb, where the acidic fluids shifted towards the albite apex. From this the release in external pressure at places within the interior-lateral zone gave rise to soda rich liquids being deposited in the fissures. These fissures provided the local release in pressure by the opening of tension fissures parallel to the foliation of the granite and the metasediments during the welling up and the expansion of the granites in the diapiric and mush room like structure. Therefore, as the vapour pressure decreased with further cooling, the behaviour of the system was reversed gradually, meaning thereby that SiO_2 and K_2O would be released alongwith the volatiles, and their quantity depended on the release in $P(H_2O)$ in the three structural zones. The mineralogy and chemistry of these structural units is quite contrasting with the exception of some overlappings at places. Therefore, the present investigations show that the pegmatitic residual solutions were derived from the albite rich solutions gradually with the introduction of K_2O and volatiles. This derivation is excellently exemplified by negative correlation of Na_2O and positive correlation of K_2O with SiO_2 and also gradual but significant increase in the rare elements.

INTRODUCTION

The acid minor bodies on which a detailed account is being presented occur closely associated with Mansehra granitic complex (Fig. 1) The Mansehra granitic complex consists of granitoid to gneisses members, tourmaline granites, micro-granites and andalusite granite (Shams 1969, 1983, and Ashraf 1974) There are all gradation between massive, semi and true gneissic types while the intensity and frequency of

foliation generally increase northwards. These granitic members are emplaced in metasedimentary Hazara and Tanol Formations of Precambrian age. This is being mentioned for the first time that Hazara Formation a pelitic facies played a major role in the formation of Mansehra granitic complex which nobody earlier envisaged. This pelitic facies of Hazara Formation is very evident in the western part of Mansehra district in Oghi and Black Mountains, having been dominantly metamorphosed from staurolite to silliminite grades.
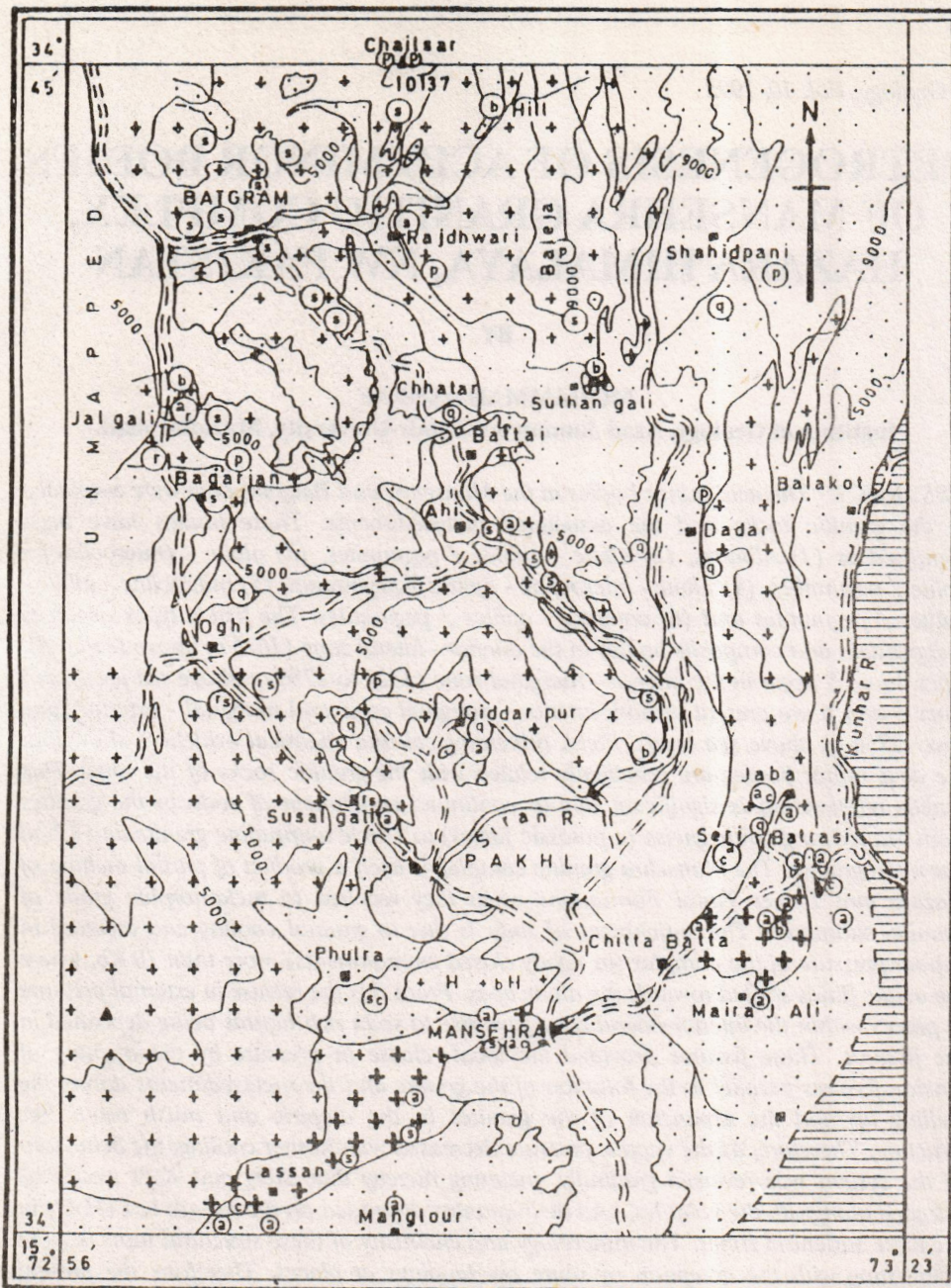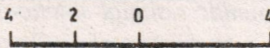
Fig. 1 Geological Map of Mansehra and Batgram Area showing Location and Distribution of Acid Minor Bodies.

2

This granitic complex has been assigned an age of lower Paleozoic by Le Fort *et al.* (1980) who also showed that similar complexes occur along the entire length of the lower Himalayas. This study thus has important regional implication. A very brief description of the occurrence of acid minor bodies was given by Shams (1969) and Shams and Rehman (1966). But a very comprehensive account was given by Ashraf (1974, 1974a, 1974b, 1975, 1983) and Ashraf and Chaudhry (1974, 1976, 1976a) on the classification, emplacement and geochemistry of acid minor bodies of Mansehra and Batgram areas.

GEOLOGY & CLASSIFICATION OF ACID MINOR BODIES

A very detailed study was carried out by Ashraf (1974, 1976) on the geology and classification of acid minor bodies (AMB) which are being described and synthesized briefly here in order to correlate them with the Mansehra granites and to understand the petrogenesis. On the basis of field evidence and subsequent laboratory studies six type groups of AMB were identified:-

(i)   Albitites.
(ii)   Albite - aplites / pegmatites.
(iii)   Albite-(microcline)-aplites/pegmatites.
(iv)   Albite-microcline-aplites/pegmatites.
(v)   Microcline - albite - aplites/pegmatites.
(vi)   Complex - aplites/pegmatites.

Keeping in view their internal structures and mineral compositions the AMB have been further subdivided (Table-1) following and modifying the zonal terminology of Heinrich (1953). The AMB type groups i to iv have been assigned to the interior - lateral zone, the type groups iv and v to interior-marginal zone and type group v and vi to exterior-marginal zone of the Mansehra granitic complex and associated metasediments. These zonal distributions show that dominantly sodic and dominantly potassic rocks show distinct spatial separation with a gradational overlap in the interior marginal zone.

The albitites and aplites of the AMB in nearly all types are found as tabular to lensoid bodies that are preferably emplaced along foliation planes of the granitic and the metamorphic rocks. The size of the AMB varies with thickness from 1.5 to 50 m. Most of the AMB emplaced in the granitic host show sharp contacts and concordant attitude, occasionally giving impression of fine - grained chilled margins, while those hosted by the metamorphic rocks exhibit gradational contacts. In the interior lateral zone the albitites and albite - aplites / pegmatites and albite - (microcline) aplites / pegmatites are closely associated as composite AMB, with sharp as well as gradational contacts, with uniform and variable grain sizes, and sometimes with sharp variations that may be present as well defined layered zones and patches (Ashraf, 1975).

The simple and complex - pegmatite occur dominantly along the foliation of the granitic rocks and the metamorphics, but also filling joints. These pegmatites exhibit spectacular variety of geometrical forms like tabular, lensoid, lenticular, lenticular branching, pod like, pinch and swell structures and as ptygmatically folded bodies. The pegmatites show concordant emplacement but occasionally those may be concordant only at one end and discordant at the other end, such a relationship exists with reference both to the contact planes as well as to internal foliation of the pegmatites. In complex pegmatites three to four zones can easily be identified. The pegmatites mostly are 1.0 to 30 m thick but they also occur commonly as stringers. Among some unusual types are the doubly convex bodies that branch off as stringers, at the both ends. Pod or orbicules (Sinclair & Richardson, 1992) like pegmatites which occur dominantly north west of Batgram are usually 5 to 25 cm across with core full of tourmaline.

Replacement type AMB occurs as irregular and ptygmatically folded bodies with diffused and somewhat sharp contacts. These bodies are a cm to about 10 m thick.

Table - 1 Detailed classification of different type-groups of acid minor bodies associated with the Mansehra granitic complex, northern Pakistan.

1.   **ALBITITES**
    i)   **Pegmatitic-albitites (associated with the granites).**
    ii)   **Medium grained-abitites (associated with the granites).**
    iii)   **Fine-grained albitites (associated with the metamorphics).**

2. APLITES

A. **Simple unzoned aplites.**
   i) Albite-aplites
      (Albite-quartz-muscovite).
   ii) Albite-(microcline) aplites
      (Albite-(microcline)-quartz-muscovite).
   iii) Albite-microcline-aplites
      (Albite-microcline-quartz-muscovite).
   iv) Microcline-albite-aplites
      (Microcline-albite-quartz-muscovite).

B. **Complex zoned aplite.**

i)	Intermediate zone	=	Microcline-quartz-albite-(green mica).
ii)	Core	=	Microcline-quartz-green mica-(albite-beryl).

(Hill)

3. SAMPLE PEGMATITES

A. **Unzoned**
   i) Albite-pegmatites
      (Albite-quartz-muscovite).
   ii) Albite-(microcline)-pegmatites
      (Albite-(microcline)-quartz-muscovite-tourmaline-garnet).
   iii) Albite-microcline-pegmatites
      (Albite-microcline-quartz-muscovite-tourmaline).
   iv) Microcline-albite-pegmatites
      (Microcline-albite-quartz-tourmaline-garnet).

B. **Zoned**

i)	a)	Outer intermediate zone	=	Graphic granite.
	b)	Inner intermediate zone	=	Muscovite-quartz.
	c)	Core	=	Quartz.

(Jabba, Batgram)

ii)	a)	Outer intermediate zone	=	Albite-muscovite-tourmaline-quartz.
	b)	Inner intermediate zone	=	Albite-muscovite-quartz.
	c)	Core	=	Quartz (albite).

(Bagarian village)

iii)	a)	Outer intermediate zone	=	Albite-muscovite-quartz.
	b)	Inner intermediate zone	=	Microcline perthite-muscovite-tourmaline-quartz.
	c)	Core	=	Quartz.

(Balhag)

iv)	a)	Intermediate zone	=	Albite-quartz-muscovite-(biotite-microcline-chess board albite).
	b)	Core	=	Albite-quartz-muscovite-(tourmaline-microcline).

(Balhag)

v)	a)	Wall zone	=	Oligoclase-quartz-muscovite-(garnet-biotite).
	b)	Outer intermediate zone	=	Albite-quartz-muscovite-(microcline-biotite).
	c)	Inner intermediate zone	=	Albite-quartz(microcline-muscovite-garnet).
	d)	Core	=	Quartz (muscovite-microcline).

(Bahishti)

vi)	a)	Intermediate zone	=	Microcline-albite-quartz-tourmaline.
	b)	Core	=	Tourmaline-quartz.

(Derai Batgram)

4. **COMPLEX PEGMATITES**
   A. **Unzoned**
      i) Microcline perthite-albite-quartz-muscovite-(tourmaline-beryl).

                                                                    (Baleja, Chail)

   B. **Zoned symmetrical.**
      i) **Pegmatitic stage**
         a) Border + wall zone   = Albite-microcline-quartz-muscovite-(tourmaline).
         b) Outer intermediate zone   = Microcline perthite-muscovite-quartz.
         c) Inner Intermediate zone   = Microcline perthite-quartz-(muscovite-garnet).
         d) Core   = Quartz-(garnet-muscovite).
         Replacement stage   = Muscovite-beryl-tourmaline.
         Hydrothermal stage   = Kaolinite.

                                                                         (Baleja)

      ii) **Pegmatitic stage.**
         a) Border + wall zone   = Albite-quartz-muscovite-(tourmaline).
         b) Intermediate zone   = Microcline perthite-muscovite-(tourmaline-garnet).
         c) Core   = Quartz.
         Pneumatolytic stage   = Cleavlandite-muscovite-beryl-tourmaline.
         Hydrothermal stage   = Kaolinite-sericite.

                                                                         (Dadar)

      iii) **Pegmatitic stage**
         a) Border + wall zone   = Albite-quartz-(tourmaline-muscovite).
         b) Intermediate zone   = Microline perthite (muscovite).
         c) Core   = Quartz.
         Pneumatolytic stage   = Beryl.
         Hydrothermal stage   = Kaolinite-sericite.

                                                                      (Rajdhawari)

   C. **Partially zoned symmetrical**
      i) **Pegmatitic stage**
         a) Border + wall zone   = Albite-quartz-(muscovite-tourmaline).
         b) Intermediate zone   = Microcline perthite-quartz-(muscovite).
         c) Core   = Microcline perthite-quartz.
         Pneumatolytic stage   = Beryl-muscovite.
         Hydrothermal stage   = Kaolinite-sericite.

                                                                         (Chail)

      ii) **Pegmatitic stage**
         a) Border + wall zone   = Albite-microcline perthite-(muscovite-biotes).
         b) Intermediate zone   = Microcline perthite-albite-(quartz-muscovite-biotite).
         c) Core   = Microcline perthite-smoky quartz-(albite).
         Pneumatolytic stage   = Beryl-cleavlandite-tourmaline.
         Hydrothermal stage   = Kaolinite-sericite.

                                                                         (Chail)

   D. **Zoned asymmetrical**
      i) **Pegmatitic stage.**
         a) Border + wall zone (western) = Albite-quartz-tourmaline-muscovite.
         b) Outer intermediate zone   = Microcline perthite-(muscovite).
         c) Inner intermediate zone   = Microcline perthite (muscovite-quartz).
         d) Core   = Quartz.

e)	Inner intermediate zone (eastern)	=	Albite-quartz (muscovite).
f)	Outer intermediate zone (eastern)	=	Graphic granite.
g)	Border + wall zones (eastern)	=	Oligoclase-quartz-tourmaline-muscovite.
	Pneumatolytic stage	=	Beryl-columbite-samarskite-muscovite-garnet-tourmaline-microcline perthite.
	Hydrothermal stage	=	Kaolinite-sericite.

(Bagarian)

ii)	Pegmatitic stage		
a)	Border + wall zone	=	Albite-quartz(muscovite).
b)	Outer intermediate zone	=	Microcline perthite.
c)	Inner intermediate zone	=	Microcline perthite-quartz (muscovite).
d)	Core	=	Quartz.
	Pneumatolytic stage	=	Beryl-blibinite-tourmaline-garnet-muscovite.
	Hydrothermal stage	=	Kaolinite-sericite.

(Rajdhawari)

5. ALBITIZED OR REPLACEMENT BODIES

i)	Oligoclase-(quartz-muscovite-biotite).	(Bandi Sadiq)
ii)	Albite-quartz-(muscovite).	(Jalgali)
iii)	Albite-quartz-(muscovite-tourmaline).	(Jalgali)
iv)	Albite-quartz-(biotite-sphene-apatite).	(Susalgali)
v)	Albite-(quartz-muscovite-chlorite-apatite).	(Susalgali)

6. COMPOSITE BODIES

i)	Pegmatitic-albitite, albite-aplite, albite-microcline-aplite/pegmatite.	(Lassan)
ii)	Fine to medium grained-albitite, layered-albitite, layered-aplite.	(Batrasi R.H.)
iii)	Pegmatitic-albitite, medium grained-albitite.	(Batrasi, Ganda)
iv)	Pegmatitic-albitite, medium grained-albitite, albite-aplite.	(Ganda, Seri)
v)	Pegmatitic-albitite, medium grained-albitite, albite-aplite, albite-(microcline)-aplite.	(Seri)
vi)	Pegmatitic-albitite, medium grained-albitite, albite-(microcline)-aplite.	(Tutgali)
vii)	Albite-(microcline)-pegmatite/aplite, fine grained and pegmatitic-albitite (xenoliths)	(Phulra)

DISCUSSION ON PETROGENESIS

The acid minor bodies evolved from the granitic rocks of the area (Fig. 8). For the sake of understanding complete process of the formation of the different phases for the development of acid minor bodies namely albitites, aplites and pegmatites, a general picture for the development of granitic rocks is necessary. For this purpose a brief resume of the petrogenesis of the granitic complex is given and various types of evidences pertaining to the problems of genesis of the acid minor bodies are also summarized before elaborating the origin of these rocks and Mansehra granitic complex.

Field evidence

(i)   The acid minor bodies are present in all types of granites and the associated metasediments.

(ii)   Each type has its own characteristic features and associations with the types and the level of the host rock they occur i.e., fine grained albitites are always associated with metasediments while medium-grained and pegmatitic albitites dominantly occur within Mansehra granite. In addition albite-aplites are also met within Mansehra granite.

(iii)   Regional zoning of Henrich (1953) has been deciphered in the area as (a) interior bodies (b) marginal bodies and (c) exterior bodies. but his zoning has been modified as in (vi).

(iv) The deeply eroded area around Mansehra has exposed the regional zoning and thus in terms of altitude it is possible to classify the AMB. In the range of 750 to 1675 m above sea level (interior - lateral zone) albitites, albite-aplites / pegmatites, albite - (microcline) - aplites / pegmatites occurs. Over 1525 m and below 2750 m above seal level (interior - marginal zone) albite rich bodies are rarely present rather albite - microcline - quartz and muscovite - bearing rocks are common with accessories like beryl, cleavelandite, bilibinite, samarskite, columbite, etc. The pegmatites above 2750 m above sea level (marginal - exterior zone) are dominantly complex.

(v) Complex pegmatites are in more than 90% cases zoned whereas some simple pegmatites are also zoned. Zoning in all the cases is quite distinct because most of the pegmatite zones have distinctly contrasting mineralogy and grain size. A few albitite bodies are also zoned with usual pegmatitic outer zone and an inner zone of medium grained albitite.

(vi) In most cases the acid minor bodies are emplaced along the foliation planes of the granites and the metamorphics. Some of them are emplaced along the joints.

(vii) Cross - cutting relation is very rare and is only found is some major pegmatites where thin veins of very simple composition (pegmatitic) are present.

(viii) Composite bodies are present around Mansehra in the deeply eroded valley. Their association and possible relationship is as follows: Albitite, albite-aplite, albite - microcline - aplite and pegmatites. In another composite body pegmatitic - albitite, medium grained albitite and albite - aplite are present.

(ix) The contacts of some bigger and coarser bodies are fine-grained.

(x) The fine-grained nature of the albitites in the matamorphics is due to chilling effect as the temperature of metasediments was evidently much lower than the soda rich magmatic solutions. The contact of the albitites with the metamorphics is diffused due to the assimilation as the magmatic solutions might have been superenriched with soda. In contrast the grain size increases in the albitite emplaced near the contact of granite and metamorphics.

(xi) Ptygmatic pegmatites are minor to quite thick and in their present form are due to the tectonic disturbance in the granites.

Mineralogical evidence

The mineralogical evidences are discussed of each structural zone to fully differenciate mineralogy of the acid minor bodies in the area. (The occurrence of minerals in different acid minor bodies is schematically presented in Fig. 7).

(A) *The interior-lateral zone has the following features:*

(i) The pegmatitic albitites have normal albite and chessboard albite with about 1 to 10% quartz and some muscovite. The medium-grained variety of albitites has essentially same mineral contents but with less quartz and muscovite. The fine grained-albitite is dominantly rich in albite with comparatively more accessories. The chessboard albite is not developed in the fine grained-albitites except in those developed near contact.

(ii) Aplites are albite-quartz-muscovite type with rare tourmaline in the rocks crystallizing near contact. Another major type crystallizing in this zone is albite-(microcline)-quartz aplite with muscovite and tourmaline. The third type is a rare one in this zone with albite-microcline-quartz and some muscovite, tourmaline etc.

(iii) Pegmatites are mostly albite-quartz with some muscovite and some of the pegmatites have albite-(microcline)-quartz-muscovite and tourmaline minerals. The latter type is present around the contact of granite and metamorphics, while the former is well inside the Mansehra granite.

(iv) Albitization or replacement by soda of granite is common in this zone.

(v) Quartz veins and dykes are commonly present in this zone and especially in the granite.

(B) *Interior-marginal zone bodies have the following mineralogic characters:*

(i) The albitite bodies are a few in number and well inside the granite which may be an overlapping zone (1525 to 1675 m). These albitites are medium - grained and slightly rich in quartz as compared to interior - lateral zone albitite bodies.

(ii) The aplites are albite - microcline - quartz - muscovite - tourmaline to microcline - albite - quartz - muscovite etc. bearing. Nowhere albite - quartz - aplite is seen in the area so far.

(iii) The pegmatites in this zone are simple as well as complex mineralogically. The simple pegmatites are albite microcline - quartz - muscovite (minor tourmaline etc.) bearing. The zoned simple pegmatites in most of the bodies have intermediate zone of graphic granite; with muscovite - quartz and quartz zones in the central portion. The zonation is perfect in most of the complex pegmatites with pneumatolytic replacement and the formation of beryl, tourmaline, samarskite, microcline perthite, columbite, bilibinite, muscovite etc. Occurrence of albite - pegmatite is rare in the interior - marginal zone, which in contrast to interior - lateral zone is partially to fully zoned. Pod like small albite - microcline and tourmaline pegmatites are abundant in this zone especially north - west of Batgram.

(iv) The albitized or replacement bodies are abundantly present in this zone consisting of albite - quartz - tourmaline - biotite and muscovite. Sometimes relict microcline grains are also met at places.

(v) The quartz-kyanite and chlorite bearing veins are present in a few localities in this zone, emplaced in metamorphics of high grade.

(C) *Marginal-exterior zone bodies*

True exterior bodies have not been found in the area studied. Though some reliable sources do confirm the occurrence of exterior pegmatites in the northern tribal area. This zone is defined as occurring above 2750 m above sea level and near the contact of granite and metamorphics.

This zone has mostly complex zoned pegmatites. The essential minerals of the pegmatites in this zone are very much like those of interior-marginal zone. But this zone has been classed as separate one because here the pegmatites are, in more than 90% cases, mineralogically complex and zoned. Moreover the albitites, albite-aplites and pegmatites are altogether absent in this zone.

Chemical Evidence

Major elements: The chemical composition of the acid minor bodies show a wide range of variations from pure sodic bodies to normal igneous pegmatites as already described in the field evidence. This means that the soda content decreases with the increase in the rest magmatic fludis rich in volatiles. From the above statement it is clear that there is wide range of chemical variations (Table - 2).

The chemical composition of the different rock units is plotted as:

(a) SiO_2 against Na_2O, K_2O, Al_2O_3, CaO, P_2O_5 and total mafic oxides in Figs. 2 & 3.)

(b) Felsic oxides against the felsic index (Fig. 4).

(c) $NaAlSi_3O_8$ - $KAlSi_3O_8$ - SiO_2 in the Luth *et al.* (1964) diagram (Fig. 5).

(d) (Or + C) - Al - (An + femic) in Brammall's (1933) diagram Fig. 6 is the improved version of the felsic index, put forward by Simpson (1954), which shows that there is a definite trend of crystallization of the granitic liquids from a partial melting of metasediments to form albitites, soda-aplite, soda-potash aplites and pegmatites.

Percent oxides

Percent SiO₂ in albitites

Fig. 2 Linear correlation diagram between SiO₂ and principal oxides.

Percent oxides

P Percent SiO₂
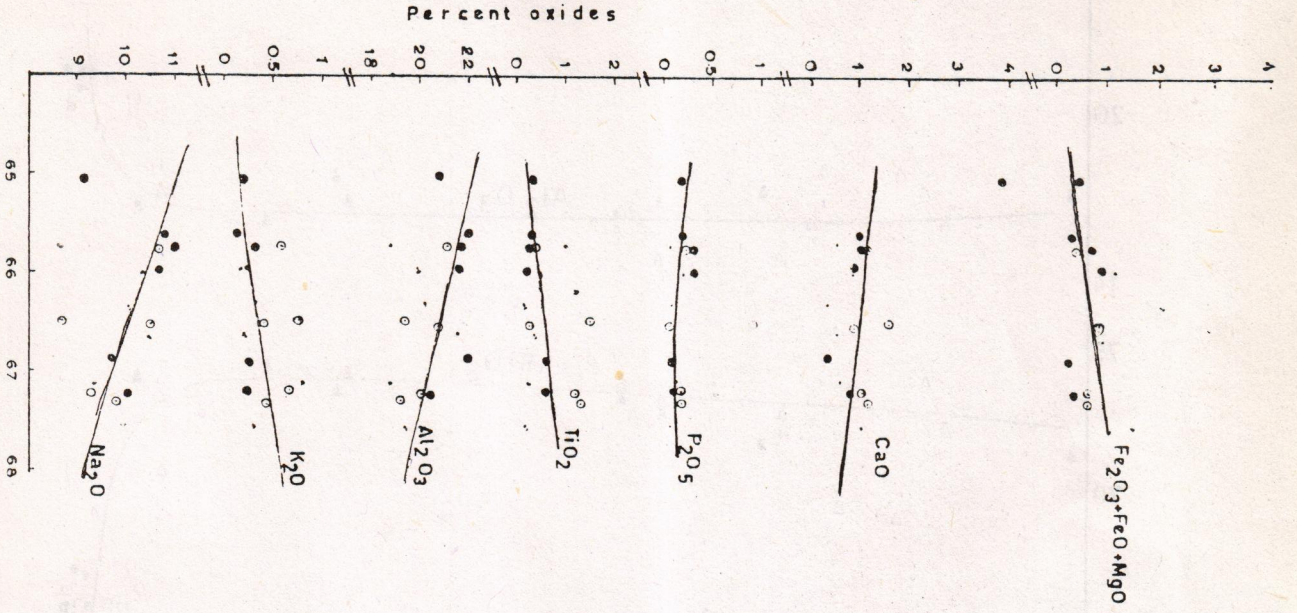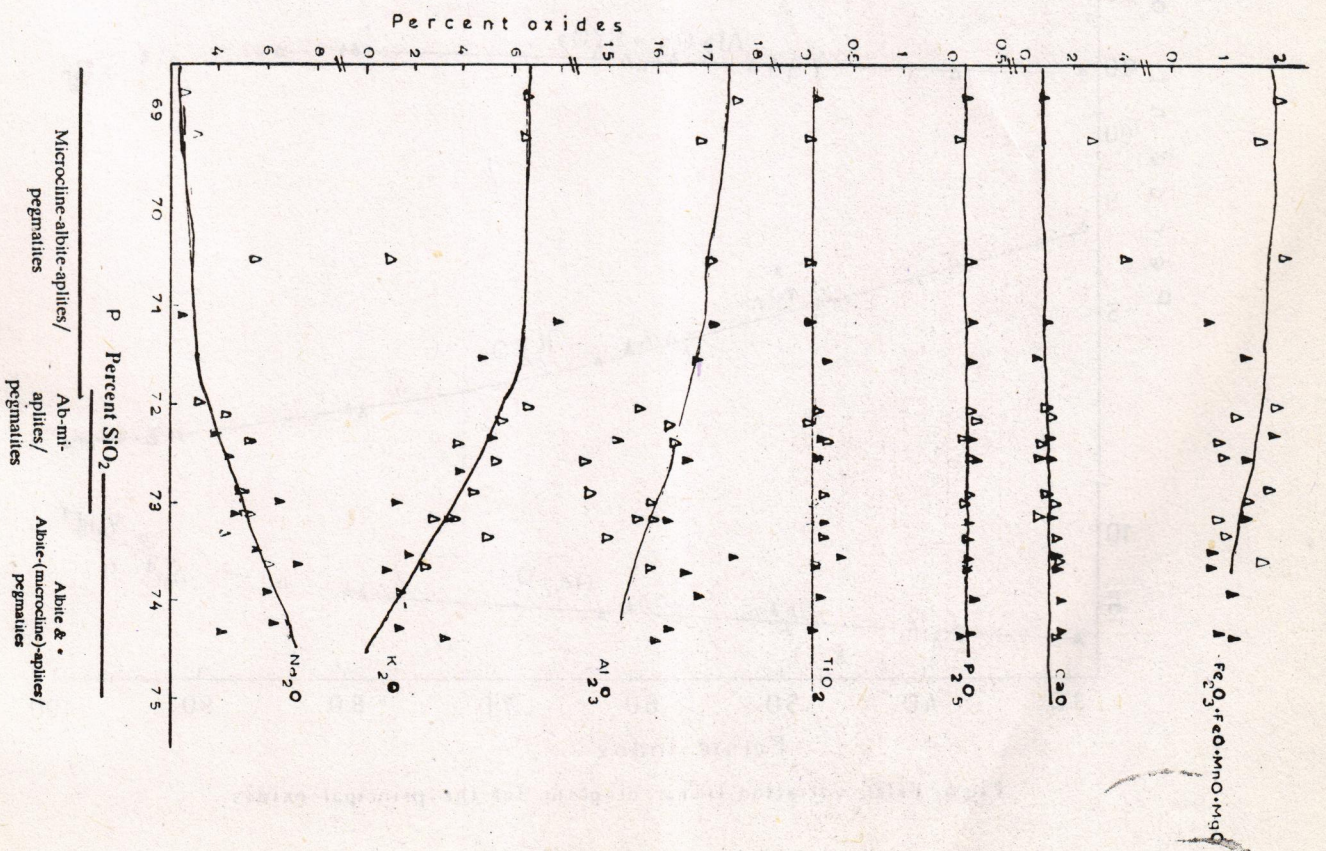
Fig. 3 Linear correlation diagram between SiO₂ and principal oxides.
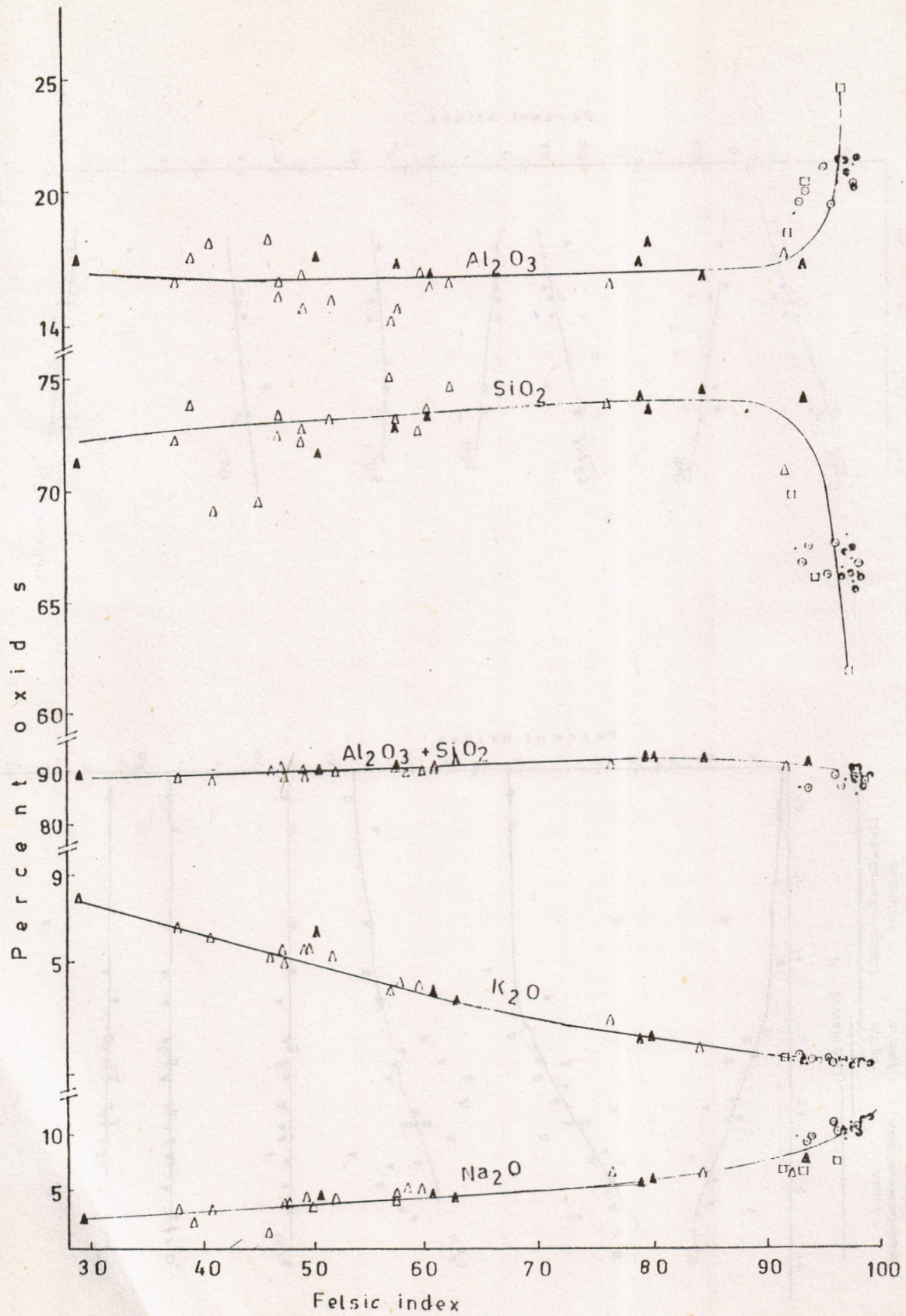
Fig.4 Felsic variation linear diagram for the principal oxides.

10
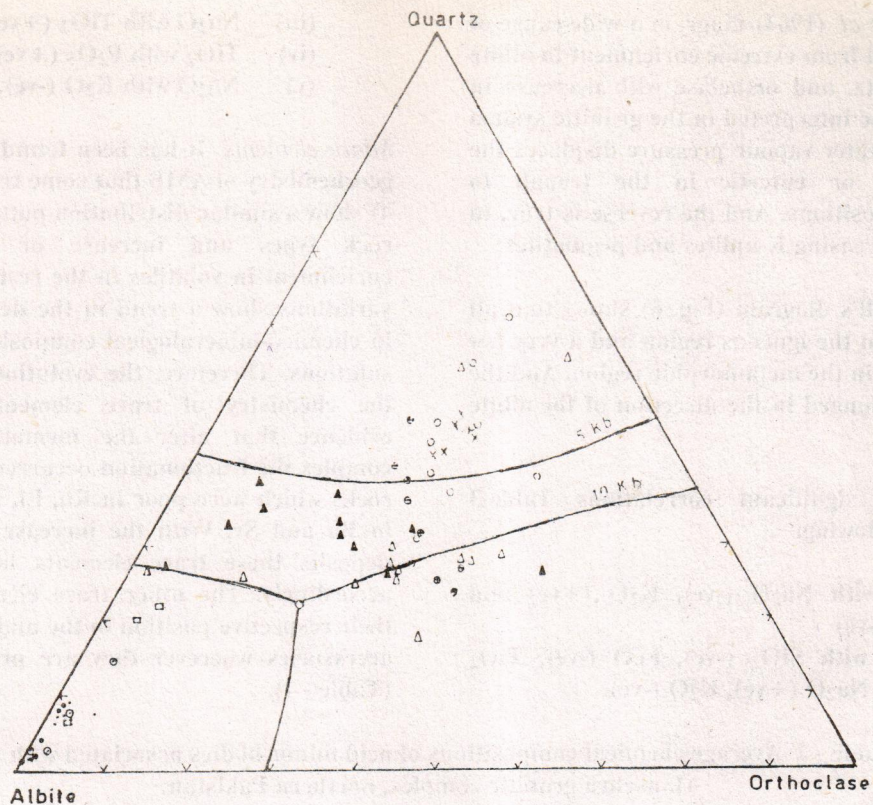
Fig. 5 Normative albite orthoclase and quartz diagram of the analysed
acid minor bodies (and granites after Shams, 1967) recalculated ∆100%.
(Luth et al., 1954)

o Susalgali granite gneiss
x Mansehra granite
⊕ Hakle tourmaline granite
△ Pegmatites
▲ Aplites
⊙ Pegmatitic albitite
• Medium grained albitite
- Fine grained   ,,
⊡ Albitized

Fig. 6 Composite Brammell diagram of the acid minor bodies and the granites.

11

In the Luth *et al.* (1964) diagram a wide range of variation is observed from extreme enrichment in albite to increase in quartz, and orthclase with decrease in PH_2O which could be interpreted in the granitic system as, the increase in water vapour pressure displaces the isobaric minimum or eutectic in the trough to increasingly sodic positions. And the reverse is true, in the formation of increasing K-aplites and pegmatites.

The Brammall's diagram (Fig. 6) shows that all the pegmatites fall in the igneous region and a very few of them are present in the metamorphic region. And the field of plots is prolonged in the direction of the albite apex.

Geochemical significant correlations Table-3 exist between the following:

(i) SiO_2 with Na_2O (-ve), K_2O (+ve) and TiO_2 (-ve)

(ii) Al_2O_3 with SiO_2 (-ve), FeO (-ve), TiO_2 (+ve), Na_2O (+ve), K_2O (-ve).

(iii) Na_2O with TiO_2 (+ve), K_2O (-ve).

(iv) TiO_2 with P_2O_5 (+ve).

(v) Na_2O with K_2O (-ve).

Minor elements: It has been found by Ashraf (1975) on geochemistry of AMB that some trace elements (Table - 4) show a similar distribution pattern within a group of rock types and increase or decrease with the enrichment in volatiles in the rest-liquids. This sort of variations show a trend in the development or change in chemico-mineralogical composition of the magmatic solutions. Therefore, the evolutionary trend shown by the chemistry of trace elements is the strongest evidence that after the formation of the granitic complex the fractionation occurred to give rise albititic rocks which were poor in Rb, Li, Pb, and Sn; and rich in Ba and Sr. With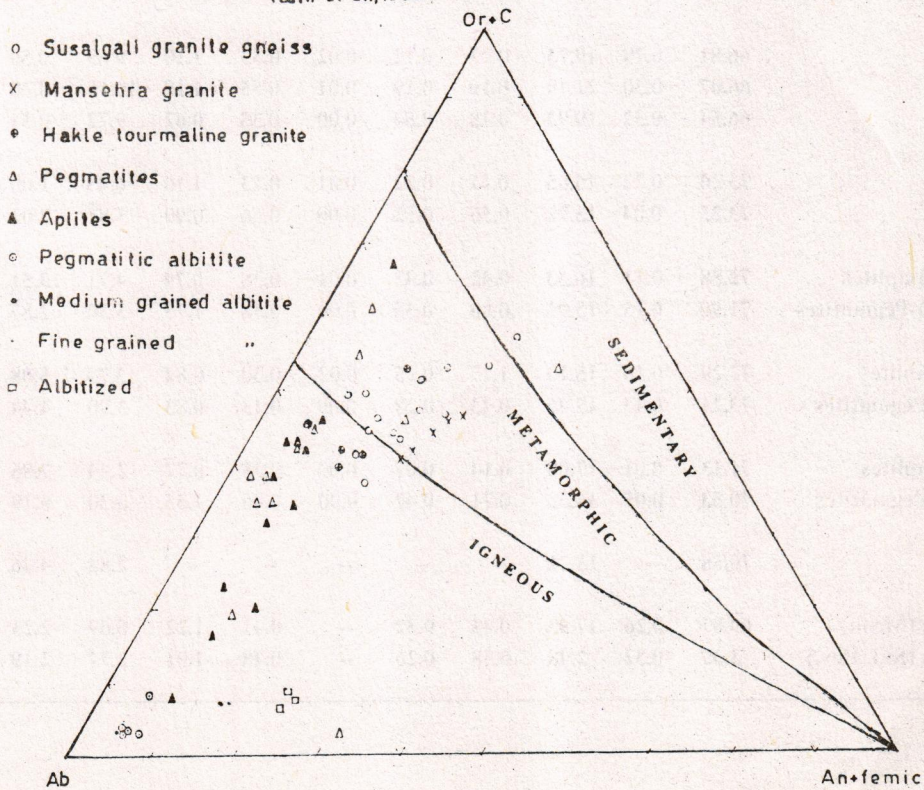 the increase in volatiles in later deposits these trace elements became rich or poor accordingly. The other trace elements are related to their respective position in the major minerals or to the accessories wherever they are present in some rocks (Table - 4).

Table - 2 Average chemical compositions of acid minor bodies associated with the Mansehra granitic complex, northern Pakistan.

	Type Rock	SiO_2	TiO_2	Al_2O_3	Fe_2O_3	FeO	MnO	MgO	CaO	Na_2O	K_2O	P_2O_5	H_2O
1.	**Albitites**												
	Coarse grained	66.81	0.79	19.73	0.27	0.12	0.02	0.33	1.10	9.65	0.50	0.27	0.32
	Medium grained	66.07	0.30	21.19	0.19	0.19	0.01	0.55	1.18	10.15	0.20	0.13	0.39
	Fine grained	66.54	0.32	19.93	0.78	0.54	0.00	0.35	0.62	9.72	0.31	0.06	0.42
2.	Albite-Aplites	73.20	0.22	16.65	0.41	0.22	0.01	0.13	1.16	6.45	1.00	0.11	0.32
	Albite-Pegmatites	73.25	0.04	15.72	0.56	0.52	0.00	0.66	0.90	5.87	2.02	0.80	0.33
3.	Albite-(microcline)-aplites	72.88	0.11	16.33	0.42	0.42	0.01	0.38	0.74	4.71	3.51	0.12	0.68
	Albite-(microcline)-Pegmatites	71.90	0.15	15.93	0.80	0.30	0.00	0.38	1.75	5.30	2.87	0.15	0.53
4.	Albite-microcline-aplites	72.29	0.16	15.10	1.17	0.25	0.02	0.30	0.84	3.79	5.08	0.16	0.75
	Albite-microcline-Pegmatites	73.21	0.13	15.46	0.43	0.28	0.00	0.13	0.83	3.90	4.44	0.16	0.95
5.	Microcline-albite-aplites	71.13	0.01	17.08	0.14	0.07	0.00	0.35	0.77	2.44	7.86	0.15	0.15
	Microcline-albite-Pegmatites	70.53	0.05	16.53	0.71	0.47	0.00	0.45	1.33	3.30	6.19	0.12	0.42
6.	Granites	70.58	--	15.21	--	--	--	--	--	2.88	4.46	--	--
7.	Acid Minor Bodies (Mean)	69.87	0.26	17.93	0.48	0.32	--	0.41	1.22	6.69	2.23	0.14	--
	Acid Minor Bodies (Std. Dev.)	3.39	0.32	2.48	0.38	0.26	--	0.48	1.01	2.77	2.19	0.13	--

Table - 3 Linear correlation coefficients between major oxides in acid minor bodies associated with the Mansehra granitic complex, northern Pakistan.

(r)

	SiO$_2$	TiO$_2$	Al$_2$O$_3$	Fe$_2$O$_3$	FeO	MgO	CaO	Na$_2$O	K$_2$O	P$_2$O$_5$
SiO$_2$		-0.42	-0.91	0.04	0.14	-0.08	-0.28	-0.73	0.57	-0.15
TiO$_2$	-3.10*		0.33	-0.23	-0.19	0.12	-0.02	0.41	-0.40	0.45
Al$_2$O$_3$	-15.16*	2.36*		-0.20	-0.33	-0.14	0.19	-0.78	-0.66	0.10
Fe$_2$O$_3$	0.26	-1.60	-1.40		0.40	0.13	0.11	-0.24	0.16	-0.12
(t) FeO	0.95	-1.28	-2.35*	2.88*		0.48	-0.14	-0.24	0.19	-0.19
MgO	-0.52	0.84	-0.92	0.87	3.70*		0.17	-0.13	-0.04	-0.09
CaO	-1.95	-0.14	1.31	0.72	-0.94	1.14		-0.07	-0.17	0.10
Na$_2$O	-7.26*	3.02*	8.48*	-1.65	-1.65	-0.90	-0.48		-0.85	0.20
K$_2$O	4.66*	-2.90*	-6.00*	1.07	1.07	-0.28	-0.28	-10.93*		-0.01
P$_2$O$_5$	1.00	3.40*	0.66	-0.78	-1.29	-0.62	0.65	0.13	0.06	

For n = 49 (r) is significant if corresponding value of student (t) is greater than 2.01 at 5%. Significant (t) is marked (*).

Table - 4 Distribution pattern of trace elements (ppm) in different acid minor bodies associated with the Mansehra granitic complex, northern Pakistan.

	MG Granite	SGN Granite	SGN Granite	A-356 Pegmatitic albitite	A-383 Medium grained albitite	A-3 Fine grained albitite	A-267 Albite-aplite	A-116'o' Complex aplite (outer zone)	A-116'i' Complex aplite (core)	A-111 Graphic granite zone	A-110M Mica+ quartz zone	Limites of sensitivity
Cr	22	15	15	14	--	450	--	800	1000	--	--	5
Sc	10	10	--	--	--	--	--	--	--	--	--	--
Co	5	5	5	--	--	--	--	--	--	40	80	5
Zr	216	180	120	300	5	140	40	300	300	--	--	5
Ni	10	8	8	--	--	--	--	--	--	--	--	2
Y	28	28	22	--	--	22	10	10	15	--	--	5
V	68	37	30	--	--	--	5	70	130	--	--	5
Ga	15	20	15	10	10	14	5	10	10	5	20	5
Sn	45	45	45	--	--	--	--	--	--	--	200	5
Pb	45	45	45	--	--	--	--	30	10	--	--	5
Ba	320	400	400	10	70	--	70	400	400	150	10	5
Sr	80	80	80	80	30	35	200	45	45	30	--	5
Rb	380	380	380	--	--	--	--	300	300	700	240	25
Li	56	43	135	1	--	--	5	15	15	2	2	1
Cs	45	--	100	--	--	--	--	--	--	--	--	--
Cu	--	--	--	4	4	10	4	10	10	4	4	4
Mo	--	--	--	--	--	--	--	--	--	--	--	2

	A-354 Ab. mi. aplite	A-354M Ab. mi. pegmatite	A-354T Ab. mi. pegmatite	A-334 Ab.-mi. pegmatite (near contract)	A-337 Ab. mi. pegmatite	A-85 Wall Zone	A-367 Graphic granite	A-365 Ab. Qtz. Zone	A-93 Qtz. Core	A-89 Microcline pegmatitic	A-291 Microcline pod pneumatolytic	A-86 Muscovite pod pneumatolytic
	Simple pegmatites unzoned					Complex pegmatite zoned						
Cr	--	--	--	--	--	13	--	--	--	30	--	--
Sc	--	--	--	--	--	--	--	--	--	--	--	--
Co	--	--	--	--	--	--	--	--	--	--	--	--
Zr	5	5	--	18	5	370	--	--	--	--	--	--
Ni	--	--	--	--	--	--	--	--	--	--	--	--
Y	--	--	--	--	--	10	--	--	--	--	--	--
V	--	--	--	--	--	--	--	--	--	--	--	--
Ga	5	5	5	5	10	20	10	14	--	5	5	40
Sn	--	--	--	--	--	200	--	--	--	--	--	500
Pb	15	10	10	--	10	10	30	--	--	15	5	--
Ba	10	10	25	25	5	--	25	10	--	10	5	--
Sr	5	5	5	5	--	5	10	--	--	5	5	--
Rb	240	240	240	180	240	240	700	25	--	3000	4500	3000
Li	1	1	2	5	15	100	40	15	--	40	40	300
Cs	--	--	--	--	--	--	--	--	--	--	--	--
Cu	10	22	4	4	4	10	4	10	10	10	--	10
Mo	--	--	--	--	--	--	--	--	--	--	--	--

Origin of the Granites

On the origin of the Mansehra granitic complex I in most cases disagree with model presented by Shams (1967, 1983) for the in situ granitization and migmatization. In my views the Mansehra granitic complex was produced from the extensive partial melting of Hazara Formation (a pelitic facies) and of a lower part of the Tanol Formation (a pelitic psammatic facies). Therefore, the protolith was almost homogeneous and metamorphosed in nature. The dominant pelitic facies occur in western area of Mansehra particularly in Oghi and Black Mountains and in southern part of Mansehra, whereas in the middle part of the complex are the pelitic psammatic facies. The age of these rock formations i.e., Hazara and Tanol Formation are 950 to 700 Ma with age of metamorphism 650 Ma (Baig *et al.*, 1989, Baig, 1991) and the age of Mansehra granite is 500 ± 16 Ma (LeFort 1980). Recent studies (Ashraf & Baig in preparation) showed that the Hazara and Tanol Formations detrital materials have been derived from basement rocks of Besham group (Baig, 1991) and Sharda group (Ghazanfar *et al.* 1983). The clasts of these groups of rocks are very evident in particularly the coarse grained varieties of Hazara Formation and in most cases of Tanol Formation. Plagioclase in Hazara Formation is from 4 to 10% in most cases and also as altered product as illite whereas K-feldspar was altered mostly to sericite 15 to 30% with relic to well preserved microcline. In Lower Tanol Formation the plagioclase is 5 to 20% with alteration to illite etc. and K-feldspar from 2 to 15% alongwith altered product of sericite and muscovite. The granitic rocks associated with both the groups i.e., of Besham and Sharda groups are well differentiated and fractionated particularly those of Sharda group where minerals like beryl, columbite, tantalite, spodumene, lepidolite etc. have been recognized in pegmatites. The composition of most parts of Mansehra granitic complex is biotite rich with minor muscovite alongwith other granite minerals suggest that a partial melting of about 40% of Hazara Formation and of Lower Tanol Formation was involved to produce Mansehra biotite granite as is also found

out, illustrated and elucidated by Shearer *et al.* (1992), Cerny *et al.* (1981) and Cerny (1982). The dehydration melting at the expense of biotite and muscovite of the Hazara Formation and Lower Tanol Formation which had been metamorphosed to kyanite-silliminite facies appear to be the most efficient means of generating the water undersaturated fertile, and peraluminous melts. That melting would produce homogeneous magmas (to form Mansehra granitic complex) with regard to major elements (Shearer *et al.* 1992).

An increase in H_2O content of the granitic melt has been illustrated to greatly decrease melt viscosity, from 10^{11} poises at 800°C and O% H_2O to 10^4 poises at 800°C and 6% H_2O (McBirney 1984). A higher content of H_2O in the low partial melt fraction may be a consequence of enhanced silicated liquid H_2O miscibility (Manning *et al.* 1980, London 1986) low degree of partial melting (Manning and Pichavant 1985), or an influx of free fluid during near solidus melting (Thompson 1982). A reduction in viscosity due to O% H_2O to 6% H_2O result in an effective efficiency of extraction of a 5% melt equivalent to a 40 to 50% partial melt (Spera 1980). The combined effect of melting accompanying the dehydration of muscovite and biotite can effectively produce large volumes of melt (Miller 1985). This sort of action of dehydration of muscovite and biotite helped to produce such a biotitic magma as is enunciated above and in this manner Mansehra granite was formed. The Mansehra granite thus formed a complex structural dome which grew upward and outward (Duke *et al.* 1990, Shams 1967, 1969) with tourmaline bearing granites. Textural interpretation suggests that tourmaline followed biotite in the sequence of crystallization. This is evident as Hakle, Sukal, Karkala and Dheri tourmaline granites, having lensoid to oval and sill like shapes of these bodies (Shams 1967).

The Hazara and Tanol Formations consist dominantly of quartz + plagioclase $\pm$ K - feldspar $\pm$ muscovite $\pm$ biotite (recent study by Ashraf & Baig unpublished), whereas their compositional variations in terms of trace elements are Rb 24-300 ppm, Li 10-100 ppm and Ba 150-700 ppm. The possible range of magmas produced by partial melting of compositionally similar to varied rocks has nearly constant concentration of Ba (320-400 ppm), Li (32-56 ppm exceptionally 135 ppm) and Rb (380 ppm) in the biotite granite (Susalgali granite gneiss and Mansehra granite of Shams, 1967). Such studies have been carried out by Duke *et al.* (1990) from the data base of Black Hills Precambrian rocks (Tuzinski 1983, Shearer *et al.* 1986 & 1987, Dewitt et al. 1986, Redden 1968 and Galbreath

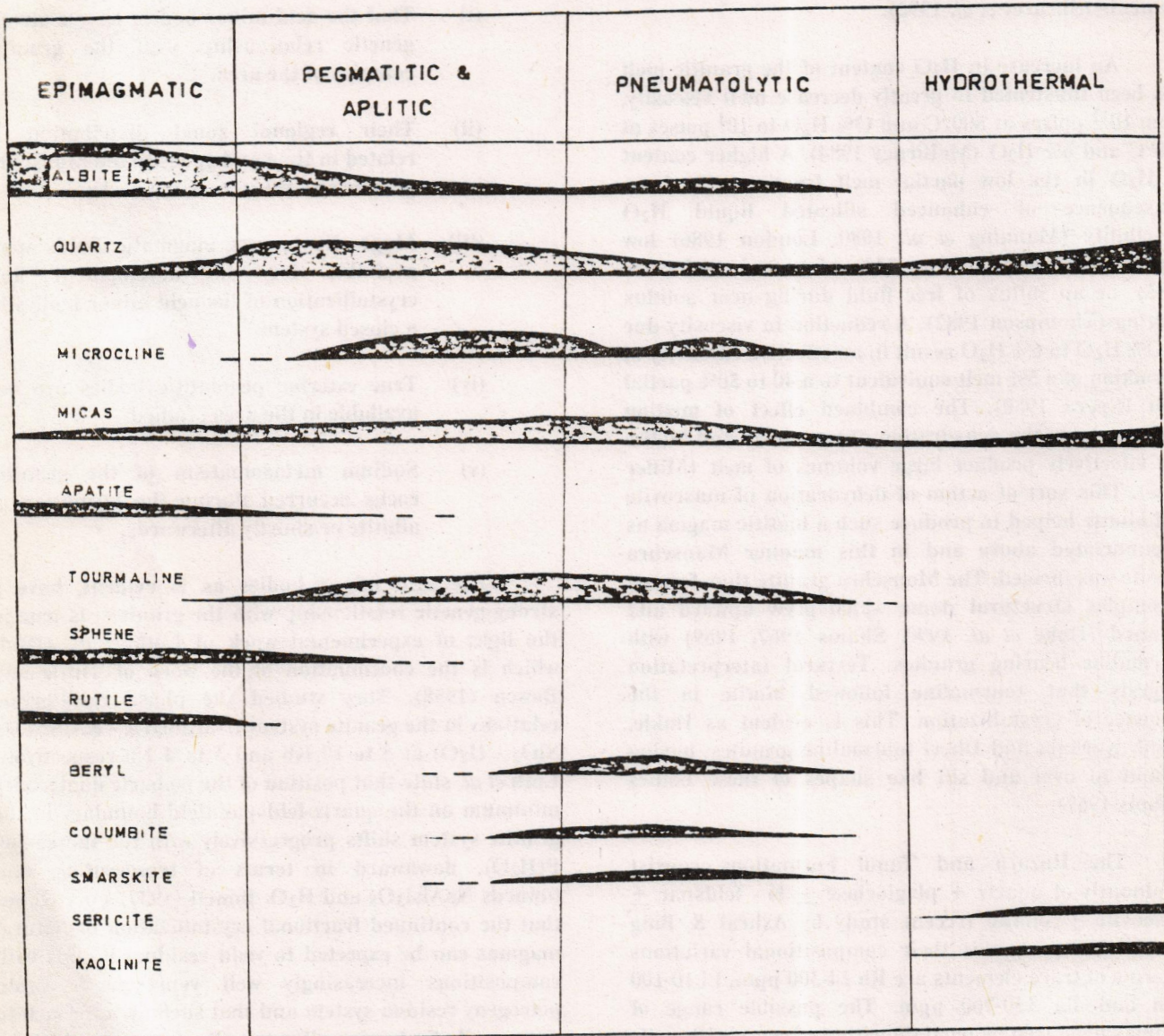*et al.* 1987) for the production Harney Peak granite.

Origin of the Acid Minor Bodies

From the description and discussions on the origin of granites, field, mineralogical and chemical evidences for the acid minor bodies; conclusions of some fundamental importance can be drawn:

(i)   That the acid minor bodies have a strong genetic relationship with the granitic complex of the area.

(ii)   Their regional zonal distribution is related in time and space to the Mansehra granite and the associated rocks.

(iii)   Magmatic to rest magmatic fluids were available for the development and crystallization of the acid minor bodies in a closed system.

(iv)   True exterior pegmatitic bodies are not available in the area studied.

(v)   Sodium metasomatism of the granitic rocks occurred during the formation of albitite or shortly afterwards.

The acid minor bodies as is evident, have a strong genetic relationship with the granites, is true in the light of experimental work of Luth *et al.* (1964) which is the continuation of the work of Tuttle and Bowen (1958). They studied the phase equilibrium relations in the granite system ($NaAlSi_3O_8$ - $KAlSi_3O_8$ - SiO_2 - H_2O) at 5 to 10 Kb and 3 to 4 Kb respectively. Luth *et al.* state that position of the isobaric quaternary minimum on the quartz-feldspar field boundary in the granite system shifts progressively with the increasing $P(H_2O)$, downward in terms of temperature and towards $NaAlSi_3O_8$ and H_2O. Bowen (1937) pointed out that the continued fractional crystallization of natural magmas can be expected to yield residual liquids with compositions increasingly well represented within petrogeny residua system and that such an approach to pure alkali-alumino-silicate liquids should be accompanied by an approach to thermal trough or belt of minimum melting in this system. At different water vapour pressures, Orville (1960), Burnham and Jahns (1962), Norton *et al.* (1962), Jahns and Tuttle (1963) and Booth (1967) have shown the composition trend from normal granitic rocks to aplites which is the projected path of the quaternary minimum and eutectic as related to increasing values of $P(H_2O)$ and to points

Fig. 7 Relative period of crystallization of the various minerals.

Fig. 7 Relative period of crystallization of the various minerals.

EPIMAGMATIC	PEGMATITIC & APLITIC	PNEUMATOLYTIC	HYDROTHERMAL
ALBITE			
QUARTZ			
MICROCLINE			
MICAS			
APATITE			
TOURMALINE			
SPHENE			
RUTILE			
BERYL			
COLUMBITE			
SMARSKITE			
SERICITE			
KAOLINITE			

Granitic magma
at $P_{H_2O} > 10$ Kbs
|
Depletion in K_2O
Enrichment in Na_2O

Pegmatitic albitite
(1.i)

Medium-grained albitite
(1.ii)

Fine-grained albitite
(1.iii)

Pegmatitic albitite

(6.ii)

Medium-grained albitite

Composite

ALBITITE

Solutions rich in Na_2O

Albitization or replacment
of granite gneiss
(5.i-v)

Release in P_{H_2O}

Composite in localized closed chamber (6.i)

Pegmatitic albite

Albite-aplite

Albite-microcline-aplite/pegmatites

Release in P_{H_2O}

Enrichment in SiO_2 and minor K_2O as muscovite.

Albite-aplite/pegmatite

Unzoned
(2 A i,3 A i)

Zoned
(3 B ii)

Increase in K_2O
as muscovite+(microcline)
with release in P_{H_2O}

Albite-(microcline)-aplite/pegmatite
(2 A.ii,3 A ii)

Further release in P_{H_2O}
Nearly equal amount of
Na_2O & K_2O

Albite-microcline-aplite/Pegmatite

Unzoned
(2 A iii,3 A iii)

Zoned
(3 B iii)

K_2O is more than Na_2O

Microcline-albite-aplite/pegmatite

Unzoned
(2 A iv,3 A iv)

Zoned
(3 B i)

Boron enrichment

Volatiles enrichment

Unzoned complex pegmatite
(4 A.i)

Zoned complex pegmatite
(4 B i-vi)

Pod pegmatite
(3 B vi)

Hydrothermal(?) veins

Quartz
(7 i)

Quartz ilmenite
(7 ii)
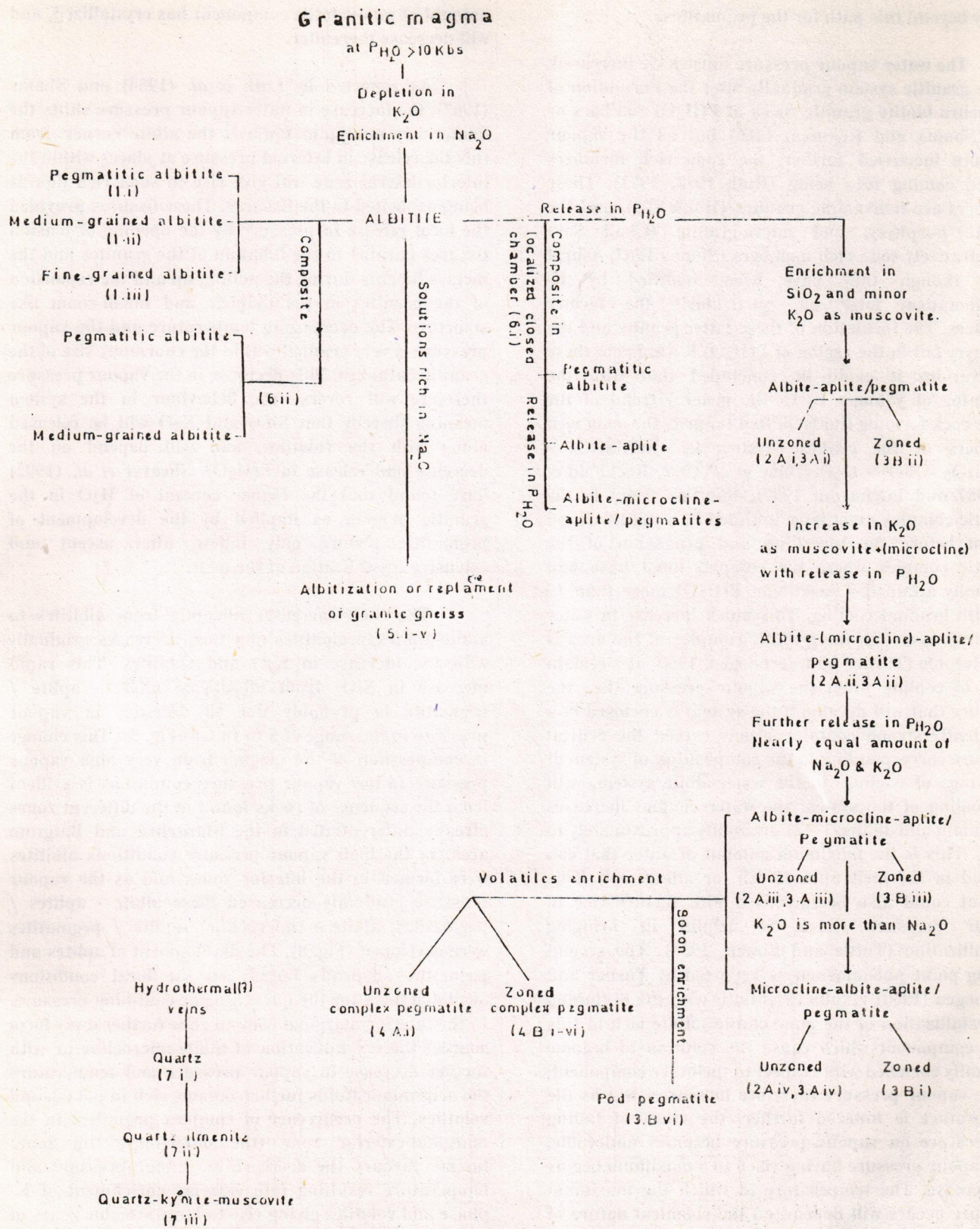
Quartz-kyanite-muscovite
(7 iii)

Fig. 8   Diagramatic outline for the derivation of water saturated granitic magma and for the crystallization of acid minor bodies.

17

wholly beyond this path for the pegmatites.

The water vapour pressure must have increased, in the granitic system gradually after the Formation of Mansehra biotite granitic rocks at $P(H_2O)$ 500 bars or less (Shams and Rehman, 1966) but as the vapour pressure increased further, the soda rich members started coming into being (Hall, 1972, 1973). These members are tourmaline granites (Hakle etc.), and the granite porphyry, and micro-granite (Chail Sar) comparatively soda rich members (Shams 1967, Ashraf 1974) though they have been modified by K-metasomatism later on, particularly the former members. The formation of these latter granite and the porphyry fall in the region of $P(H_2O)$ 5 Kb. From these observations it could be concluded that with the upcoming of younger rocks the general trend of the acidic rock forming fluids shifted towards the soda rich members of the granitic system i.e. $NaAlSi_3O_8$ - $KAlSi_3O_8$ - SiO_2 - H_2O (Duke et al. 1992, Rockhold et al. 1987 and Pitchavant 1987). But this trend in the granitic complex must have initiated in a tightly closed system before the upwelling and expansion of the granitic complex where the complex must have had gradually attained a maximum $P(H_2O)$ more than 10 Kb with gradual cooling. This much increase in water vapour pressure in the granitic complex of the area is conceiveable (Turner and Verhoogen, 1960) at a certain stage of cooling when the vapour pressure (i.e., the pressure that will develop if the system is enclosed in a sufficiently strong container) may exceed the critical pressure corresponding to the composition of system at this stage of cooling. In the water-albite system, with the cooling of the system the water content increases (Burnham and Jahns, 1962) gradually approximately to 16.8%. This is the maximum amount of water that can be held in the melt upto 10 Kb for albite melt. This amount could also be increased with further rise in vapour pressure which is helpful in bringing crystallization (Tuttle and Bowen, 1958). The second boiling point phenomenon as reported by Turner and Verhoogen (1960) results essentially with the beginning of crystallization of the non-volatile (albite rich in this case) component which cause the solution to become gradually enriched with respect to the other component; whose vapour pressure therefore increases. But as the temperature is lowered further, the effect of falling temperature on vapour pressure becomes noticeable; and vapour pressure having risen to a maximum begins to decrease. The temperature at which the maximum pressure occurs will depend on the chemical nature of the system i.e., the effect of the increasing concentration of which might predominate so that the vapour pressure would rise continuously until the whole amount of non-volatile component has crystallized, and will decrease thereafter.

As reported by Luth et al. (1964) and Shams (1967), the increase in water vapour pressure shifts the quaternary minimum towards the albite corner. from this the release in external pressure at places within the interior-lateral zone will give rise to soda rich liquids being deposited in the fissures. These fissures provided the local release in pressure by the opening of tension fissures parallel to the foliation of the granites and the metasediments during the welling up and the expansion of the granites in the diapiric and mush-room like structure. The decrease in temperature and the vapour pressure is very gradual within the enormous size of the granitic batholith. This decrease in the vapour pressure therefore will reverse the behaviour in the system meaning thereby that SiO_2 and K_2O will be released along with the volatiles, and will depend on the decrease and release in $P(H_2O)$. Shearer et al. (1992) have found that the higher content of H_2O in the granitic magma as implied by the development of pegmatitic texture only follow, after ascent and extensive crystalization of the melt.

The SiO_2 increases abruptly from albitites to albite-aplites/pegmatites and then decreases gradually with the increase in K_2O and volatiles. This rapid increase in SiO_2 from albitite to albite - aplite / pegmatite is probably due to decrease in vapour pressure in the range of 5 to 10 Kb (Fig. 5). This change in composition of the magma from very high vapour pressure to low vapour pressure conditions is evident from the sequence of rocks found in the different zones already differentiated in the Mansehra and Batgram area. In the high vapour pressure conditions albitites were formed in the interior zones and as the vapour pressure gradually decreased these albite - aplites / pegmatites, albite - (microcline) -aplite / pegmatites were developed (Fig. 8). The development of aplites and pegmatites depends largely on the local conditions available there for the quenching or confining pressure. In the interior-marginal zone (a zone further away form source) the crystallization of albite-microcline or with further decrease in vapour pressure and temperature the acid minor fluids further became rich in potash and volatiles. The occurrence of complex pegmtites in the marginal-exterior zone (the outer-most top zone) further favours the decrease in vapour pressure and temperature resulting into extreme enrichment of K-phase and volatiles giving rise to large sizeable zones of microcline-perthite and development of rare minerals at the pneumatolytic stage. Therefore from the above statement it could be concluded that the entire mass of

granite acted as a closed system in the case of individual acid minor bodies where the vapour pressure and temperature decreased from the interior of the granitic complex upwards to the roof. Whereas the composite bodies acted simply in a localized closed system (e.g., Lassan composite body, Ashraf 1975) were the depositions occurred in the same vapour pressure conditions as stated above.

Origin of the Albitites

The albitites and soda aplites are very rare bodies in the world and they have been recorded mostly in the basic and ultrabasic rocks and rarely in the acidic rocks. Larsen (1928) (describing some examples) has postulated hydrothermal origin for corundum and albitite bodies. Walker (1932) noted an albitite body from Shetland Isles. Anderson (1937) found albitites bodies in northern Inyo Range which were formed by replacement of the metasediments. Joplin (1957) reported several albitites associated with K-granite and has commented that K-granite magma assimilated with NaCl of the sediments to give rise to soda rich differentiate of small volume. Barth (1965) has given a diagram after Winkler and Platen (1961) showing CIPW - normative proportions of Ab: Or: Q of 112 granitoid rocks of the Precambrian of southern Norway. These plots show a definite trend towards albititic rocks from granites. Golden (1965) gave an example of magnetite - sphalerite albitite of metasomatic origin from quartzite. Boguslavskiy et al. (1965) found some albitites of metasomatic origin in Russia. Gladyshevskaya et al. (1966) reported an albitite from drilhole in Russia and classed as a syenite. Leonaridos et al. (1966) reported albitites developed by contact metasomatism during serpentinization, and albitites are thought to have been derived from volcanic rocks and sediments.

In the present studies albitites have been recorded from the granites and the associated metasedimentary rocks. As already mentioned in the preceding pages that the albitite magma was evolved from the granitic magma with the increasing water vapour pressure. This thing could also be explained in term of immiscibility in the granitic system at $P(H_2O)$ more than 10 Kb. This can be proved by further research work in this field beyond 10 Kb.

The experimental work of Orville (1963) also shows that an albititic magma can be created in early high temperature (more than 630°C) environments. The high temperature conditions might have been favourable in the interior zone of the Mensehra granitic

complex where enrichment in albite occurred gradually to form albitites and the potash moved towards the lower temperature (less than 600°C) regions.

In nature the release in $P(H_2O)$ is provided by the natural tension fissures and joints. The fissures were widely formed during the welling up and expansions of the granite complex. This sort of expansion is postulated due to development of mushroom and diapiric structure. The fissures are parallel to the foliation of the granites and metasediments. In the metasediments the fissures were developed contemporaneously with those in the granites and follow the same trend. So if these fissures would have been filled with the albititic liquids, the crystallization would start in a closed chamber and had given rise to the albitites bodies, at high PH_2O conditions. As the bodies are coarse, medium and fine-grained from place to place and as composite too so the physico-chemical conditions must have been the controlling factors. The coarse or pegmatitic albitites were formed in an environment of closed system with the surroundings. That is why the grain size of that albitite type is generally 3 to 30 mm. The albitites which have comparatively more temperature gradient than the coarser variety crystallized in the range of 1 to 3 mm grains-a medium-grained variety. In the case of albitites which are present in the metasediments the quenching was much more than those present in the granitic rocks as the relative temperature of the granites was much more than that of the metasediments because the acid minor bodies came into being just after the development of the granitic rocks. It can be observed in the field that as one moves away from the contact towards the metasediments the grain size of the albitite bodies decreases so much that the identification of the albite grains from quartz becomes difficult because twinning is absent or very vague and the grains are quite anhedral as compared to those subhedral to euhedral in the bodies near the contact of the granite and the metasediments. So the identity of this fine-grained albitite was proved by chemical analyses and X-ray diffraction method.

The above examples can be proved by the laboratories and field observations: (i) an albitite body about 30 metres from the granite contact in the metasediments near Batrasi rest house on road cut has grain size 0.15 to 0.30 mm in general (ii) a body near Maira J. Ali about 800 metres away from the contact has grains 0.1 to 0.15 mm with nearly 1% grains 0.2 to 0.3 mm and (iii) in this case the albitite body is about 2 kilometres away form the contact in the metasediments near Giddarpur and has grain size 0.02 to 0.04 mm.

The contact relations of the albitite with the granites are sharp which show that the nature of the bodies is intrusive and there is no exchange of material across the contacts. Even with the composite pegmatitic albitite, medium-grained albitite the contact is comparatively sharp which shows a sudden change in the local environmental conditions. The contact of fine-grained albitite with metasediments is sharp to somewhat diffused. This diffused phenomenon is due to Na - metasomatism, simultaneous with the emplacement of albitite or just occurred after the crystallization of the albitite.

The role of volatiles is very poor in the development of albitite. Only in one case tourmaline was observed. Moreover, the introduction of muscovite phase is also very minor but hydrothermally formed sericite is in a few cases upto 7% in albitites.

Origin of Albite, Albite-(Microcline)-Aplites and Pegmatites

These bodies occur in interior-lateral zone, sometime closely associated with albitites. Like pure albitites and quartz bearing pegmatitic albitites, these aplites and pegmatites are thought to have formed at slightly lower $P(H_2O)$ as compared to albitites. This thing could be evidently correlated in the normative and modal plots of the acid minor bodies in the granitic system where the trend without doubt, is towards albite end though the phases occur close to the albite-quartz baseline. The normative orthoclase in albite-aplites and pegmatites is due to the presence of muscovite in place of microcline is possible in these bodies in the light of highly sodic nature of the magma and at a higher $P(H_2O)$ (Luth *et al.,* 1964) and temperature (Orville, 1963) than the occurrence of microcline or orthoclase bearing bodies which form at relatively lower temperature. The lower contents of microcline and higher contents of white mica in some rocks favour these above views.

Origin of Albite-Microcline and Microcline-Albite-Aplites and Pegmatites.

In the section on the mineralogical evidence it has been explained that albite-microcline and microcline - albite - aplites and pegmaties are present in the interior - marginal zone, zone between 1525 to 2750 m above sea level. In this zone K-rich aplites and pegmatites were formed later than the albitites, albite - aplites and pegmatites and albite- (microcline) - aplites and pegmatites. In the present case, it appears as if $P(H_2O)$ was reduced and the system was reversed to the

plotted area in the petrogeny residua showing a composition well within the granitic magma. This reversal to the granitic system is excellently exemplified by a composite body with series of different rocks right from albitite, albite - aplite, albite - microcline - aplite and pegmatites occurring near Lassan in association showing different environment conditions of high water vapour pressure to the resulting normal $P(H_2O)$ in the formation of pegmatites (Ashraf, 1975). Therefore at high $P(H_2O)$ albitite was formed and with lowering of this pressure K-minerals were also released alongwith albite which slowly and gradually turned out to be albite-microcline aplite and pegmatite. Thereafter aplite and pegmatite are mineralogically and chemically same and composite but may be conformable to discordant in details (Heinrich, 1965). The outer pegmatite is slightly discordant with aplite which shows that the crystallization started in a gradually confined environments. The inner pegmatite on the other hand has sharp contact with aplite and shows that the confining pressure increased much more quickly than the outer pegmatite (Ashraf, 1975). According to Jahns (1955) and Jahns and Tuttle (1963), Windley and Bridgewater (1965), the aplites are generally considered as product of volatile poor magma that were otherwise similar to pegmatite forming magmas. On the other hand Miguel (1969) suggested that aplite-pegmatite association developed in two stages by metamorphic and metasomatic processes. Their view could be outrightly rejected in this case as the difference in volatiles in both aplite and pegmatites is not appreciably greater rather boron was much more active in the aplitic phase than the pegmatitic phase. It can be concluded that these aplites are, indeed, the quenched rocks - the result of the pressure quench without the escape of volatiles while in the formation of pegmatites the confining pressure increased. The information gathered from this composite body may have considerable bearing on the ideas about the crystallization of albitites, aplites and pegmatites of the whole area under consideration.

In some aplites and pegmaties, the K-feldspar contents increase much more than the albite. In these aplites and pegmatites the dominance of K-phase could be explained due to K-enrichment with further decrease in $P(H_2O)$ and temperature of the interior-marginal zone. This sort of K-enrichment is very difficult to explain by K-metasomatism as no where K-phase has been noticed replacing Na-phase. Moreover in a highly K-rich feldspar bearing aplites both albite and K-feldspar are untwined or the latter is faintly twinned in some grains, that hardly an idea of twinning could be postulated (staining technique was used to differentiate

20

the K-phase from the Na-phase in the thin sections).

The albite microcline and microcline albite aplites and pegmatites are ptygmatically folded and sometimes do show pinch and swell structure. The host granitic rocks are similarly folded ptygmatically. These aplites and pegmatites are folded ptygmatically as envisaged by Ramberg (1956) due to one or two dimensional compression of the plastic host rocks and consequent folding of the less plastic aplites and pegmatites. The pinch and swell structure is also visible in the same area where ptygmatic pegmatites are absent. This shows that with compression ptygmatic bodies were formed and with tension pinch and swell structure was observed in the pegmatites.

Origin of the Major Pegmatites Including the Zoned Bodies.

In the above those aplites and pegmatites have been described which were formed immediately after the crystallization of the sodic bodies and they were derived from the poorly aqueous silicate melt and do not fully represent all the stages of development of the pegmatites including pneumatolytic and hydrother-mal stages.

As was envisaged in the preceding discussion, that a sodic magma came into being during the last phase of the consolidation of granitic rocks. This sodic magma was enriched with soda-potash phase gradually and with its upward movement in the batholith. With subsequent increase in height the true pegmatitic rest magma started coming into being near marginal and marginal exterior zones having almost all the properties of a rest magma, becoming richer in aqueous fluids in association with silicate melt. This thing is again emphasized that the rest-liquids, derived in the present studies, are not directly related with the granitic magma as is schematically illustrated by Jahns and Burnham (1969). Anyhow a gradual uprise was from albitites to simple pegmatite involving the introduction of K-phase and some aqueous fluids. Therefore, as the melt cools and the system becomes saturated gradually with water a free aqueous phase would begin to separate as scattered units of submicroscopic size doubtless unevenly distributed through the melt if the thermal and compositional inhomogeneities were present (Jahns and Burnham, 1969). This phase probably would accumulate as thin films along the crystal-melt interfaces. Discrete bubbles may also be expected in the earlier stages and will increase in number and size. With a density considerably less than that of the silicate melt, the aqueous phase could migrate slowly upward through the crystal-bearing liquid.

Systematic thermal gradients are thought to be present in these cooling igneous bodies and in pegmatite forming systems (Jahns and Burnham, 1969) they would have been responsible for compositional gradients in the aqueous phase. The compositional variations of temperature dependent have been determined experimentally for feldspar bearing natural and synthetic system by Orville (1963) and Jahns and Burnham (1969). Therefore, they regard the aqueous stage that which separate from a cooling and crystallizing pegmatite magma as a powerful moving agent and transporting medium because it can extract portion of various constituents from the much more viscous (sodic) melt and it can serve as an avenue for ready movement of these constituents from one part of the system (sodic) to another (sodic-potassic to potassic-aqeous system).

The unzoned pegmatites could have developed from the rest magmatic melt with low aqueous fluids at high thermal gradient and low confining pressure. In these bodies the border zone is usually richer in albite, microcline and quartz etc. and gradually enriches in microcline and quartz $\pm$ albite. The occurrence of muscovite, tourmaline, beryl etc. depends on the amount of aqueous phase and volatiles available. With increasing amount of aqueous fluids available, the growth of crystals becomes larger due to physical segregation of the growing crystalline phases and the reaction between crystalline and fluids phases. The fine or medium grained texture of the border zone observed in the numerous unzoned pegmatites of the area can be attributed to the loss of the water during the crystallization, in such situations the water having migrated into the enclosing country rocks.

Landes (1933) and Derry (1931) regard simple pegmatites as due to magmatic crystallization and complex pegmatites as essential products of strong subsequent pneumatolytic and hydrothermal replacement while Jahns (1955) regards magmatic crystallization as of primary importance and subsequent replacement as trivial in the formation of the complex pegmatites. The views of Quensel (1955) and Varlamoff (1946) lie in between the two different ideas. According to Nawaz (1967) none of the views are universally applicable and that each of the case ought to be judged on its own merits. He regards, in the case of Meldon aplite, the complex pegmatites as product of direct crystallization from a melt and regarded simple pegmatites as derivatives of the complex pegmatites by

a decrease in fluorine and water, which may also results in suppression of zonal structure. Jahns and Burnham (1969) think that the reaction between crystals and silicate melt would be expected to continue after the appearance of a free aqueous phase in the system and the reaction will be more vigorous between crystals and aqueous fluids and attendant replacement phenomena may be more rapid and extensive. According to London (1992) typical granite to pegmatite is transition of texture that the pegmatitic grain size marks the point of aqueous vapour (over) saturation to magma. Those actions of an aqueous vapour phase together with silicate melt make pegmatites as opposed to granite.

Some of the pegmatites of the area show magmatic and pegmatitic stages of their development (Fig. 8). In those bodies the development of succeeding pneumatolytic and hydrothermal stages have played a very minor role. In those pegmatites the formation of different zones is quite clear. Worth mentioning are the zoned pegmatites of Jabba, Batgram, Bahishti, Bagarian village and Balhag. In these bodies the development of different zones is quite clear and compositionally different zonal distribution is due to the availability of the pegmatitic type material in those very places where they crystallized. In the complex pegmatites, following stages have been observed pegmatitic, pneumatolytic and hydrothermal and are elaborated as regards their occurrence and position in the bodies.

The pegmatitic stage is the initial zonal consolidation of the pegmatite in a closed system. Marked segregation on the scale of individual crystal group is extended to larger and larger domains with increasing general migration of the nourishing constituents through the aqueous phase to some preferred parts of the system prior to precipitation. Much of the coarse-grained quartz in pegmatites represented through the aqueous phase of silica, that was not being fixed in feldspars and micas, and therefore, formed graphic intergrowth with K-feldspars (in Bagarian, Batgram and some other pegmatites) and with Na-feldspar (in the Balhag pegmatite). The quartz has also been found to occur interstitially among the large crystals of feldspar. The quartz also formed enormous aggregates completely separate in most zoned pegmatites and partially in a few of them (in the Chail Sar pegmatites). This showed that segregation increased in scale with progressive consolidation of the pegmatite body. In this way different zones were constituted that is a most conspicuous feature of granitic pegmatites for common development of sharply bounded internal mineralogical zones (London, 1992),

(a) the border zone (b) the wall zone (c) the outer intermediate and inner intermediate zones (d) the core which denote the sequence of consolidation from the wall inwards. The zonal sequence of the pegmatites fit into some of the types of Turner and Verhoogen (1960).

The border and wall zones are inconspicuously developed in most cases. They are rarely developed in simple zoned pegmatites. In most complex zoned pegmatites these are higher temperature zones than the succeeding zones because the mineral assemblage is usually of albite or oligoclase, whereas, generally in the intermediate zone the dominant mineral is microcline. The occurrence of muscovite, microcline and tourmaline in some pegmatites is due to replacement, as that sometimes the crystals there attain dimensions extraneous of the wall zone in general but characteristic of the sequent intermediate zone.

The intermediate zones are developed intermediate between wall zone the core. They could be divided into outer intermediate and inner intermediate zones (Quensel, 1955). The essential mineral in the outer intermediate zone of the simple zoned pegmatites are albite-quartz-muscovite with microcline or graphic granite sometimes. The essential minerals in the outer intermediate zone of the complex zoned pegmatite are microcline with minor quartz, muscovite, etc. This shows that the simple pegmatites represent higher temperature outer intermediate zone as it has albite (slightly more calcic than the albite in the interior zones) and graphic granite (Barth, 1965 and Brotzen, 1959). In the inner intermediate zone of the simple pegmatites the essential minerals are albite-quartz-muscovite with comparatively higher percentage of microcline than the outer zone. While in the complex pegmaties microcline is again the essential and major mineral. This shows that the inner zone might have developed at lower temperature. Due to decreasing temperature and in closed system environments the crystal size increases extensively from wall inward. The Rb content also increases in this zone in the microcline from the wall zone towards the core (Table - 3).

The core generally represents the ultimate stage of consolidation of zonal pegmatites (Quensel, 1955). In most pegmatites the core consists of only pure quartz. The core, in most of the pegmatites is centrally located. It might have crystallized at about 300°C as found out by Babu (1970) who correlated his work with that of Fersman (1960).

The pneumatolytic stage: It will be used here to denote the phases of replacement which follows the zonal

consolidation of the pegmatitic stage. The pneumatolitic activity displays successive depositions, replacing pre-existing mineral assemblage and depositing new minerals in stead. The phases of such replacement are signified as replacement units. This replacement in most of the simple zoned pegmatites is minor but is well marked to very extensive in the complex zoned pegmatites e.g., Bagarian, Rajdhwari, Chail Sar and Baleja.

The high temperature phase is represented by development of beryl in many pegmatites. In the Hawagali pegmatites only beryl is a mineral being formed as a replacement unit between core and intermediate zone cross-cutting a part of both the zones. But in many other pegmatites the black tourmaline, beryl, columbite/tantalite, Rb microcline, Li-muscovite, fuschitic muscovite replace mostly quartz and feldspars or form as miarolite deposits.

The lower temperature phase - the solutions of this unit are found to traverse and replace all earlier consolidated mineral assemblages (Quensel, 1955). The minerals in this replacement unit are not represented in the earlier zones or units. The dominant mineral of this unit is cleavelandite. It is most extensively developed in the Dadar pegmatites (Ashraf and Chaudhry, 1974a). In one of the pegmatites the replacement of the zones is so extensive that only remnants of the primary zonation is present. In Chail pegmatites it replaces microcline in the intermediate zone of the pegmatite where relict microcline is still present. It also replaces beryl in Dadar pegmatites. Muscovite is also developing within this phase as pods.

The hydrothermal stage: It is represented by last phase of activity in connection with paragenetic deposition of the pegmatites (Quensel, 1955). The most pronounced minerals belonging to this stage are quartz, kaolinite and sericite. The latter minerals are generally developed as an alteration product of feldspars, columbite and beryl under higher thermal activity. The development of kaolinite is on the surface of most of the feldspar grains. The sericite develops along the weak zones. The hydrothermal stage on minor scale throughout is found all in the acid minor bodies.

CONCLUSIONS

(1) The Mansehra granitic complex was produced by extensive partial melting of Hazara Formation and a lower part of the Tanol Formation (which are dominantly pelitic in nature) rather than in situ granitization and migmatization.

(2) The composition of most parts of Mansehra granitic complex is biotite rich with minor muscovite along with other granite minerals, suggest that a partial melting of about 40% of the Hazara Formation and of Lower Tanol Formation was involved for such a complex.

(3) The acid minor bodies (AMB) i.e., (i) albitites, (ii) albite - aplites / pegmatites, (iii) albite - (microcline) - aplites / pegmatites, (iv) albite - microcline - aplites / pegmatites, (v) microcline - albite - aplites / pegmatites and (vi) complex - aplites / pegmatites are rocks evolved from Mansehra granites.

(4) The assciations of the above AMB is with Mansehra granites and enclosing metasediments and the mineralogical & chemical evidences suggest that AMB type groups i to iv occur in interior - lateral zone (upto 1675 m above sea level), type groups iv and v occur in interior - marginal (zone (1525 to 2750 m) and type group v and vi ar present in both interior - marginal and marginal - exterior zone (above 2750 m).

(5) Sodic magma was evolved at high $P(H_2O)$ more than 10 Kb which with gradual cooling and upwelling of the Mansehra granitic complex gave rise albitite and with decreasing $P(H_2O)$ gradually produced type groups ii to vi given above in 3.

(6) Complex pegmatites like Bagarian are the most evolved rocks mineralgically and chemically forming complete zones like border + well zones, outer and inner intermediate zones, pneumatolytic miarotitic stage and hydrothermal stage.

(7) Economically important rocks are the albitites whereas the pegmatitic very pure minerals are microcline and quartz; and pneumatolytic minerals are ores of beryl (Be ore), columbite (Nb-Ta ore) & samarskite (U ore). High Sn values from 200-500 ppm suggest that Sn can be found in most evolved pegmatites at highest contour level in the true exterior structural zone.

ACKNOWLEDGEMENTS

Dr. M. Nawaz Chaudhry and F. A. Shams for all sorts of discussions, help and introduction to the project. The help of locals of Mansehra cannot be neglected far localting AMB and hospitality. Prof. S. R. Nockold and Mr. Allen of Cambridge University are acknowledged for analysing trace elements.

REFERENCES

Anderson, G.H., (1937). Granitization, albitization and related phenomena in the northern Inyo Range of California-Neveda. *Bull. Geol. Soc. Amer.,* Vol. 48, pp. 1- .

Ashraf, M., (1983). Geochemistry of acid minor bodies associated with the Hazara granitic complex, Hazara Himalayas, Northern Pakistan. In: granites of Himalayas, Karakorum and Hindukush (F.A. Shams, ed). *Inst. Geol. Punjab Univ.* Spec, publication, pp. 123-141.

Ashraf, M., (1975). Composite albitite - aplite and pegmatite from Mansehra and Batgram area, Hazara District, Pakistan. Spec Issue IMA Papers, 9th meeting Berlin, *Fortschr. Miner.* Vol. 52, pp. 329-344.

Ashraf, M., (1974). Geochemistry and petrogenesis of acid minor bodies of Mansehra and Batgram area, Hazara District. *Ph.D. thesis Punjab Univ. Lahore, Pakistan.*

Ashraf, M., (1974a). Geology and petrology of acid minor bodies from Mansehra and Batgram area, District Hazara Pakistan. *Geol. Bull. Punjab Univ. Lahore,* Vol. 11, pp. 81-88.

Ashraf, M., (1974b). Geochemistry and petrogenesis of albitites from Mansehra and Batgram area, Hazara District, Pakistan. *Geol. Bull. Punjab Univ. Lahore,* Vol. 11, p. 97.

Ashraf, M., and Chaudhry, M.N., (1974). Geology of Dadar pegmatites, Mansehra area, Hazara District. *Geol. Bull. Punjab Univ. Lahore,* Vol. 10, pp. 59-66.

Ashraf, M., and Chaudhry, M.N., (1976). Geology and classification of acid minor bodies of Mansehra and Batgram area, Hazara Division, Pakistan. *Geol. Bull. Punjab, Univ. Lahore,* Vol. 12, pp. 1-16.

Ashraf, M., and Chaudhry, M.N., (1976a). Origin of chess-board albite present in the acid minor bodies of Mansehra and Batgram area, Hazara Division, Pakistan. *Geol. Bull. Punjab, Univ. Lahore,* Vol. 13, pp. 93-98.

Baig, M.S., (1991). Geochronology of pre-Himalayan and Himalayan tectonic events, northwest Himalaya Pakistan. *Kashmir Jour. Geol.,* Vol. 8 & 9, pp. 197.

Baig, M.S., Snee, L.W., LaFortune, R.J. and Lawrence, R.D., (1989). Timing of pre-Himalayan oregenic events in the Northwest Himalaya, $^{40}Ar/^{39}Ar$ constraints. *Kashmir Jour. Geol.,* Vol. 6 & 7, pp. 29-40.

Barth, T.F.W., (1965). Aspects of the orystallization of quartzofeldspathic plutonic rocks. *Tsch. Min. Petr. Mitt.,* Vol. 11, (3-4), pp. 210- .

Babu, V.R.R.M., (1969). Temperature of formation of pegmatites of Nellore Mica Belt, Andhra Pradesh, India. *Econ. Geol.,* Vol. 64, pp. 66.

Bouguslavskiy, I.S., Kaleno, A.D., and Egel, L.Y., (1965). The metasomatic albitite found for the first time in the MPR. *Doklady Akademii Nauk SSSR.,* Vol. 168 (5), pp. 1154.

Booth, B., (1967). Land's end granite and their relation to the experimental granite system. *Nature.,* March 4. p. 869.

Bowen, N.L., (1937). Recent high temperature research on silicates and its significance in igneous geology. *Amer. Jour. Sci., 5th Ser.,* Vol. 33, pp. 1- .

Brammall, A., (1933). Syntaxis and differentiation. *Geol. Mag.,* Vol. 70, pp. 97- .

Brotzen, O., (1959). Outline of mineralization in zoned granitic pegmatites. *Geol. Foren. Stockholm Forth.,* Vol. 81, pp. 98- .

Brunham, C.W., and Jahns, R.H., (1961). Experimental studies of pegmatite genesis. The composition of pegmatite fluids (abstract). *Geol. Soc. Amer., Special paper.,* Vol. 68, pp. 143.

Burnham, C.W., and Jahns, R.H., (1962). A method for determining the solubility of water in silicate melts. *Amer. Jour. Sci.,* Vol. 260, pp. 721- .

Cerny, P., (1982). Petrogenesis of granite pegmatites. In: Grnaitic pegmatites in science and industry (P. Cerny, ed.). *Mineral. Assoc. Can., short Course Hand Book,* Vol. 8, pp. 405-461.

Cerny, P., Trueman, D.I., Ziehlke, D.V., Goad, P.E. and Paul, B.J., (1981). The cat Lake-Winnipeg River and Wekusho Lake pegmatite fields, Monitoba. *Man. Mineral. Res. Div., Geol. Rep.* ER 80-1.

Derry, D.R., (1931). The genetic relationship of pegmatites, aplites and tin veins. *Geol. Mag.,* Vol. 8, pp. 454- .

Dewitt, E., Redden, J.A, Wilsen, A.B., and Buscher, D., (1986). Minerla resource potential and geology of the Black Hills National Forest, South Dakota and Wyoming. *U.S. Geol. Surv. Bull.* No. 1580.

Duke, E.F., Papike, J.J., and Laul, J.C., (1992). Geochemistry of a boron-rich peraluminous granite pluton. The Clamity Peak layered granite-pegmatite complex, Black Hills, South Dakot. *Canadian Mineral.,* Vol. 30, pp. 811-833.

Duke, E.F., Shearer, C.K., Redden, J.A., and Papike,

JJ., (1990). Proterozoic granite-pegmatite magmatism, Block Hills, South Dakota: structure and geochemical zonation. In: The Early Proterozoic Trans-Hudson Oregon of N. America (J.W. Lewry & M.R. Stauffer, eds). *Geol. Assoc. Canada, Spec., Pap,* Vol. 37, pp. 253-269.

Fersman, A.E., (1060). Collected works of A.E. Fersman, VI. Pegmatite (in Russian). *Acad. Sci., U.S.S.R., Moscow 742.*

Galbreath, K.C., Duke, E.F., Papike, J.J. and Laul, J.C., (1987). Mass transfer during wall rock alteration: an exmaple from a quartz-graphite vein, Black Hills, South Dakota. *Geochem. Cosmochim. Acta,* Vol. 52, pp. 1905-1918.

Ghazanfar, M., Baig, M.S., and Chaudhry, M.N., (1983). Geology of Tithwal - Kel area, Neelum Valley, Azad Jammu & Kashmir. *Kashmir Jour. Geol.* Vol. 1, pp. 1-10.

Gladyshevskaya, N.N., Sakhatskiy, I.I., Safronov, I.L., and Skarzhinskiy, V.I., (1966). Albitite form Bantyshevo station area of the Donets Basin. *Doklady Akademii Nauk SSSR.* Vol. 167 (3), pp. 663.

Goldin, B.A., (1965). Magnetite-sphalerite albitite in the Pechora Urals. *Doklady Akademii Nauk SSSR,* Vol. 162 (3), pp. 662.

Hall A., (1972). Regional geochemical variation in the Caledonian and Variscan granites of Western Europe. 24th IGC, pp. 171.

Hall, A., (1973). Geochemical control of granite compositions in the Variscan Orogenic belt. *Nature Phy. Sci.,* Vol 242 (118), pp. 72.

Heinrich, E.W., (1953). Zoning in pegmatite districts. *Amer. Mineral.,* Vol. 38, pp. 68- .

Heinrich, E.W., (1965). Composite-aplite pegmatites of the Frnakalin-Sylva district, North Carolina. *Amer. Mineral.,* Vol. 50, pp. 1681.

Jahns, R.H., (1955). The study of pegmatites. *Econ. Geol., 50th anniversary.* Vol. pp. 1025-1130.

Jahns, R.H., and Tuttle, O.F., (1963). Layered pegmatite-aplite intrusives. *Mineral. Soc. Amer., Special Paper I.,* pp. 78- .

Jahns, R.H., and Burnham, C.W., (1969). Experimental studies of pegmatite genesis: I. A model for the derivation and crystallization of granitic pegmatites. *Econ. Geol.,* Vol. 64, pp. 843- .

Joplin, G.A., (1957). On the association of albitites and soda-aplites with potash granites in the Precambrian and old Paleozoic of Australia. *Jour. Proc. Royal Soc. N.S. Wales.,* Vol. 90, pp. 80- .

Landes, K.K., (1933). Origin and classification of pegmatites. *Amer. Mineral.,* Vol. 18, pp. 33-95.

Larsen, E.S., (1928). A hydrothermal origin of corundum and albitite bodies. *Econ. Geol.,* Vol. 23, pp. 398- .

LeFort, P., Debon, F., and Sonet J., (1980). The lesser Himalayan cordierite granite belt, typology and age of pluton of Mansehra, Pakistan. *Geol. Bull. Peshawar Univ.,* Vol. 13, pp. 51-61.

Leonardos, O.H.Jr., and Fyfe, W.S., (1966). Serpentinite and associated albitites Maccasin quadrangle California. *Amer. Jour. Sci.,* Vol. 265, pp. 609- .

London, D., (1992). The applicatoin of experiemental petrology to the genesis and crystalization of granitic pegmatites. *Canadian Mineral.* Vol. 30, pp. 499-540.

London, D., (1986). Internal differentiation of rare element pegmatites, effects of boron, phosphorous, and fluourine. *Geochem. Cosmochim Acta,* Vo.. 51, pp. 403-420.

Luth, W.C., Jahns, R.H., and Tuttle, O.F., (1964). The granite system at pressure of 4 to 10 Kilobars. *Jour. Geophys. Res.,* Vol. 69, pp. 759- .

Manning, D.A.C., and Pichavant, M., (1985). Volatiles and their bearing on the behaviour of metals in granitic systems. In: Granite - related mineral deposits - geology, petrogenesis, and tectonic setting (R.P. Taylor & D.F. Storng, eds.. *Canadian Inst. Min. Metall.,* Extended Asbstract., pp. 184-187.

Manning, D.A.C., Hamilton, D.L., Henderson, C. M.B., and Dempsey, M.J., (1980). The probable occurrence of interstitial Al in hydrous, F-bearing and F-free aluminosilicate melts. *Contrib. Mineral Petrol.* Vol. 75, pp. 1351-1358.

McBirney, A.R., (1984). Igneous Petrology. Freeman, Cooper and Company, San Francisco, California.

Miguel, A.S., (1969). The aplite-pegmatite association and its petrogenetic interpretatoin. *Lithos,* Vol. 2, pp. 25- .

Miller, C., (1985). Arc peraluminous magmas derived from pelitic sedimentary source. *Jour. Geol.,* Vol. 93, pp. 673-689.

Nawaz, M., (1967). The mineralogy and geochemistry of the Meldon aplite Devonshire, and associated rocks. *Ph.D. thesis London University.*

Norton, J.J., Page, L.R., and Probst, D.A., (1962). Geology of the Hugo pegmatite, Keystone, South Dakota. *U.S. Geol. Surv. Prof. Pap.,* Vol. 267-B, pp. 49- .

Orville, P.M., (1963). Alkali ion exchange between vapour and feldspar phases. *Amer. Jour. Sci,* Vol. 26, pp. 201- .

Orville, P.M., (1960). Petrology of several pegmatites in the Keystone District, Black Hills, South Dakota.

Bull. Geol. Soc. Amer., Vol. 71, pp. 1467- .

Pitchavant, M., (1987). Effect of B and H_2O on liquidus phase relations in the haplogranite system at 1 Kbar. *Amer. Mineral.,* Vol. 72, pp. 1056-1070.

Quensel, P., (1955). The paragenesis of the Varutrask pegmatite. *Arkiv. Mineralogi, Och. Geologi. Stockholm,* Vol. 2, (2) pp. 9- .

Ramberg, H., (1956). Pegmatites in west Greenland. *Bull. Geol. Soc. Amer.,* Vol. 67, pp. 185- .

Redden, J.A., (1968). Geology of the Berne quardrangle, Black Hills, South Dakota. *U.S. Geol. Surv. Profess. Paper,* No. 297.

Rockhold, J.r., Nabelek, P.I., and Glascock, M.D., (1987). Origin of rhythmic layering in the Calamity Peak satellite pluton of the Harney Peak granite, South Dakota: the role of boron. *Geochem. Cosmochim Acta,* Vol. 51, pp. 487-496.

Shams, F.A., (1983). Granites of the NW Himalays in Pakistan. In: Granites of Himalayas Karakorum and HIndukush (F.A. Shams, ed). *Inst. Geol. Punjab, Univ. Spec. Publication,* pp. 75-121.

Shams, F.A,, (1967). Granites of the Mansehra-Amb State area and the associated metamorphic rocks. *Ph.D. thesis Punjab University, Lahore.*

Shams, F.A,, (1969). Geology of the Mansehra-Amb State area Northern West Pakistan. *Geol. Bull. Punjab, Univ.,* Vol. 8, pp. 1- .

Shams, F.A., and Rehma, F.U., (1966). The petrochemistry of the granitic comp;lex of the Mansehra-Amb State area Northern West Pakistan. *Jour. Sci. Res. Punjab, Univ,* Vol. 1, pp. 47- .

Shearer, C.K., Papike, J.J. and Jolliff, B.L., (1992). Petrogenetic links among granites and pegmatites in the Harney Peak rare-element granite-pegmatite system, Black Hills, South Dakota. *Canadian Mineral.,* Vol. 30, pp. 785-809.

Shearer, C.K., Papike, J.J., Simon, S.B., Walker, R.J., and Laul, J.C., (1987). Origin of pegmatitic granite segregations, Willow Creek, Black Hills, South Dakota. *Canadian Mineral.,* Vol. 25, pp. 159-171.

Shearer, C.K., Papike, J.J., Simon, S.B., and Laul, J.C., (1986). Pegmatite-wall -rock interactions, Black Hills, South Dakota: Interactions between pegmatite derived fluids and quartz-mica schist wall rock. *Amer. Mineral.,* Vol. 71, pp. 518-539.

Simpson, E.S.W., (1954). On the graphical representation of differentiation trends in igneous rocks. *Geol. Mag.,* Vol. 91, pp. 233- .

Sinclair, W.D., and Richardson, J.M., (1992). Quartz-tourmaline orbicules in Seagull bathobith, Yukon Territory. *Canadian Mineral.,* Vol. 30, pp. 923-935.

Spera, F.J., (1980). Aspects of magma transport. In: Physics of magmatic processes (R.B. Harqraves, ed.). Princeton University Press, New Jersey, pp. 265-324.

Thomson, A.B., (1982). Dehydration melting of pelitic rocks and the generation of H_2O - undersaturated granitic liquids. *Amer. Jour. Sci.,* Vol. 282, pp. 1567-1595.

Turner, F.W., and Verhoogen, J., (1960). Igneous and Metamorphic Petrology. McGraw-Hill, Book Co. New York.

Tuttle, O.F., and Bown, N.L., (1958). Origin of granite in the light of experimental studies in the system $NaAlSi_3O_8$ - SiO_2 - H_2O. *Geol. Soc. Amer. Mem.,* Vol. 74, pp. 153- .

Tuzinski, P., 1983). Rare alkali halos (Li, Rb. Cs) surrounding the Bob Iggersoll lithium pegmatite mine in Keystonec, Black HIlls, South Dakota. *M.S. Thesis, Ohio State Univ., Columbus, Ohio.*

Varlamoff, H., (1946) La repartition de la mineralisation d'apres la clef geochemique de Fersman, *Soc. Geol. Belgique Annals,* Vol. 70, pp. 108-

Walker, F., (1932). An albitite from Ve Skerries Shetland Isles. *Min. Mag.,* Vol. 23, pp. 239- .

Windley, B., and Bridgewater, D., (1965). The layered aplite-pegmatite sheets of Kinalik, South Greenland. Medd. om Gronland, Vol. 179, Nr. 10.

Winkler, H.G.F., and Von Platen, H., (1961). Experiment elle gesteinmena-morphose. V. Experimentelle anatektische schemizen nnd ihre petrogenetische Bedutung. *Geochim. Cosmochim. Acta,* Vol. 24, pp. 250.

GEOLOGY AND GEOCHEMISTRY OF INDIAN PLATE ROCKS SOUTH OF THE INDUS SUTURE ZONE, BESHAM AREA, NORTHWEST HIMALAYA, PAKISTAN

By

J. R. LA FORTUNE*, L. W. SNEE** & M. S. BAIG***

*Geosciences Department, Oregon State University, Corvallis, Or, 97331, U.S.A.
**U.S. Geological Survey, Denver Federal Center, M.S. 905, Box 25046, Denver, Co, 80225, U.S.A.
***Institute of Geology, University of Azad Jammu and Kashmir, Muzaffarabad, Pakistan.

ABSTRACT: *The Himalayan mountains are the geologic manifestation of continental collision, and in northern Pakistan the Main Mantle Thrust (MMT) is a major suture along which the collision occurred. The basement rocks near Besham village in southern Kohistan, adjacent to the MMT, are bounded on the east and west by north-trending high-angle faults. These basement rocks that are significantly different from any of the other plutonic and metamorphic rocks of southern Kohistan and that are not seen elsewhere in the Pakistan Himalaya west of the Nanga Parbat-Haramosh massif (NPHM).*

Rocks of the Besham area are subdivided from oldest to youngest into five groups. The oldest rocks of the Besham area are; (1) the metasediments and heterogeneous gneisses of the Besham group. In conjunction with field evidence, major, trace and rare earth element analyses of Besham gneisses suggest that the quartzofeldspathic gneisses formed in situ from a sedimentary protolith. The presence of both quartzofeldspathic gneiss and sodic quartzofeldspathic gneiss in the Besham group may be attributable to variable protolith composition or more likely, the sodic gneiss was derived from intrusive protolith that was strongly transposed during deformation. These sodic gneisses are equivalent to the previously named Lahor granite. The Besham group was intruded by (2) mafic dikes that were subsequently metamorphosed to amphibolites. Geochemical data suggest that these tholeiitic dikes have island arc geochemical affinities. (3) The third group of rocks comprise cogenetic, small granitic intrusions and associated pegmatites; the Shang granite, the Dubair granodiorite and the Shorgara pegmatite. Unconformably lying upon these three units is (4) the Karora group, which comprises conglomeratic, calcareous and carbonaceous sedimentary rocks. The Karora group provides evidence for more than one metamorphic event in the Besham area, i.e., the Karora group is metamorphosed to lower greenschist facies, in contrast, the underlying Besham group is metamorphosed to epidote amphibolite facies. The youngest unit observed in the Besham area is (5) a relatively undeformed leucogranite that intrudes both the Karora group and the Besham group. The metamorphic and granitic rocks of the Besham area may be correlative with the basement rocks of the Nanga Parbat-Haramosh Massif. Specifically, the quartzofeldspathic gneisses of the Besham group may correlate with the Nanga Parabat gneisses, and the amphibolites found in the Besham area may correlate with mafic dikes of the massif. Further study of both the Besham area and the Nanga Parabat-Haramosh Massif can provide a better understanding of Precambrian basement rocks of northern Pakistan.

INTRODUCTION

The Himalayan mountains, which stretch from Pakistan in the west to Bhutan in the east is a southward-convex arc for 2400 km across south central Asia, are the geological manifestation of continental collision. This enormous mountain range formed largely in response to the collision of the northward-moving Indo-Pakistan plate with Asia beginning in the Paleocene and Eocene (Molnar and Tapponnier, 1975; Powell, 1979; Klootwijk et al., 1985). The seismic, geodetic and geologic evidence indicates that India continues to plow northward into Asia today at a rate of 4-5 mm/yr (Jacobs and Quittmeyer, 1979; Seeber et al., 1981; Molnar, 1986). The rocks of the Himalaya are more than a record of the collision between India and Asia; they also contain clues to the pre- and post-collisional history (Baig and Lawrence, 1987; Baig et al., 1988; Baig and Snee, 1989; Baig et al., 1989; Baig, 1990; Baig, 1991).

The suture along which India collided with Asian or Cimmerian microplates (Sengor, 1979) is known as the Indus-Tsangpo Suture Zone (ITSZ). In northern Pakistan, the ITSZ bifurcates into two major faults, which surround a mainy Cretaceous-Paleogene island arc terrain, the Kohistan-Ladakh arc. The northern branch is known as the Main Karakorum Thrust (MKT); the southern branch is the Main Mantle Thrust (MMT; Tahirkheli and Jan, 1979). The MMT, which was first recognized as a through going suture by Tahirkheli and Jan (1979), separates ultramafic and mafic oceanic rocks of the southern margin of Kohistan from gneisses, granites and metasediments of the northern margin of the Indo-Pakistan plate.

As the MKT and MMT resulted from the collision (and possible later adjustment) of India and Asia, tectonostratigraphic subdivisions of the northern margin of the Indo-Pakistan plate in northwest Pakistan also reflect this collision (Fig. 1; Tahirkheli and Jan, 1979; Yeats and Lawrence, 1984). From north to south, these subdivision are; (1) the southern Kohistan metamorphic and plutonic terrain, located adjacent to the MMT (Tahirkheli and Jan, 1979; Martin et al., 1962; Calkins et al., 1975), (2) the Hill Ranges, where shelf sediments on the northern margin of the Indian continent were thrusted south over the Potwar Plateau along the Main Boundary Thrust (MBT), which is late Tertiary (Yeats and Hussain, 1987) and (3) the Salt Range-Potwar Plateau molasse basin, where Late Cenozoic molasse is cut by active faults (Yeats et al., 1984).

A newly recognized basement of the Indo-Pakistan plate exists in southern Kohistan (Baig and Lawrence, 1987; Baig and Snee, 1989; Baig et al., 1989; Baig, 1990), adjacent to the MMT (Fig. 2). The north-trending high-angle Thakot and Puran faults bound the basement on the east and west respectively (Fig. 2; Baig and Lawrence, 1987; Baig and Snee, 1989; Baig et al., 1989; Baig, 1990). The fault on the east is shown in Fig. 2. The fault on the west is located 2 Km west of the western margin of Fig. 2.

The Besham area basement exposes basement crystalline gneisses unconformably under sedimentary rocks. Both this basement and its cover are significantly different from any of the other plutonic and metamorphic rocks of southern Kohistan. They are not seen elsewhere in the Pakistan Himalaya west of the Nanga Parabat-Haramosh Massif (NPHM). They may correspond to the older basement exposed in the massif.

The purpose of this study, therefore, is to geologically and geochemically characterize the basement near the village of Besham.

GEOLOGIC SETTING

The geology of the Besham area was generally outlined by Ashraf et al. (1980), Butt, (1983) and Fletcher et al. (1986) in geological studies of larger areas within the southern Kohistan metamorphic and plutonic terrain. All of these studies were primarily concerned with the origin and association of lead-zinc deposits in this region. Informal nomenclature for rock units of the Besham area was established in these earlier works, and the present study has confirmed the usefulness of some of these names. During this study the area west of Indus River, near the village of Besham has been mapped (Fig. 2).

The rocks of the Besham area generally can be subdivided from oldest to youngest into five groups. The oldest rocks, which were named the Besham group by Fletcher et al. (1986) are heterogeneous gneisses and metasediments. The sodic quartzofeldspathic gneisses of the Besham group of rocks have been named the Lahor granite by Ashraf et al. (1980). The second-oldest rocks are mafic dikes that intruded the Besham group and were metamorphosed to amphibolites. The third group of rocks includes cogenetic, small granitic intrusions and associated pegmatites. The Shang granite and Dubair granodiorite, previously named by Ashraf et al. (1980), who considered them to be late-

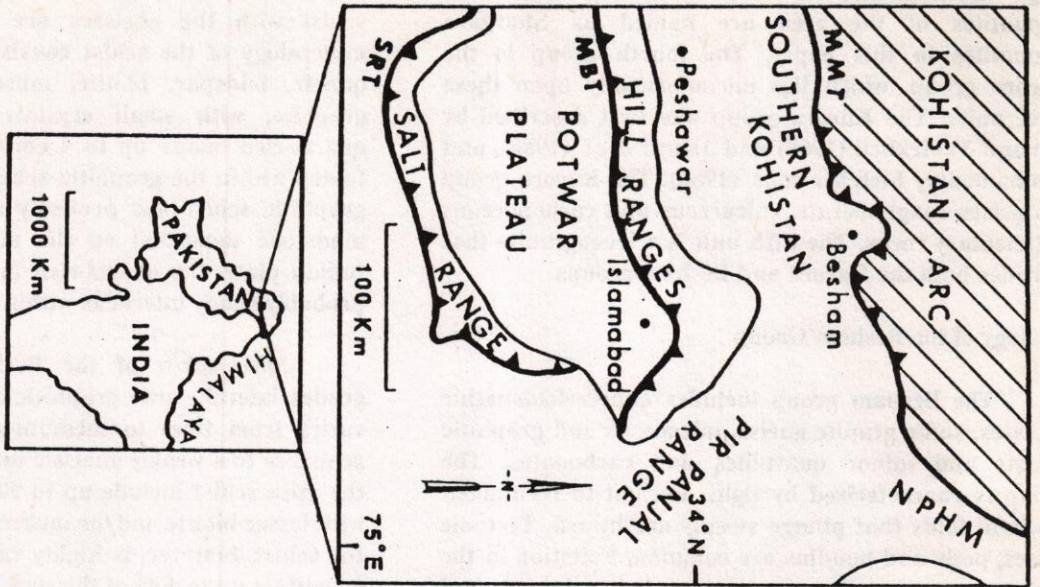Fig. 1. Tectonic subdivisions of northern Pakistan. MMT = Main Mantle Thrust, NPHM = Nanga Parbat-Haramosh Massif, MBT = Main Boundary Thrust, SRT = Salt Range Thrust.

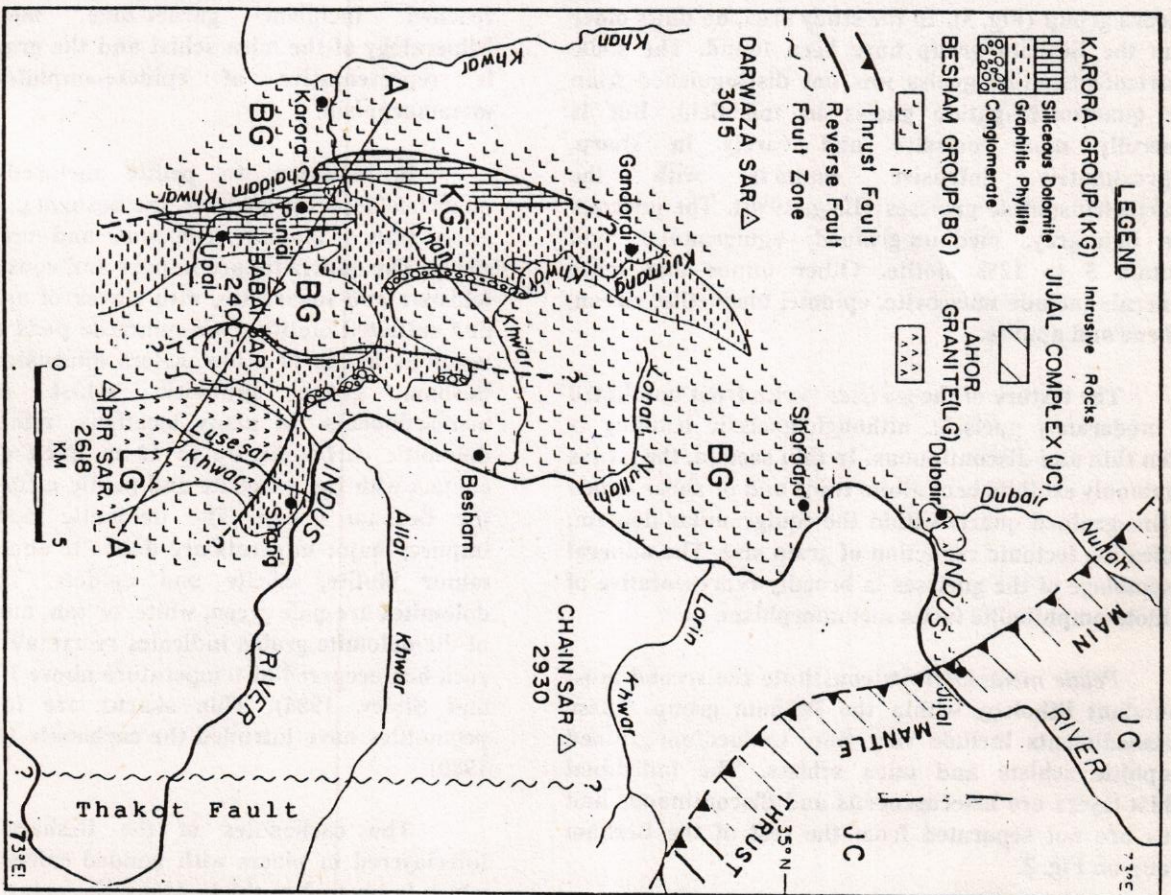Fig. 2. Geologic map of the Besham area, northern Pakistan.

LEGEND

KARORA GROUP (KG)
- Siliceous Dolomite
- Graphitic Phyllite
- Conglomerate

BESHAM GROUP (BG)

JIJAL COMPLEX (JC)

LAHOR GRANITE (LG)

Intrusive Rocks

Thrust Fault
Reverse Fault
Fault Zone

stage differentiates of the Lahor granite. The pegmatites of the area are named as Shorgara pegmatites in this paper. The fourth group is the Karora group, which lies unconformably upon these three units. The Karora group was first described by Jan and Tahirkheli (1969) and Ashraf *et al.* (1980), and was named by Fletcher *et al.* (1986). The Karora group comprises conglomerate, calcareous and carbonaceous sedimentary rocks. The fifth unit is a leucogranite that intrudes both the Karora and Besham groups.

Geology of the Besham Group

The Besham group includes quartzofeldspathic gneisses, sodic granite gneiss, micaceous and graphitic schists and minor quartzites and carbonates. The group is characterized by tight, upright to recumbent isoclinal folds that plunge steeply northward. Tectonic lenses, pods and boudins are common. Foliation in the Besham group strikes predominantly northward, and dips steeply west or east. All units in the Besham group were intruded by the Shang granite or Dubair granodiorite and are unconformably overlain by the Karora group (Fig. 3). In the study area, no units older than the Besham group have been found. The sodic quartzofeldspathic gneiss was not distinguished from the quartzofeldspathic gneiss in the field. But is generally more massive and rarely in sharp, approximately intrusive contacts with the quartzofeldspathic gneisses (Baig, 1990). The gneisses are light-grey, medium-grained, equigranular and contain 5 to 12% biotite. Other minor and trace minerals include muscovite, epidote, magnetite, zircon, sphene and apatite.

The texture of the *gneisses* varies from unfoliated to moderately gneissic, although gneissic banding is often thin and discontinuous. In thin section, the gneiss commonly exhibits bent albite twins and or shear bands of fine-grained quartz within the equigranular domain, indicating tectonic reduction of grain size. The mineral assemblage of the gneisses is broadly representative of epidote-amphibolite facies metamorphism.

Pelitic metasediments constitute the second most abundant lithology within the Besham group. These metasediments include very fine- to medium-grained graphitic schists and mica schists. The individual schist layers are heterogeneous and discontinuous and thus are not separated from the rest of the Besham group on Fig. 2.

Highly sulfurous *graphitic schist* within the Besham group occurs as laterally discontinuous layers and pods up to 30 m thick. Contacts of the graphitic schist with the gneisses are generally sharp. The mineralogy of the schist consists of very fine-grained quartz, feldspar, biotite, muscovite and 4 to 10% graphite, with small crystals of pyrite. Abundant quartz-rich bands up to 4 cm thick are ptygmatically folded within the graphitic schist. The protolith of the graphitic schist was probably an anoxic marine silty mudstone deposited on the northern margin of the Indian plate; the quartz-rich layers in the schist were probably sandy interbeds within the clay-rich muds.

Mica schist of the Besham group commonly grades laterally into graphitic schist. The mica schist varies from fine- to medium-grained, and from the schistose to a weakly gneissic fabric. Major minerals in the mica schist include up to 90% quartz and feldspar, with lesser biotite and/or muscovite. Mineral content of the schist, however, is highly variable, and biotite may constitute up to 40% of the rock. Zircon, apatite, sphene and graphite are typical accessory minerals. A trace of garnet may be present, and garnet is commonly intergrown with biotite, suggesting that the rock reached incipient garnet-zone metamorphism. Mineralogy of the mica schist and the graphitic schist is representative of epidote-amphibolite facies metamorphism.

In addition to pelitic metasediments and quartzofeldspathic gneisses, the Besham group includes *minor beds of quartzite, carbonate* and *rare calc-silicate gneiss.* The quartzites are impure and consist of quartz, feldspar and muscovite, with traces of sphene, zircon and rutilated biotite. Pure quartzite pods uncommonly occur as lenses of a few meters dimension within the Besham group graphitic schist and pelitic metasediments. In many locations, minor lenses of dolomitic carbonate up to 10 m thick are in sharp contact with the quartzite and pelitic metasediments of the Besham group. The dolomitic carbonates are impure; major minerals are dolomite and quartz, with minor biotite, calcite and epidote. The siliceous dolomites are pale green, white, or tan, and the texture of the dolomite grains indicates recrystallization of the rock has occurred at temperature above 100° C (Gregg and Sibley, 1984). Thin skarns are formed where pegmatites have intruded the carbonate (Ashraf *et al.,* 1980).

The carbonates of the Besham group are interlayered in places with banded calc-silicate gneiss which is up to 2 m thick. Along Kurmang Khwar (Fig. 2), the calc-silicate gneiss consists of bands of coarse-grained actinolite up to 30 cm thick that alternate with
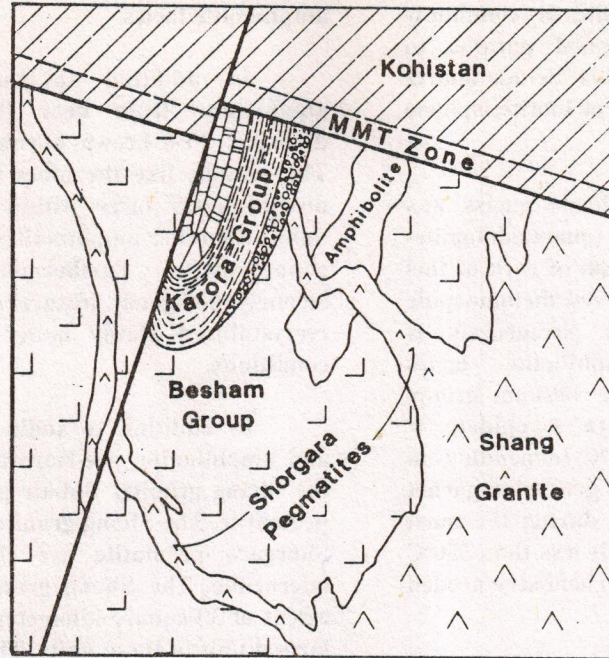
Fig. 3. Stylized sketch of surface geology demonstrating cross-cutting relationships in the Besham area. No scale is implied.
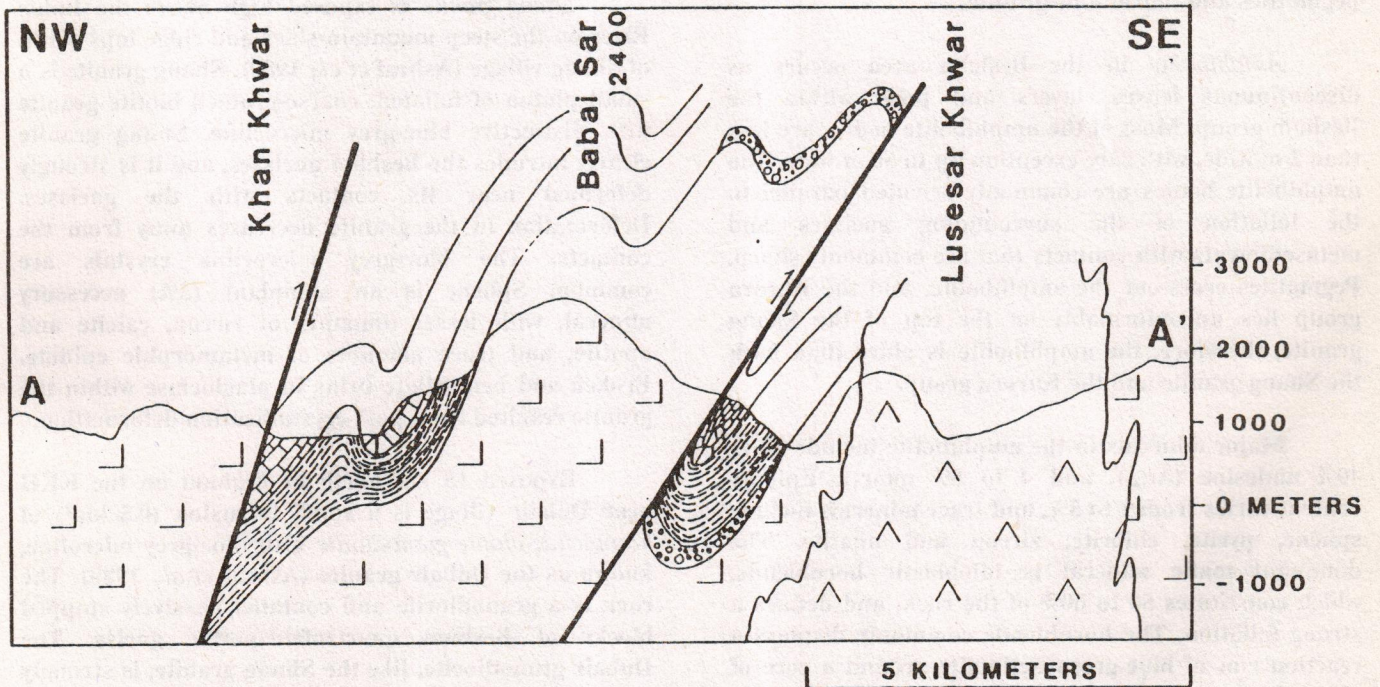

Fig. 4. Geologic cross-section of the Besham area along A-A'. For identification of symbols, see Figure 2.

31

felsic bands. The contact between the felsic bands and the darker actinolite-rich bands is marked by a 2 mm thick band of epidote. The actinolite is commonly poikiloblastic and only weakly aligned parallel to gneissic layering. Other major minerals include quartz and plagioclase, with trace amounts of biotite, sphene and chlorite.

The protolith for the calc-silicate gneiss was probably a calcareous arenite (quartz-dolomite-feldspar-clay). Prograde metamorphism of rock of this composition would produce the observed metamorphic mineral assemblage. This mineral paragenesis is consistent with the epidote-amphibolite facies metamorphism noted throughout the Besham group. Because the mineral reaction quartz + epidote = grossular garnet occurs at about 550°C (depending on epidote composition), the absence of grossular garnet indicates that the peak temperature during the most recent metamorphic event was probably less than 550°C and/or that the protolith lacked the chemistry needed to form garnet.

Geology of the Pre-Karora Group Intrusives

Pre-Karora group intrusives include amphibolite, the sodic quartzofeldspathic gneiss, the Shang granite and Dubair granodiorite, the Shorgara pegmatites and tourmaline granite.

Amphibolite in the Besham area occurs as discontinuous lenses, layers and pods within the Besham group. Most of the amphibolite bodies are less than 2 m wide, with rare exception up to 50 m wide. The amphibolite bodies are commonly oriented parallel to the foliation of the surrounding gneisses and metasediments with contacts that are commonly sharp. Pegmatites cross-cut the amphibolite, and the Karora group lies unconformably on the top of the Shang granite; therefore, the amphibolite is older than both the Shang granite and the Karora group.

Major minerals in the amphibolite include 20 to 40% andesine (An$_{48}$), and 4 to 8% quartz. Epidote content varies from 1 to 5%, and trace minerals include sphene, pyrite, chlorite, zircon and apatite. The dominant mafic mineral is idioblastic hornblende, which constitutes 50 to 60% of the rock, and defines a strong foliation. The hornblende commonly displays a reaction rim of blue-green actinolite around a core of brown-green hornblende. These retrograde reaction rims may have occurred during the original metamorphism, or they indicate a pre-Himalayan polymetamorphic history for the amphibolite (Baig *et*

al., 1989; Baig, 1990). The mineralogy and texture of the amphibolite indicate metamorphism to epidote-amphibolite facies.

In addition to the above minerals, one amphibolite from near the MMT contains 25% diopside, 30% brown hornblende and 35% andesine. The sample, like the other amphibolites, occurs as a discontinuous layer within the Besham group, but unlike the other amphibolites, it contains poikiloblastic clinopyroxene. Furthermore, the coarse-grained, strongly polygonal texture of sample implies that it recrystallized slowly under static, near equilibrium conditions.

In addition to sodic quartzofeldspathic gneiss and amphibolite, pre-Karora group intrusives include the Shang granite, Dubair granodiorite and Shorgara pegmatite. The Shang granite, Dubair granodiorite and Shorgara pegmatite are characterized by blue-grey microcline. The Shang granite, which has a mapped extent of 30 square kilometers in the study area, is the largest unit of these units. The Shang granite continues beyond the southern boundary of the study area (Baig, 1990). The Dubair granodiorite is a small body of about 0.5 square kilometer. The Shorgara pegmatite is the youngest of these units.

Shang granite is exposed high above the Indus River on the steep mountain-sides and ridge tops south of Shang village (Ashraf *et al.,* 1980). Shang granite is a small pluton of foliated, coarse-grained biotite granite with distinctive blue-grey microcline. Shang granite clearly intrudes the Besham gneisses, and it is strongly deformed near its contacts with the gneisses. Deformation in the granite decreases away from the contacts. The blue-grey microcline crystals are common. Sphene is an abundant (3%) accessory mineral, with lesser amounts of zircon, calcite and apatite, and trace amounts of metamorphic epidote. Broken and bent albite twins in plagioclase within the granite resulted from post-crystallization deformation.

Exposed 15 km north of Besham on the KKH near Dubair village is a small intrusion (0.5 km^2) of *hornblende-biotite granodiorite* with blue-grey microline, known as the Dubair granite (Ashraf *et al.,* 1980). The rock is a granodiorite and contains passively stopped blocks of Besham quartzofeldspathic gneiss. The Dubair granodiorite, like the Shang granite, is strongly deformed near its contacts, and deformation decreases away from the contacts. The mineral content of the Dubair granodiorite and Shang granite is similar, except that the Dubair granodiorite contains more

mafic minerals, including 7% hornblende, and less sphene, about 1%. In addition, plagioclase in the Dubair granodiorite is partially altered to sericite.

The *Shorgara pegmatite* is a distinctive "blue" pegmatite with abundant blue-grey microcline and for that reason may be related to the Shang granite and/or Dubair granodiorite. The pegmatite includes both "blue" and/or white microcline. Biotite and black tourmaline are common, though not ubiquitous, accessory minerals in the white pegmatites. The Shorgara pegmatite intrudes all the lithologies of the Besham group. Contact between the Shorgara pegmatite and the Besham group rocks are sharp, except at the Besham gneisses/pegmatite, where both gradational and sharp contacts are noted. Thin skarns formed where the pegmatite intruded siliceous dolomite of the Besham group (Ashraf *et al.*, 1980; Chaudhry *et al.*, 1983). The pegmatite is best exposed near the small village of Shorgara on the KKH midway between Besham and the MMT.

The pegmatites are extensively boudinaged, isoclinally folded and metamorphosed. Along the KKH between Dubair village and the MMT the pegmatite bear the same blastomylonitic overprint as the gneisses and metasediments of the Besham group (Lawrence and Ghauri, 1983). The pegmatites are truncated by the unconformity separating the Besham group from the Karora group.

The presence of abundant bluish-grey microcline in all three units is considered to be evidence that they may be comagmatic. Furthermore, Shorgara pegmatite cross-cuts all units of the Besham group, yet it is found only at the margins of the Shang granite. Although these three units are not in immediate proximity with each other, they are all younger than the Besham group but older than the Karora group. The chemical data suggesting this correlation are presented below.

In addition to these three felsic granitic units that intruded the Besham group, *tourmaline granite* probably intruded within or near the study area before deposition of the Karora group. The tourmaline granite occurs only as a large (0.3 x 0.2 m) boulder within the basal conglomerate of the Karora group. The boulder is a relatively underformed, coarse-grained granite with 5% magmatic muscovite, 3% black tourmaline, and no biotite. The source region for the granite boulder is not known, but it is assumed that it was not transported far.

Geology of the Karora group

The name Karora group is misnomer because rocks of the Karora group do not cropout at Karora village, however, the name will be used in this work in order not to confuse the terminology established by Fletcher *et al.* (1986). The Karora group is a sequence of marine metasediments that was deposited unconformably on top of the rocks of the Besham group. Foliation in the Karora group, like that of the enveloping Besham group, is primarily north-trending and steeply east or west dipping. The distinctive unconformity between the Karora group and the Besham group, first recognized by Jan and Tahirkheli (1969) and Ashraf *et al.* (1980), is marked by a metamorphosed pebble conglomerate that grades upward into a thick unit of graphitic phyllite, which is overlain by a jointed siliceous dolomite. Gradations between these units and wide variations within them are common.

Biotite, chlorite and muscovite are present in the Karora group of rocks and garnet is absent, thus the grade of metamorphism is of lower greenschist facies (Baig, 1990). The areal extent of the Karora group has been substantially underestimated by previous workers (e.g., Jan and Tahirkeli, 1969; Ashraf *et al.*, 1980; Butt, 1983; Coward *et al.*, 1982; Fletcher *et al.*, 1986). The eastern and southern contacts of the Karora group, in particularly, extend much farther than previously believed (Fig. 2). Indeed, the basal pebble metaconglomerate lies as close as 1 km to the Karakorum Highway at Chaman village, 3 km north of Shang.

The *pebble metaconglomerate* of the Karora group is exposed irregularly along the eastern edge of the Karora group, at the unconformity with the Besham group. The metaconglomerate is 6-10 meters thick and poorly sorted, and clasts include subrounded to angular pebbles and cobbles of the underlying basement complex. Boulders range up to 40 cm long. The conglomerate is clast-supported nearest the unconformity and for about 5 meters above the basal contact. The clast-matrix ratio diminishes as the metaconglomerate grades upwards into fine-grained graphitic phyllite.

The mineralogy of the black, pelitic matrix of the metaconglomerate consists of very fine-grained feldspar, quartz and lithic fragments, with minor biotite and trace amounts of graphite, muscovite, sphene and detrital zircon. Most lithic fragments are poorly sorted and angular, although they commonly lie

parallel to the weak foliation of the matrix. The matrix contains quarzt-rich and mica-rich segregation bands that define foliation; detrital zircon and sphene tend to concentrate within the mica-rich bands. The relative proportion of mica and graphite to quartz and feldspar increases rapidly and gradationally upwards into overlying graphitic phyllite.

The metaconglomerate is deformed. The amount of deformation of pebbles within a single outcrop varies according to competency of pebble lithology. Pebbles of competent rock such as tourmaline granite lack the flattening and folding seen in the less competent carbonate and graphitic clasts.

Discontinuous beds of intraformational, matrix-supported pebble metaconglomerate are common within the massive graphitic phyllite, however, they are inseparable from the graphitic phyllite at the scale of this study. The principal difference between the intraformational and the basal metaconglomerates are (1) the intraformational beds are not clast-supported and (2) pebbles are mostly graphitic schists, quartzite and carbonate, and lack the granitic clasts common to the basal unit.

Massive, fine-grained graphitic phyllite is the most extensive unit of the Karora group, and is relatively easily recognized throughout the field area. The Karora group graphitic phyllite is more extensive in outcrop than the lithologically similar graphitic schist of the Besham group. Excellent exposures of massive, poorly indurated, black graphitic phyllite cropout in roadcuts along the Besham-Karora road. The rock invariably contains abundant, discontinuous, ptygmatically folded quartzose veinlets up to 3 cm wide and 10 cm long. Crenulation cleavage is common.

The mineralogy of the graphitic phyllite consists of dusty, submicroscopic graphite, quartz ribbons with ragged, sutured quartz-quartz grain boundaries, fine-grained plagioclase, biotite, muscovite, minor epidote and chlorite and trace amounts of detrital zircon. The epidote occurs as amorphous masses within quartz- and plagioclase-rich domains.

The Karora group graphitic phyllite commonly grades into extremely fine-grained, black, dirty quartzite and/or metapelite. The best exposures of these two lithologies occur along the Kurmang Khwar on the road near Gandorai (Fig. 2). Major minerals in the dirty quartzite include very fine-grained quartz, feldspar, biotite and anhedral muscovite blades, with trace amounts of graphite, zircon and tourmaline. The

extremely fine grain size (< 0.1 mm) of the dirty black quartzite gives the rock a homogeneous bluish-black appearance, and there is a weak, slaty parting parallel to foliation. Thin folia and quartz veinlets are less than 1 mm apart, and on some surfaces a slight phyllitic sheen is evident.

Graphitic phyllite locally grades into metapelites, ranging from medium-grained psammitic biotite schist to extremely fine-grained muscovite-biotite metapelite. The metapelites occur in discontinuous beds less than 20 m thick. The muscovite-biotite metapelites typically weathers to a light brown-orange colour, and is locally aphanitic. Quartz, feldspar and micas compose the major minerals, with traces of zircon, graphite and sphene.

The metapelites and graphitic phyllite are in sharp conformable contact with the Karora group carbonates. The carbonate is exposed in an elongate north-trending unit that reaches its maximum thickness of about 500 meters between Upal and Panial villages. It pinches out laterally to the south of Upal and to the north of the Besham-Karora road.

The most abundant carbonate is a dark grey to black siliceous metadolomite that is well exposed along the Beṣham-Karora road. The rock has quartzose interlayers in vein-like segregations up to 4 cm thick. Mineralogy of the siliceous metadolomite consists of 70% fine-grained (< 0.2 mm) dolomite and 30% strained, subangular quartz with a trace of muscovite. Both dolomite-dolomite and quartz-quartz grain boundaries are sutured and irregular. The nonrhombic, mosaic texture of the dolomite crystals is typical of xenotopic-A (anhedral) dolomite, which is thought to result from either recrystallization of a preexisting dolomite at temperature above 100°C and/or from replacement of a limestone by dolomite (Gregg and Sibley, 1984). Both Karora group and Besham group dolomites clearly display this recrystallized texture.

There are many lithologic variations within this relatively extensive carbonate sequence. For example, the 40-m-wide carbonate outcrop west of the mouth of Chaidam Khwar on the Besham-Karora road is made up of two distinctive lithogies. The outcrop nearest Chaidam Khwar is a tan-buff coloured sandy dolomite that powders easily to a yellowish grit. Farther from the stream is a more crystalline, white siliceous dolomite with two pressure solution cleavage planes spaced 2 cm apart that cause the rock to break readily into elongate, rectangular prisms.

Other variations within the carbonates of the Karora group include etched grey-blue limestone that commonly cropsout as discontinuous beds within the massive graphitic phyllite. Also, a 100 m long by 10 m thick outcrop of limestone breccia was found at 1785 m elevation on the steep ridge northeast of Punial village. Clasts in the breccia are angular grey-blue limestone up to 5 cm long, and subangular dissolution pits are prominent where the clasts have dissolved/eroded more rapidly than the limey sand matrix, commonly leaving fragile, reddish-brown skeletal clasts in the pits. The breccia indicates that instability and slumping occurred within the Karora carbonate.

Geology of a Post-Karora Group Intrusive

Near the western contact of the Karora group (Fig. 2) with the Besham group along the Besham-Karora road the graphitic phyllite of the Karora group is intruded by a small sill of equigranular, medium-grained leucogranite of colour index 2 to 7. Small sills of the leucogranite also intrude the Besham group west of the mouth of Chaidam Khwar. The leucogranite is important because it is the only post-Karora group intrusive unit found within the Besham area, and because it is clearly younger than the Karora group, which was previously considered to be the youngest unit within the basement block (Ashraf et al., 1980; Butt, 1983; Coward et al., 1982; Fletcher et al., 1986).

The leucogranite is faint red on fresh surfaces and weathers white. Its best exposure is located east of the mouth of Chaidam Khwar, where the largest sill is 25 m thick. Karora group graphitic phyllite within a few meters of the contact is baked to an extremely hard, dense and coarse-grained graphitic schist. Mineralogy of the leucogranite consists of oligoclase that is altered to sericite (with optically continuous unaltered oligoclase overgrowths), quartz, microcline, biotite and accessory pyrite and sphene. Quartz-quartz grain boundaries are sutured to weakly polygonal. Plagioclase is occasionally myrmekitic. Biotite defines a very weak foliation in the leucogranite, which provides evidence for at least minor deformation after metamorphism of the Karora group and emplacement of the leucogranite.

Geology of Units Adjacent to the Besham Area

The geology of two units of regional significance will be briefly discussed below in order to better constrain the geology of the Besham area. The two units are the Mansehra granite gneiss and the Swat granite

gneiss.

Late Pecambrain-Cambrain Mansehra granite intrudes metasedimentary rocks of possible Precambrian age southeast of Besham (Ashraf et al., 1980; Baig and Lawrence, 1987; Baig, 1990). This porphyritic granite is truncated against the Thakot fault that separates the Besham basement complex from the Mansehra pluton and associated metasediments (Baig and Lawrence, 1987; Baig and Snee, 1989; Baig et al., 1989; Baig, 1990). The fault is located on the east side of the Indus River (Fig. 2). Mansehra granite is a peraluminous, corderite-bearing pluton, dated by Le Fort et al. (1980) at 516 ± 16 Ma. An analysis of major element and rare earth (REE) data from the Mansehra granite will be presented in the geochemistry section.

The Swat granite is a suite of porphyritic granites that is similar in lithology to the Mansehra granite (Baig, 1990) and is exposed in the lower Swat region (Martin et al., 1962; King, 1964), west of Besham. The age of the Swat granite gneiss is not known, but is probably similar to the age of the Mansehra granite. The oldest unit of the Swat granite gneiss, the Choga granite, cropsout west of the Puran fault, which is the western boundary of the Basham block (Baig and Snee, 1989; Baig et al., 1989; Baig, 1990). The Choga granite is a porphyritic biotite-garnet-bearing granite with a moderate to strong gneissic texture. An analysis of geochemical data from the Choga granite will be presented in the geochemistry section.

STRUCTURE OF THE BESHAM ARÉA

The Besham basement block is bounded on the east and west by high-angle, north-trending Thakot and Puran faults respectively (Fig. 1; Baig and Lawrence, 1987; Baig et al., 1989; Baig, 1990). The structures found within the basement include tight, upright to recumbent isoclinal folds with an amplitude of 1.3 meters. The discontinuous tectonic lenses, pods and boudins show strong tectonic transposition parallel to layring. In addition, major north-trending, upright folds with a wavelength of 1.2 km affect all the units of the Basham area (Fig. 4). The Karora group was deposited unconformably on the top of the Besham group, then enveloped and preserved within synclines formed by these folds. Within the field area, the western limbs of these synclines are cut by high-angle north-trending faults (Figs. 2 and 4), some of them offset the MMT Zone (Baig and Snee, 1989; Baig, 1990; Fig. 3).

The Besham group, later granitic intrusives and

Karora group exhibit a predominantly north-trending foliation that dips steeply to the east or west. The exception to this dominant foliation occurs adjacent to the MMT, where Indian plate rocks are overprinted by a strong blastomylonitic fabric that is parallel to the orientation of the MMT (Lawrence and Ghauri, 1983). The leucogranite has a very weak foliation defined by biotite, and is the least foliated of the units within the Besham area.

GEOCHEMISTRY

Nineteen samples from the Besham area were analysed for major and selected trace elements. Sample locations are shown on Fig. 5. The samples included two quartzofeldspathic and three sodic quartzofeldspathic gneisses of the Besham group, four amphibolites, two Shang granites, one Dubair granodiorite, the tourmaline granite boulder and the post-Karora group leucogranite. In addition, one sample of the adjacent Mansehra granite and two samples of the Swat granite gneiss were analysed. Geochemical data are presented in Table-1. Major element concentrations are given in weight percent (wt. %), trace element concentrations in parts per million (ppm). In the context of this paper, the term major element is used for chemical constituents whose abundance in common rocks is normally greater than 0.1 wt. %; trace element is used for an element whose abundance in common rocks is less than 0.1 wt. %.

Major Elements

The Besham group gneisses include sodic quartzofeldspathic gneiss and quartzofeldspathic gneiss. Both types of gneisses are equigranular, peraluminous, calcium-poor (< 1.5 wt. % CaO) and corundum normative. An A-C-F diagram clearly demonstrates their bimodal nature (Fig. 6; Ca = CaO, K = K_2O, Na = Na_2O). On a ternary Q-A-P diagram of normative quartz-alkali feldspar-plagioclase feldspar the bimodal nature of the gneisses is also evident, i.e., the sodic quartzofeldspathic gneiss contains only 5% normative potassium feldspar, whereas the quartzofeldspathic gneiss contains 34% normative potassium feldspar (Fig. 7). Fig. 8 shows an A-F-M diagram of major element composition of five Besham gneisses, in addition to twelve other samples from the Besham area (A = Na_2O + K_2O, F = FeO^*, and M = MgO). The FeO^*/Na_2O + K_2O ratio of the sodic

quartzofeldspathic gneiss exhibits a wide range of values, whereas the quartzofeldspathic gneiss values are more consistent. Mg content is relatively constant for both types of gneiss.

Spider diagrams of the Besham gneisses exhibit depletion of TiO_2 relative to average Archean upper crust in both the sodic quartzofeldspathic gneiss and the quartzofeldspathic gneiss (Figs. 9 and 10). All values presented in spider diagrams in this study are chondrite normalized (after Thompson, 1982) except rubidium, potassium and phosphorus, which are normalized to primitive mantle values after Sun (1980). TiO_2 ranges from 0.13 to 0.25 wt.% in the sodic quartzofeldspathic gneiss, and is 0.18 wt.% in the quartzofeldspathic gneiss. A negative trough is also seen for P_2O_5.

The scatter seen in the major element data, particularly in sodium and potassium, for the Besham gneisses may be due to variability in the composition of the sediments that comprised the protolith of the gneisses. This compositional variability relative to protolith is observed in the A-C-F diagram (Fig. 6); the quartzofeldspathic gneiss plots near the field of rocks with a protolith of clays and shales containing 0-35% carbonate, and sodic quartzofeldspathic gneiss plots within or near the field of aluminum-rich clays and shales.

The amphibolite bodies found within the Besham area are classified as tholeiitic based on their major element content, as shown by the A-F-M diagram (Fig. 8; Irvine and Baragar, 1971). The four amphibolite samples plot within the tholeiite field, near the calcalkaline/tholeiite discrimination line. Other diagrams that distinguish tholeiitic from calcalkaline magmas (SiO_2 vs. FeO^* and SiO_2 vs. FeO^*/MgO; Miyashiro, 1974) suggest a tholeiitic protolith for the amphibolite (Figs. 11 and 12).

A spider diagram of the amphibolites shows a negative trough for P_2O_5 relative to the international standard basalt BHVO-1 (Fig. 13). Phosphorous content varies from 0.06 to 0.1 wt.%. Titanium is also depleted relative to BHVO-1, although TiO_2 does not plot as a trough on the spider diagram. Potassium, a volatile-lithophile element, is depleted relative to BHVO-1, perhaps due to its mobility during metamorphism.
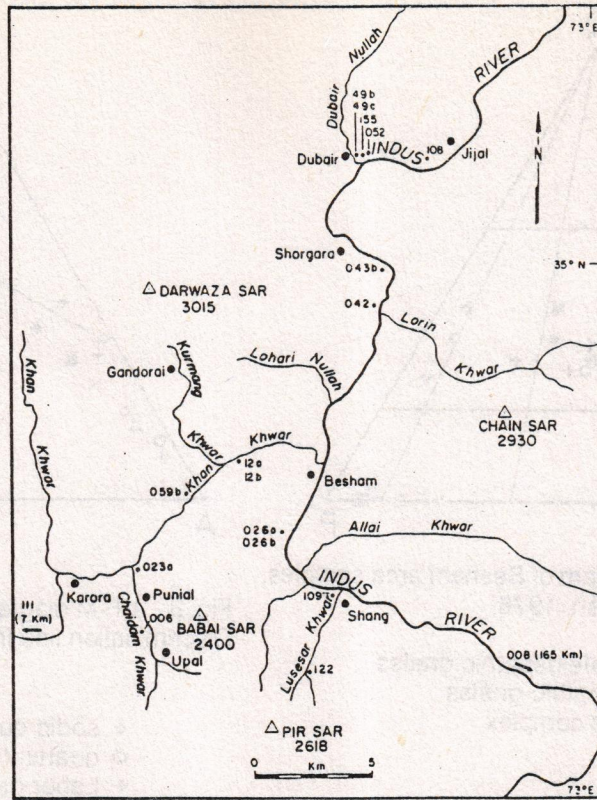
Fig. 5. Sample location map.

1 Al-rich clays and shales

2 Clays and shales containing
0-35% carbonate

3 Greywackes
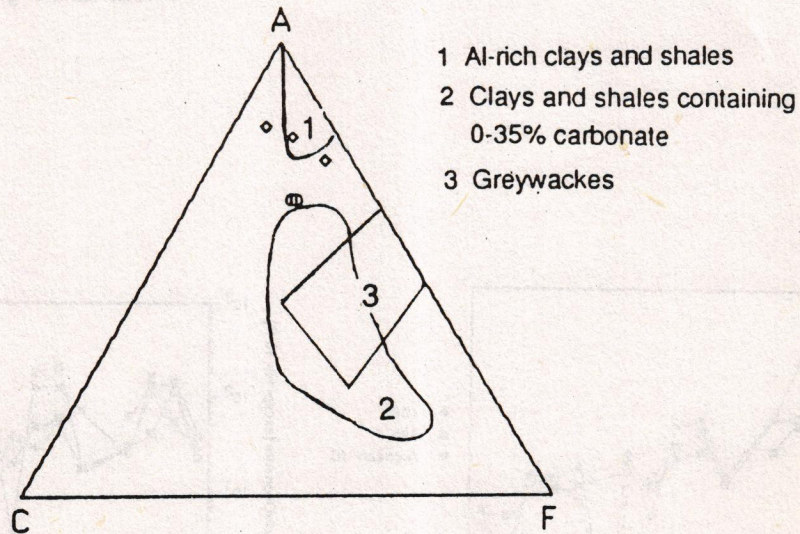
Fig. 6. A-C-F ternary diagram delineating protolith fields for Besham area samples. Plot after Nockolds, 1954.

◇ sodic quartzofeldspathic gneiss
○ quartzofeldspathic gneiss
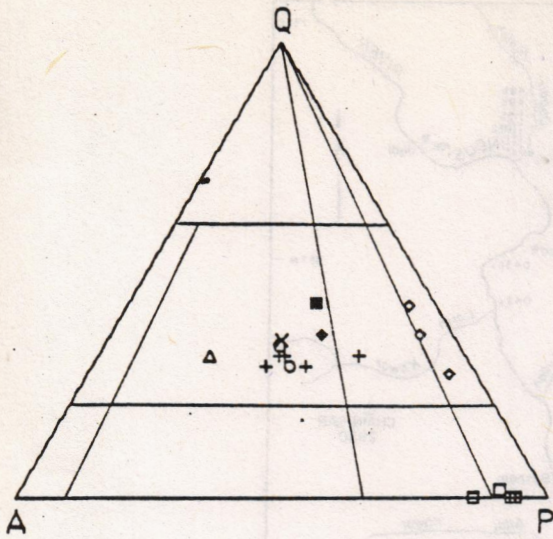
Fig. 7. Normative Q-A-P diagram of Besham area samples. Base diagram after Streckeisen, 1976.

◇ sodic quartzofeldspathic gneiss
○ quartzofeldspathic gneiss
+ Lahor granitic complex
□ amphibolite
▲ leucogranite
✖ Mansehra granite
◆ Choga granite
■ tourmaline granite boulder

Fig. 8. A-F-M diagram of Besham area samples. Discrimination line from Irvine and Baragar, 1978.

◇ sodic quartzofeldspathic gneiss
○ quartzofeldspathic gneiss
+ Lahor granitic complex
□ amphibolite
▲ leucogranite
✖ Mansehra granite
◆ Choga granite
■ tourmaline granite boulder

Fig. 9. Spidergrams for quartzofeldspathic gneiss. Archean upper crust from Taylor and McClennan, 1985.
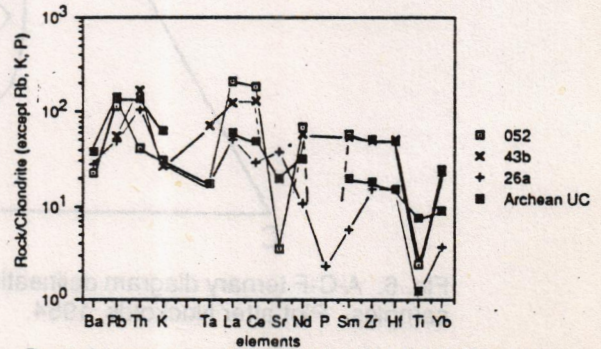
Fig. 10. Spidergrams for sodic quartzofeldspathic gneiss. Archean upper crust from Taylor and McClennan, 1985.

Table - 1 Geochemistry of Representative Samples from the Besham Area, Northern Pakistan.

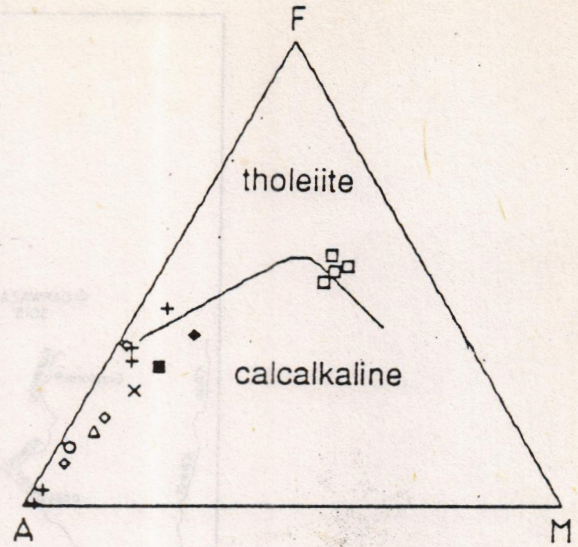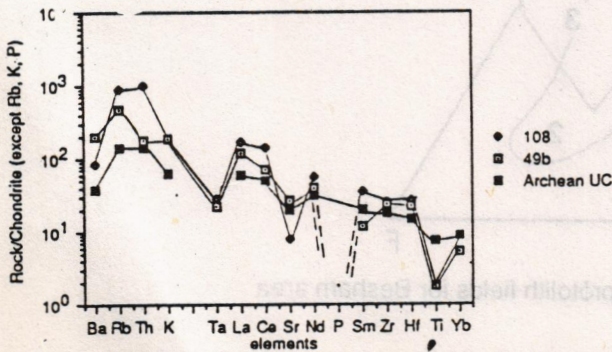| Rock type:	Sodic quartzofeldspathic gneiss			Quartzofeldspathic gneiss		Amphibolite		
Sample	052	43b	26a	108	49b	042	12b	006
SiO_2 (wt. %)	74.4	75.8	72.7	73.6	71.7	50.8	49.5	51.8
Al_2O_3	12.3	12.8	15.7	13.5	14.5	13.4	13.8	15.3
FeO	2.20	0.91	0.44	0.68	0.70	8.63	8.04	6.78
Fe_2O_3	1.83	0.70	0.39	0.56	0.70	3.61	3.48	3.47
MgO	0.16	0.45	0.28	0.22	0.25	6.74	7.17	6.38
CaO	0.52	0.80	1.47	1.28	1.54	10.2	10.7	9.83
Na_2O	6.12	5.34	6.86	2.90	3.32	2.80	2.62	3.60
K_2O	0.89	0.78	0.83	5.48	5.52	0.68	1.19	0.56
TiO_2	0.25	0.29	0.13	0.18	0.18	1.08	0.89	0.59
P_2O_5	<0.05	<0.05	0.05	<0.05	<0.05	0.10	0.09	0.1
MnO	<0.02	<0.02	<0.02	<0.02	<0.02	0.22	0.20	0.19
La (ppm)	70.6	41.8	16.5	56.4	37.9	6.98	7.07	11.2
Ce	162.0	115.0	25.0	123.0	60.5	15.2	14.2	20.0
Nd	42.6	36.2	6.8	35.0	17.1	--	16.0	--
Sm	11.8	10.7	1.14	7.16	2.41	3.02	2.62	2.65
Eu	1.94	1.63	0.48	0.55	0.83	1.14	0.90	0.79
Tb	1.8	1.5	0.17	0.79	0.25	0.60	0.51	0.46
Yb	5.4	5.0	0.8	2.0	1.2	2.6	2.4	1.8
Lu	0.85	0.77	0.09	--	0.15	0.47	0.32	0.22
Sc (ppm)	2.39	7.84	1.32	2.58	2.12	47.2	45.4	37.1
Cr	2.8	3.5	1.8	2.5	1.8	99.0	188.0	79.0
Co	1.4	0.8	1.2	0.9	1.2	52.1	51.0	31.0
Zn	9.0	20.0	10.0	18.0	18.0	150.0	140.0	130.0
Rb	40.3	19.8	16.7	303.0	163.0	21.3	33.6	21.3
Sr	40.0	--	450.0	90.0	470.0	260.0	200.0	400.0
Cs	1.2	0.8	0.5	3.4	1.7	--	0.9	--
Ba	157.0	--	195.0	563.0	1350.0	--	558.0	--
Zr	320.0	330.0	110.0	170.0	170.0	190.0	140.0	120.0
Hf	9.8	9.9	3.0	5.3	4.6	2.2	1.5	2.0
Ta	0.35	1.4	0.34	0.55	0.45	0.35	0.17	0.34
Th	1.7	7.0	4.4	55.0	7.5	2.2	2.7	2.6
U	3.2	3.4	2.3	7.0	--	--	--	--

Table - 1 (Continued)

| Rock type: | Amphibolite | Shang granite | | Shorgara pegmatites | | Leuco-granite | Tour. granite | Dubair, granodiorite |
Sample	155	122	109	12a	26b	23a	59b	49c
SiO_2 (wt. %)	48.3	70.2	69.6	74.0	72.7	71.5	73.7	66.0
Al_2O_3	14.2	13.0	12.9	14.7	14.7	14.3	14.5	13.2
FeO	11.61	2.16	2.41	0.17	0.04	0.92	0.37	3.57
Fe_2O_3	3.66	1.99	4.62	0.15	0.04	0.85	0.35	2.92
MgO	7.46	0.56	0.40	0.16	0.16	0.47	0.14	0.68
CaO	12.9	1.70	2.07	1.20	0.58	1.39	0.53	3.14
Na_2O	2.64	2.92	2.80	4.86	3.37	3.78	4.34	2.86
K_2O	0.56	5.25	5.27	3.18	6.30	4.36	3.88	4.50
TiO_2	0.94	0.60	0.66	0.04	<0.02	0.30	0.03	1.09
P_2O_5	0.08	0.13	0.14	<0.05	<0.05	0.05	0.37	0.30
MnO	0.19	0.03	0.04	<0.02	<0.02	<0.02	<0.02	0.07
La (ppm)	3.95	361.0	261.0	7.07	1.81	2.49	11.1	103.0
Ce	8.67	712.0	539.0	11.7	1.50	39.1	19.2	201.0
Nd	--	120.0	96.0	--	--	--	8.9	72.0
Sm	2.16	28.9	24.5	0.49	0.18	2.22	2.06	13.5
Eu	0.85	1.29	1.25	0.60	0.64	0.41	0.30	1.89
Tb	0.44	3.0	2.8	0.04	0.02	0.23	0.29	1.7
Yb	2.4	8.5	8.7	--	--	1.3	1.0	4.8
Lu	--	0.89	0.90	0.04	--	0.08	0.10	0.76
Sc (ppm)	37.1	6.07	0.61	0.15	0.15	2.28	6.84	11.2
Cr	122.0	5.7	5.8	1.8	1.3	3.2	2.9	5.1
Co	53.4	3.7	3.3	0.2	0.1	2.4	0.4	6.2
Zn	120.0	50.0	60.0	4.0	2.0	20.0	30.0	80.0
Rb	19.1	282.0	316.0	64.4	151.0	123.0	153.0	178.0
Sr	140.0	--	180.0	250.0	340.0	460.0	63.0	229.0
Cs	0.5	5.0	7.1	0.8	1.0	3.3	7.1	3.1
Ba	--	827.0	--	1710.0	6140.0	766.0	350.0	1370.0
Zr	--	570.0	650.0	94.0	41.0	176.0	77.0	540.0
Hf	1.5	16.0	18.0	3.0	0.3	4.6	1.0	15.0
Ta	0.30	2.2	2.3	0.03	0.05	1.5	5.0	2.0
Th	--	91.3	94.9	1.8	0.2	12.2	0.7	20.6
U	--	95.0	9.4	--	--	4.4	1.0	4.9

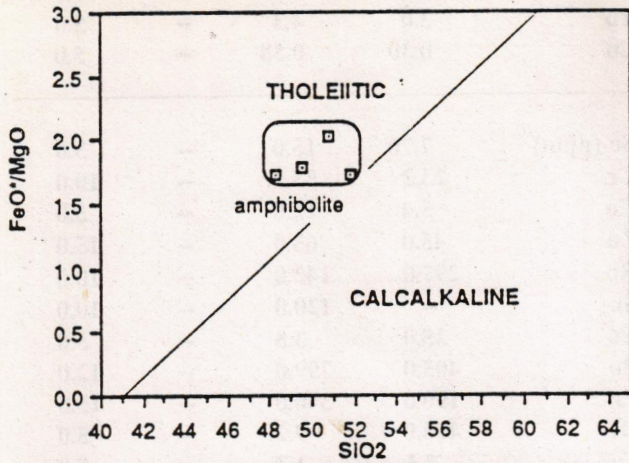Fig. 11. SiO2 vs. FeO*/MgO diagram for mafic rocks of the Besham area. Thol./Calkalk. determination line from Miyashiro, 1974.
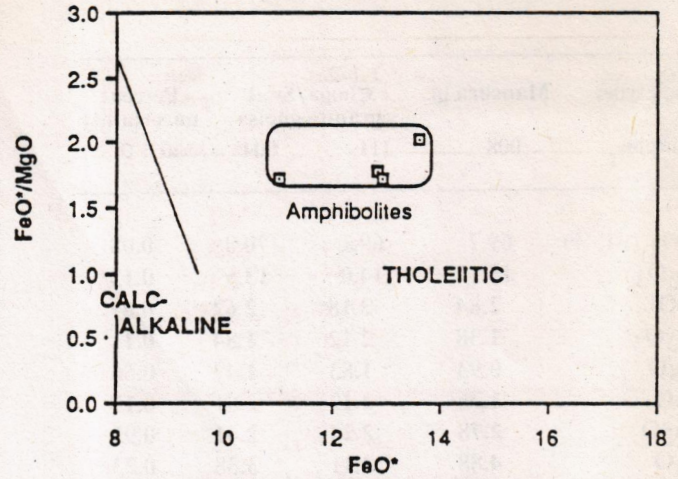

Fig. 12. FeO* vs. FeO/ MgO diagram for mafic rocks of the Besham area; after Miyashiro, 1974.
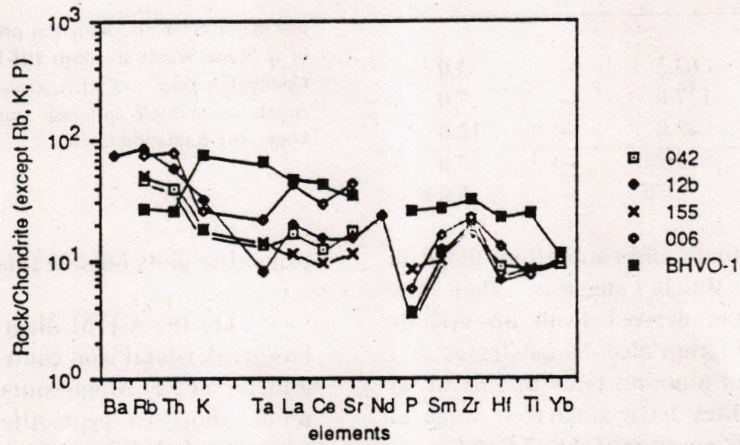

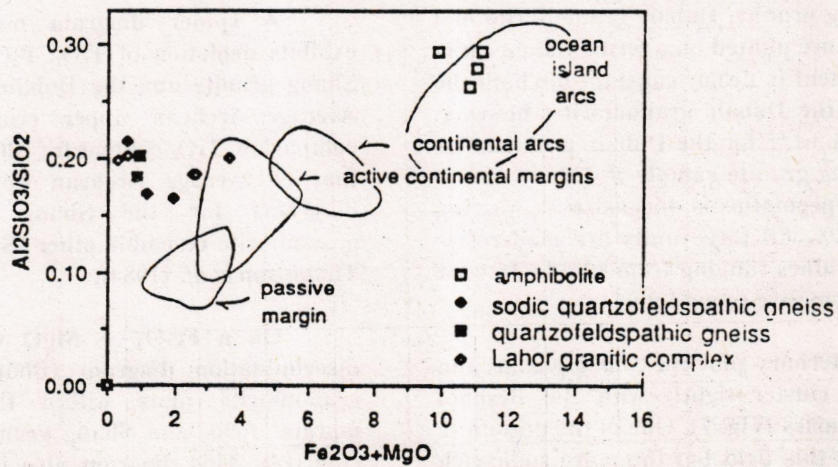Fig. 13. Spidergrams for amphibolites. BHVO-1 from Taylor and McClennan, 1985.

Fig. 14. Tectonic discrimination diagram of Besham area samples. After Bhatia, 1983.

41

Table - 1 (Continued)

Rock type:	Manshra gr.	Choga/Swat granite gneiss		Percent uncertainty at 1σ
Sample	008	111	004	
SiO_2 (wt. %)	69.7	69.1	70.0	0.08
Al_2O_3	15.1	14.0	13.6	0.12
FeO	2.84	3.18	2.62	0.01
Fe_2O_3	1.38	2.12	1.84	0.11
MgO	0.93	1.83	1.49	0.56
CaO	1.36	2.17	2.01	0.15
Na_2O	2.78	2.24	2.41	0.93
K_2O	4.88	3.11	3.38	0.23
TiO_2	0.47	0.97	0.80	1.1
P_2O_5	0.21	0.06	0.1	1.7
MnO	0.05	0.1	0.06	5.5
La (ppm)	30.3	63.3	--	3.0
Ce	76.0	127.0	--	7.0
Nd	29.0	42.0	--	12.0
Sm	6.65	9.94	--	5.0
Eu	0.92	1.59	--	5.0
Tb	0.83	1.1	--	5.0
Yb	3.0	4.3	--	5.0
Lu	0.30	0.58	--	5.0
Sc (ppm)	7.70	15.0	--	3.0
Cr	23.2	53.2	--	10.0
Co	5.4	12.0	--	5.0
Zn	45.0	68.0	--	15.0
Rb	297.0	142.0	--	10.0
Sr	--	120.0	--	10.0
Cs	25.0	3.8	--	5.0
Ba	405.0	799.0	--	12.0
Zr	190.0	340.0	--	15.0
Hf	470.0	9.2	--	5.0
Ta	2.1	1.3	--	5.0
Th	19.6	27.6	--	5.0
U	3.0	2.8	--	7.0

For major elements, analytical precision in based on replicate counts of in-house basalt standard BB-1 reported by USGS Denver XRF facility. For trace and REE, analytical precision is based on replicate counts of multiple in-house standards reported by Oregon State University Radiation Center.

Fig. 14 is a tectonic discrimination diagram (after Bhatia, 1983) which suggests that the amphibolite protolith was derived from an oceanic island arc setting. The diagram also demonstrates that silica (48 to 52 wt.%) and alumina (13.4 to 15.3 wt.%) content in the amphibolites have a narrow range of concentrations, as does magnesium (6.4 to 7.5 wt.%).

Major element oxides of calcium, potassium and sodium of the Shang granite, Dubair granodiorite and Shorgara pegmatite are plotted on a ternary diagram in Fig. 15. Sodium content is nearly constant for both the Shang granite and the Dubair granodiorite; however, CaO varies from 3.1 wt.% for the Dubair granodiorite to 1.7 wt.% for Shang granite sample # 122. The ratio K_2O/Na_2O for the pegmatite is inconsistent, varying from 0.65 to 1.9 wt.%. All three units are moderately high in Al_2O_3, with values ranging from 12.9 to 15 wt.% but none contain normative corundum.

On a Q-A-P ternary plot the *Shang granite* and *Dubair granodiorite* cluster tightly with the Besham quartzofeldspathic gneiss (Fig. 7). One of the pegmatite sample also plots in this field but the more sodic-rich pegmatite plots outside this cluster.

On the A-F-M diagram the Dubair granodiorite has greater total iron content than the Shang granite by a factor of 1.5. Magnesium content is similar for both units. Shorgara pegmatite data plot near the alkali apex, an indication of their extremely fractionated, felsic mineralogy.

A spider diagram normalized to chondrite exhibits depletion of TiO_2, P_2O_5 and K_2O in both the Shang granite and the Dubair granodiorite (Fig. 16). Average Archean upper crust is also shown for comparion. TiO_2 content for Shang granite is similar to that of average Archean upper crust. The spider diagrams for the Shang granite and Dubair granodiorite resemble other "S-type" granites noted by Thompson *et al.* (1984).

On a Fe_2O_3 + MgO vs. Al_2O_3/SiO_2 tectonic discrimination diagram (Bhatia, 1983), the Dubair granodiorite plots within the "active continental margin" field, and Shang granite plots near the field (Fig. 14). This diagram also illustrates the iron and
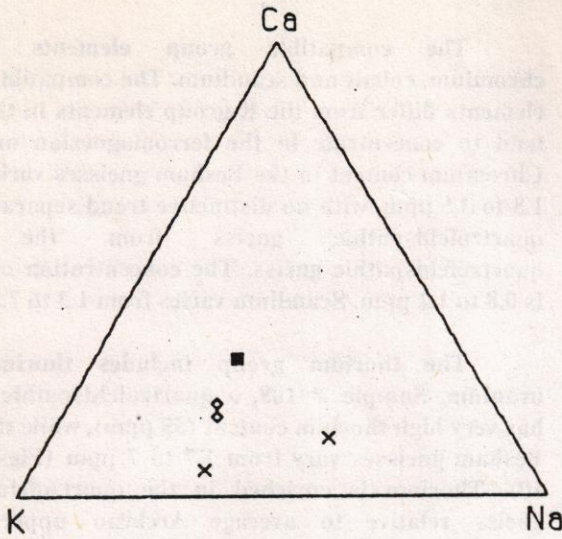
Fig. 15. Ca-K-Na diagram of Lahor granitic complex.

◇ Shang granite
■ Dubair granite
✕ Shorgara pegmatite
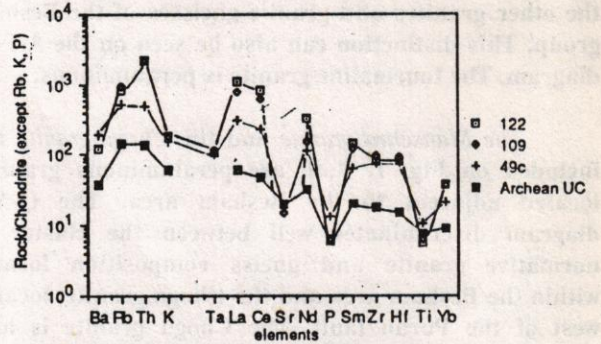
Fig. 16. Spidergrams for the Shang granite (122 and 109) and Dubair granite (49c). Archean upper crust from Taylor and McClennan, 1985.
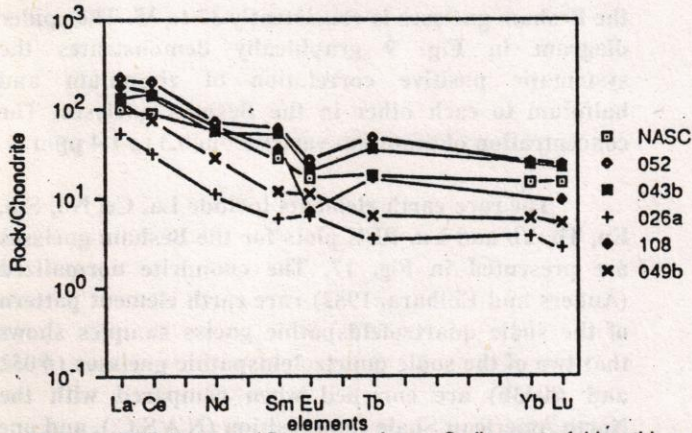
Fig. 17. REE diagram of Besnam gneisses. Sodic quartzofeldspathic gneiss (052, 043b, 026a), quartzofeldspathic gneiss (108, 049b), and NASC (from Haskin et al., 1968).
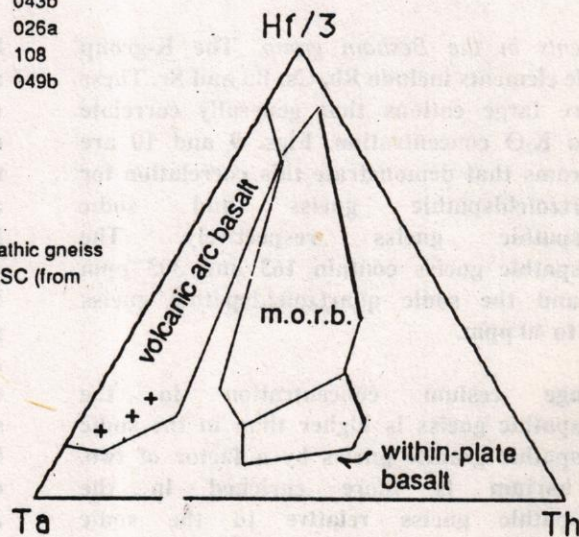
Fig.18. Th-Hf/3-Ta tectonic discrimination diagram for amphibolites. Plot after Wood et al., 1979.

magnesium enrichment of the Shang granite and Dubair granodiorite relative to the Besham gneisses.

On a Q-A-P diagram the *tourmaline granite* boulder does not plot in a cluster with any of the above units or Besham group rocks (Fig. 7). The tourmaline granite is more siliceous and slightly less alkalic than the other granites and granite gneisses of the Besham group. This distinction can also be seen on the A-F-M diagram. The tourmaline granite is peraluminous.

The Mansehra granite and the *Choga granite* are included on Fig. 7. Both are peraluminous granites located adjacent to the Besham area. The Q-A-P diagram discriminates well between the cluster of normative granite and gneiss composition located within the Besham area and the Choga granite, located west of the Puran fault. The Choga granite is also enriched in iron and magnesium relative to the Mansehra granite and the Besham area rocks. The sample of Mansehra granite has similar Q-A-P normative wt.% to Besham quartzofeldspathic gneiss # 108.

Trace Elements

The concentration of Rb, Cs, Ba, Sr, Cr, Co, Sc, Zn, Zr, Hf, Ta, Th, U and the rare earth elements (REEs) La, Ce, Nd, Sm, Eu, Tb, Yb and Lu are presented in Table - 1. The chondrite normalized incompatible element patterns of representative samples from the Besham area are presented on both spider diagrams.

Trace elements in the Besham group: The K-group incompatible elements include Rb, Cs, Ba and Sr. These elements are large cations that generally correlate positively to K_2O concentration. Figs. 9 and 10 are spider diagrams that demonstrate this correlation for the quartzofeldspathic gneiss and sodic quartzofeldspathic gneiss respectively. The quartzofeldspathic gneiss contain 163 and 303 ppm rubidium, and the sodic quartzofeldspathic gneiss contains 17 to 40 ppm.

Average cesium concentration in the quartzofeldspathic gneiss is higher than in the sodic quartzofeldspathic granite gneiss by a factor of two. Likewise, barium is more enriched in the quartzofeldspathic gneiss relative to the sodic quartzofeldspathic gneiss by a factor of 5. Strontium in the Besham gneisses is less systematic, with quartzofeldspathic gneiss concentrations of 90 and 470 ppm, and sodic quartzofeldspathic gneiss values

ranging from 40 to 450 ppm.

The compatible group elements include chromium, cobalt and scandium. The compatible group elements differ from the K-group elements in that they tend to concentrate in the ferromagnesian minerals. Chromium content in the Besham gneisses varies from 1.8 to 3.5 ppm, with no distinctive trend separating the quartzofeldspathic gneiss from the sodic quartzofeldspathic gneiss. The concentration of cobalt is 0.8 to 1.2 ppm. Scandium varies from 1.3 to 7.8 ppm.

The thorium group includes thorium and uranium. Sample # 108, a quartzofeldspathic gneiss, has very high thorium content (55 ppm), while the other Besham gneisses vary from 1.7 to 7 ppm (Figs. 9 and 10). Thorium is enriched in the quartzofeldspathic gneiss relative to average Archean upper crust. Conversely, thorium is generally depleted in the sodic quartzofeldspathic gneiss relative to average Archean upper crust. Uranium content varies from 2.3 to 7.0 ppm.

The high field strength elements include zirconium, hafnium and tantalum. These elements have high charge/ionic radius and are not incorporated into most of the common minerals. The ratio of Zr/Hf for the Besham gneisses is consistently 32 to 35. The spider diagram in Fig. 9 graphically demonstrates the systematic positive correlation of zirconium and halfnium to each other in the Besham gneisses. The concentration of tantalum varies from 0.3 to 1.4 ppm.

The rare earth elements include La, Ce, Nd, Sm, Eu, Tb, Yb and Lu. REE plots for the Besham gneisses are presented in Fig. 17. The chondrite normalized (Anders and Ebihara, 1982) rare earth element pattern of the sodic quartzofeldspathic gneiss samples shows that two of the sodic quartzofeldspathic gneisses (#052 and #043b) are enriched when compared with the North American Shale Composition (N.A.S.C.), and one (#026a) is not enriched. The composition of average North American Shale is thought to represent the average chemical composition of the earth's upper continental crust (Haskin *et al.,* 1968). Compared with C1 chondrite, most material at or near the earth's surface are enriched in the REE, for example, the N.A.S.C. The same two enriched sodic quartzofeldspathic gneisses also display a negative Eu anomaly.

Most evolved protoliths are more enriched in the light rare earth elements (LREE) than in the heavy rare earth elements (HREE), as shown by a high ratio of

La/Lu for chondrite normalized (cn) abundances. The average La/Lu (cn) of the two sodic quartzofeldspathic gneisses is 7.6 versus 6.8 for N.A.S.C. La/Lu (cn) for the third sodic quartzofeldspathic gneiss is 18.9, which is similar to the average value of 20.9 for the quartzofeldspathic gneisses.

One quartzofeldspathic gneiss (#108) has a strong, negative Eu anomaly, while the other (#049b) has a slightly positive Eu anomaly and a lower overall concentration of REE relative to N.A.S.C., in particular a depletion of HREE.

Trace Elements in the Amphibolites: Chondrite normalized spider diagrams for the amphibolite are shown in Fig. 13. The incompatible element data for this plot have been "double-normalized" to Yb(n) = 10 after Thompson *et al.* (1984). This convention makes incompatible element patterns of basic rocks easier to compare. In addition, the international standard basalt BHVO-1 is plotted for comparison.

The K-group elements in the amphibolite are enriched 2 to 3x relative to BHVO-1. Rubidium concentrations in the amphibolites are in the range of 19-34 ppm, with K/Rb ratios consistently 111 to 143. Cesium and barium concentrations are below detectable limits for two of the four amphibolites analysed. For the other two amphibolites, cesium is 0.5 to 0.9 ppm, and barium is 558 ppm in sample #12b.

The compatible elements are enriched in the amphibolite. Chromium ranges from 79 to 188 ppm, cobalt from 31 to 53 ppm and scandium from 37 to 47 ppm.

Thorium in the amphibolite ranges from 2.2 to 2.7 ppm. Ternary plots of Th-Hf/3-Ta are utilized to discriminate tectonic setting for rocks of basaltic composition (Fig. 18; Wood *et al.*, 1979). The amphibolite of the Besham area is consistent with a volcanic arc basalt. Uranium concentrations are below detectable limits for all four amphibolite samples analysed.

The high field strength elements in the amphibolite are depleted relative to BHVO-1. The spider diagram also shows a peak at zirconium. Zr/Hf ratios are high, ranging from 58 to 95.

The REE pattern of the Besham area amphibolite shows at a LREE enrichment of 10 times chondrite at 20-25 times chondrite, a HREE enrichment of 10 times chondrite, and a relatively flat pattern with

average (La/Lu) cn = 2.7 (Fig. 9). The pattern is typical of island arc affinities.

Trace Elements in the Shang Granite, Dubair Granodiorite and Shorgara Pegmatite: The K-group elements in the Shang, Dubair and Shorgara units are enriched relative to average Archean upper crust, except strontium, which has a similar concentration to upper crust (Figs. 16 and 20). Rubidium concentration in the Shang granite and Dubair granodiorite is 179 to 316 ppm. Rubidium is variable in the Shorgara pegmatite at 64 and 151 ppm.

Cesium content is 3 to 5 ppm in the Shang and Dubair plutons, and 1 ppm in Shorgara pegmatite. Barium is extremely enriched (6100 ppm) in the more sodic of the two pegmatites (#26b).

The compatible group elements have concentrations in these units typical for granitic rocks, with the more mafic rocks containing more compatible elements. Chromium values range from 5 to 6 ppm in the Shang and Dubair plutons to 1.3 ppm in the Shorgara pegmatite. The fact that scandium, like chromium and cobalt, is preferentially crystallized in the lattice of mafic minerals is evident from the scandium concentration of 7 to 12 ppm in the Shang and Dubair plutons respectively, and only 0.1 to 0.6 ppm in the Shorgara pegmatite.

Thorium concentration displays a positive peak of enrichment at 1300x chondrite for Shang granite, and 500x chondrite for Dubair granodiorite. Shorgara pegmatite demonstrates the opposite characteristic, i.e., a negative trough for thorium. Uranium values in the Shang and Dubair intrusive rocks are 5 to 10 ppm; uranium was below detectable limits in the sampled pegmatites.

Concentrations of the high field strength elements are consistent within the Shang and Dubair plutons (Zr/Hf = 35, Ta = 2 ppm), but less consistent within the Shorgara pegmatite (Zr/Hf = 31 and 150, Ta = 0.04). These trends can be seen on their respective spider diagrams.

The REE plot shows that the Shang and Dubair plutons are extremely enriched relative to C1 chondrite in all the REE and have a large, negative Eu anomaly, while the Shorgara pegmatite is only slightly enriched in REE and demonstrates a large positive Eu anomaly (Fig. 21). The average (La/Lu) cn for the highly fractionated and evolved Shang granite is 35, whereas the ratio is 11.6 for the pegmatite.
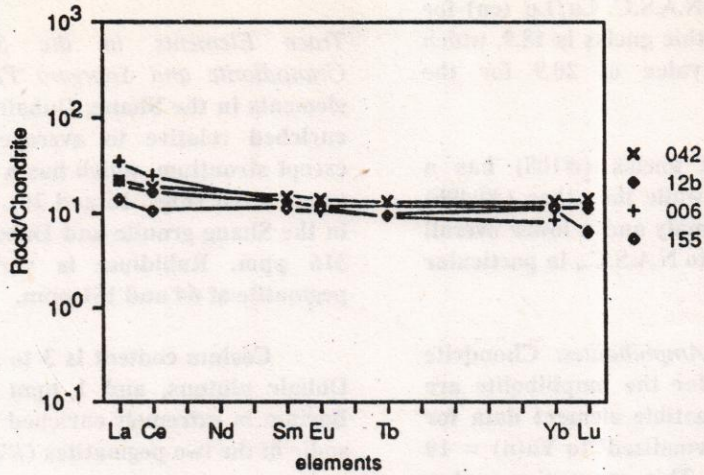
Fig. 19. REE diagram of amphibolites (042,12b,006, and 155).
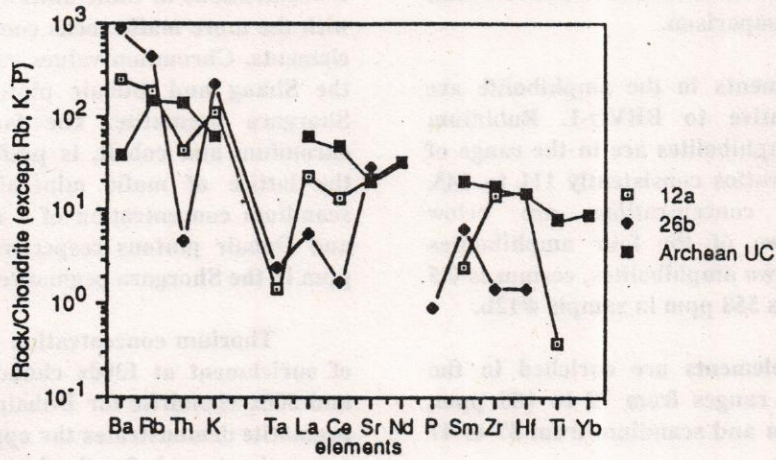
Fig. 20. Spidergrams for Shorgara pegmatite. Archean upper crust from Taylor and McClennan, 1985.
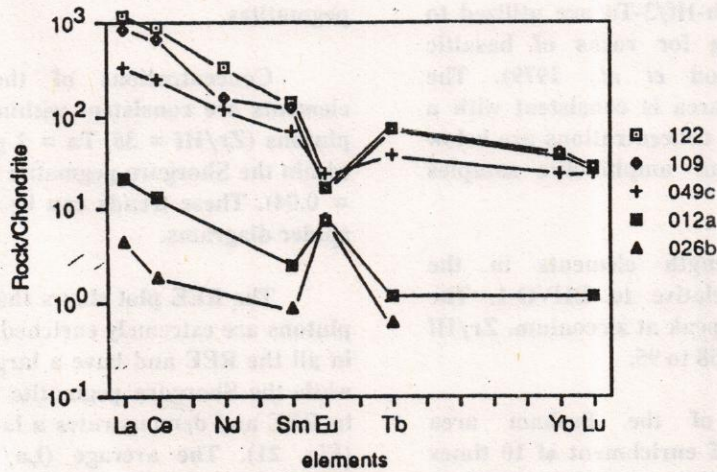
Fig. 21. REE diagram of Lahor granitic complex. Shang granite (122 and 109), Dubair granite (049c), and Shorgara pegmatite (012a and 026b).
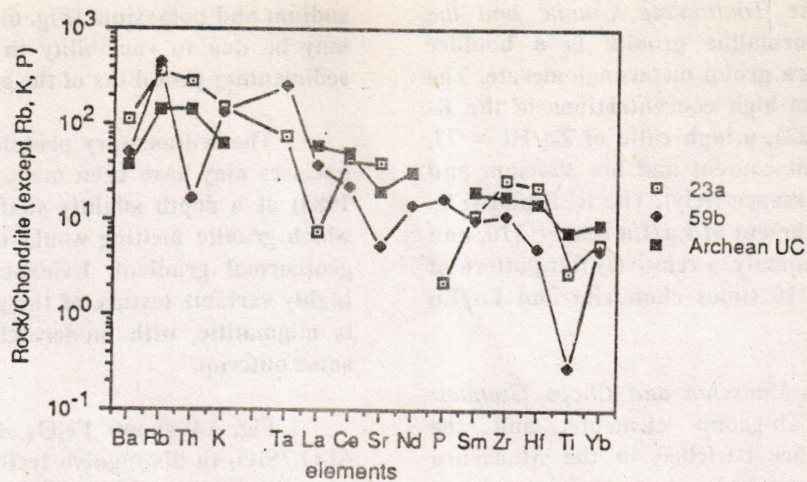
Fig. 22. Spidergrams for leucogranite (23a) and tourmaline granite (59b).
Archean upper crust from Taylor and McClennan, 1985.
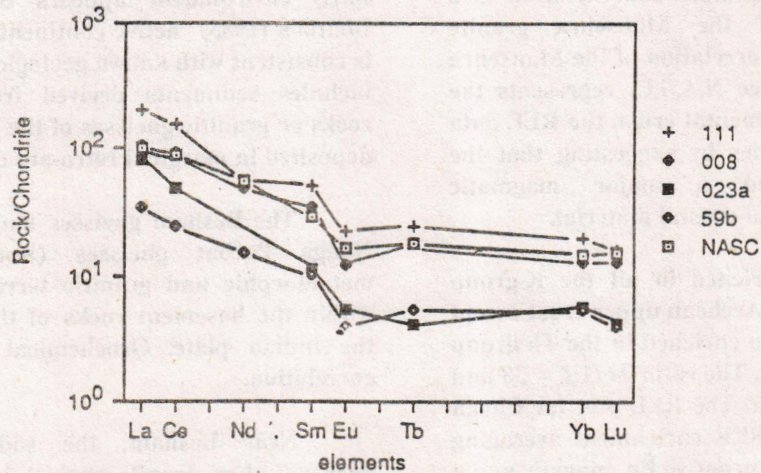
Fig. 23. REE diagram of Choga granite (111), Mansehra granite (008), leuco-
granite (023a), tourmaline granite (059b), and NASC (from Haskin et al., 1968).
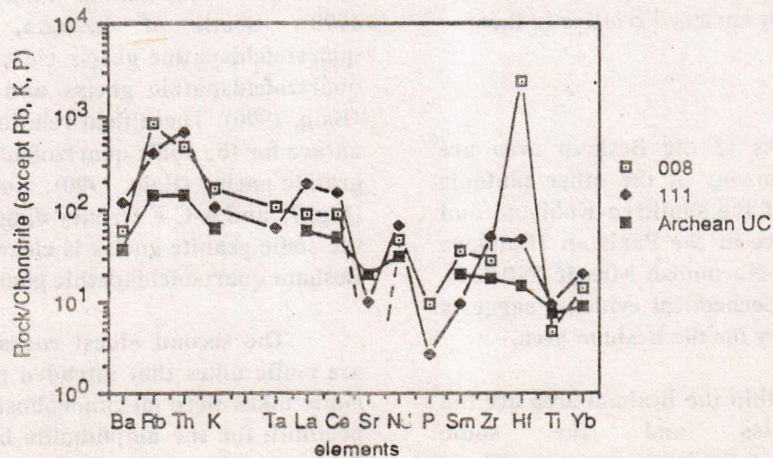
Fig. 24. Spidergrams for Mansehra granite (008) and Choga granite (111).
Archean upper crust from Taylor and McClennan, 1985.

Trace Elements of the Tourmaline Granite and the Leucogranite: The tourmaline granite is a boulder deposited in the Karora group metaconglomerate. The tourmaline granite has high concentrations of the K-group elements (Fig. 22), a high ratio of Zr/Hf = 77, low compatible element content and low thorium and uranium (0.7 and 1.0, respectively). The REE plot (Fig. 23) shows LREE enrichment at La/Lu (cn) = 110, and a slight negative Eu anomaly, a relatively flat pattern of HREE enrichment of 10 times chondrite and La/Lu (cn) = 31.

Trace Elements of the Mansehra and Choga Granites: The K-group, the Th-group elements, and the compatible elements are enriched in the Mansehra granite relative to average Archean upper crust, as seen on the spider diagram presented in Fig. 24. The high field strength elements are enigmatic, with an unusually low Zr/Hf ratio of 0.4. Tantalum concentration is 2 ppm. The REE plot of the Mansehra granite demonstrate a remarkable correlation of the Mansehra granite to the N.A.S.C. Since N.A.S.C. represents the average composition of continental crust, the REE data complements previous studies by suggesting that the Mansehra pluton derived a major magmatic contribution from continental crustal material.

Choga granite is enriched in all the K-group elements relative to average Archean upper crust except strontium (Fig. 24). It is also enriched in the Th-group and the compatible elements. The ratio Zr/Hf = 38 and Tantalum content is 1.3 ppm. The REE plot for Choga granite shows significant LREE enrichment averaging 180 times chondrite, a slight negative Eu anomaly and a flat HREE pattern at 20 times chondrite (Fig. 23). The ratio of (La/Lu) cn = 13. The REE pattern for the Choga granite mimics the pattern for Mansehra granite and N.A.S.C., but is slightly enriched relative to them.

DISCUSSION

The basement rocks of the Besham area are significantly different from any of the other plutonic and metamorphic rocks of the southern Kohistan and that are not seen elsewhere in the Pakistan Himalaya west of the Nanga Parbat-Haramosh Massif (NPHM). Field, petrographic and geochemical evidence suggests a complex geological history for the Besham area.

The oldest rocks within the Besham area are the quartzofeldspathic gneiss and the sodic quartzofeldspathic gneiss of the Besham group. These quartzofeldspathic gneisses are peraluminous. The scatter seen in the major element data, particularly in

sodium and potassium (Fig. 6) for the Besham gneisses may be due to variability in the composition of the sedimentary protoliths of the gneisses.

The sedimentary protolith of the Besham group gneisses may have been metamorphosed in situ (Butt, 1983) at a depth slightly shallower than the depth at which granite melting would occur for that particular geothermal gradient. Evidence for this includes the highly variable texture of the gneisses, which in places is migmatitic, with moderately gneissic fabric in the same outcrop.

Fig. 14 shows Fe_2O_3 + MgO plotted against Al_2O_3/SiO_2 to distinguish tectonic setting in which the protolith sedimentary rocks of the Besham gneisses were deposited (Bhatia, 1983). Fields are derived from Paleozoic rocks of known tectonic setting. The most likely environment appears to be associated with Bhatia's (1983) "active continental margin" field, which is consistent with known geologic constraints. This field includes sediments derived from siliceous volcanic rocks or granitic gneisses of the Besham area that were deposited in marginal retro-arc or pull apart basins.

The Besham gneisses may be correlative to the Nanga Parbat gneisses (Butt, 1983). Both are metamorphic and granitic terrains, and both occurs within the basement rocks of the northern margin of the Indian plate. Geochemical data also allow this correlation.

Near Besham, the sodic quartzofeldspathic gneiss (Lahor granite gneiss) is difficult to separate from the Besham quartzofeldspathic gneiss, due to migmatization, multiple injections and strong pre-Himalayan deformation and metamorphism (Baig, 1990). South of Besham, near Thakot, sodic quartzofeldspathic gneiss clearly intrudes the Besham quartzofeldspathic gneiss and contains its xenoliths (Baig, 1990). These field relations confirm a magmatic nature for the sodic quartzofeldspathic gneiss or Lahor granite gneiss (Baig, 1990). Normative Q-A-P diagram (Fig. 7) and A-C-F ternary diagram (Fig. 6) shows that the sodic granite gneiss is clearly separatable from the Besham quartzofeldspathic gneisses.

The second oldest rocks of the Besham group are mafic dikes that intruded the Besham area. These mafic dikes were metamorphosed to amphibolites. The protolith for the amphibolite bodies found within the Besham area is classified as tholeiitic based on its major element oxides content, as shown on four separate diagrams (Figs. 8, 11, 12 and 14). Field

evidence indicating a protolith for the amphibolite was ambiguous, however, marl was considered to be a potential protolith. This ambiguity was largely due to the transposition of bedding that formed tectonic lenses, pods and boudins in most of the pre-Karora group rocks, thereby disguising cross-cutting relationships.

Trace and major element analyses of the amphibolite suggest that the protolith was tholeiitic, not sedimentary. For example, the concentration of compatible elements (Cr, Co and Sc) are high in the amphibolite. Chromum in the amphibolite varies from 79 to 188 ppm, which is 2 to 5x higher than values reported for sedimentary rocks (Wedepohl, 1978) that could be metamorphosed to produce an amphibolite. Cobalt concentration in the amphibolite is also about 2x higher than values expected for potential sedimentary protoliths.

Trace element abundances may also serve as discriminators of tectonic setting. For example, the REE plot of the Besham area amphibolites is typical of rocks with island arc affinities (Fig. 19). A tectonic discrimination diagram of Th/Hf/3-Ta for the amphibolite is also consistent with a volcanic arc basalt (Wood et al., 1979). Island arc affinities, however, are not particularly consistent with known continental tectonic setting of the Besham area. Continental rift basalt is consistent with known tectonic constraints, and might be a reasonable protolith for the amphibolite. Indeed, values for chromium reported from African rift basalts (Wedepohl, 1978) are similar to chromium concentrations in the amphibolite. Baig and Snee (1991) reported amphibolite of komatiitic affinity from the Besham basement complex on the basis of major element chemistry. They suggested that some of the amphibolites are the metamorphic equivalent of rift-related basaltic komatiites.

The ratio K/Rb may be used as another tectonic discriminator for the amphibolite. K/Rb in the amphibolite ranges from 111 to 143. These values, however, are 0.5x less than values reported for African rift basalts (Wedepohl, 1978).

Geochemical evidence allows, therefore, that the protolith of the amphibolite has volcanic island arc affinities. Furthermore, REE signatures of some mafic dikes in the Nanga Parbat gneiss (Verplanck, 1986) are similar to signatures of amphibolites from the Besham area.

Field and geochemical evidence suggests that

Shang granite, Dubair granodiorite and Shorgara pegmatite are comagmatic. Both the Shang granite and the Dubair granodiorite are peraluminous plutons that intrude the Besham group gneisses and metasediments, and both contain abundant blue-grey microcline. Shorgara pegmatites intrude all the pre-Karora group rocks of the Besham area except the Shang granite and the Dubair granodiorite. Shorgara pegmatite is found only at the margins of the Shang and Dubair plutons, and their abundance rapidly diminishes towards the centers of the plutons.

The spider diagrams for Shang granite and Dubair granodiorite resemble other "S-type" granites (Fig. 16; Thompson et al., 1984). The systematic downward slope from left to right and the strong, negative troughs at strontium, phosphorous and titanium are common characteristics of granites derived from sediments.

On a Q-A-P ternary diagram the Shang and Dubair plutons plot in a tight cluster with the Besham gneiss, thus the sedimentary protolith of the Shang and Dubair plutons may be the same sedimentary protolith from which the Besham gneisses formed (Fig. 7). At some depth below where sedimentary rocks were being metamorphosed into Besham gneisses, melting of the sedimentary protolith might have occurred. This melt might then have migrated upwards into the overlying Besham gneisses as a small intrusion. Pegmatites associated with the small intrusion would cross-cut all the units of the Besham group.

REE plots of the Shang and Dubair plutons (Fig. 21) and the Besham gneisses (Fig. 17) allow the above hypothesis as a model of the relationship between these units. A magma with the REE signature of sample #49c cloud represent the composition of the early melt. The slight positive Eu anomaly progressively became a strong negative anomaly as first melts gave way to melts dominated by potassic feldspar rather than calcic feldspar. REE-enriched sample #122 could represent the end member of the system. The REE signature of the Shorgara pegmatite is also shown on Fig. 21. Potassium feldspar may be responsible for the Eu peak observed in the REE plot of the pegmatite (Grommet and Silver, 1983).

The unconformity above the Besham group separates rocks that have been metamorphosed more than once from rocks that were subjected to only one metamorphic event. Based on field and petrographic evidence, the Karora group has been metamorphosed to lower greenschist facies (Baig, 1990). This most recent

event masks vestiges of earlier event, however, the sediments that comprised the protolith of the Besham gneisses, Shang granite, Dubair granodiorite and Shorgara pegmatite were probably metamorphosed to epidote-amphibolite facies before deposition of the Karora group. The evidence for a pre-Karora group metamorphic event includes the presence of clasts of the Besham gneiss and Shang granite (which are foliated) deposited within the Karora group conglomerate. It is probable that this foliation existed before the clasts were deposited in the conglomerate. Furthermore, pre-Karora group lithologies all demonstrate some degree of tectonic disruption and boudinage. The Karora group apparently has not been subjected to this degree of deformation, as lateral continuity of units is more common in the Karora group than in the pre-Karora group lithologies. The pre-Karora group metamorphic events are dated between 1,840 Ma to 2,000 Ma (Baig and Snee, 1989; Baig et al., 1989; Baig, 1990; Baig et al., 1992; Treloar and Rex, 1990).

The leucogranite intrudes both the Besham group and the Karora group. It is relatively undeformed and unmetamorphosed.

The Mansehra and Choga granites are present on the east and west of the Besham area. The REE plot of the Mansehra granite demonstrates a remarkable correlation of the Mansehra granite to the N.A.S.C. (Fig. 23). Since N.A.S.C. represents the average composition of continental crust, the REE data compliments previous studies by suggesting that the Mansehra granite was derived from continental crust.

The Swat granite gneiss is a suite of porphyritic granites that is similar to the Mansehra granite and is exposed in the lower Swat region, west of Besham (Martin et al., 1962; King, 1964). The REE pattern for the Choga granite mimics the pattern for Mansehra granite and N.A.S.C., but is slightly enriched relative to them (Fig. 23).

CONCLUSIONS

The Besham gneisses were formed from sedimentary protolith. The sodic quartzofeldspathic gneiss (Lahor granite gneiss), Shang granite, Dubair granodiorite and Shorgara pegmatite were formed from the same sedimentary protolith as the Besham gneisses.

Variable protolith composition may be responsible for the bimodal chemistry of the Besham group quartzofeldspathic and sodic quartzofeldspathic gneisses.

Mafic dikes that intrude the pre-Karora group rocks are tholeiitic and have island arc affinities.

There is evidence for more than one metamorphic event in pre-Karora group rocks.

Leucogranite is the youngest unit in the study area.

Gneisses and amphibolites of the Besham area may be correlative to Nanga Parbat gneisses and mafic dikes respectively.

ACKNOWLEDGEMENTS

REFERENCES

Anders, E., and Ebihara, M., (1982). Solar-System abundances of the elements. Geochem. Cosmochem. acta, Vol. 46, pp. 2363-2380.

Ashraf, M., Chaudhry, M.N., and Hussain, S.S., (1980). General geology and economic significance of the Lahor granite and rocks of southern ophiolite belt in Allai-Kohistan area. Geol. Bull. Univ. Peshawar, Vol. 13, pp. 207-213.

Baig, M.S., and Lawrence, R.D., (1987). Precambrian to early Paleozoic orogenesis in the Himalaya. Kashmir Jour. Geol., Vol. 5, pp. 1-22.

Baig, M.S., Lawrence, R.D., and Snee, L.W., (1988). Evidence for late Precambrian to early Cambrian orogeny in northwest Himalaya, Pakistan. Geol. Mag., Vol. 125, No. 1, pp. 83-86.

Baig, M.S., and Snee, L.W., (1989). Pre-Himalayan dynamothermal and plutonic activity preserved in the Himalayan collision zone, NW Pakistan. Geol. Soc. Am. Abst. with Programs, Vol. 21, No. 6, pp. 264.

Baig, M.S., Snee, L.W., LaFortune, J.R., and Lawrence, R.D., (1989). Timing of pre-Himalayan orogenic

events in the northwest Himalaya: $^{40}Ar/^{39}Ar$ constraints. *Kashmir Jour. Geol.*, Vol. 6 & 7, pp. 29-39.

Baig, M.S., (1990). Structure and geochronology of pre-Himalayan and Himalayan orogenic events in the northwest Himalaya, Pakistan, with special reference to the Besham area. Unpublished Ph.D. thesis, Oregon State University, Corvallis, Oregon, U.S.A. 397 p.

Baig, M.S., and Snee, L.W., (1991). A discovery of Late Archean to Early Proterozoic Komatiite from the northwestern margin of the Indian plate Besham area, Northwest Himalaya Pakistan. *Kashmir Jour. Geol.*, Vol. 8-9, pp. 19-23.

Baig, M.S., (1991). Geochronology of pre-Himalayan and Himalayan tectonic events, northwest Himalaya, Pakistan. *Kashmir Jour. Geol.*, Vol. 8-9, pp. 197.

Baig, M.S., Snee, L.W., and Lawrence, R.D., (1992). Early Proterozoic to Late Paleozoic tectonic history of the northwest Himalaya, Pakistan: $^{40}Ar/^{39}Ar$ constriants. *Geol. Soc. Am. Abst. with Programs*, Vol. 24, pp. 250.

Bhatia, M.R., (1983). Plate tectonics and geochemical composition of sandstones. *Jour. Geol.*, Vol. 91, pp. 611-627.

Butt, K.A., (1983). Petrology and geochemical evolution of Lahor pegmatoid/granite complex, northern Pakistan, and genesis of associated Pb-Zn-Mo and U mineralization. In: Granites of the Himalayas, Karakorum and Hindu Kush (Ed. F.A. Shams), *Institute of Geology, Punjab University, Lahore, Pakistan.* pp. 309-326.

Calkins, J.A., Offield, T.W., Abdullah, S.K.M., and Ali, S.T., (1975). Geology of the southern Himalayas in Hazara. *U.S.G.S. Prof. Paper 716-C*, 29 p.

Chaudhry, M.N., Ashraf, M., and Hussain, S.S., (1983). Lead-Zinc mineralization of Lower Kohistan District, Hazara Division, NW Frontier Province, Pakistan. *Kashmir Jour. Geol.*, Vol. 1, No. 1, pp. 31-37.

Coward, M.P., and Jan, M.Q., (1982). Geotectonic framework of the Himalaya of N. Pakistan. *Jour. Geol. Soc., London*, Vol. 139, pp. 299-308.

Fletcher, C.J.N., Leake, R.C., and Haslam, H.W., (1986). Tectonic setting, mineralogy and chemistry of a metamorphosed stratiform base metal deposit within the Himalayas of Pakistan. *Jour. Geol. Soc., London*, Vol. 143, pp. 521-536.

Gregg, J.M., and Sibley, D.F., (1984). Epigenetic dolomitization and the origin of xenotopic dolomite texture. *Jour. Sed. Petrol.*, Vol. 54, No. 3, pp. 908-931.

Grommet, L.P., and Silver, L.T., (1983). Rare earth element distributions among minerals in a granodiorite and their petrogenetic implications. *Geochem. Cosmochem. Acta*, Vol. 47, pp. 925-939.

Haskin, L.A., Haskin, M.A., Frey, F.A., and Wildeman, T.R., (1968). Relative and absolute abundances of the rare earth elements. In: Origin and Distribution of Elements (Ed. L.H. Ahrens), *Pergamon, Oxford Press*, pp. 889-912.

Irvine, T.N., and Baragar, W.R.A., (1971). A guide to the chemical classification of the common volcanic rocks. *Canadian Jour. Earth. Sci.*, Vol. 8, pp. 523-548.

Jacob, K.H., and Quittmeyer, R.C., (1979). The Markran region of Pakistan and Iran: trench-arc system with active plate subduction. In: Geodynamics of Pakistan (Eds. A. Farah and K.A., DeJong), *Geological Survey Pakistan, Quetta, Pakistan*, pp. 305-317.

Jan, M.Q., and Tahirkheli, R.A.K., (1969). The geology of the lower part of Indus Kohistan (Swat), West Pakistan. *Geol. Bull. Univ. Peshawar*, Vol. 4, pp. 1-13.

Klootwijk, C.T., Conaghan, P.J., and Powell, C., (1985). The Himalayan Arc: large-scale continental subduction, oroclinal bending and back-arc spreading. *Earth Planet. Sci. Lett.*, Vol. 75, pp. 167-183.

King, B.H., (1964). The structure and petrology of part of Lower Swat, West Pakistan, with special reference to the origin of granite gneisses, Unpublished Ph.D. thesis, University of London, 130 p.

Lawrence, R.D., and Ghauri, A.A.K., (1983). Observations on the structure of the Main Mantle Thrust at Jijal, Kohistan, Pakistan. *Geol. Bull. Univ. Peshawar*, Vol. 16, pp. 1-10.

Le Fort, P., Debon, F., and Sonet, J., (1980). The "Lesser Himalayan" cordierite granite belt, typology and age of the pluton of Mansehra, Pakistan. *Geol. Bull. Univ. Peshawar*, Vol. 13, pp. 51-62.

Martin, N.R., Siddiqui, S.F.A., and King, B.H., (1962). A geological reconnaissance of the region between the lower Swat and Indus Rivers of Pakistan. *Geol. Bull. Univ. Peshawar*, Vol. 2, pp. 1-14.

Molnar, P., (1986). The geological history and structure of the Himalaya. *American Scientist*, Vol. 247, pp. 321-355.

Molnar, P., and Tapponnier, P., (1975). Cenozoic tectonics of Asia: effects of a continental collision. *Science*, Vol. 189, pp. 419-426.

Miyashiro, A., (1974). Volcanic rock series in island arcs and active continental margin. *Am. Jour. Sci.*, Vol. 247, pp. 321-355.

Powell, C. A., (1979). A speculative tectonic history of Pakistan and surroundings: some constraints from the Indian Ocean. In: Geodynamics of Pakistan (Eds. A. Farah and K.A., DeJong), *Geological Survey Pakistan, Quetta, Pakistan*, pp. 5-24.

Seeber, L., Armbruster, J.G., and Quittmeyer, R.C., (1981). Seismicity and continental subduction in the Himalayan arc. In: Zagros, Hindu-Kush, Himalaya. Geodynamic Evolution (Eds. H.K. Gupta and F.M. Delany). *A.G.U. Geodyn. Ser.*, Vol. 3, pp. 215-242.

Sengor, A.M.C., (1979). Mid-Mesozoic closure of Permo-Triassic Tethys and its implications. *Nature*, Vol. 279, pp. 590-593.

Sun, S.S., (1980). Lead isotopic study of young volcanic rocks from mid-ocean ridges, ocean islands and insland arcs. *Phil. Trans. Royal Soc., London, Ser. A.*, Vol. 297, pp. 409-445.

Tahirkheli, R.A.K., and Jan, M.Q., (1979). A preliminary geological map of Kohistan and adjoining areas, N. Pakistan. 1: 1,000,000. *Geol. Bull. Univ. Peshawar*, Vol. 11.

Taylor, S.R., and McClennan, S.M., (1985). The continental crust; its composition and evolution (Ed. A. Hallam), *Blackwell Scientific Publications,* Palo Alto, CA., 312 p.

Treloar, P.J., and Rex, D.C., (1990). Cooling and uplift histories of the crystalline thrust stack of the Indian plate internal zones west of Nanga Parbat, Pakistan Himalaya. *Tectonophysics*, Vol. 180, pp. 323-349.

VerPlanck, K.H., (1986). A field and geochemical study of the boundary between the Nanga Parbat-Haramosh Massif and the Ladakh Arc terrance, northern Pakistan. Unpublished M.S. thesis, Oregon State University, U.S.A. 136 p.

Wedepohl, K.H., (1978). Handbook of Geochemistry *Springar-Verlag, New York, NY.* Vol. 2.

Wood, D.A., Joron, J.L., and Treuil, M., (1979). A reapppraisal of the use of trace elements to classify and discriminate between magma series erupted in different tectonic settings. *Earth Planet. Sci. Lett.*, Vol. 45, pp. 326-336.

Yeats, R.S., and Lawrence, R.D., (1984). Tectonics of the Himalayan thrust belt in northern Pakistan. In Marian Geology and Oceanography of Arabia Sea and Coastal Pakistan (Eds. B.U. Haq and J.D. Milliman), *Van Nostrand Reinhold*, pp. 177-198.

Yeats, R.S., and Hussain, A., (1987). Timing of structural events in the Himalayan foothills of northwestern Pakistan. *G.S.A. Bull.*, Vol. 99, pp. 161-176.

BULK-ROCK AND MINERAL CHEMISTRY OF ANATECTIC AND FRACTIONATED ACIDIC ROCKS COEXISTING IN THE BELA OPHIOLITE

By

ZULFIQAR AHMED[*]

National Centre of Excellence in Mineralogy, University of Balochistan, G.P.O. Box 43, Quetta, Pakistan.

ABSTRACT: *Acidic rocks are extensively developed in the Bela ophiolite. They occur as large as well as small-sized bodies in a variety of forms. There are two distinct rock suites. The oceanic plagiogranite consists of dioritic rocks, tonalites, trondjhemites, albite granites and other leucocratic rocks formed by fractional crystallization from a basic magma. This rock suite makes the uppermost plutonic-rock unit of the ophiolite. The associated anatectic acidic rock suite is made of potash-rich granites, granophyres and trondhjemites developed by anatexis caused probably by the heat of the ophiolite. Most outcrops occur in the upper peripheral part of the ophiolite. The differences in the whole-rock and phase chemistry between these two rock suites are highlighted and interpreted in this study.*

INTRODUCTION

Ophiolites often carry leucocratic rocks collectively named oceanic plagiogranite by Coleman & Peterman (1975). The plagiogranites are soda-rich, potash-poor rocks comprised of one or more of the following rock units: trondhjemite, albite granite, tonalite, quartz diorite, keratophyre and albitite. These rocks often form by low-pressure differentiation of sub-alkaline basaltic magma favoured by the slow-spreading centres. The fractionation model has been supported in subsequent studies (e.g. Pallister & Knight 1981). Later work (e.g., Gerlach et al., 1981; Pedersen & Malpas, 1984; Flagler & Spray, 1991) has convinced that the plagiogranitic rocks also form by the anatexis of amphibolite. Gerlach et al. (1981) presented field and geochemical evidence from the Canyon Mountain ophiolite, Oregon, for the production of plagiogranite by partial melting of basic rocks under hydrous conditions. Flagler and Spray (1991) presented field, geochronological and rare earth element (REE) evidence for generation of plagiogranite in the Fournier oceanic fragment by the anatexis of amphibolite formed along shear zones in gabbro caused by dynamothermal processes in proximity to a spreading centre.

Previous studies have also recognized more than one genetic type of leucocratic rock suites from individual ophiolites. The leucocratic rocks of the Sarmiento ophiolite complex, southern Chile, were shown geochemically by Saunders et al. (1979) to belong to two types; (a) trondhjemites and granophyres formed by refusion and assimilation of continental sialic material around the mafic rocks; and, (b) plagiogranites as defined by Coleman and Peterman (1975) formed by high level differentiation of the mafic magma.

Pedersen and Malpas (1984) found two suites of leucocratic rocks in the plutonic zone of Karmoy ophiolite of western Norway: one suite formed by the anatexis of amphibolite and the other by the filter pressing of a differentiated interstitial liquid plus autometasomatism.

Pearce (1989) recognized sub-ophiolitic granitic rocks formed by the anatexis of sedimentary rocks in the high T/P metamorphic aureoles of three ophiolite complexes: the Semail thrust sheet of Oman, the Guevgueli complex of northern Greece and the Lizard complex of SW England. The first two of these possess plagiogranites as well.

---

[*] Present address: Institute of Geology, Punjab University, New Campus, Lahore.

This paper includes field relations, geochemistry, petrology and phase chemistry of the leucocratic rocks of the Bela ophiolite which comprise fractionated plagiogranite as well as the anatectic acidic rocks (Map A).

FIELD RELATIONS AND PETROGRAPHY

The Bela ophiolitic rocks are excellently exposed in a general N-S trend for over 400 km length between Gadani Hill, west of Karachi city (Gansser, 1979) and Karku Jhal, NW of Nal town in Khuzdar District. In addition, tectonically emplaced minor outcrops occur several km away from the main outcrops, such as the basaltic body at Pir Umar, Khuzdar District, and the ophiolitic melange at Takhte Siah, Kalat District. The N-S elongation of the ophiolite parallels and lies close to the western margin of the Indian plate. Earlier workers (e.g., Kazmi, 1979) believed that the western margin of the Indian plate is defined by the zone of transform faults called Chaman Fault. However, the recent study of the Bela ophiolite by the author conforms to the idea that the Bela ophiolite itself may lie at the western boundary of the Indian plate in this sector. The minimum age of the Bela ophiolite, based upon palaeontological evidence of overlying strata is late Eocene (Allemann, 1979).

The Bela ophiolite shows development of all the members of a typical stratigraphic sequence of ophiolites. These include: lherzolite, harzburgite, wehrlite, dunite, podiform chromitite, clinopyroxenite, layered gabbro, isotropic gabbro, sheeted diabase dykes, basaltic pillow lavas, chert interbedded with volcanics, shale, limestone, plagiogranite and keratophyre. Pyroxenite and dolerite also occur as satellitic dykes inside ultramafic rock outcrops. Rock units of the mantle sequence are much less in volume relative to the crustal units. An ophiolitic melange constitutes a large part of the ophiolite outcrops. However, the ophiolitic rocks occur in typical sequence intact at many places, especially the large massif around Lak Baran area.

The leucocratic rocks are commonly conspicuous on outcrops except in a few cases of darkish weathering colour. The leucocratic rocks form discrete major bodies, upto a few km in longer dimensions, as well as minor, dyke-like, vein-shaped and lensoid bodies. The outcrops are surrounded by rocks of mafic to intermediate compositions. All the leucocratic rock outcrops lie in the land area of Khuzdar District. This forms the northern and mid-northern section of the over 400 km north-south length of the ophiolite. Along

length, the ophiolite stretches from 25° N to 27° 52′ N latitude. The leucocratic rocks are restricted to the stretch between 27° N and 27° 52′ N latitudes. Longitudinally, they lie between 66° 8′ 66° and 25′ E.

The anatectic acidic rocks comprise bodies of granites with included pegmatites, granophyres and trondhjemites. They often make large masses upto several hundred metres in longer dimensions.

In the area comprising rocky outcrops south of the alluvial plain of Wadh town, a few km long zone of dyke-like to lensoid bodies of acidic plutonic rock occurs intruding the sheeted doleritedkyes.

At Purwait Bhut, further south from Wadh town, a conspicuous white mound comprises acidic plutonic rock that is intrusive into underlying diorite. The contact zone shows diorite xenoliths trapped in the acidic rock which has sent apophyses into the diorite. However, these features are restricted to the contact zone only and do not pervade within the outcrop of either rock type.

There are also small lensoid bodies of acidic rock emplaced tectonically into mafic rocks near Lohi Jhal, south of Wadh town.

NW of Nal town, about 2 km west from Karku Jhal, greyish coloured biotite granite is present. The rock is traversed by veins of pinkish pegmatite and of quartz breccia. The biotite granite is in contact with pillowed basalts and Mn-bearing sediments.

Another big outcrop of pink granite is exposed on the left bank of Porali River about 6 km north of Khazini in Khuzdar District.

The term plagiogranite is followed here from Coleman & Peterman (1975), and includes the spectrum from dioritic to trondhjemitic rocks. The lithologies include leucogabbro, diorite, quartz diorite, tonalite, trondhjemite, albite granite and keratophyre. There are also trondhjemites that contain fresher, greenish, epidote with magmatic appearance. The plagiogranites form one big outcrop overlying isotropic gabbro and dolerite. This outcrop appears to lie undisturbed in its position in the ophiolitic sequence which begins with the ultramafic lherzolite and harzburgite near Lak Baran. It is succeeded north- and east-wards by the cumulate dunite with mineable chromitite bodies of lenticular layer type. Further up-section one successively finds pyroxenite horizon, layered gabbro, isotropic gabbro, diorite and acidic
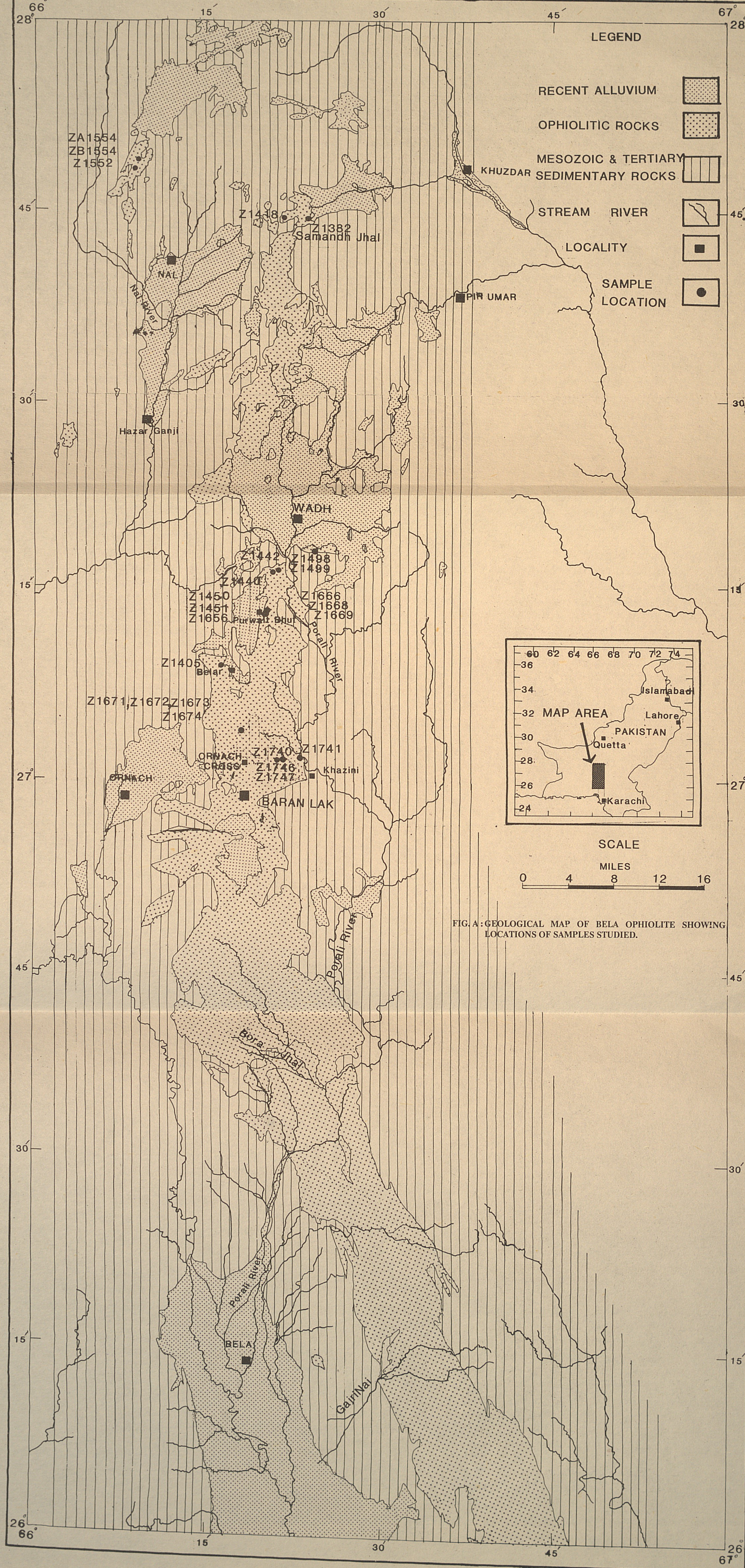
FIG. A : GEOLOGICAL MAP OF BELA OPHIOLITE SHOWING LOCATIONS OF SAMPLES STUDIED.

LEGEND

RECENT ALLUVIUM

OPHIOLITIC ROCKS

MESOZOIC & TERTIARY SEDIMENTARY ROCKS

STREAM   RIVER

LOCALITY

SAMPLE LOCATION

ZA1554
ZB1554
Z1552

KHUZDAR

Z1448
Z1382
Samandh Jhal

NAL

Nal River

PIR UMAR

Hazar Ganji

WADH

Z1442
Z1498
Z1499
Z1440
Z1450
Z1451
Z1656 Purwali Bhul

Z1666
Z1668
Z1669

Porali River

Z1405
Belar

Z1671 Z1672 Z1673
Z1674

ORNACH
CROSS
Z1740
Z1741
Z1746
Z1747
Khazini

ORNACH

BARAN LAK

Bora Jhal

Porali River

BELA

Gar Nai

MAP AREA

Islamabad
Lahore
PAKISTAN
Quetta
Karachi

SCALE

MILES

0   4   8   12   16

plagiogranite. A big keratophyre outcrop is present near Goth Shafi, north of Wadh town. Minor outcrops of keratophyre occur near Belar.

BULK-ROCK CHEMISTRY

The bulk-rock samples were analyzed for their major-, trace- and rare earth - elements employing the x-ray fluorescence (XRF), direct current plasma (DCP), and inductively coupled plasma atomic emmission spectrometric (ICP-AES) techniques. The details of the procedures employed and precision are given in Ahmed (1991).

The results of whole-rock analyses are displayed graphically is Figs. 1 to 5. High soda and very low potash are characteristic of plagiogranites (Fig. 1).

The plagiogranite analyses display high silica, low to moderate alumina, low total iron magnesium and extremely low potash characteristic of oceanic plagiogranite. Normative orthoclase is below 1 mol %, and the normative An content of the plagioclase ranges from An_{21} to An_{51}, except one sample with An_{10}. The wide range in An content shows differentiation from gabbroic composition towards leucocratic types. The plot of normative Or, An and Ab (Fig. 5) reveals that the plagiogranites fall within the low-pressure one-feldspar boundary.

The normative feldspar content of the anatectic rocks is usually high and may contain upto 51 % Or.

The differentiation of plagiogranites is also shown on the triangular Alk-F-M diagram after Coleman & Peterman (1975) in Fig. 3. The samples seem to follow the ophiolitic tholeiite differentiation trend.

The anatectic rocks also show a tholeiitic trend but contain more iron and potash than the plagiogranites.

It is generally held that the high-field-strength elements (HFSE: Ti, Zr, Y, Nb, Ta, Hf), transition metals (TM: Sc, V, Cr, Ni) and REE are essentially immobile during all but the most severe seafloor hydrothermal alteration. Low-field-strength elements (LFSE: Cs, Rb, Ba, Sr) and certain other elements like

Si, K and Na are mobile in hydrous fluids (e.g., Pearce, 1975; Humphris & Thompson, 1978; Wood et al., 1979; Middleburg et al., 1988).

Samples of the anatectic acidic rocks especially more K-rich types are, in general, richer in incompatible trace elements compared to the plagiogranite samples (Fig. 2).

In terms of tectonic classes of granites established by Pearce et al. (1984), the plagiogranitic rocks belong to the "ocean ridge granites" and "volcanic arc granites" categories.

The REE data on acidic rock samples (Table 2) shows the presence of two distinct types of chondrite-normalized behaviour. The anatectic potassic granites (e.g., sample Nos. Z1440, Z1450) show LREE-enrichment with distinct negatively anomalous values of Eu. Elements Sm - La range from 19 to 65 times chondritic values. The feature resembles the pattern of sodic Fournier plagiogranite supposedly formed by amphibolite anatexis (Flagler & Spray, 1991, Fig. 3A). However, the HREE part of the potassic Bela samples is different and does not show a gradient. It stays around 11 to 16 times chondritic values for the elements Gd to Lu. The Bela samples are also different from the amphibolite- anatectic plagiogranites of East Karmoy which display lower REE abundances combined with anomalously higher Eu (Pedersen & Malpas, 1984). The anatectic rocks of Bela possess REE similar to the pattern of sample OM2 of the anatectic granite from Oman ophiolite thrust sheet (Pearce, 1989, Fig. 4a) supposedly formed by melting of crustal sediments.

The REE contents of plagiogranite sample (No. Z1673, Table 2) does not show large variations, and the abundances stay between 13 and 18.5 times chondritic. There is only slight LREE depletion relative to HREE. The Eu values are not anomalous. Such values resemble those of the Visnes-type plagiogranite of Pedersen & Malpas (1984) which, however, differs in possessing higher REE and distinctly negative Eu anomaly. The plagiogranites of Ibra area of the Samail ophiolite (Pallister & Knight, 1981) also differ in their higher REE abundances, negative Eu anomalies and stronger LREE depletions.
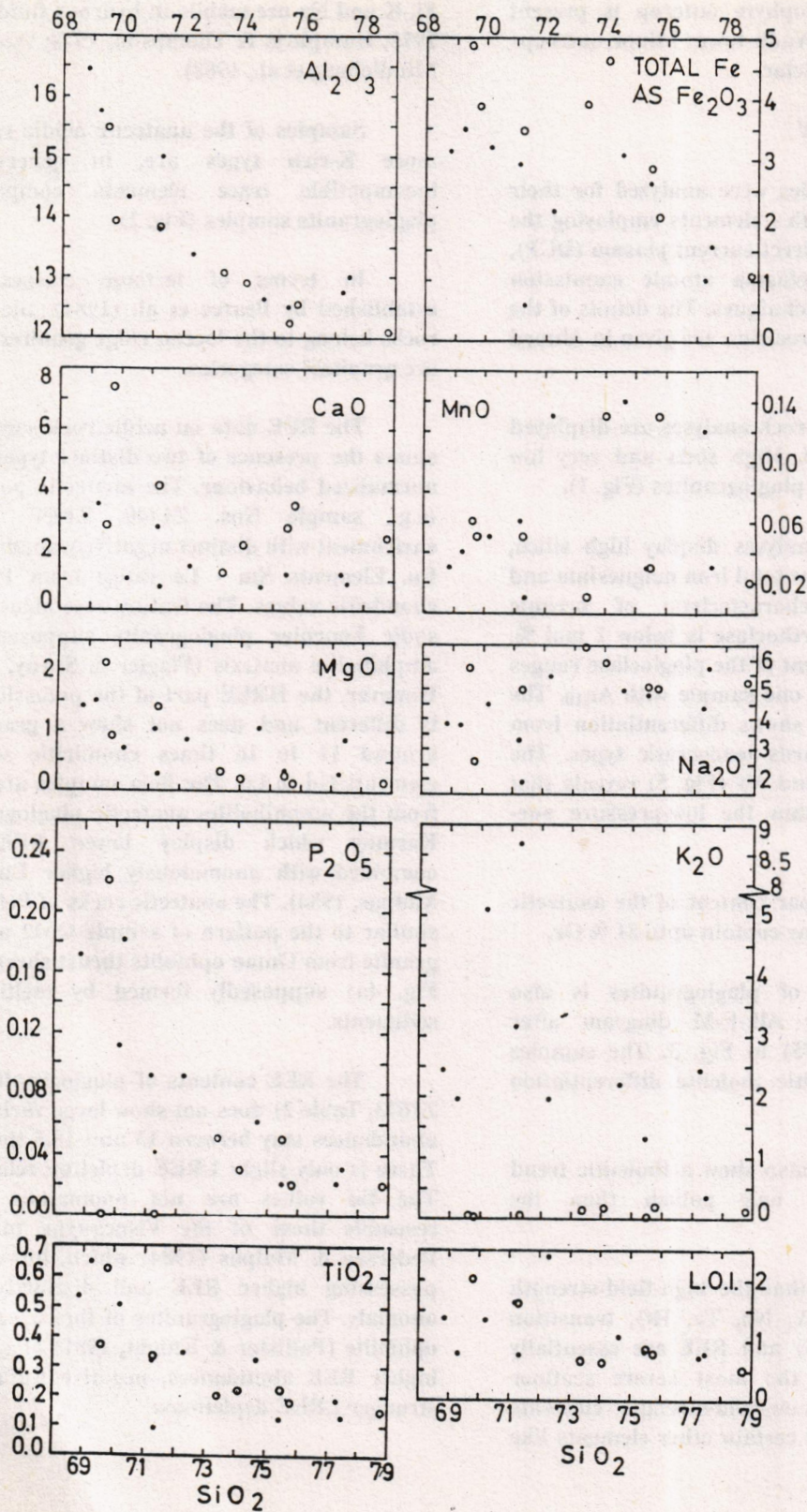
Fig. 1. Covariation diagrams for wt % major elements versus SiO₂ for the two acidic rock suites of Khuzdar District representing magma-fractionated (circles) and anatectic (dots) rocks.
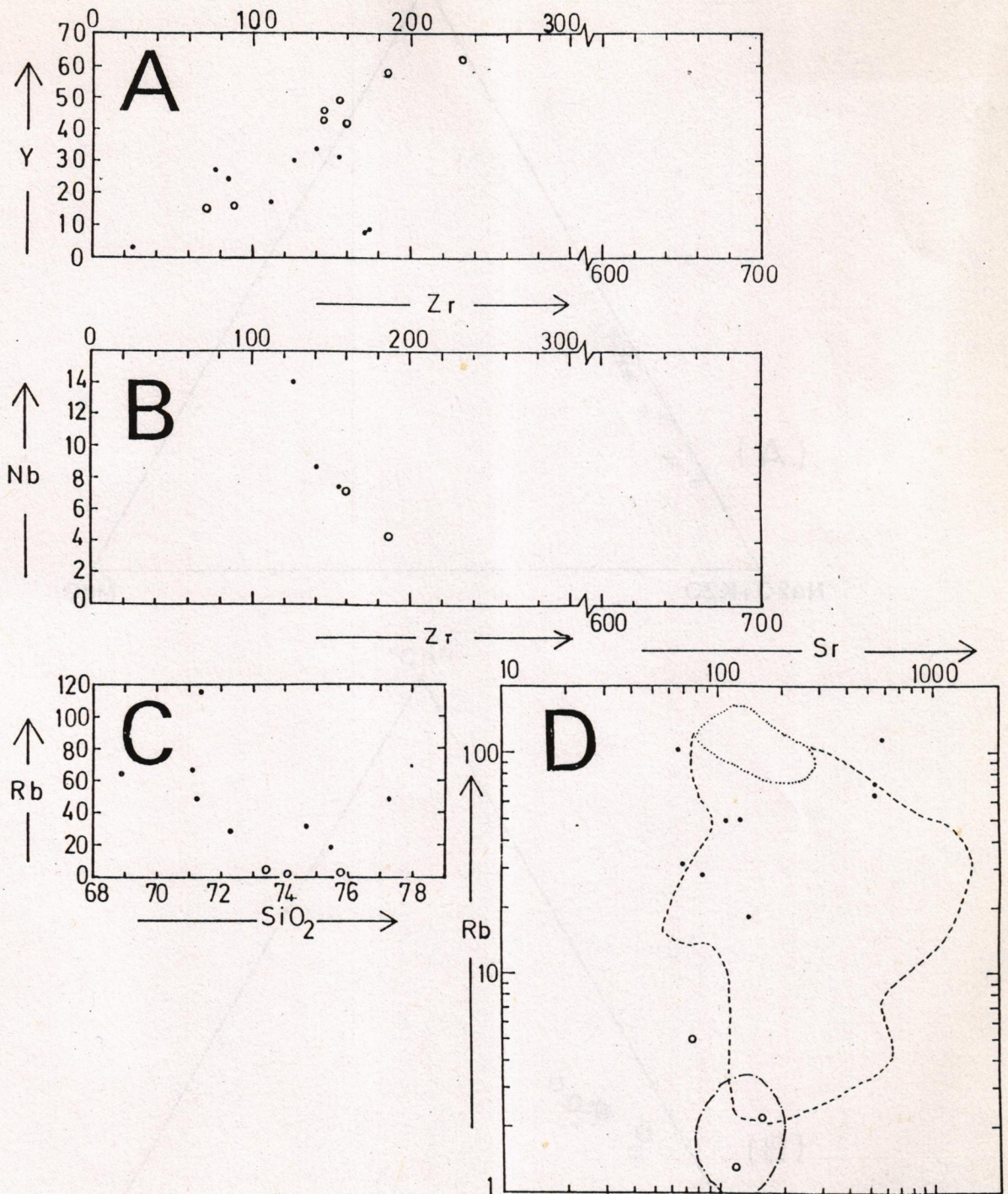
Fig. 2. (A to D) Bivariant plots of trace elements for the magma-fractionated acidic rock suite (circles) and anatectic acidic rock suite (dots). Values are in p.p.m. except for SiO_2 in wt. %. Fields drawn in Fig. 4D are after Coleman & Peterman (1975) and represent oceanic plagiogranite (dash-dot outline), continental granophyres and Iceland pitchstone (dotted outline), and island arc and continental margin calc-alkaline basalt to rhyolite rocks (dashed outline).
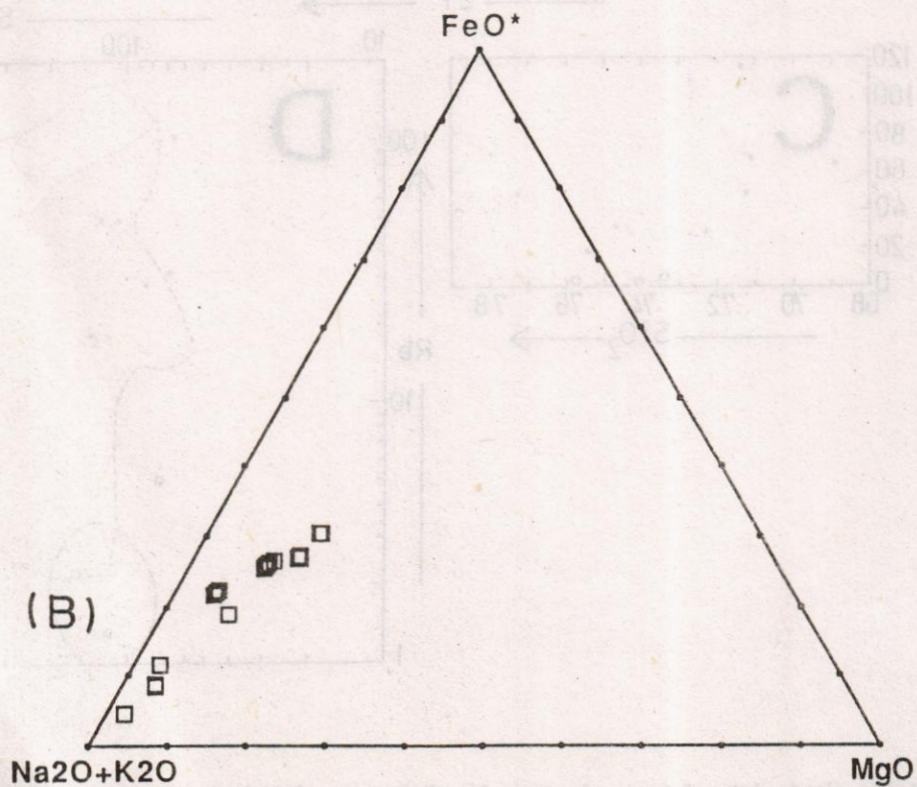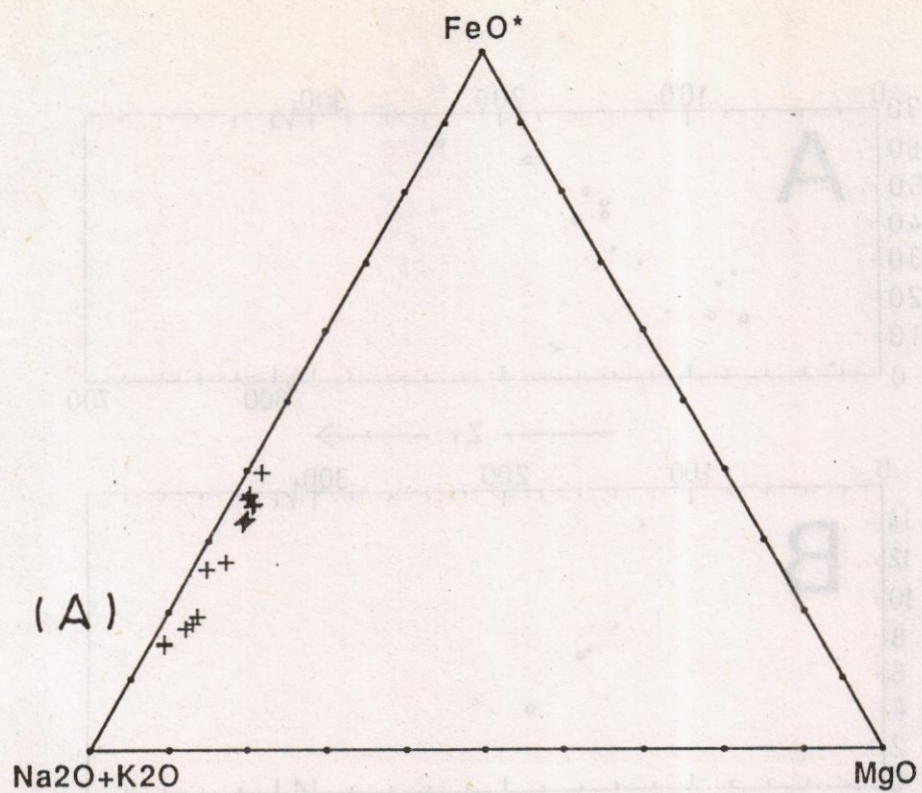
Fig. 3.   Alk - F - M diagram after Coleman & Peterman (1975) for the acidic rocks of the Bela ophiolite showing the variation in (A) magma fractionated; and (B) anatectic acidic rocks.
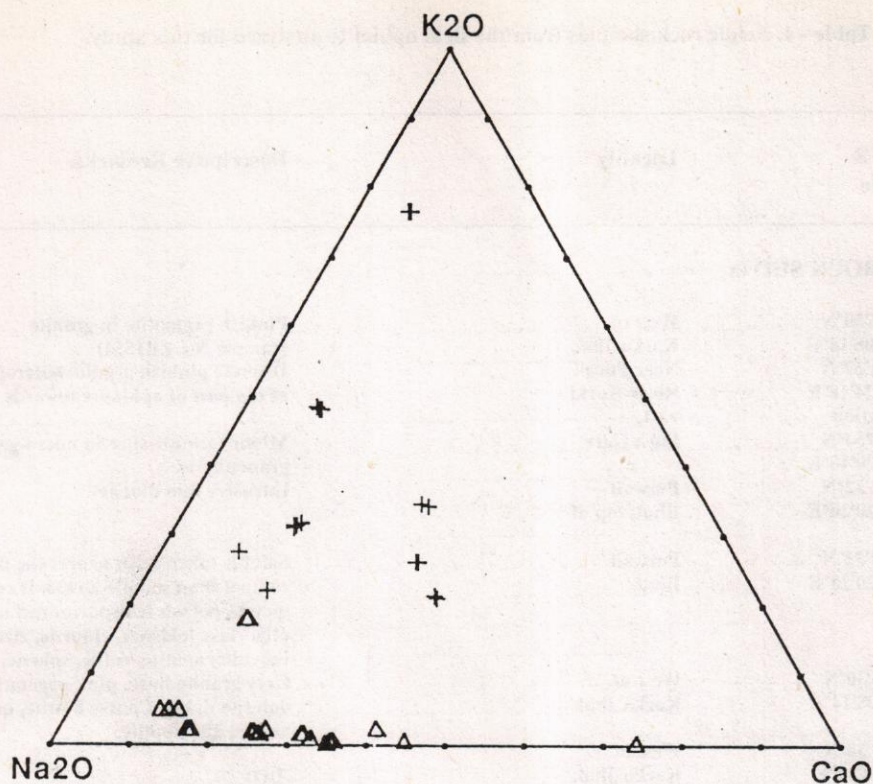
Fig. 4.   CaO - Na₂O - K₂O plot for the acidic rocks of Bela ophiolite, plotting separately the sodic acidic rocks (triangles) and potassic granitic rocks (crosses).
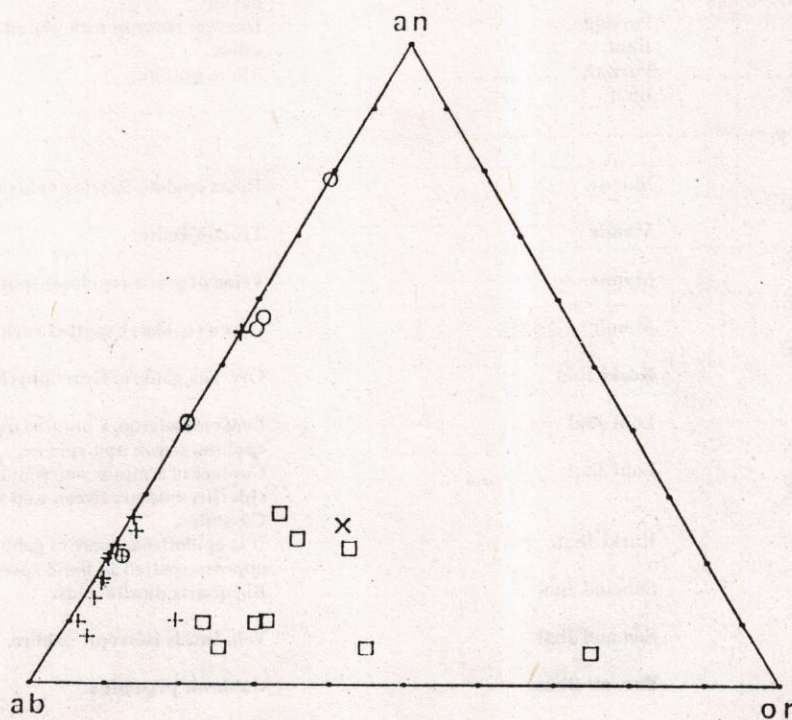
Fig. 5.   Triangular diagram showing the normative content of ab, an and or for leucocratic rocks of the Bela ophiolite. The oceanic plagiogranites with acidic (plus sign) and subacidic (circles) silica content are distinct from the coexisting anatectic acidic rocks (squares) and diorite (X). The latter plot in the same space as the continental trondhjemites and granophyres (Coleman & Peterman, 1975).

59

Table - 1. Acidic rock samples from the Bela ophiolite analyzed for this study.

Sample No.	latitude & longitude	Locality	Descriptive Remarks.
I. ANATECTIC ACIDIC ROCK SUITE:			
ZA1554	lat. 27°45'30"N long. 66°08'14"E	West of Karku Jhal.	Pinkish pegmatite in granite (sample No. ZB1554)
Z1741	lat. 27°01'57"N long. 66°24'18"E Jhal Junction	Near Porali River-Kurki east.	Discrete pinkish granite outcrop at top part of ophiolite towards
Z1442	lat. 27°15'54"N long. 66°20'40"E	Laya Garr	Minor tectonic slice in micro-gabbro. It is granophyric.
Z1450	lat. 27°12'32"N long. 66°20'20"E hillock.	Purwait Bhut; top of	Intrusive into diorite.
Z1656	lat. 27°12'32"N long. 66°20'20"E	Purwait Bhut.	Sample taken from nearer the diorite contact than sample Z1450. It contains quartz, potash feldspar, zoned albite-oligoclase feldspar, chlorite, zircon, ilmenite, apatite, rutile, sphene.
ZB1554	lat. 27°45'30"N long. 66°08'14"E	West of Karku Jhal.	Grey granite hosts pink pegmatite and dolerite dykes. Coarse biotite, quartz, zircon, and apatite.
Z1552	lat. 27°45'30"N long 66°08'14"E	West of Karku Jhal.	-DO-
Z1440	lat. 27°16'14"N long. 66°20'33"E	Laya Garr,	Keratophyre that occurs as a cluster of dykes interdigitating with diabase.
Z1405	lat. 27°08'51"N long. 66°16'40"E	Belar	Keratophyre; hosts dykes of porphyritic basalt
Z1666	lat. 27°12'49"N long. 66°20'24E	Purwait Bhut	Discrete outcrop with abundant quartz, albite.
Z1451	lat. 27°12'54"N long. 66°20'24"E	Purwait Bhut	Albite granite.
II. FRACTIONATED ROCKS SUITE:			
Z1672	lat. 27°03'41"N long. 66°17'44"E	Mamir.	Hosts epidote-bearing veins (sample Z1671).
Z1673	lat. 27°03'41"N long. 66°17'43"E	Mamir	Trondhjemite.
Z1671	lat. 27°03'41"N long. 66°17'44"E	Mamir	Veins of green (epidote) spotted rock.
Z1674	lat. 27°03'41"N long. 66°17'44"E	Mamir	Green (epidote) spotted rock as discrete outcrop.
Z1747	lat. 27°01'40"N long. 66°22'E	Kurki Jhal	Overlies gabbro. Granophyric textured, non-spotted.
Z1498	lat. 27°18'17"N long. 66°24'05"E	Lohi Jhal	Lensoid outcrop. Contains quartz, albite, chlorite, epidote, zircon and sphene.
Z1499	lat. 27°18'17"N long. 66°24'05"E	Lohi Jhal	Contact of a minor outcrop; contains quartz, albite, chlorite, epidote, zircon and sphene. Richin green Cu-stains.
Z1746	lat. 27°01'40"N long. 66°22'E	Kurki Jhal.	It is epidotized, overlies gabbro, and appears spotted in hand speeimens.
Z1418	lat. 27°44'13"N long. 66°20'26"E	Samand Jhal	Big quartz diorite body.
Z1382	lat. 27°44'36"N long. 66°23'E	Samand Jhal	Vein inside isotropic gabbro.
Z1669	lat. 27°12'49"N long. 66°20'24"E	Purwait Bhut.	Gabbroic pegmatite.
Z1668	lat. 27°12'49"N long. 66°20'24"E	Purwait Bhut	Diorite.
Z1740	lat. 27°01'27"N long. 66°23'09"E	2.5 km NE of Khushhal Garr	Diorite.

Table 2. Rare-earth element analyses from plagiogranite and anatectic acidic rock samples.

Concentrations in p.p.m.:				Chondrite-normalized values:		
Sample No:	Z1673	Z1440	Z1450	Z1673	Z1440	Z1450
La	4.30	19.60	21.40	13.0	59.4	64.8
Ce	12.10	38.00	41.70	14.0	43.9	48.2
Pr	2.00	4.51	4.66	16.4	37.0	38.2
Nd	9.80	16.00	17.40	15.6	25.4	27.6
Sm	3.44	3.98	3.88	16.9	19.6	19.1
Eu	1.32	1.03	0.73	17.1	13.4	9.5
Gd	4.78	4.37	3.85	17.4	15.9	14.0
Dy	6.31	5.07	4.27	18.5	14.8	12.5
Ho	1.22	0.98	0.82	16.1	12.9	10.8
Er	3.93	3.09	2.57	17.5	13.7	11.4
Yb	3.89	3.09	2.83	17.7	14.0	12.9
Lu	0.58	0.47	0.43	17.1	13.8	12.6

MINERAL CHEMISTRY

The rock samples were made into polished thin sections and after carbon-coating, analyzed with the JEOL-733 SUPERPROBE instrument set up at the California Institute of Technology (CALTECH), U.S.A. Standard procedures for wavelength-dispersive analyses were employed to acquire high-quality data. The cationic mineral formulae were calculated, in most cases, by MINTAB computer programme written by Rock & Carroll (1990).

Feldspar Compositions

The plagioclase is rather variable in composition. Albite is most abundant. More calcic laths are saussuritized. There are symplectic and myrmekitic intergrowths between sodic plagioclase and quartz. Graphic intergrowths of albite and quartz are also present in some samples. Granophyric texture is extensively developed. Polysynthetic albite twinning is common.

Representative feldspar compositions for the anatectic acidic rock samples are provided in Table 3 and those for the plagiogranitic samples in Table 4. The structural formulae of analyses in Tables 3 and 4 are calculated to 8 oxygens. Most of them are fairly close to the ideal formula of $Z = 4$ and $X = 1$. The Z totals are slightly more than 4 and X slightly less than one for 27 out of 44 analyses reported. The problem of silica excess is common in plagioclases (Deer *et al.*, 1962). The anorthite contents of the analyses closely match those optically determined. The extent of substitution for Mg, Ti and Fe is trivial in all the feldspars, especially for the former two elements. Phosphorus is below detection level in all the analyses.

In plagiogranitic rocks of acid composition (Table 4) all analyses conform to albite composition. The most calcic composition has $An_{8.77}$. Within-sample variation is not large, and remains within the albite range. Such compositions normally result from crystallization differentiation in igneous rocks; although metasomatic albitization is also possible.

K-feldspar occurs only in samples Z1656 and Z1442; both are of anatectic granites. Sample Z1656 also has zoned plagioclase with rather high An content. This Ca could have come from wall-rock assimilation, and is in contrast to the low Ca content for the acidic plagiogranite formed by fractional crystallization

Table - 3 Feldspar compositions from anatectic acidic rocks of Khuzdar District. Total iron assumed as ferric.

Anal. No.	617	616	614	613	609	608	754	753	749	745	750	765	743	766	742	752
Sp. No.	Z1552	Z1656	Z1552	Z1442	Z1552	Z1552	Z1656	Z1656	Z1656	Z1656	Z1656	Z1656	Z1656	Z1656	Z1656	Z1656
	CORE	RIM	CORE	RIM			CORE	RIM								
SiO_2	62.35	61.95	60.01	62.96	59.26	57.22	64.26	65.42	70.05	73.08	70.51	65.98	70.10	71.83	72.07	71.83
Al_2O_3	24.46	24.04	24.84	24.07	24.66	24.33	22.00	21.47	22.22	21.05	20.69	20.73	20.61	19.86	19.59	19.37
Fe_2O_3	0.03	0.05	0.02	0.03	0.06	0.02	0.19	0.09	0.07	0.04	0.01	0.22	0.06	0.11	0.00	0.06
MnO	0.00	0.00	0.00	0.00	0.02	0.01	0.03	0.00	0.00	0.00	0.01	0.00	0.00	0.00	0.01	0.00
CaO	5.94	5.45	6.41	5.63	6.47	6.35	3.56	2.92	2.46	0.75	1.56	1.78	1.49	0.55	0.23	0.23
BaO	0.07	0.04	0.01	0.00	0.06	0.06	0.08	0.03	0.04	0.00	0.00	0.03	0.00	0.04	0.00	0.00
SrO	0.17	0.00	0.04	0.01	0.16	0.23	0.04	0.03	0.00	0.01	0.05	0.08	0.08	0.03	0.01	0.00
Na_2O	6.64	6.51	7.85	7.31	8.00	7.93	7.41	7.55	3.20	2.70	6.58	9.35	8.31	6.10	6.57	8.78
K_2O	0.27	0.16	0.29	0.61	0.20	0.32	0.07	0.00	0.18	0.03	0.14	0.47	0.22	0.16	0.15	0.00
Total	99.93	98.20	99.47	100.17	98.83	96.47	97.57	97.48	98.22	97.67	99.55	98.65	100.87	98.68	98.63	100.27
Cations to 8 Oxygens:																
Si	2.76	2.77	2.69	2.77	2.68	2.65	2.87	2.91	3.02	3.13	3.04	2.93	3.01	3.09	3.11	3.08
Al	1.27	1.27	1.31	1.25	1.31	1.33	1.16	1.13	1.13	1.06	1.05	1.09	1.04	1.01	1.00	0.98
Ca	0.28	0.26	0.31	0.27	0.31	0.32	0.17	0.14	0.11	0.04	0.07	0.08	0.07	0.03	0.01	0.01
Na	0.57	0.57	0.68	0.62	0.70	0.71	0.64	0.65	0.27	0.22	0.55	0.81	0.69	0.51	0.55	0.73
K	0.02	0.01	0.02	0.01	0.01	0.02	0.02	0.02	0.01	0.00	0.01	0.03	0.01	0.01	0.01	0.00
Molecular ratios in percents:																
Ab	65.74	67.62	67.77	69.44	68.34	68.07	76.76	79.98	68.41	86.00	87.34	87.82	89.57	93.66	96.68	98.43
An	32.50	31.28	30.58	29.56	30.54	30.12	20.38	17.09	29.06	13.38	11.44	9.22	8.87	4.71	1.87	1.43
Or	1.76	1.09	1.55	1.00	1.12	1.81	2.86	2.93	2.53	0.63	1.22	2.97	1.56	1.63	1.45	0.15

Anal. No.	746	741	625	628	629	622	51	50	44	45	56	57	41	52	55	65
Sp. No.	Z1656	Z1656	Z1442	Z1442	Z1442	Z1442	Z1451	Z1451	Z1451	Z1451	Z1451	Z1451	Z1451	Z1451	Z1451	Z1451
					RIM	CORE	RIM	RIM	RIM	RIM					CORE	RIM
SiO_2	69.98	68.09	69.28	67.70	69.52	72.52	70.28	65.29	67.54	67.36	66.42	66.97	64.26	66.45	66.64	75.14
Al_2O_3	19.04	18.64	18.73	18.85	19.83	19.42	21.79	20.58	19.65	19.56	20.96	20.36	21.34	20.59	19.78	15.84
Fe_2O_3	0.08	0.04	0.02	0.14	0.01	0.12	0.02	0.20	0.03	0.00	0.03	0.05	0.14	0.08	0.06	0.06
MnO	0.02	0.01	0.00	0.00	0.01	0.01	0.00	0.03	0.03	0.00	0.00	0.02	0.02	0.00	0.06	0.00
CaO	0.03	0.05	0.01	0.06	0.81	0.21	2.08	2.36	0.93	0.93	2.00	1.28	3.29	2.00	1.38	0.57
BaO	0.07	0.00	0.55	0.83	0.00	0.02	0.00	0.05	0.00	0.00	0.04	0.00	0.06	0.00	0.00	0.04
SrO	0.00	0.05	0.11	0.09	0.00	0.00	0.00	0.02	0.05	0.00	0.00	0.12	0.00	0.02	0.00	0.02
Na_2O	0.90	0.95	0.39	0.43	8.18	7.60	4.97	10.28	11.36	11.24	10.44	11.00	9.65	10.95	10.52	9.40
K_2O	9.70	12.84	12.33	11.80	0.09	0.02	0.07	0.18	0.04	0.05	0.26	0.25	0.37	0.00	0.08	0.04
Total	99.82	100.67	101.42	99.81	98.45	99.92	99.21	98.99	99.60	99.14	100.15	100.05	99.13	100.10	98.56	101.20
Cations to 8 oxygens:																
Si	3.10	3.05	3.08	3.06	3.04	3.00	3.02	2.91	2.97	2.97	2.91	2.94	2.86	2.92	2.96	3.19
Al	0.99	0.99	0.98	1.00	1.02	0.98	1.10	1.08	1.02	1.02	1.08	1.05	1.12	1.07	1.04	0.79
Ca	0.00	0.00	0.00	0.00	0.04	0.01	0.10	0.11	0.04	0.04	0.09	0.06	0.15	0.09	0.07	0.03
Na	0.08	0.08	0.04	0.04	0.69	0.63	0.41	0.89	0.97	0.96	0.89	0.94	0.83	0.93	0.91	0.78
K	0.55	0.74	0.70	0.68	0.01	0.00	0.00	0.01	0.00	0.00	0.02	0.01	0.02	0.00	0.01	0.00
Molecular ratios in per cents:																
Ab	12.33	10.08	4.58	5.23	94.09	98.33	80.61	87.84	95.46	95.36	89.11	92.66	82.40	90.24	92.81	96.53
An	0.23	0.29	0.07	0.40	5.15	1.50	18.64	11.14	4.32	4.36	9.43	5.96	15.52	9.11	6.73	3.20
Or	87.44	89.63	95.35	94.37	0.76	0.17	0.75	1.01	0.22	0.28	1.46	1.39	2.08	0.65	0.46	0.27

Analyses joined by bars in pairs are parts of the same individual grains.

Table 4. Feldspar compositions from acidic Plagiogranites of Khuzdar District.

Anal. No.	767	785	784	783	645	644	642	634	633
Sp. No.	Z1498	Z1498	Z1498	Z1498	Z1671	Z1671	Z1671	Z1747	Z1747
SiO_2	72.82	67.66	72.55	67.69	69.82	67.72	72.13	71.73	70.62
Al_2O_3	19.32	19.16	19.24	19.07	20.92	19.38	19.43	20.18	19.55
Fe_2O_3	0.04	0.00	0.07	0.06	0.22	0.00	0.02	0.06	0.00
MnO	0.03	0.02	0.01	0.03	0.00	0.00	0.06	0.00	0.00
MgO	0.11	0.00	0.03	0.00	0.00	0.00	0.01	0.00	0.00
CaO	0.14	0.29	0.17	0.16	1.61	0.56	0.56	0.44	0.81
BaO	0.00	0.00	0.00	0.00	0.00	0.00	0.01	0.00	0.00
SrO	0.00	0.05	0.00	0.00	0.00	0.00	0.08	0.02	0.00
Na_2O	5.72	11.86	6.56	11.63	9.15	8.28	9.57	7.71	8.15
K_2O	0.04	0.06	0.02	0.04	0.17	0.04	0.02	0.04	0.03
Total	98.22	99.10	98.65	98.68	99.90	98.02	101.89	100.54	98.80

Cations to 8 Oxygens:

	767	785	784	783	645	644	642	634	633
Si	3.14	2.99	3.12	3.00	2.96	3.06	3.06	3.06	3.07
Al	0.98	1.00	0.98	1.00	1.08	1.00	0.97	1.01	1.00
Ca	0.01	0.01	0.01	0.01	0.08	0.03	0.03	0.04	0.02
Na	0.48	1.02	0.55	1.00	0.77	0.70	0.79	0.64	0.69
K	0.00	0.00	0.00	0.00	0.01	0.00	0.00	0.00	0.00

Molecular ratios in per cents:

	767	785	784	783	645	644	642	634	633
Ab	98.19	98.31	98.36	99.00	90.11	96.10	96.74	94.21	96.88
An	1.35	1.36	1.44	0.77	8.77	3.59	3.13	5.47	2.89
Or	0.46	0.33	0.20	0.23	1.12	0.31	0.13	0.32	0.24

(Table 4).

Epidote Compositions

Epidote is a common constituent in plagiogranites and granites of Khuzdar District. In some samples of acidic plagiogranite, radiating crystal aggregates of fresh coarse prismatic crystals are conspicuously developed.

Representative epidote analyses are provided in Table 5, and exhibit the variations in chemical composition of epidote.

The hypothetical pistacite (Ps) content in epidote ranges from 12.42% to 28.06% in the analyzed samples. There is large variation in the Ps content observed within individual samples. The distinction between the granitic and trondhjemitic samples is not apparent. The content of Si in none of the analyses is below the ideal 3 atoms per formula unit, and all Al is octahedrally coordinated. Maximum amount of Ti is seen in sample Z1498, with TiO_2 at 0.29 wt. %. In granitic samples, Sr is present upto 0.19 wt. per cent, but the trondhjemitic samples contain no Sr in their epidote. Na_2O is below 0.03 per cent. V_2O_3 does not exceed 0.07 wt. per cent. P_2O_5 is below detection level in all the analyses. MnO is below 0.44% in all but one of the analyses. This one analysis shows 1.05 % MnO which may be an analytical uncertainty in view of the other analyses from the same sample with much less MnO. Although the epidote in igneous rocks is generally supposed to form by autometasomatism (e.g., Deer et al., 1986); the epidote that forms long prisms in radiating aggregates in the fractionated trondhjemitic samples shows primary magmatic texture (e.g., sample no. Z1671).

Chlorite Composition

Chlorite analyses (Table 6) do not discriminate between granitic and trondhjemitic rock samples. Two main textural types of chlorite, i.e., spherulitic and flaky, are present but they lack distinction on chemical basis. The chemical variations amongst chlorites are not large, except one trondhjemite sample (Z1747) which shows widely different Mg and Fe contents within the same sample. This anomalous sample may indicate altered chlorite or may represent submicroscopic intergrowths of chlorite with other phyllosilicates. The rest of the samples show quite uniform compositions. In terms of the nomenclature scheme of Hey (1954), all these chlorites are termed "ripidolites". Ripidolite is the main type of chlorite in the latest magmatic differentiates from the Sakhakot-Qila ophiolite as well (Ahmed, 1988). CaO is below 0.15% except for one analysis showing 0.29% CaO. The cationic proportions of chlorite microprobe analyses reported in Table 6 are obtained by normalization to 28 oxygens, assuming the total iron to be Fe^{2+}.

A review of a large number of published chlorite analyses (Foster, 1962; Deer et al., 1962; Shirozou, 1978) shows that trivalent iron typically constitutes less than 5% of the total iron. Such trivalent iron occurs mainly in the Fe-richer and Mg-poorer chlorites. Thus, in the present study, like some earlier works (e.g., Cathelineau & Nieva, 1985), consideration of all iron in the formula to be divalent, is more appropriate than adopting certain arbitrary assumptions such as those made by McDowell & Elders (1980) who assume 10% Fe - Fe^{3+}; or Walshe & Solomon (1981) who balance the trivalent charge in tetrahedral and octahedral sites to reach a zero vacancy.

Al substitution limits in chlorites are known to be about 0.8 to 3.6 Al atoms per 8 tetrahedral positions (Bailey, 1988). The chlorites analyses in Table 6 shows the samples analyzed contain more than two Al iv atoms per formula unit. Thus, the chlorites have high levels of Al 3+ in tetrahedral positions.

The temperatures of chlorite crystallization (Table 6) are calculated after the methods of Cathelineau (1988) using the equation:

$$T^o(C) = -61.92 + 321.98 (Al^{iv}).$$

These range from 315°C to 369°C for the chlorites of anatectic acidic rocks. For plagiogranitic acidic rocks, the range is 329°C to 400°C except for one anomalous low value at 244°C. Thus, relatively slightly higher temperatures of crystallization for the plagiogranitic chlorites are indicated.

Mica Compositions

Coarse-grained primary biotite flakes are abundant in the biotite granite (Z1552) outcrop near Karku Jhal. Analyses of this biotite are given in Table 7. Other acidic rock samples do not show such a higher content of discrete coarse crystals of biotite. This biotite has TiO_2 content commonly above 3%. Fe/(Fe + Mg) ratio varies from 54.76 to 58.4%. Slight amounts of Ba, Zn and V are present. The analyses do not record significant changes in crystallization history. However, presence of biotite may reflect the K and water content of the magma source and lower temperature for this

Table - 5 Epidote Analyses

Anal. No.	747	748	621	620	627	632	782	780	781	773	646	636	637	638
Sp. No.	Z1656	Z1656	Z1442	Z1442	Z1442	Z1442	Z1498	Z1498	Z1498	Z1498	Z1671	Z1447	Z1447	Z1447
SiO_2	39.30	38.18	37.78	37.85	37.09	37.60	37.73	38.43	36.34	36.34	41.98	35.82	37.01	36.43
TiO_2	0.00	0.00	0.00	0.07	0.15	0.00	0.00	0.29	0.18	0.19	0.02	0.05	0.08	0.40
Al_2O_3	28.53	25.74	25.97	23.87	23.19	22.78	26.92	26.81	23.73	22.16	20.34	23.12	23.21	22.49
Cr_2O_3	0.00	0.00	0.00	0.00	0.00	0.00	0.04	0.03	0.00	0.00	0.01	0.05	0.02	0.00
V_2O_3	–	–	0.00	0.05	0.07	0.04	0.04	0.03	0.04	0.04	0.00	0.00	0.01	0.00
Fe_2O_3	6.31	9.02	8.97	12.15	13.39	13.88	5.89	8.48	11.04	12.90	12.37	11.78	12.52	12.92
MnO	0.14	0.14	0.44	0.31	1.05	0.08	0.09	0.07	0.42	0.11	0.00	0.06	0.16	0.902
MgO	0.02	0.03	0.01	0.02	0.05	0.01	0.03	0.08	0.05	0.05	0.00	0.00	0.02	0.00
CaO	23.14	23.05	22.77	23.16	21.70	23.21	22.72	23.30	21.88	23.34	18.38	22.67	22.81	22.63
SrO	0.19	0.15	0.15	0.12	0.00	0.04	–	–	0.41	–	0.05	–	0.02	0.06
ZnO	–	–	0.01	0.03	0.08	0.00	–	–	–	–	2.88	0.01	0.00	0.00
Na_2O	0.03	0.00	0.01	0.01	0.01	0.00	–	–	–	–	0.12	0.00	0.00	0.00
K_2O	0.00	0.00	0.00	0.00	0.00	0.00	–	–	–	–	–	0.00	0.00	0.00
Total	97.66	96.31	96.10	97.64	96.78	97.60	93.42	97.51	93.68	95.13	96.19	93.51	95.84	94.95

Number of cations on the basis of 12.5 (O) ignoring water:

	747	748	621	620	627	632	782	780	781	773	646	636	637	638
Si	3.09	3.10	3.09	3.10	3.09	3.12	3.11	3.08	3.08	3.09	3.46	3.07	3.10	3.09
Al^{vi}	2.65	2.47	2.50	2.31	2.29	2.23	2.61	2.53	2.37	2.22	1.98	2.34	2.29	2.25
Ti	–	–	–	0.01	0.01	–	–	0.02	0.01	0.01	0.01	0.01	0.01	0.03
V	–	–	–	–	–	–	0.01	–	0.01	–	–	–	–	–
Fe	0.38	0.55	0.55	0.75	0.84	0.87	0.37	0.51	0.71	0.83	0.77	0.76	0.79	0.83
Mn	0.01	0.01	–	0.02	0.08	0.01	0.01	0.01	0.03	0.01	–	0.01	0.01	–
Mg	0.01	0.01	–	0.01	0.01	–	0.01	0.01	0.01	0.01	–	0.01	0.01	–
Ca	1.95	2.01	1.99	2.04	1.94	2.06	2.00	2.00	1.99	2.13	1.62	2.08	2.05	2.06
Sr	0.01	0.01	0.01	0.01	–	–	–	–	0.02	–	0.01	0.01	0.01	–
Zn	–	–	–	–	–	–	–	–	–	–	–	–	–	–
Na	0.01	–	–	–	0.01	–	–	–	–	–	0.46	–	0.01	–
$Ps=100 \times Fe/(Fe+Al)$:	12.59	18.21	18.03	24.51	26.84	28.06	12.42	16.78	23.05	27.21	28.00	24.52	25.65	26.96

65

Table - 6 Chlorite Analyses

Sp. No.	Z1656	Z1656	Z1656	Z1442	Z1451	Z1451	Z1451	Z1451	Z1451	Z1498	Z1498	Z1498	Z1498	Z1498	Z1671	Z1747	Z1747
SiO_2	26.35	26.23	25.51	26.91	25.31	25.89	24.91	25.54	25.16	26.35	25.77	27.22	26.96	26.74	27.95	23.36	27.91
TiO_2	0.06	0.03	0.06	0.01	0.07	0.08	0.05	0.08	0.09	0.03	0.02	0.00	0.01	0.04	0.01	0.02	0.04
Al_2O_3	20.55	19.46	18.54	18.91	22.44	19.99	21.52	20.87	21.20	20.24	19.48	18.64	19.60	20.22	19.25	19.95	19.80
Cr_2O_3	--	0.01	0.01	0.00	0.01	0.02	0.00	0.10	0.05	0.00	0.03	0.03	0.00	0.01	--	--	--
V_2O_3	--	--	--	--	0.03	0.01	0.02	0.01	0.03	--	0.03	--	--	--	--	--	--
FeO	27.61	27.83	28.65	25.71	25.54	27.11	27.39	28.47	29.44	22.69	25.64	26.51	26.59	27.11	13.21	38.17	30.36
MnO	0.55	0.69	0.59	0.49	0.47	0.48	0.34	0.33	0.38	0.32	0.41	0.30	0.28	0.42	0.08	0.42	0.25
MgO	14.47	14.16	14.03	15.70	12.09	14.71	13.18	12.42	12.62	17.12	15.38	14.38	14.01	13.78	26.36	5.44	7.39
NiO	--	--	0.05	0.11	0.00	0.04	0.03	0.01	0.03	0.01	0.04	--	--	0.02	0.09	0.00	0.00
CaO	0.08	0.07	0.15	0.29	0.04	0.05	0.10	0.14	0.05	0.04	0.03	0.07	0.03	0.04	0.03	0.09	0.15
BaO	--	--	--	--	0.06	0.00	0.00	0.01	0.03	--	--	--	--	--	--	--	--
SrO	--	--	--	--	0.22	0.00	0.17	0.17	0.11	--	--	--	--	--	--	--	--
Na_2O	0.04	0.05	0.05	--	0.07	0.02	0.01	0.03	0.03	0.98	--	--	--	--	0.00	0.02	0.11
K_2O	0.00	0.00	0.00	--	0.72	0.00	0.00	0.00	0.00	--	--	--	--	--	0.00	0.00	0.56
ZnO	0.12	0.09	0.09	0.10	0.01	0.09	0.06	0.07	0.07	--	--	--	--	--	0.07	0.10	0.03
Cl	--	--	--	--	0.03	0.02	0.01	0.01	0.01	--	--	--	--	--	--	--	--
Total	89.83	88.62	87.73	88.23	87.11	88.51	87.79	88.25	89.27	86.80	86.86	87.15	87.48	88.38	87.05	87.57	86.60

Atomic proportions of elements calculated 50 28 oxygens:

Sp. No.	Z1656	Z1656	Z1656	Z1442	Z1451	Z1451	Z1451	Z1451	Z1451	Z1498	Z1498	Z1498	Z1498	Z1498	Z1671	Z1747	Z1747
Si	5.49	5.56	5.51	5.66	5.41	5.47	5.32	5.45	5.33	5.35	5.46	5.23	5.26	5.13	5.57	5.34	6.10
Al^{vi}	2.53	2.42	2.23	2.35	3.06	2.45	2.73	2.70	2.62	2.19	2.33	1.45	1.77	1.70	2.09	2.71	3.20
Ti	0.01	0.01	0.01	0.00	0.01	0.01	0.01	0.01	0.01	0.01	0.00	0.00	0.00	0.01	0.00	0.00	0.01
Fe	4.81	4.93	5.18	4.53	4.57	4.79	4.89	5.08	5.22	3.85	4.55	4.26	4.34	4.35	2.20	7.29	5.55
Mn	0.10	0.12	0.11	0.09	0.09	0.09	0.06	0.06	0.07	0.06	0.07	0.05	0.05	0.07	0.01	0.08	0.05
Mg	4.49	4.48	4.52	4.93	3.85	4.63	4.19	3.95	3.99	5.18	4.86	4.12	4.08	3.94	7.83	1.85	2.41
Ca	0.02	0.02	0.04	0.07	0.01	0.01	0.02	0.03	0.01	0.01	0.01	0.01	0.01	0.01	0.01	0.02	0.04

Nomenclature after Hey (1954) (RI = ripidolite, PY = pycnochlorite; BH = brunsvigite):

| | RI | RI | RI | PY | RI | RI | RI | RI | RI | RI | RI | RI | RI | RI | RI | RI | BR |

T(°C) after Cathelineau (1988):

| | 342 | 331 | 339 | 315 | 355 | 345 | 369 | 349 | 368 | 365 | 347 | 384 | 379 | 400 | 329 | 366 | 244 |

66

Table - 7 Biotite (1-5) and phengite (6) analyses.

	1	2	3	4	5	6
Anal. No.	605	604	606	610	618	623
Sp. No.	Z1552	Z1552	Z1552	Z1552	Z1552	Z1442
SiO_2	34.75	35.31	34.40	35.71	35.49	47.88
TiO_2	2.25	3.26	3.58	3.28	--	0.10
Al_2O_3	16.58	16.99	16.62	16.79	16.79	27.99
Cr_2O_3	0.00	0.02	0.01	0.00	--	--
V_2O_3	0.07	0.15	0.13	0.13	--	--
FeO	20.28	20.59	21.25	21.35	21.73	3.79
MnO	0.20	0.26	0.15	0.28	0.29	0.02
MgO	9.40	8.81	8.53	8.53	8.73	1.55
CaO	0.01	0.00	0.01	0.00	0.00	0.30
BaO	0.36	0.28	0.31	0.26	0.33	0.04
SrO	0.36	0.00	0.00	0.00	0.07	0.00
ZnO	0.09	0.08	0.16	0.16	--	0.00
Na_2O	0.09	0.08	0.06	0.05	0.05	0.12
K_2O	8.92	9.37	9.54	7.82	9.13	9.30
P_2O_5	0.01	0.01	0.03	0.00	--	0.00
Cl	0.06	0.05	0.00	0.05	--	0.00
Total	93.43	95.26	94.78	94.41	92.59	90.99

Cations on the basis of 22 oxygens:

	1	2	3	4	5	6
Si	5.47	5.45	5.37	5.52	5.56	6.71
Al^{iv}	2.53	2.55	2.63	2.48	2.35	1.29
Al^{vi}	0.55	0.54	0.43	0.58	0.80	3.33
Ti	0.27	0.38	0.42	0.38	--	0.01
V	0.01	0.02	0.02	0.02	--	--
Fe^{2+}	2.67	2.66	2.78	2.76	2.89	0.44
Mn	0.03	0.03	0.02	0.04	0.04	0.00
Mg	2.21	2.03	1.99	1.97	2.07	0.32
Ca	0.00	0.00	0.00	0.00	0.00	0.05
Ba	0.02	0.02	0.02	0.02	0.02	0.00
Sr	0.03	0.00	0.00	0.00	0.01	0.00
Zn	0.01	0.01	0.02	0.02	--	0.00
Na	0.03	0.02	0.02	0.02	0.02	0.03
K	1.79	1.84	1.90	1.54	1.86	1.66
Cl	0.02	0.01	0.00	0.01	0.00	0.00

- = Not determined.

Table - 8 Sphene Analyses. Total Fe is Assumed as Ferric.

Anal.No.	761	48	49	46	64	779	640
Sp. No.	Z1656	Z1451	Z1451	Z1451	Z1451	Z1498	Z1747
SiO_2	29.67	31.23	30.42	31.34	28.82	29.58	29.75
TiO_2	39.63	24.41	31.96	32.67	40.11	32.25	30.66
Al_2O_3	0.07	6.68	5.04	5.13	0.36	3.78	6.04
V_2O_3	0.92	0.62	0.79	0.71	0.90	0.90	0.75
Fe_2O_3	1.17	10.15	2.53	0.68	1.88	1.49	0.52
MnO	0.02	0.15	0.04	0.04	--	--	--
MgO	0.00	1.75	0.64	0.00	--	0.06	0.02
NiO	0.01	--	--	--	--	--	0.02
ZnO	--	0.03	--	--	0.02	--	0.05
CaO	28.20	20.88	26.47	28.98	26.66	27.83	28.54
BaO	--	0.16	0.14	0.22	0.20	--	--
SrO	--	0.05	0.05	0.09	--	--	--
Na_2O	--	0.10	0.00	0.12	--	--	0.04
K_2O	0.01	0.06	0.00	0.01	0.00	0.05	0.00
P_2O_5	--	0.04	0.07	0.02	0.05	--	--
Cl	--	0.03	0.02	0.00	--	--	--
Total	99.70	96.34	98.17	100.01	101.00	95.94	96.39

Cations on the basis of four silicon:

Si	4.00	4.00	4.00	4.00	4.00	4.00	4.00
Ti	4.02	2.35	3.16	3.14	4.18	3.28	3.10
Al	0.01	1.01	0.78	0.77	0.38	0.60	0.96
V	0.10	0.07	0.08	0.07	0.10	0.10	0.08
Fe	0.12	0.97	0.25	0.07	0.19	0.15	0.05
Mn	0.00	0.02	0.01	0.00	0.00	0.00	0.00
Mg	0.00	0.33	0.13	0.00	0.00	0.01	0.00
Ca	4.07	2.87	3.72	3.96	3.96	4.03	4.11
Na	0.00	0.03	0.00	0.03	0.00	0.00	0.01
K	0.00	0.01	0.00	0.00	0.00	0.00	0.00
P	0.00	0.01	0.01	0.00	0.01	0.00	0.00
O	20.41	18.56	19.75	19.61	21.28	19.80	20.00

nor western outcrop. Alternatively, this biotite granite may be a hybrid rock. Phengite in anatectic granitic rocks is illustrated by one analysis from sample Z1442 (Table 7).

Sphene compositions

The analytical data of sphene from both the rock suites are reported in Table 8. Sphene is commonly present in late stage plagiogranitic differentiates of ophiolites (e.g., Ahmed, 1987). Sphene from granitic rocks is generally richer in REE. However, in the samples from the Bela ophiolitic granitic rocks (Table 8), REE are not present. The analyses 761, 64 are close to ideal sphene composition except that Fe is slightly higher and Ca lower (Deer *et al.*, 1982).

V_2O_3 ranges from 0.62 to 0.92 wt. per cent. In the Y (octahedral sites) Al predominates over Fe^{3+} for the trondhjemitic rock suite. The granitic sample shows reverse behaviour. All Al and Fe has been assigned to the octahedral sites, and tetrahedral sites are assumed to be filled by Si alone (Higgins & Ribbe, 1976). The substitution of Na, Mg or Mn for Ca is extremely small.

Apatite Composition

Apatite analyses from the biotite granite (Z1552) and other potash-rich samples are reported in Table 9. Apart from major amounts of CaO (51.57 to 55.89 wt. %) and P_2O_5 (41.57 to 42.33 wt. %), minor amounts of MnO, ZnO and ZrO_2 are noteworthy. Y is present in Z1656 and Z1451.

Table 9. Apatite Analyses.

Anal. No.	619	759	763	59
Sp.No.	Z1552	Z1656	Z1656	Z1451
SiO_2	0.19	0.35	0.56	0.30
TiO_2	0.00	0.39	0.00	0.05
Al_2O_3	0.02	0.00	0.01	0.01
Cr_2O_3	0.00	0.03	0.00	0.04
V_2O_3	0.00	0.01	0.00	0.01
FeO	0.00	0.70	0.08	0.62
MnO	0.08	0.46	0.31	0.43
MgO	0.00	0.00	0.00	0.04
NiO	0.02	0.03	0.00	0.00
CaO	55.89	53.03	51.57	54.47
BaO	0.00	0.00	0.07	0.00
ZnO	0.40	2.67	4.83	0.28
Y_2O_3	0.00	0.19	0.57	0.17
ZrO_2	1.27	1.25	1.19	1.05
Cl	0.02	0.17	0.10	0.00
P_2O_5	41.57	42.33	42.03	41.95
Cl	0.02	0.17	0.10	0.00
Total:	99.48	101.78	101.42	99.42

Table - 10 Zircon Analyses from Acidic Anatectic Rocks (1-4) and Plagiogranite (5).

Anal. No.	607	611	744	751	778
Sp. No.	Z1552	Z1552	Z1656	Z1656	Z1498
SiO_2	32.62	31.81	32.70	32.86	32.29
Al_2O_3	0.00	0.02	0.05	0.02	0.01
Cr_2O_3	0.01	0.05	0.00	0.01	0.00
MnO	0.02	0.00	0.03	0.00	0.01
MgO	0.01	0.01	0.00	0.04	0.00
NiO	0.00	0.00	0.03	0.03	0.00
CaO	0.00	0.01	0.04	0.03	0.00
BaO	0.04	0.00	0.01	0.05	0.00
SrO	0.09	0.00	0.00	0.02	0.09
ZnO	0.10	0.08	0.06	0.10	0.00
Na_2O	0.00	0.00	0.03	0.02	0.00
K_2O	0.03	0.01	0.00	0.00	0.01
ZrO_2	68.18	66.63	67.92	67.46	67.06
Cl	0.00	0.01	0.02	0.01	0.00
Total	101.10	98.63	100.89	100.65	99.47

Cations to 16 oxygens:

Si	3.96	3.95	3.97	4.00	3.97
Al	--	--	0.01	--	--
Cr	--	0.01	--	--	--
Ca	--	--	0.01	--	--
Sr	0.01	--	--	--	0.01
Zn	0.01	0.01	0.01	0.01	0.00
Zr	4.03	4.04	4.02	4.00	4.02
Na	--	--	0.01	--	--
K	0.01	--	0.01	--	--

Zircon Composition

Euhedral zircon is ubiquitous accessory in all the acidic rocks of Khuzdar District. Compositions from three samples are given in Table 10. Analyses from sodic plagiogranite (Z1498) and potassic granitic rocks (Z1552 and Z1656) overlap. Trace elements display negligible concentrations. Crystals are unaltered and lack inclusions and various trace elements that are frequently present. Thus, there are no Hf, Y, P, U, Th or rare-earth elements detectable with

the technique employed. Si values close to 4 in Table 10 show the analyses are of good quality.

Fe-Ti oxides

The Fe, Ti-oxide phase compositions in the acidic leucocratic rocks are reported for three rock samples in Table 11. The plagiogranite sample Z1747 contains ilmenite which shows differences with ilmenite from anatectic rock sample Z1656. The former has much higher TiO_2 and FeO and lower Fe_2O_3 and MnO

Table - 11 Analyses of Fe-Ti Oxides.

Anal. No.	760	758	762	53	639
Sp. No.	Z1656	Z1656	Z1656	Z1451	Z1747
SiO_2	0.00	0.02	0.01	0.04	0.01
TiO_2	99.35	49.82	47.73	0.50	52.17
Al_2O_3	0.01	0.00	0.01	0.36	0.00
V_2O_3	2.33	1.08	1.09	0.11	1.07
Fe_2O_3	--	6.14	8.42	67.89	1.38
FeO	0.78	39.23	37.42	31.80	44.50
MnO	0.00	5.18	5.04	0.02	2.03
MgO	0.01	0.06	0.04	--	0.03
NiO	0.05	--	0.04	--	0.02
CaO	0.50	0.19	0.23	0.02	0.19
Total	103.03	101.72	100.03	100.74	101.40
Oxygens	2	3	3	32	3
Si	--	--	--	0.01	--
Ti	0.97	0.93	0.91	0.12	0.98
Al	--	--	--	0.13	--
V	0.02	0.02	0.02	0.03	0.02
Fe^{3+}	--	0.12	0.16	15.59	0.03
Fe^{2+}	0.01	0.82	0.79	8.12	0.93
Mn	--	0.11	0.011	0.01	0.04
Ca	0.01	0.01	0.01	0.01	0.01

than the latter. Both types contain about 1% V_2O_3 and 0.2% CaO as well. Czamanske & Mihalik (1972) presented a model for the development of Mn-rich ilmenites in oxidizing magma systems. Thus, Mn-richer ilmenites, if not reequilibrated, may represent more oxidizing melts of anatectic rocks than those of plagiogranites. Chemical differences between whole-rock analyses of Z1747 and Z1451 are not large.

Rutile and magnetite analyses from anatectic rock sample Z1656 and Z1451, respectively, are reported in Table 11. Rutile contains 2.33 wt. % V_2O_3. V_2O_3 is low in magnetite.

DISCUSSION

Amongst the mechanisms proposed for the formation of plagiogranite, those involving the processes of Na-metasomatism or liquid immiscibility are discounted for the leucocratic rocks of the Bela ophiolite because of the reasons mentioned below.

The range of whole-rock compositions and petrographic rock types do not reveal any gap implied by the possibility of genesis of these rocks as immiscible liquids in equilibrium with conjugate mafic melts. Experimental production of two immiscible liquids of plagiogranitic and Fe-rich basalt compositions by Dixon & Rutherford (1979) was found to be inapplicable to natural plagiogranite at the Canyon Mountain ophiolite by Gerlach et al. (1981). At Bela, the large size of soda-rich plagiogranitic outcrops and existence of rocks of diorite and granodiorite compositions do not favour the model of liquid immiscibility.

Na-metasomatism of a K-rich precursor (Gilluly, 1933; Brown et al., 1979) does not seem viable for the Bela rocks, as the sodic and potassic acidic rock types are texturally similar and form discrete magmatic bodies lacking metasomatic texture and appearance. There is not much age difference between the two (Ahmed, 1991).

The field relations and geochronological studies of the two rock suites suggest coeval formation. Both outcrop in close spatial association in the northern half of the Bela ophiolite and are exposed within the limits of Khuzdar District.

The plagiogranites initially defined by Coleman and Peterman (1975) and later reported from many ophiolites in the world, are often regarded as products of magmatic differentiation of a basic magma (e.g.,

Pallister & Knight, 1981; Lippard et al., 1986). These plagiogranites crystallize from a circa 10% residual liquid formed during the low-pressure, hydrous crystal fractionation of a subalkaline, low-K tholeiitic magma. The REE data on the plagiogranite (e.g., sample Z1673) correspond to the essential features of the model of fractional crystallization of the gabbro parent given by Flagler & Spray (1991).

Many plagiogranites are now considered to result from anatexis of amphibolite, e.g., part of the Karmoy ophiolite (Pedersen & Malpas, 1984), the Fournier ophiolite from the Canadian Appalachians (Flagler & Spray, 1991).

The REE data on the samples Z1450 and Z1440 is in good agreement with the REE pattern calculated by Flagler & Spray assuming 10-20 % partial melting of amphibolite parent of plagiogranite.

The Sarmiento ophiolite complex, southern Chile, is an autochthonous ophiolite formed on the floor of an extensional marginal basin behind a continental margin volcanic arc (Saunders et al., 1979). The "trondhjemite-granophyre" rocks of this complex were derived by remelting and assimilation of older sialic material bordering the mafic complex. Some larger bodies were explained as stoped blocks of sialic crust inside marginal gabbros (Saunders et al., 1979). The chondrite-normalized REE plots of such rocks show certain resemblances with the properties of such plots of anatectic acid rocks from Bela. These include LREE enrichment relative to HREE, with a distinct negative Eu anomaly. However, the anatectic acid rocks from Bela possess a rather flat HREE part of the pattern that does not show a steep gradient. The plagiogranites of Sarmiento ophiolite possess a distinct negative Eu anomaly. They also exhibit higher abundances of REE which vary from 50 to 100 times chondritic values, compared to those from Bela ophiolite at 12 to 18 times chondritic values.

The feldspar compositions are dominantly albitic in both the rock suites. However, a distinction can be drawn on the basis of orthoclase and more calcic plagioclase both of which are found in the anatectic rock suite only. The differences in Fe-Ti oxide phases and ilmenite compositions are also described above.

CONCLUSIONS

In the Bela ophiolite, leucocratic rocks are well-developed, as are all the other rock units of a typical ophiolite sequence. The leucocratic rocks occur only in

the northern outcrops of the Bela ophiolite and display variations in their mode of occurrence, geochemistry and mineral chemistry. The plagiogranitic and anatectic rock suites co-exist in the Bela ophiolite. The former consist of dioritic rocks, tonalites, trondhjemites, albite granites and keratophyre, all formed by fractional crystallization from the basic magma. The anatectic rock suite is made of potash-rich granite, granophyre, acid pegmatite and trondhjemite; and is derived by crustal anatexis due to ophiolitic heat. The distinction between the two rock suites is explicit in terms of trace element and rare-earth element geochemistry. It is further enhanced when the evidence from mode of occurrence, mineral chemistry and major element chemistry is added.

Feldspar in the acidic plutonic rocks of plagiogranitic suite is exclusively albite. In the anatectic rock suite, albite is accompanied by more calcic plagioclase and in some cases orthoclase is associated. Primary biotite in coarse flakes is present only in the anatectic granitic rocks. The anatectic rocks mineral assemblage contains rutile and magnetite in addition to its abundant ilmenite. In fractionated acidic rocks, the ilmenite has comparatively higher TiO_2 and lower Fe_2O_3 and MnO.

ACKNOWLEDGEMENTS

REFERENCES

Ahmed, Z., (1987). Mineral chemistry of the Sakhakot-Qila ophiolite, Pakistan: Part 1, monosilicates. *Acta Mineralogica Pakistanica*, Vol. 3, pp. 26-41.

Ahmed, Z., (1988). Mineral chemistry of the Sakhakot-Qila ophiolite, Pakistan: Part 3, phyllosilicates. *Acta Mineralogica Pakistanica*, Vol. 4, pp. 45-64.

Ahmed, Z., (1991). A supra-subduction zone origin of the Bela ophiolite indicated by the acidic rocks, Khuzdar District, Pakistan. *Acta Mineralogica Pakistanica*, Vol. 5, pp. 9-24.

Allemann, F., (1979). Time of emplacement of the Zhob Valley ophiolites and Bela ophiolites. In: Geodynamics of Pakistan (Ed. A. Farah & K.A. De Jong), *Geol. Surv. Pakistan, Quetta*, pp. 215-242.

Bailey, S.W., (1988). Chlorites: structures and crystal chemistry. In: Hydrous Phyllosilicates (Ed., S.W. Bailey), *Min. Soc. Amer. Rev. Mineralogy*, Vol. 19, pp. 347-403.

Brown, E.H., Bradshaw, J.Y. and Mustoe, G.E., (1979). Plagiogranite and keratophyre in ophiolite on Fidalgo Island, Washington. *Geol. Soc. Amer. Bull.*, Vol. 90, No. 1, pp. 493-507.

Cathelineau, M., (1988). Cation site occupancy in chlorites and illites as a function of temperature. *Clay Minerals*, Vol. 23, pp. 471-485.

Cathelineau, M. and Nieva, D., (1985). A chlorite solid solution geothermometer: The Los Azufres (Mexico) geothermal system. *Contrib. Mineral. Petrol.*, Vol. 91, pp. 235-244.

Coleman, R.G. and Peterman, Z.E., (1975). Oceanic plagiogranite. *Jour. Geophys. Res.*, Vol. 80 No. 8, pp. 1099-1108.

Czamanske, G.K. and Mihalik, P., (1972). Oxidation during magmatic differentiation, Finnmarka complex, Oslo area, Norway, 1, The opaque oxides. *Jour. Petrol.*, Vol. 13, pp. 493-509.

Deer, W.A., Howie, R.A. and Zussman, J., (1962). Rock-Forming Minerals. Vol. 3, Sheet Silicates. Longmans, London. 270p.

Deer, W.A., Howie, R.A. and Zussman, J., (1982). Rock-Forming Minerals, Vol., 1A, Orthosilicates (second edition). Longmans, London. 919 p.

Deer, W.A., Howie, R.A. and Zussman, J., (1986). Rock-Forming Minerals: Vol. 1-B, Disilicates and Ring Silicates. Longman Group U.K. Limited, England. 629 p.

Flagler, P.A. and Spray, J.G., (1991). Generation of plagiogranite by amphibolite anatexis in oceanic shear zones. *Geology*, Vol. 19, pp. 70-73.

Foster, M.D., (1962). Interpretation of the composition and a classification of the chlorites. *U.S. Geol. Surv. Prof. Pap.* 414-A, pp. 1-27.

Gansser, A., (1979). Reconnaissance visit to the ophiolites in Baluchistan and the Himalaya. In: Geodynamics of Pakistan. (Eds. A. Farah and K.A. De Jong), *Geol. Surv. Pakistan, Quetta*. pp. 193-214.

Gerlach, D.C., Leeman, W.P. and Ave-Lallemant, H.G., (1981). Petrology and geochemistry of plagiogranite in the Canyon Mountain ophiolite, Oregon. *Contrib. Mineral. Petrol.*, Vol. 77, pp. 82-92.

Hey, M.H., (1954). A new review of the chlorites. *Mineral. Mag.*, Vol. 30, pp. 277-292.

Higgins, J.B. and Ribbe, P.H., (1976). The crystal chemistry and space groups of natural and synthetic titanites. *Amer. Mineral.*, Vol. 61, no. 9-10, pp. 878-888.

Kazmi. A.H., (1979). Active fault systems in Pakistan. In: Geodynamics of Pakistan (Eds. A. Farah and K.A. De Jong), *Geol. Surv. Pakistan, Quetta.*, pp. 285-294.

McDowell, S.D. and Elders, W.A., (1980). Authigenic layer silicate minerals in borehole Elmore 1, Salton Sea geothermal field, California. *Contrib. Mineral. Petrol.*, Vol. 74, pp. 293-310.

Pallister, J.S. and Knight, R.J., (1981). Rare-earth element geochemistry of the Samail ophiolite near Ibra, Oman. *Jour. Geophys. Res.*, Vol. 86, no. B4, pp. 2673-2697.

Pearce, J.A., (1989). High T/P metamorphism and granite genesis beneath ophiolite thrust sheets. *Ofioliti*, Vol. 14, No. 3, pp. 195-211.

Pedersen, R.B. and Malpas, J., (1984). The origin of oceanic plagiogranites from the Karmoy ophiolite, Western Norway. *Contrib. Mineral. Petrol.*, Vol. 88, pp. 36-52.

Rock, N.M.S. and Carroll, G.W., (1990). MINTAB: A general purpose mineral recalculation and tabulation program for Macintosh microcomputers. *Amer. Mineral.*, Vol. 75, pp. 424-430.

Saunders, A.D., Tarney, J., Stern, C.R. and Dalziel, I.W.D., (1979). Geochemistry of Mesozoic marginal basin floor igneous rocks from southern Chile.

Shirozu, H., (1978). Chlorite minerals. In: Developments in sedimentology, Vol. 26, pp. 243-264. Elsevier, Amsterdam.

Walshe, J.L. and Solomon, M., (1981). An investigation into the environment of formation of the volcanic hosted Mt. Lyell copper deposits using geology, mineralogy, stable isotopes and a six component chlorite solid solution model. *Econ. Geol.*, Vol. 76, pp. 246-284.

GEOLOGY, PETROLOGY AND GEOCHEMISTRY OF DADELDHURA GRANITE MASSIF, FAR WESTERN NEPAL

By

K.P. KAPHLE
Department of Mines and Geology, Kathmandu, Nepal.

ABSTRACT: *In Nepal granite bodies are known from the Higher Himalaya, north of Main Central Thrust (MCT) as well as from the Lesser Himalaya, north of Main Boundary Thrust (MBT). Dadeldhura granite is one of the Lesser Himalayan cordierite bearing two mica granite of 470 ± 5.6 Ma age. From field and laboratory study Dadeldhura granite massif has been found to consist of four types of granites as (1) gneissic granite (GGR), (2) biotite granite (BGR), (3) muscovite granite (MGR) (4) aplitic tourmaline granite (TGR). Petrographic characteristics and geochemistry has confirmed that they are the result of magmatic differentiation of same granitic magma.*

In general the Dadeldhura granite is rich in silica, alumina, and potash and comparatively low in soda. Geochemistry of various types of Dadeldhura granite shows a remarkable variation by the general increase in SiO_2, Al_2O_3, K_2O, Na_2O, P_2O_5 and decrease in CaO, MgO, Fe_2O_3 and TiO_2 towards later part of differentiation. The evolutionary trend is in the direction of alkaline rich liquid. Trace element chemistry in various types also suggests an increasing tendency in the ratio between Rb/Ba, Rb/Sr and decreasing tendency in the ratio between Ba/K from gneissic granite, biotite granite to muscovite granite and tourmaline granite. Rb - Ba - Sr ternary diagram, Rb vs K, Rb vs Ba and Rb vs Sr variation diagrams and mineral chemistry revealed a clear-cut differentiation trend of the granitic magma. High Sr 87/Sr 86 initial ratio (0.7266 ± 0.0012) and rock geochemistry has confirmed that Dadeldhura granite is a S-type granite.

INTRODUCTION

Nepal Himalaya fall in the central part of the Main Himalayan Range extending from Bhutan in the east to Pakistan in the west. It can be divided into three main lithomorphotectonic zones sharply separated by two prominent thrusts. The Main Boundary Thrust (MBT) separate the Lesser Himalaya from Sub Himalaya and Main Central Thrust (MCT) separates the Higher Himalaya from Lesser Himalaya (Fig. 1). In Nepal a number of scattered granite bodies of various size are located in the Higher Himalaya as well as in the Lesser Himalaya region. On the basis of geographical position they are known as the Higher Himalayan granites and the Lesser Himalayan granites (Fig. 1). Out of these granites only few e.g. Manaslu and Makalu granites of Higher Himalaya and Dadeldhura, Palung and Simchar (Agra) granites of Lesser Himalaya are partly studied by Nepalese and foreign geologists. Department of Mines and Geology (1977 -

1984) partly explored the Dadeldhura granite. Similarly Department of Mines and Geology/UNDP Mineral Exploration Development Board (1975 - 1980) did very preliminary mineral prospection works around some part of Ipa, Palung, Simchar, an Udayapur granites with a view to find out the economic mineral deposits related to the respective granites. Except some minor tin occurrences and low grade copper - tungsten mineralization in the exocontact zones (northern contact) of Dadeldhura granite and minor occurrences of cassiterite + molybdenite in the pegmatites and quartz + tourmaline veins within 100 to 150 m from the granite/schist contact in Palung and Ipa granites (Joshi 1988) and recovery of few cassiterite grains in the heavy concentrate samples derived form the granitic terrain in Dadeldhura granite and Palung granite no other potential thin and tungsten mineralization were recorded within or around these granites. Kaphle (1984, 1988) did a fairly detail works on petrology and geochemistry of Dadeldhura granite.
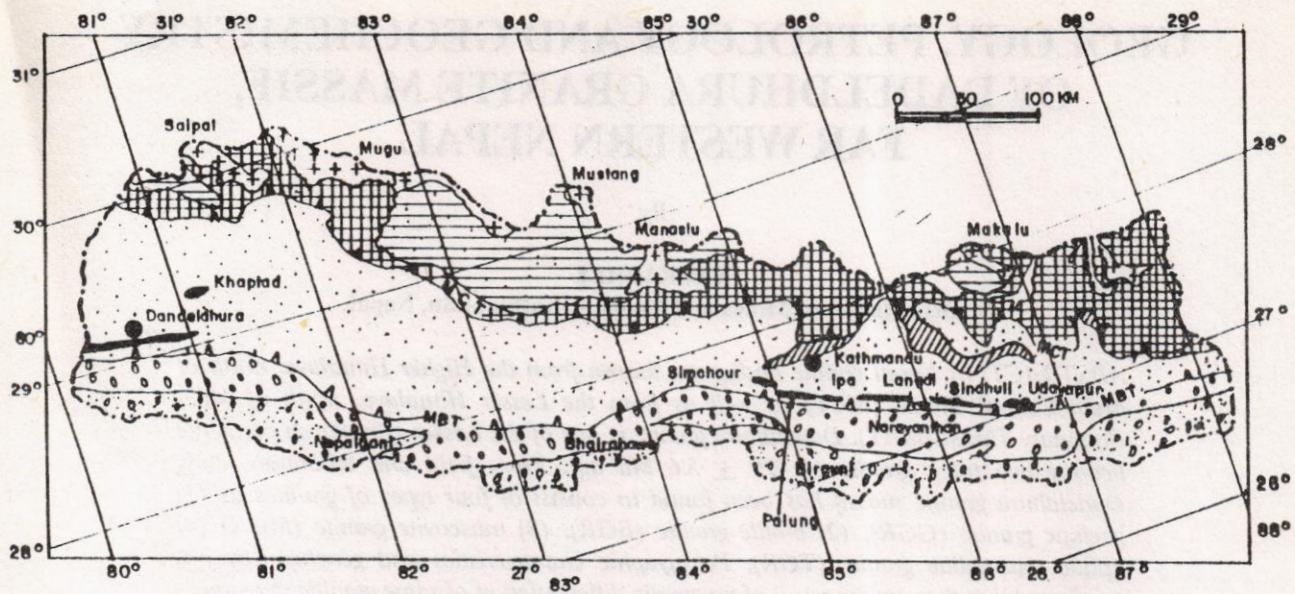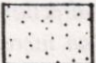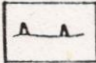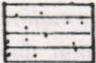
INDEX
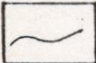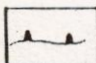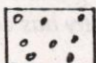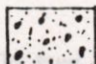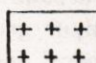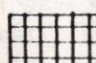
Boundary between different units.	Lesser Himalayan Metamorphics
Main Boundary Thrust (MBT)	Tethyan Sediments
Main Central Thrust (MCT)	Siwalik Sediments
Lesser Himalayan cordierite bearing two mica grahites.	Alluvial deposits
Higher Himalayan Granites	
Central Crystalline (Augen gneiss, Kyanite-sillimanite gneiss/schist) with minor grainitic bodies.	
Augen gneiss (South of Main Central Thrust)	

Fig. 1   Distribution of granites in Nepal Himalaya.

Prepared by : K. P. Kaphle.

76

Present paper is based on his field observation and laboratory studies carried out during his research work on Dadeldhura granite.

GEOLOGICAL SETTING

Heim and Gansser (1939), Gansser (1964) and Remmy (1976) considered that the Dadeldhura complex is the eastward extension of Almora nappe which is possibly equivalent to Kathmandu complex (Stocklin & Bhaltarai, 1977) Hagen (1969) is of the view that granites, gneisses, various schists, phylites and quartzites of this area are the possible eastern extension of the frontal rocks of Almora nappe and interpreted these rocks to form an allochthonous anticlinal structure and to be pushed and slightly overturned towards south. Talalov (1972) considered the area to be a block faulted zone. In Dadeldhura area Bashyal (1981, 1986) has recognized two main tectonic units, Bunder metasedimentary unit of parautochthonous character being thrusted by allochthonous Dadeldhura Complex. In this area towards south Bunder Metasedimentary Complex directly comes in contact with the Tertiary Siwalik sedimentary rock which are separated by MBT. This Bunder Metasedimentary Complex is possibly an equivalent unit to Nawakot Complex of Central Nepal.

The author and Upreti (1990) have similar views that the Dadeldhura complex towards north as well as towards south is bounded by North Dadeldhura Thrust (NDT) and South Dadeldhura Thrust (SDT) respectively. Dadeldhura Complex is divided into two groups (1) the Dadeldhura crystalline group of Precambrian age is emplaced by Dadeldhura granite of Ordovician age and (2) Damgad metasedimentary group (Early Cambrian ?) The Dadeldhura crystalline group is further divided into four formations eg. (1) Sirsegad Formation (SGD), (2) Gaira Formation (GRA) (3) Bherupani Formation (BPN) and Raduwagad Formation (RGD) and represented by different types of phyllites, quartzites, slates, carbonaceous schist, quartz mica schist, quartzo felspathic mica schist, garnetiferous mica schist, gneisses and amphibolites (Fig. 2, Table 1) Except Raduwagad Formation all other formations are traceable on both the flanks of Dadeldhura syncline. Small bodies of porphoroids, granites, pegmatites, aplites and basic rock bodies are recorded at different localities. Towards north east side the stratigraphy continued with unfossiliferous metasediments of Damgad metasedimentary group. It is represented by both calcareous as well as arenaceous rocks and divided into two formations (1) Damgad Carbonate

Formation represented by finely crystalline creamy whitish yellowish to whitish gray dolomite with 1 to 3 m thick bands of bluish gray limestone and (2) Dhanekhola Formation represented by fine grained quartzite and quartzitic sandstone. The Damgad metasedimentary group is separated from underlying rocks by partially well developed unconformity (2 to 3m thick pebble conglomerate bed in Korail Khola section) and form the overlying rocks (towards north) by a thrust which extends from west and separate the low metamorphic rocks from the medium grade metamorphic rocks of Dadeldhura crystalline group. The Bunder metasedimentary complex is separated from Dadeldhura complex by SDT and from the Siwaliks by MBT. This complex is represented by low grade metamorphic rocks of Precambrian age (?). It has only one formation named as Bunder Formation. This Formation is further divided into (1) Bunder quartzite member, represented by thinly to thickly bedded various coloured quartzites interbedded with various coloured phyllites. At places small basic rock bodies are present and (2) Rupaskanra phyllite member is represented by gray to greenish gray and brownish gray phyllite interbedded with quartzites and chloritic mica schist. Amphibolite bodies are quite common in this unit. Further south of MBT the Siwalik group is represented by sandstone, siltstone, mudstone, shale and conglomerate of Mid·Miocene to Pleistocene age.

DADELDHURA GRANITE

The Dadeldhura granite massif is a NW-SE elongated lenticular body (90 * 5 to 20 km) which has emplaced slightly south of the axis of Dadeldhura synform during Ordovician time (470 $\pm$ 5.6 ma, Hohendorf, Kaphle and Einfalt, 1991). It extends further west across Nepal/India boarder to Kumaun, India. Like other Lesser Himalayan granites of Nepal, India and Pakistan this granite also comprises both gneissic and massive granite. On the basis of field relations, state of deformation, petrographical characteristics and rock geochemistry Dadeldhura granite is further divided into (1) Gneissic granite (GGR), (2) Biotite granite (BGR), (3) Muscovite granite (MGR) and (4) Tourmaline granite (TGR). It is believed that these four types of granites are the result of differentiation of the same granitic magma. In the peripheral region the Dadeldhura granite body is strongly deformed and gneissic. Whereas the central part is occuped by undeformed very poorly foliated to massive granite. Small bodies of leucocratic muscovite granite and aplitic tourmaline granite are the later product of differentiation and occur in association with

Fig.2, GEOLOGICAL MAP OF DADELDHURA AND ADJACENT AREA FAR WESTERN NEPAL

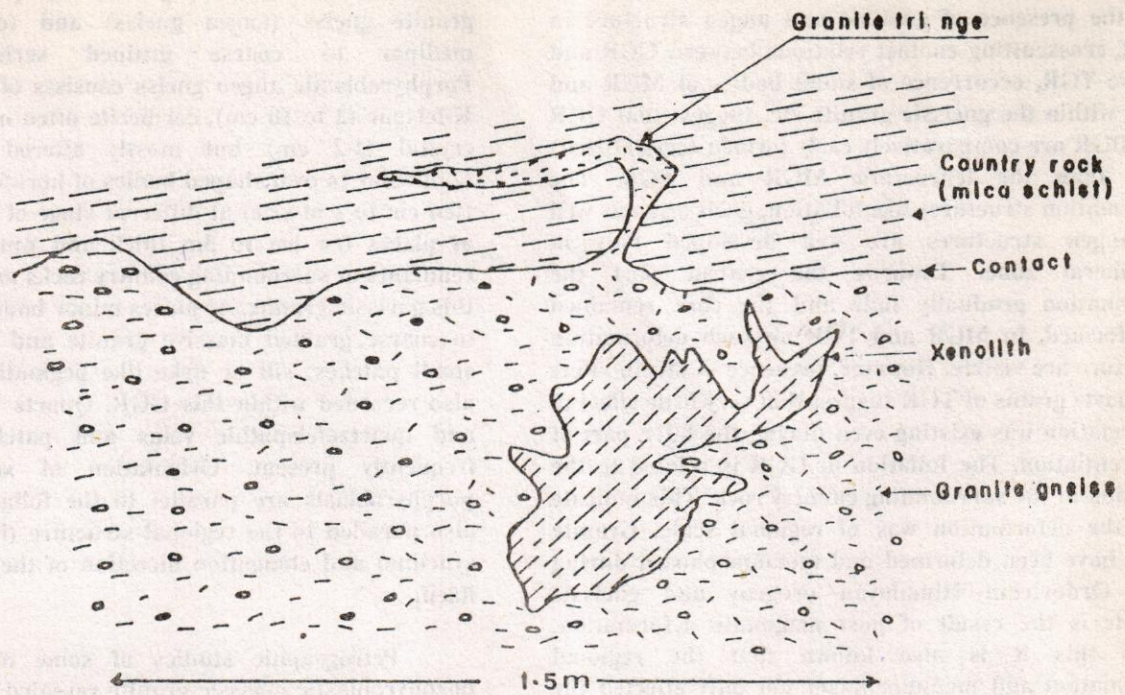SECTION ALONG A — B

Mapped by K.P. Kaphle

Fig. 3 Sketch section of the granite / country rock contact exposed in Rumail Khola.
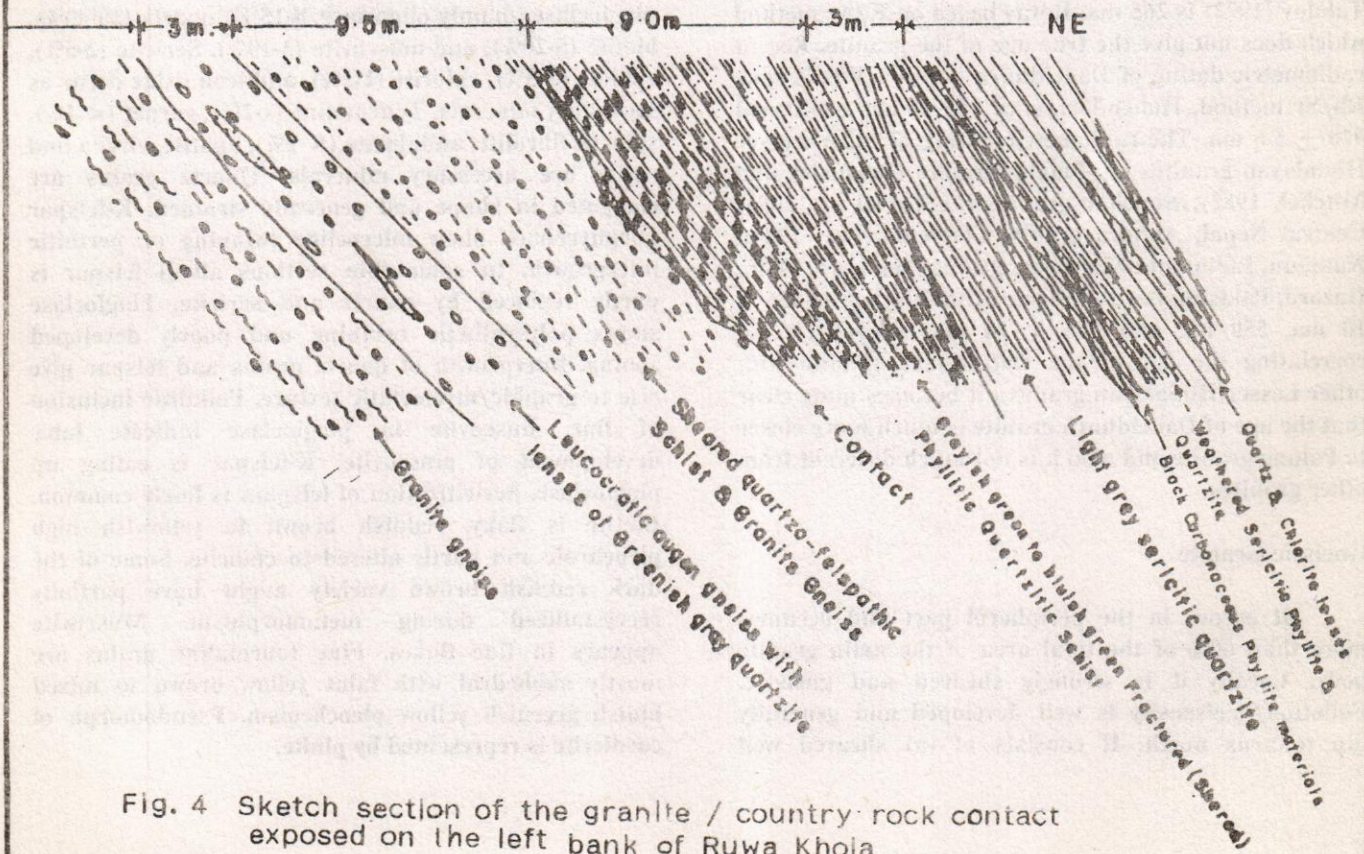

Fig. 4 Sketch section of the granite / country rock contact exposed on the left bank of Ruwa Khola

gneissic and massive biotite granite. Field evidences like the presence of gneissic and augen structure in GGR, crosscutting contact relations between GGR and aplitic TGR, occurrence of small bodies of MGR and TGR within the gneissic granite etc. suggest that GGR and BGR are comparatively early formed (crystallized) ones than the leucocratic MGR and TGR. The deformation structures like foliation, gneissosity as well as augen structures are well developed only in peripheral zone. Towards the central part the deformation gradually fade and the core remained undeformed. In MGR and TGR no such deformation structure are visible. However, presence of strain effect on quartz grains of TGR suggest that very little effect of deformation was existing even during the later part of differentiation. The foliation in GGR is related to the foliation in the surrounding country rock. This indicate that the deformation was of regional scale. Granite must have been deformed and metamorphosed during post Ordovician Himalayan orogeny and gneissic granite is the result of post magmatic deformation. From this it is also known that the regional deformation and metamorphism not only affected the surrounding rocks but also the granite body as well.

The age of Dadeldhura granite as assigned by Talalov (1972) is 265 ma. It was based on K/Ar method which does not give the true age of the granite. Recent radiometric dating of Dadeldhura granite (Whole rock Rb/Sr method, Hohendorf, et al., 1991) has confirmed 470 $\pm$ 5.6 ma. The radiometric dating of other Lesser Himalayan granites eg. Plaung granite (Bekinsley and Mitchel, 1982), Simchar granite (LeFort et al., 1983) Central Nepal; Almora granite (Trivedi et al., 1984), Kumaun, India; and Mansehra granite (Le Fort, 1980), Hazara, Pakistan have confirmed that they are of 486 $\pm$ 10 ma, 550 ma and 516 $\pm$ 16 ma respectively. In correlating the age of the Dadeldhura granite with other Lesser Himalayan granites it becomes quite clear that the age of Dadeldhura granite is much more closer to Palung granite and also it is not much different from other granites.

Gneissic Granite

It occurs in the peripheral part and occupies more than 60% of the total area of the main granite body. Locally it is strongly sheared and gneissic. Foliation/gneissosity is well developed and generally dip towards north. It consists of (a) sheared well foliated coarse grained gneiss, (b) porphyroblastic granite gneiss (augen gneiss) and (c) leucocratic medium to coarse grained sericitic gneiss. Porphyroblastic augen gneiss consists of megacryst of K-felspar (2 to 10 cm), cordierite often occur as green crystal (1-2 cm) but mostly altered into pinite. Lenticular to oval shaped bodies of hornfelsic xenoliths (few cm to 1 m size) at different stage of digestion and at places few cm to 3m thick and upto 35 m long remnants of surrounding country rocks are recorded in this gneissic granite. At places minor bodies of medium to coarse grained massive granite and a number of small patches, sill or dyke like pegmatite and aplite also recorded within this GGR. Quartz + tourmaline and quartzofelspathic veins and patches are also frequently present. Orientation of xenoliths and porphyroblasts are parallel to the foliation which is also paralled to the regional structure (i.e. axis of the syncline) and elongation direction of the granite body itself.

Petrographic studies of some of the typical porphyroblastic gneissic granite revealed that they are coarse grained, well foliated with or without augen structure. They mainly consist of tabular K-flespar (microcline and orthoclase 15-40%), fairly altered plagioclase (mainly oligoclase, 8-15%), quartz (20-40%), biotite (5-20%), and muscovite (3-10%). Sericite (2-5%), epidote (1-3%), chlorite (1-2%), and iron oxide occur as secondary minerals. Tourmaline (1-2%), garnet (< 1%), sphene, fibrolite, andalusite (< 1%), apatite, zircon and rutile are accessory minerals. Quartz grains are elongated in shape and generally strained. K-felspar porphyroblast show microcline twinning or perthitic intergrowth. In some thin sections alkali felspar is partly replaced by quartz and sericite. Plagioclase shows polysynthetic twinning and poorly developed zoning. Intergrowth of quartz grains and felspar give rise to graphic/myrmekitic texture. Poikilitic inclusion of fine muscovite in plagioclase indicate later development of muscovite. K-felspar is eating up plagioclase. Sericitization of felspars is fairly common. Biotite is flaky, reddish brown to yellowish high pleochroic and partly altered to chlorite. Some of the dark reddish brown variety might have partially recrystallized during metamorphism. Muscovite appears in fine flakes. Fine tourmaline grains are mostly subhedral with faint yellow brown to mixed bluish greenish yellow pleochroism. Pseudomorph of cordierite is represented by pinite.

Table 1.--Litho-Tectonic units in Dadeldhura area

Age	Complex	Group	Formation		Lithology
			Main Boundary Thrust	(MBT)	
Tertiary		Siwalik group	Siwalik Formations	(SW)	Sandstone, mudstone, shale and conglomerates.
Ordovician (470 ± 5.6 ma)	Dadeldhura Complex.	Dadeldhura granite massif	Tourmaline granite	(TGR)	Aplitic leucocratic granite
			Muscovite granite	(MGR)	Coarse grained leucocratic granite
			Biotite granite	(BGR)	Coarse grained massive granite
			Gneissic granite	(GGR)	Coarse grained gneissic granite
Early Cambrian (?)		Damgad meta sedimentary group.	Dhanekhola formation	(DQS)	Well bedded fine to medium grained quartzite and quartzitic sandstone
			Damagad carbonate "	(DLL)	Fairly well bedded fine grained gray dolomite with interbeds of bluish gray limestone and conglomerate at the base.
			Unconformity		
Pre-Cambrian (?)		Dadeldhura crystalline group.	Raduwagad Formation	(RGD)	Repeated interbed of green to greenish gray sericitic chloritic phyllite, quartzites, slates, carbonaceous phyllite, chloritic mica schist and sericitic quartzites.
			Bherupani Formation	(BPN)	Gray to light greenish gray sericitic phyllite, quartzite, very few fine garnet bearing, chloritic mica schist and micaceous quartzites.
			Thrust ——— x ———		Thrust ——— x
			Gaira Formation	(GRA)	Shining gray to greenish gray garnetiferous mic schist, felspatic schist, quartzite and sheared gneisses with minor granite bodies.
			Siresegad Formation	(SGD)	Quartzofelspathic schist, gneiss, quartzite, and few garnet bearing chloritic mica schist and amphibolite. At places small bodies of basic rocks and pegmatites.
Thrust ——	Thrust ——		Thrust ——		
Pre-Cambrian (?)	Bunder meta sedimentary Complex		Bunder Formation	(BDR)	
			(b) Rupaskanra phyllite Member	(RPH)	Sericitic chloritic phyllite interbedded with micaceous quartzites, at places with some amphiolite bodies.
			(a) Bunder Quartzite Member	(BQZ)	Various coloured quartzite and thin phyllite interbeds, at places with small basic rock bodies.

81

Biotite Granite

It occurs in the central part and occupies almost 33% of the total area of the massif. It is a medium to coarse grained holocrystalline, porphyritic to massive granite. Poorly developed mineral lineation is traceable only close to the granite gneiss (eg. in Rupaligad section). Euhedral phenocryst of K-felspar (1-6 cm size) in the matrix of medium to coarse grained quartz, felspar and micas give rise to porphyritic texture. Occasionally quartz + tourmaline veins and pegmatite lenses are also observed within this granite. Xenoliths of compact hard quartz biotite schist and micaceous quartzite (1-15 cm to 50 cm size) are common.

Petrographic study of this granite reveals that it consists of anhedral to globular quartz (20-35%), subhedral K-felspar (mainly microcline and perthitic megacryst, 18-40%), coarse euhedral plagioclase (10-24% oligoclase corroded by quartz and K-felspar), biotite (5-15%) and muscovite (5-8%). Secondary minerals are sericite (2-9%), chlorite (2-12%) and epidote (< 1%). Almost all cordierite has altered into green pinite. tourmaline, sphene, rutile and few zircon and apatite occur as accessory minerals. Sericitization of K-felspar results to development of quartz and sericite. However, inclusion of ilmenite and rutile in biotite, and sphene and muscovite in felspar are common. In some thin sections biotite seems to have partially crystallized. Deuteric alteration of felspar is evidenced by the alteration of felspar into sericite and clay and introduction of pneumatolytic minerals eg. tourmaline.

Muscovite Granite

It is an elongated and comparatively small body. It occupies the central part of the massif and lies close to the contact of granite gneiss and massive biotite granite (Fig. 2). It is a highly differentiated muscovite rich leucogranite. At places small coarse grained pegmatite lenes, patches and veins are commonly observed (eg. around Matkatypa village). Here the rocks are highly fractured. Small but numerous muscovite granite fringes (apophyses) and lenses are common in the granite gneiss.

It is a coarse grained equigranular massive to porphyritic granite. It mainly consists of violet gray quartz (20-40%), gray K-felspar (30-56%), greyish white plagioclase (10-18%), flaky muscovite (5-15%) and very few biotite (1-5%). Tourmaline, zircon and apatite occur as rare minerals. Some chlorite and sericite occur as secondary minerals.

Tourmaline Granite

Aplitic tourmaline granite bodies of mappable size are extremely rare. However, a number of minor scattered, concordant to disconcordant bodies (50 cm - 16 m thick and above 100 m long) and irregular patches are noted mainly in the western slope of Kopersad area and Khar khola section. All these granite bodies are recorded within the granite gneiss. This indicates that they are the youngest of all granite types and possibly related to pneumatolitic phase of differentiation of granitic magma as evidenced by the presence of tourmaline, apatite and rarely flourite.

It is medium grained, equigranular, massive aplitic in texture. It consists of quartz (30-55%), K-felspar (28-35%), plagioclase (oligoclase upto 15%) and tourmaline (4-10%). Idiomorphic tourmaline grains are pleochroic and show zoning. Sericitization of K-felspar and staining of dirty dull earthy (clay) materials are fairly common. Garnet, apatite, and very rarely flourite occur as accessory minerals. Presence of few strained quartz and development of biotite flakes along the deformation plane indicate some deformation effect even in the later part of differentiation of granitic magma.

Pegmatite and Aplite

Minor irregular and lenticular bodies as well as veins and dyke like bodies (few cm to 1 m thick) of pegmatites and aplites are present at various places within the different types of granite. They are the last product of differentiated magma. The crosscutting relations with each other revealed that they are possibly of three generations.

Contact Relations

The northern margin of this granite in the stream bed at Rumail khola (Fig. 3) is sharp. Granite gneiss dips below the schist (country rock). At this point a contact metamorphic effect is marked by the presence of about 50 m thick fine grained, compact, tough, biotite rich hornfelsic rock (with few grains of andalusite and garnet) and passes transionally into sericitic chloritic phyllite. Similar situations are also seen in some other contacts as well. The hornfelsic rock is quite similar to some of the xenoliths in their texture and mineralogy. At this contact a 3 cm wide quartz - tourmaline vein forms the actual schist/granite contact

which dips at 50° towards north. Here the foliation of granite gneiss is oblique to the contact and the country rocks are penetrated by few aplitic granite dykes and fringes. The contact exposed along Dhangarhi - Dadeldhura road near Dhundhune and shyaule bazar are also sharp where a number of granite fringes are penetrating the Phyllitic country rock. This relations clearly indicate an intrusive nature of the granite. Similarly the contact observed on the foot track from Ruwa khola to Bandal, Surnayagad section, Dotigad, Khar khola and right at left bank of Rawa khola is very sharp. However, at few places the contact is faulted and the rocks are fairly well sheared (Fig. 4).

In general granite gneiss at the contact becomes more leucocratic but in Khar khola section and in Ghanteshwar area it is biotite rich (15-30%). At few other places, at the contact the local effect of sericitization and greisenisation causes development of a narrow border zone which becomes rich in muscovite, quartzofelspathic minerals and few tourmaline. Its southern contact with the country rock at Rapaligad, Poknagad, Ghanghat khola, Khaluwagad and Ghanteshawar area is also intrusive. However, biotite content in the granite at the southern contact zone is higher than in the northern contact. It may be due to different type of country rocks which come at the contact and their intermixing effect.

Table 2a: Major Elements in Dadeldhura granite (values in %).

	S. No.	SiO$_2$	Al$_2$O$_3$	Fe$_2$O$_3$	MnO	MgO	CaO	Na$_2$O	K$_2$O	P$_2$O$_5$	TiO$_2$	LOI	Total
GGR	5	71.25	14.10	3.87	0.04	0.82	0.98	2.20	4.59	0.16	0.53	1.15	99.69
	406	73.90	13.90	1.64	0.03	0.04	0.55	2.92	5.25	0.17	0.15	0.89	99.44
	425	70.40	13.92	3.77	0.07	0.25	2.04	3.22	4.42	0.11	0.41	0.78	99.39
	439	72.98	13.37	2.62	0.06	0.36	1.44	2.98	4.63	0.11	0.31	0.68	99.54
	441	74.81	12.77	2.53	0.04	0.56	1.95	2.65	3.23	0.14	0.34	0.69	99.71
	455	71.97	15.67	2.57	0.04	0.00	0.44	3.71	4.03	0.28	0.07	0.75	99.53
	536	75.73	12.23	2.57	0.04	0.41	1.06	2.36	3.90	0.20	0.34	0.88	99.72
	543	73.97	13.72	2.23	0.05	0.57	0.92	2.79	4.06	0.16	0.27	0.88	99.62
	605	76.48	10.61	3.65	0.04	1.35	0.52	1.55	3.19	0.12	0.55	1.26	99.32
	707	74.87	13.22	1.55	0.02	0.10	0.50	2.89	5.00	0.22	0.11	0.94	99.42
	714	72.11	13.86	3.48	0.04	0.84	1.32	2.58	3.78	0.19	0.48	1.03	99.71
	824	73.64	13.56	1.85	0.03	0.16	0.63	3.24	4.93	0.19	0.12	1.20	99.55
	828	70.64	14.79	2.24	0.04	0.48	1.43	2.82	5.59	0.13	0.30	1.00	99.46
	829	73.37	13.39	2.61	0.04	0.55	0.87	2.66	4.33	0.17	0.28	1.23	99.50
	830	71.18	13.84	4.03	0.05	0.83	1.12	2.32	4.01	0.15	0.51	1.44	99.48
Avg. of 15 samples		73.15	13.53	2.75	0.04	0.49	1.05	2.73	4.33	0.17	0.32	0.99	99.54
BGR	1	75.15	13.62	1.43	0.02	0.13	0.74	2.84	4.53	0.22	0.10	0.90	99.68
	1a	74.30	13.43	2.06	0.04	0.15	0.48	2.87	4.91	0.18	0.12	0.98	99.52
	2	75.43	13.67	1.40	0.03	0.08	0.52	2.97	4.62	0.23	0.07	0.76	99.78
	493	73.90	12.72	3.07	0.04	0.69	1.02	2.39	3.94	0.18	0.43	1.00	99.38
	521	72.21	13.98	2.80	0.04	0.63	0.85	2.50	5.01	0.20	0.32	1.06	99.60
	527	70.26	14.61	3.55	0.06	0.77	1.09	2.55	4.55	0.23	0.48	1.10	99.25
	540	76.42	12.54	1.91	0.04	0.20	0.94	2.68	3.54	0.18	0.25	0.79	99.49
	548	71.74	14.08	3.43	0.05	0.81	1.33	2.64	3.70	0.19	0.50	1.14	99.61
	554	74.34	12.95	2.91	0.06	0.55	0.87	2.40	3.86	0.17	0.38	1.01	99.50
	566	72.13	14.52	2.09	0.04	0.34	0.99	3.13	4.82	0.20	0.24	0.81	99.31
	708	73.08	14.36	1.66	0.04	0.14	0.58	3.42	4.85	0.20	0.15	0.74	99.72
	709	73.25	13.47	2.90	0.06	0.66	0.96	2.47	4.06	0.17	0.38	1.20	99.58
	710	75.09	12.37	3.13	0.05	0.74	0.94	2.38	3.45	0.15	0.41	0.79	99.50
	710a	71.82	13.84	3.33	0.05	0.75	0.99	2.47	4.45	0.14	0.39	1.20	99.43
	822	70.90	14.68	3.13	0.05	0.62	0.89	2.82	4.85	0.17	0.35	1.05	99.51

S.No.												Total
825	74.13	13.50	1.71	0.03	0.15	0.57	3.14	4.96	0.17	0.11	1.04	99.58
826	73.45	12.86	3.08	0.04	0.53	0.99	3.00	4.11	0.10	0.36	0.96	99.57
827	72.67	13.62	2.46	0.04	0.45	0.84	3.22	4.53	0.14	0.28	1.24	99.56
Avg. of 18 samples	73.35	13.60	2.56	0.04	0.47	0.87	2.77	4.37	0.18	0.30	0.99	99.50
MGR 496	73.80	14.81	0.87	0.03	0.00	0.34	3.66	4.45	0.26	0.05	1.20	99.47
499	73.13	13.91	1.91	0.03	0.39	0.72	2.76	5.42	0.18	0.25	0.88	99.63
570	73.72	14.42	1.57	0.03	0.00	0.50	3.23	5.03	0.18	0.15	0.83	99.66
573	78.28	11.90	0.89	0.02	0.00	0.31	3.24	3.76	0.27	0.05	0.75	99.47
Avg. of 4 samples	74.73	13.76	1.31	0.03	0.10	0.47	3.22	4.67	0.22	0.13	0.92	99.56
TGR 581	74.31	14.39	0.97	0.03	0.13	0.53	3.80	4.35	0.21	0.11	0.68	99.54
583	76.37	14.51	0.66	0.01	0.17	0.43	5.84	0.57	0.29	0.06	0.51	99.42
Avg. of 2 samples	75.34	14.45	0.82	0.02	0.15	0.48	4.82	2.46	0.25	0.09	0.60	99.48
Whole average of 39 samples	73.52	13.63	2.41	0.04	0.42	0.87	2.90	4.28	0.18	0.27	0.95	99.49

Values < 3, 5, 10, 15, 20 ppm are converted to 1.5, 2.5, 5, 7.5, 10 ppm for calculation.

Table 2b.--Trace elements in Dadeldhura granite (value in ppm.)

	S.No.	Ba	Ca	Nb	Pb	Rb	Sn	Sr	Ta	Th	U	W	Y	Zn	Zr
GGR	5	391.0	67.0	15.0	38.0	222.0	34.0	90.0	8.0	25.0	4.0	2.5	26.0	77.0	212.0
	406	111.0	32.0	16.0	34.0	396.0	10.0	29.0	2.5	14.0	35.0	2.5	24.0	47.0	86.0
	425	669.0	72.0	14.0	41.0	215.0	24.0	110.0	2.5	20.0	6.0	2.5	35.0	62.0	209.0
	439	421.0	81.0	7.0	36.0	264.0	10.0	74.0	2.5	20.0	3.0	6.0	36.0	41.0	138.0
	441	244.0	70.0	6.0	32.0	192.0	10.0	88.0	2.5	20.0	8.0	6.0	30.0	50.0	160.0
	455	7.5	10.0	10.0	23.0	343.0	10.0	8.0	10.0	2.5	5.0	2.5	6.0	108.0	9.0
	536	113.0	45.0	13.0	31.0	236.0	10.0	52.0	2.5	12.0	1.5	5.0	28.0	56.0	133.0
	543	136.0	37.0	12.0	32.0	319.0	26.0	54.0	2.5	13.0	3.0	2.5	18.0	49.0	112.0
	605	353.0	83.0	11.0	19.0	219.0	10.0	41.0	2.5	20.0	4.0	2.5	32.0	38.0	272.0
	707	7.5	10.0	14.0	37.0	383.0	10.0	15.0	2.5	8.0	1.5	2.5	21.0	39.0	58.0
	714	311.0	84.0	11.0	42.0	197.0	10.0	100.0	2.5	16.0	1.5	2.5	18.0	67.0	188.0
	824	80.0	35.0	17.0	33.0	398.0	35.0	11.0	5.0	15.0	2.5	5.0	15.0	45.0	75.0
	828	891.0	75.0	17.0	35.0	271.0	32.0	83.0	5.0	24.0	2.5	5.0	29.0	36.0	161.0
	829	238.0	42.0	18.0	22.0	321.0	47.0	51.0	5.0	12.0	2.5	5.0	15.0	62.0	120.0
	830	381.0	87.0	20.0	34.0	213.0	15.0	88.0	5.0	19.0	2.5	5.0	14.0	71.0	212.0
Avg. of 15 samples		290.3	54.2	13.4	32.6	279.3	19.5	59.6	4.0	16.0	5.5	3.8	23.1	56.5	143.0
BGR	1a	72.0	35.0	19.0	34.0	442.0	15.0	2.5	5.0	5.0	2.5	5.0	16.0	52.0	45.0
	1	72.0	16.0	12.0	35.0	365.0	10.0	19.0	7.0	15.0	1.5	2.5	15.0	34.0	60.0
	2	0.0	3.0	13.0	36.0	430.0	20.0	10.0	2.5	2.5	1.5	12.0	8.0	38.0	48.0
	493	158.0	73.0	11.0	40.0	292.0	10.0	54.0	2.5	20.0	1.5	2.5	28.0	54.0	189.0
	521	131.0	53.0	13.0	32.0	291.0	21.0	58.0	7.0	16.0	7.0	10.0	28.0	59.0	144.0
	527	186.0	99.0	19.0	37.0	307.0	10.0	66.0	6.0	23.0	5.0	6.0	34.0	64.0	187.0
	540	101.0	10.0	14.0	29.0	283.0	10.0	41.0	9.0	15.0	9.0	6.0	24.0	50.0	108.0
	548	181.0	111.0	16.0	24.0	245.0	10.0	75.0	2.5	24.0	1.5	2.5	22.0	73.0	219.0

	554	227.0	35.0	19.0	28.0	286.0	24.0	57.0	7.0	18.0	12.0	2.5	36.0	63.0	157.0
	566	168.0	25.0	9.0	44.0	304.0	10.0	67.0	2.5	9.0	10.0	6.0	21.0	49.0	103.0
	708	95.0	37.0	14.0	32.0	406.0	10.0	30.0	2.5	11.0	1.5	2.5	12.0	52.0	65.0
	709	181.0	73.0	18.0	30.0	301.0	10.0	56.0	2.5	22.0	1.5	2.5	24.0	58.0	180.0
	710	122.0	84.0	11.0	38.0	228.0	10.0	53.0	2.5	18.0	3.0	2.5	37.0	61.0	182.0
	710a	291.0	86.0	17.0	44.0	267.0	31.0	60.0	5.0	18.0	5.0	5.0	22.0	64.0	168.0
	822	194.0	83.0	22.0	39.0	337.0	15.0	48.0	5.0	16.0	2.5	5.0	21.0	62.0	139.0
	825	69.0	41.0	19.0	37.0	427.0	57.0	10.0	5.0	12.0	2.5	5.0	11.0	41.0	64.0
	826	245.0	71.0	17.0	44.0	241.0	39.0	58.0	5.0	16.0	8.0	5.0	27.0	52.0	164.0
	827	269.0	35.0	17.0	48.0	325.0	42.0	52.0	5.0	5.0	2.5	5.0	16.0	75.0	135.0
Avg. of 18 samples		149.6	51.9	15.6	36.2	320.9	19.7	45.4	4.6	14.7	4.3	4.9	22.3	55.6	130.9
MGR	496	7.5	10.0	27.0	18.0	602.0	21.0	1.5	7.0	5.0	1.5	19.0	9.0	52.0	40.0
	499	343.0	39.0	10.0	40.0	338.0	21.0	59.0	6.0	19.0	1.5	2.5	21.0	42.0	127.0
	570	111.0	10.0	14.0	40.0	353.0	10.0	24.0	2.5	7.0	5.0	2.5	24.0	62.0	67.0
	573	0.0	0.0	14.0	29.0	387.0	10.0	3.0	8.0	2.5	1.5	2.5	1.5	28.0	2.5
Avg. of 4 samples		115.4	14.8	16.3	31.8	420.0	15.5	21.9	5.9	8.4	2.4	6.6	13.9	46.0	59.1
TGR	581	140.0	10.0	10.0	29.0	245.0	41.0	61.0	2.5	7.0	4.0	2.5	14.0	44.0	38.0
	583	0.0	4.0	5.0	5.0	34.0	10.0	19.0	8.0	2.5	1.5	10.0	8.0	33.0	21.0
Avg. of 2 samples		70.0	7.0	7.5	17.0	139.5	25.5	40.0	5.3	4.8	2.8	6.3	11.0	38.5	29.5
Whole Avg. of 39 samples		196.1	16.7	14.4	33.4	305.8	19.5	48.2	4.6	14.1	4.5	4.7	21.2	54.1	123.0

Values < 3, 5, 10, 15, 20 ppm are converted to 1.5, 2.5, 5, 7.5, 10 ppm for calculation.

The contracts between different types of granite are well defined only at few places. Presence of similar mineralogy and grain size the contact between massive BGR and GGR is gradational. At places the massive granite grade progressively into orthogneiss. The foliation in gneiss also decreases towards the central part and appear as massive granite. Due to hard nature of granite the deformation effect could not reach to the central part (Le Fort, 1983).

The contact between MGR and GGR is fairly sharp. The mineral composition, grain size and leucocratic nature of MGR help to distinguish it from GGR. Similarly the contact between aplitic TGR and GGR is very sharp. TGR in most places has cross cut relation with GGR. The contact between BGR and MGR is rather gradational as a result it is difficult to put sharp boundary line between the two units. However, the amount of biotite and muscovite help to separate two rock types. At places xenoliths of fine grained biotite schist and micaceous quartzite are noted within GGR and BGR.

GEOCHEMISTRY

More than 39 rock samples of different types of granite and 3 xenoliths were analysed for major and trace elements by XRF. some of the representative analysis are giren in the table (Table 2a, and 2b). Comparative study on chemical characteristics of various types of granite shows a range of distribution pattern in silica (70.26 - 78.28%), alkalis 3.7 - 10.19% and alumina (10.61 - 15.67%) content. Where as Rb (34-602 ppm), Sr (3-110 ppm), Ba (0.891 ppm), Zr (< 5-272 ppm) and Pb (5-48 ppm) show a wide range of distribution pattern.

Inter elements variation within the massif are more irregular (Fig. 5), however, there exist a positive correlation between SiO_2 vs Na_2O, K_2O, Al_2O_3, P_2O_5 and Rb (Fig. 5a, 5b, 5c, 5d, 5i) and negative correlation between SiO_2 vs CaO, MgO, TiO_2, FeO and Sr (Fig. 5e, 5f, 5g, 5h and 5j).
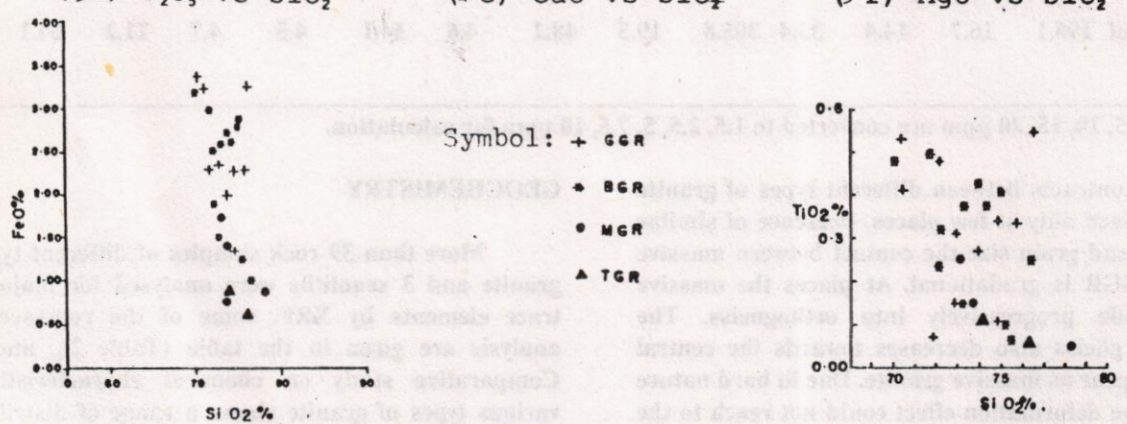
Triangular plot of normative quartz - Orthoclase - Palgioclase (QAP diagram) show that they fall within the field of granite (Fig. 6) Most of the granites cluster
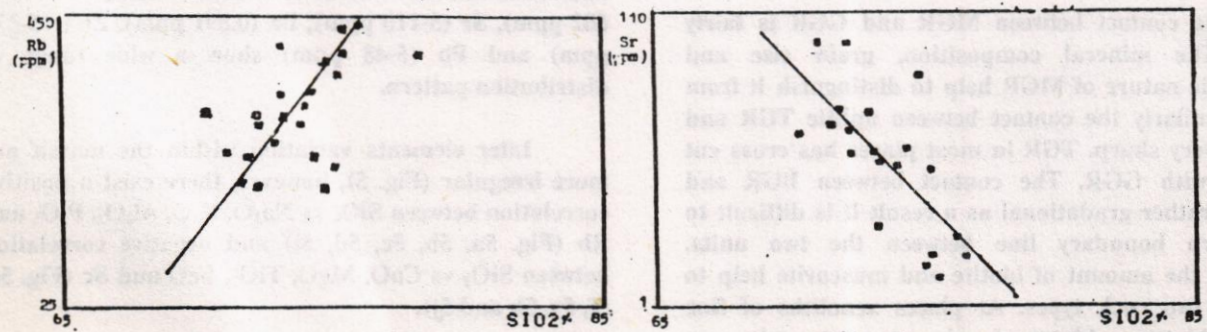
(5a) Na₂O vs SiO₂
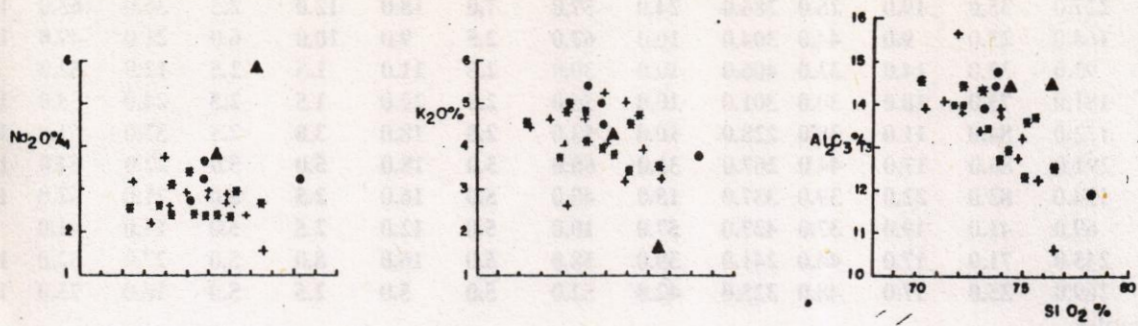
(5a) Na$_2$O vs SiO$_2$

(5b) K$_2$O vs SiO$_2$

(5c) Al$_2$O$_3$ vs SiO$_2$
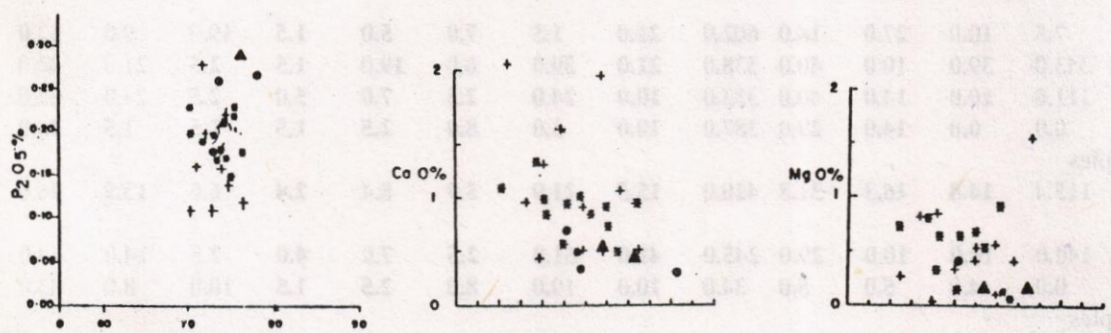
(5d) P$_2$O$_5$ vs SiO$_2$

(5e) CaO vs SiO$_2$

(5f) MgO vs SiO$_2$

Symbol: + GGR
■ BGR
● MGR
▲ TGR

(5g) FeO vs SiO$_2$

(5h) TiO$_2$ vs SiO$_2$

(5i) Rb vs SiO$_2$

(5j) Sr vs SiO$_2$

26

Fig. 5 Variation diagrams SiO$_2$ vs Major oxides and SiO$_2$ Vs Trace elements.
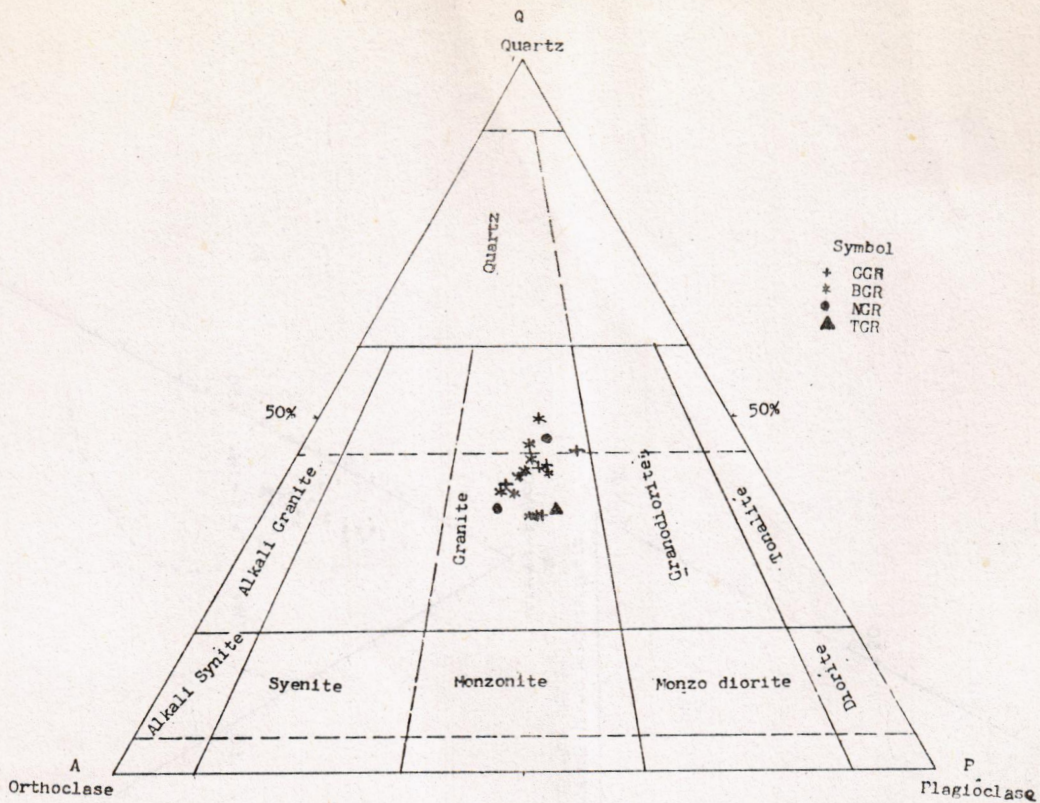
Fig. 6   Triangular diagram showing distribution of Dadeldhura granite using CIPW norm. Quartz - Qrthoclase - Plagioclase on a quantitative mineralogical Classification of Ingenous rock (Strekeisen, 1967).
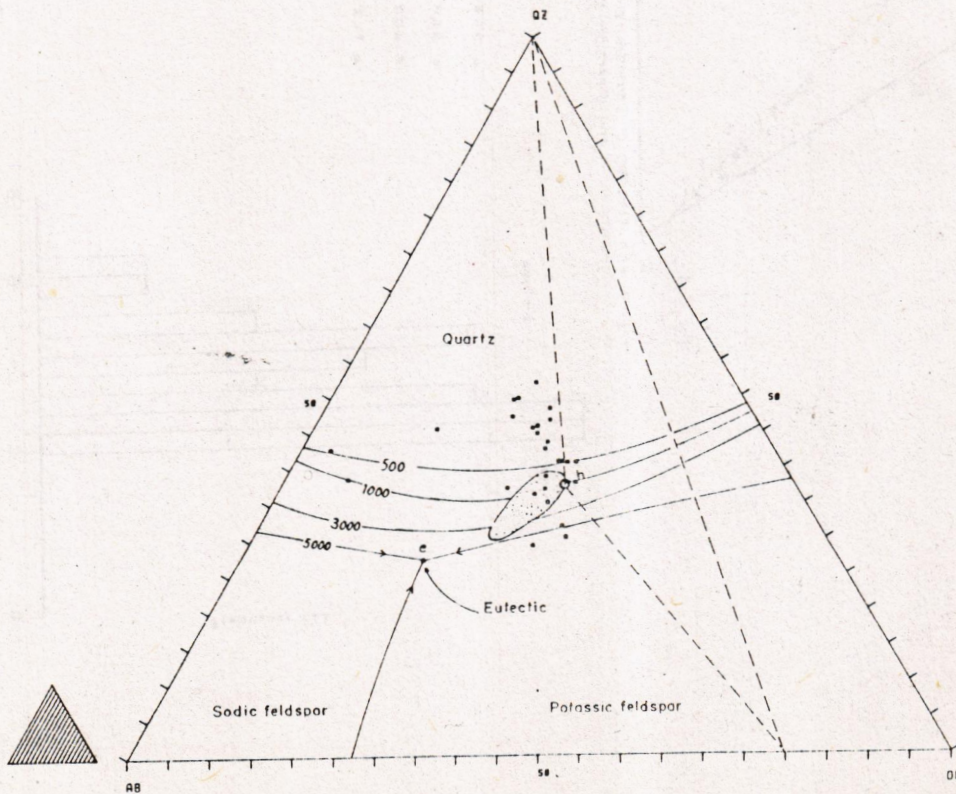
Fig. 7   Triangular plot of Dadeldhura granite using CIPW norm. Quartz - Albite - Orthoclase. (Tuttle & Bowen, 1958).
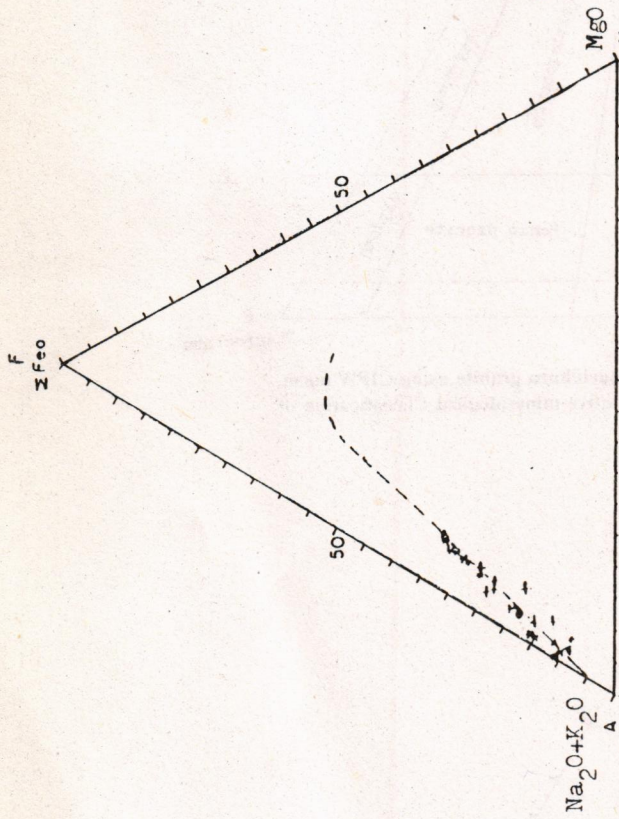
Fig. 8 AFM diagram of Dadeldhura granite (variation trend in Dadeldhura granite is in the direction of a more alkali rich liquid).

Fig. 10 ACF diagram of Dadeldhura granite (diagram after Takahasni et al. 1981, for I – type and S – type granites).

Fig. 9 Histogram showing mol. Al2O3 / (Na2O +K2O+ CaO) in Dadeldhura granite.
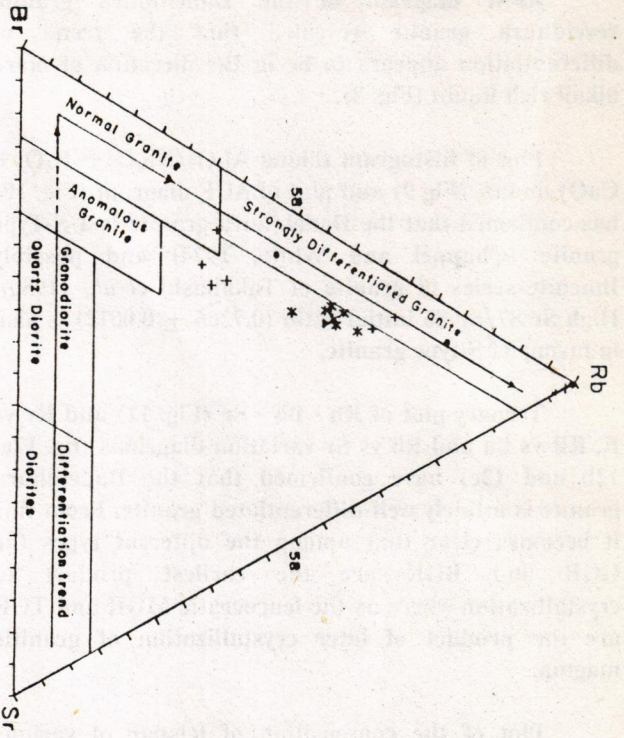
Fig. 11 The application of the different fields of the Ternary relation Rb - Ba - Sr on Dadeldhura granite (Diag. after Bouseily and Sokkory, 1975).
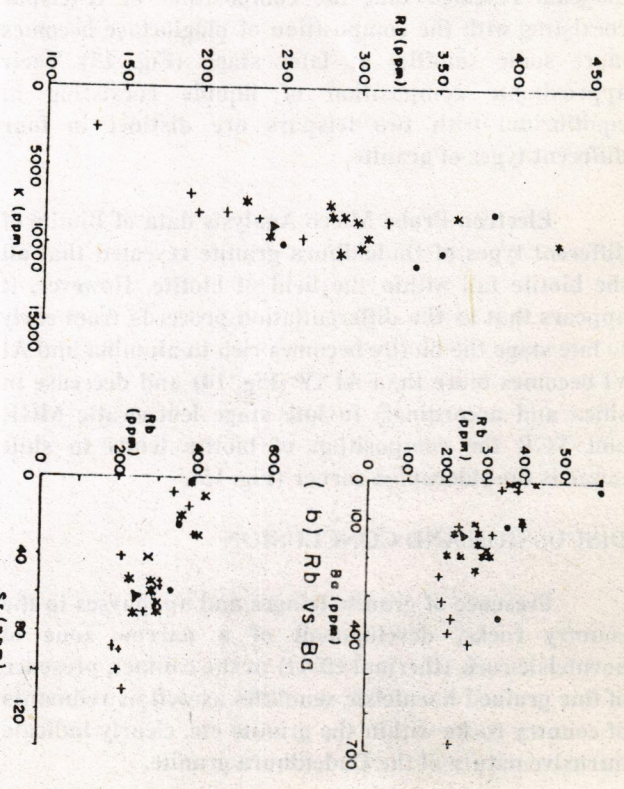
Fig. 12 Variation diagrams (a) Rb vs K, (b) Rb vs Ba, (c) Rb vs Sr.

(a) Rb vs K

(b) Rb vs Ba

(c) Rb vs Sr
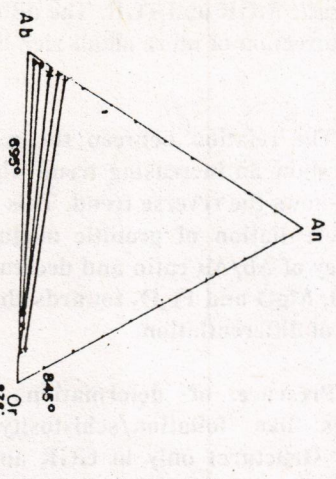
Fig. 13 Plot of the composition of felspar of Dadeldhura granites on Ab - An - Or triangular diagram showing approximate composition of liquids coexisting in equilibrium with two felspars (Diagram after, Carmichael, 1963).
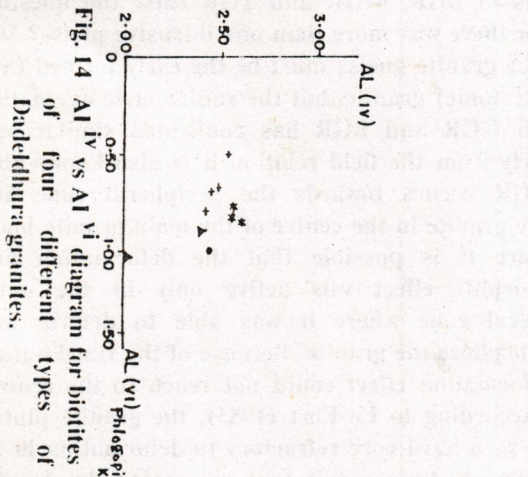
Fig. 14 Al iv vs Al vi diagram for biotites of four different types of Dadeldhura granites.
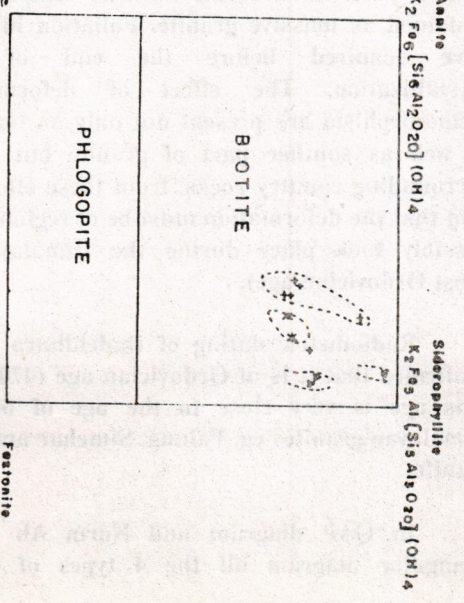
Fig. 15 Plot of the composition of biotites of Dadeldhura granite on phlogopite - Biotite compositional field.

PHLOGOPITE

BIOTITE

Annite
$K_2 Fe_6 [Si_6 Al_2 O_{20}] (OH)_4$

Siderophyllite
$K_2 Fe_5 Al [Si_5 Al_3 O_{20}] (OH)_4$

Phlogopite
$K_2 Mg_6 [Si_6 Al_2 O_{20}] (OH)_4$

Eastonite
$K_2 Mg_5 Al [Si_5 Al_3 O_{20}] (OH)_4$

around <500 to 2000 bars (Fig. 7) which indicates that P_{H_2O} of magma generally does not exceeds 2000 bars (Tuttle and bowen, 1958) with some exceptions.

AFM diagram of the Dadeldhura granite reveldhura granite revealed that the trend of differentiation appears to be in the direction of more alkali rich liquid (Fig. 8).

Plot of histogram taking $Al_2O_3/Na_2O + K_2O + CaO)$ molar, (Fig 9) and plot of ACF diagram (Fig. 10) has confirmed that the Dadeldhura granite is a S-Type granite (Chappel and White, 1974) and possibly Ilmenite series of granite of Takahashi et al., (1980). High Sr 87/Sr 86 initial ratio (0.7266 $\pm$ 0.0012) is also in favour of S-type granite.

Ternary plot of Rb - Ba - Sr (Fig. 11) and Rv vs K, RB vs Ba and Rb vs Sr variation diagrams (fig. 12a, 12b and 12c) have confirmed that the Dadeldhura granite is a fairly well differentiated granite. From this it becomes clear that among the different types the GGR and BGR are the earliest product of crystallization where as the leucocratic MGR and TGR are the product of later crystallization of granitic magma.

Plot of the composition of felspar of various types of Dadeldhura granite on Ab - An - Or triangular diagram revealed that the composition of K-felspar coexisting with the composition of plagioclase becomes more sodic (albitic) at later stage (Fig. 13) Their approximate composition of liquids coexisting in equilibrium with two felspars are distinct in four different types of granite.

Electron Probe Micro Analysis data of Biotite of different types of Dadeldhura granite revealed that all the biotite fall within the field of biotite. However, it appears that as the differentiation proceeds from early to late stage the biotite becomes rich in alumina and Al VI becomes more than Al IV (Fig. 14) and decrease in silica and accordingly in late stage leucocratic MGR and TGR the composition of biotite tends to shift towards the siderophyl corner (Fig. 15).

DISCUSSION AND CONCLUSION

Presence of granite fringes and apophyses in the country rocks, development of a narrow zone of hornfelsic rock (thermal effect) at the contact, presence of fine grained hornfelsic xenoliths as well as remnants of country rocks within the granite etc. clearly indicate intrusive nature of the Dadeldhura granite.

Dadeldhura granite is a fairly well differentiated granites. Differentiation trend is marked by the increase in alkalis, silica, alumina and Rb content and decrease in lime, magnesia, iron and Ba content from early crystallized GGR and BGR to later crystallized leucocratic MGR and TGR. The differentiation trend is in the direction of more alkali rich liquid (calk alkaline trend).

The relation between the ratio of Rb/Ba and Rb/Sr show an increasing trend where as the ratio of Ba/K shows the reverse trend. This is due to the result of differentiation of granitic magma. The increasing tendency of Ab/An ratio and decreasing of the amount of CaO, MgO and Fe_2O_3 towards the later stage are in favour of differentiation.

Presence of deformation and metamorphic features like foliation/schistosity and gneissosity (augen structure) only in GGR and absence of such features in BGR, MGR and TGR raise the question whether there was more than one intrusive phase? If it is so the granite gneiss must be the early formed (Syn or pretectonic) granite. but the radiometric age dating of both GGR and BGR has confirmed similar age. Similarly from the field relation it is also known that the GGR occurs towards the peripheral zone and massive granite in the centre of the main granite body. Therefore it is possible that the deformation and metamorphic effect was active only in the outer peripheral zone where it was able to deform and metamorphose the granite. Because of the Hard nature the deformation effect could not reach to the central part. According to Le Fort (1983), the granite pluton behave as a hard core refractory to deformation in its central part. As a result towards centre the granite remained as massive granite. Foliation in GGR must have acquired before the end of magmatic crystallization. The effect of deformation and metamorphism are present not only on both northern as well as souther part of granite but also in the surrounding country rocks. from these effect it can be said that the deformation must be of regional scale and possibly took place during the Himalayan orogeny (Post Ordovician age).

Radiometric dating of Dadeldhura granite has confirmed that it is of Ordovician age (470 $\pm$ 5.6 ma). This age is very close to the age of other Lesser Himalayan granites eg. Palung, Simchar and Mansehra granite.

In QAP diagram and Norm Ab - An - Or triangular diagram all the 4 types of Dadeldhura

granite fall within the field of granite. They are peraluminous, quartz rich, potassic granite. Petrography and geochemistry of Dadeldhura granite confirm that it is a S-type granite.

The chemico-mineralogical characteristics and age of the Dadeldhura granite are similar to that of other Lesser Himalayan granites eg. Manserah granite of Hazara, Pakistan and Plaung and Simchar granite of central Nepal. As in Mansehra granite the Dadeldhura granite shows a remarkable evolutionary trend which is marked by the increase of Soda, potash, silica and alumina and similarly felspar dominate over the dark minerals and muscovite over the biotite.

ACKNOWLEDGEMENTS

REFERENCES

Bashyal, R. P., (1981). Geology of Dhanagarhi - Dadeldhura road section and its regional significance. *Jour. Nepal Geol. Soc.* Vol. 1, No. 1.

Bashyal, R. P., (1981). Geology of Lesser Himalaya, Far Western Nepal. *Sci. de la terre*, Memorie 47, pp. 31-42.

Gansser, A. (1964). Geology of Himalaya. *Int. Sci. Pub.* London, New York.

Hagen, T. (1969). Report on Geological Survey of Nepal, Vol. 1, Preliminary reconnaissance, Denkschar, Schweiz, Naturt. Zurich.

Heim, A. and Gansser, A. (1939). Central Himalaya geological observations of the Swiss expedition, 1936, *Mem. Soc. Helv. Sci. Nat.*, Vol. 37, (1).

Hohendorf, A., Kaphel, K. P. and Einflat, H. C., (1991). Rb - Sr whole rock age determination of Dadeldhura granite, Far-Western Nepal (in press).

Joshi, P. R., (1973). Report on the Geological investigation of mineral resources around Palung granite, Makwanpur district, Narayani Zone. DMG. Unpub. report.

Joshi, P. R., (1974). Report on geological investigation of the mineral resources around Kapre and Ipa-Arkhaule granite. Lalitpur, district, Bagmati zone. DMG Unpub. report.

Joshi, P. R., (1978). Report on geological and geochemical investigation of mineral resources in Dadeldhura granite, Dadeldhura, Mahakali zone. DMG Unpub. report.

Joshi, P. R., (1988). Geology and exploration for tin mineralization in the Himalayas of Nepal. Hutchinsons Edt. "Geology of Tin Deposits in Asia and the Pacific. UN/ESCAP.

Kaphle, K. P. and Adhikary, G. R., (1980). Report on geological and geochemical prospecting of Bamangaon copper - Tungsten prospect and Meddi Tin prospect, Dadeldhura, Mahakali zone Far Western Nepal. DMG Unpub. report.

Kaphle, K. P., (1981). Geological and geochemical exploration of Cu - W prospect at Bamangaon and adjacent areas, Dadeldhura, Far Western Nepal. ESCAP/RMRDC, "Symp. on Tungsten Geology", Jiangxi, China.

Kaphle, K. P., (1984). Report on follow-up geochemical and geological survey of Ruwa Khola area with special emphasis on petrology, chemistry and genesis of Dadeldhura granite, Dadeldhura, Far Western Nepal. DMG. Unpub. Report.

Kaphle, K. P., (1988). Geology, Petrology and chemistry of Dadeldhura granite Far Western Nepal, Paper presented to the international Seminar on *"Geodynamics of Nepal Himalaya"*, Kathmandu, Nepal.

Kaphle, K. P., (1992). The Dadeldhura Granite, Far-Western Nepal: A comparison with other Lesser Himalayan Granites. Paper presented at the *First South Asia Geological Congress (GEOSAS-I)*, *Islamabad*, Pakistan.

Kaphle, K. P., (1991). Geochemistry of Dadeldhura granite and its mineral potential. *Jour. Nepal Geol. Soc.*, Vol. 7, pp. 21-38.

Klominisky and Groove (1970). In J. C. Blockley's

paper (1980) on petrography and chemistry of granites associated with Western Australian tin deposits. Book Chapter. 5 pp. 109.

Le Fort, P. *et al.* (1980). The Lesser Himalayan cordierite granite belt, Typology and age of the Pluton of Mansehra (Pakistan). Procidings of the Int. Geodynamic conf. *Geol. Bull. of Univ. Peshawar*, Spec. Issue.

Le Fort, P. *et al.* Lower Paleozoic emplacement for granites and granitic gneisses of the Kathmandu nappe, Central Nepal. Terra Cognita Spec. issue, i, 30, 72.

Le Fort, P. *et al.* (1983). The Lower Paleozoic Lesser himalayan granite belt, emphasis on the Simchar pluton of Central Nepal. F. A. Shams Edt. "Granites of Himalayas, Karakorum and Hindukush" *Inst. Geol. Punjab Univ. Lahore, Pakistan.*

Mitchell, A.H.G. *et al.* (1983). Granitic rocks of the Central Himalaya, their tectonic setting and mineral potential. F. A. Shams edt. "Granites of Himalayas, Karakorum and Hindukush", *Inst. Geol. Punjab Univ. Lahore, Pakistan.*

Remmy, J. M., (1975). Geology of Nepal, West of Nepal Himalayas, CNRS (Ed). Paris, 72 p.

Shams, F. A., (1969). Geology of Mansehra - Amb state area, Northern W. Pakistan. *Geol. Bull. Punjab Univ. Lahore,* Vol. 8, p. 1-31.

Shams, F. A., (1980). An anatectic liquid of granitic composition from Hazara Himalaya. Pakistan and its petrogenetic importance. *R. C. Accad. Naz. Lincei.* Vol. 68, pp. 207-215.

Shams, F. A., (1983). Granite of the North West Himalayas in Pakistan. F. A. Shams edt. "Granites of Himalayas, Karakorum and Hindukush". *Inst. Geology, Punjab Univ. Lahore, Pakistan.*

Sharma, M. P., (1983). Mineralogy and geochemistry of Palung granite massif. *Jour. Nepal Geol. Soc.,* Vol. 2, No. 1.

Stocklin J., and Bhattaria, K. D., (1977). Geology of Kathmandu area and Central Mahabharat range, Nepal Himalaya, Kathmandu. *DMG/UNDP Tech. Report PG/11/77.*

Thakur, V. C., (1983). Granites of Western Himalayas and Karakourm, Structural framework Geochronology and Tectonics. F. A., Shams edt. "Granites of Himalayas, Karakorum and Hindukush". *Inst. Geology, Punjab Univ. Lahore, Pakistan.*

Trivedi, J. R., *et al.* (1984). Rb - Sr ages of granitic rocks within the Lesser HImalayan nappes, Kumaun, India. *Jour, Geol. Soc. India,* Vol. 25, No. 10.

Upreti, B. N., (1990). An outline geology of Far Western Nepal. *Jour. Himalayan Geology,* Vol. 1, pp. 93-102.

Valdiya, K. S., (1980). Geology of the Kumaun HImalaya, Wadia Institute of Himaalayan Geology, Dehradun, pp. 1-291.

Valdiya, K. S., (1983). Tectonic setting of Himalayan granites. F. A. Shams edt. "Granites of Himalayas, Karakorum and Hindukush". *Inst. Geology, Punjab Univ. Lahore, Pakistan.*

ASYMMETRICALLY ZONED COMPLEX PEGMATITE OF BAGARIAN AREA NORTH OF OGHI, MANSEHRA DISTRICT, HAZARA HIMALAYA, PAKISTAN

By

MOHAMMAD ASHRAF
Institute of Geology Azad Jammu & Kashmir University Muzaffarabad.

ABSTRACT: The Bagarian asymmetrically zoned complex pegmatite occur associated with Mansehra granitic complex in the interior-marginal zone near Oghi subdivision of Mansehra district. This pegmatite body is the most developed zonally and is most evolved with contrasting mineral composition on both sides of the quartz core. The zones on east side of core are border + wall zones with oligoclase, muscovite quartz and tourmaline; outer intermediate zone-microcline graphic granite; inner intermediate zone-subgraphic albite, quartz and muscovite. The zones on west side of quartz core are border + wall zone with albite, tourmaline, quartz and muscovite; outer intermediate zone-microcline perthite & minor muscovite; and inner intermediate zone-microcline perthite with minor quartz. Miarolitic cavity filled minerals of aqueous vapour phase are beryl columbite, samarskite Rb-rich translucent microcline, Rb & Li-rich muscovite. The Mansehra granitic magma was formed after 40% partial melting of Hazara and LowerTanol Formation pelites, which in turn gave rise pegmatitic magmatic solution to develop Bagarian pegmatite and aqueous phase modified for miarolitic minerals. It is envisaged that 75-90% fractional crystallization of granitic rest magma was responsible for the present shape of Bagarian pegmatite.
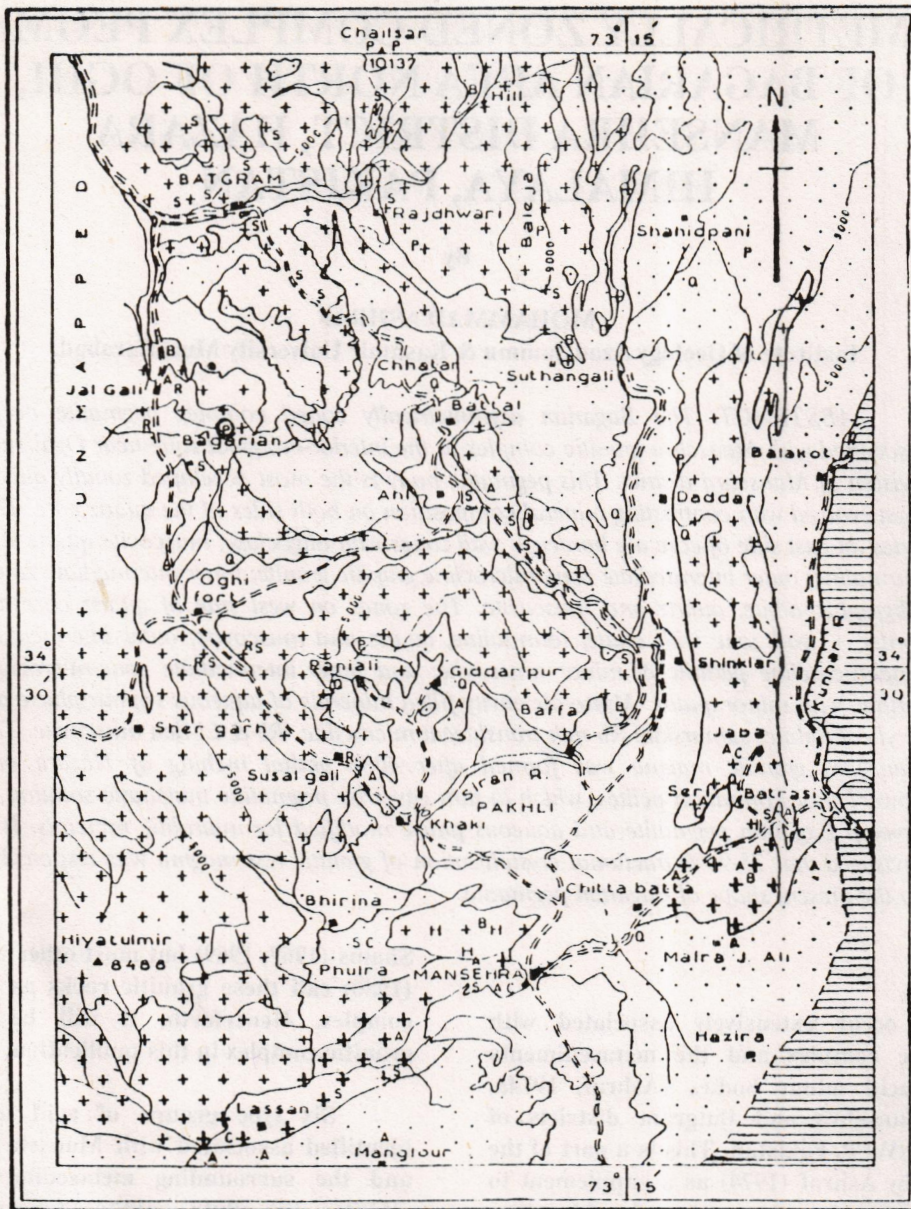
INTRODUCTION

Pegmatites occur extensively associated with Mansehra granitic complex and the metasediments alongwith other acid minor bodies (Ashraf, 1974a, 1974b) in the Mansehra and Batgram districts of Hazara Division, NWFP, Pakistan. This is a part of the work carried out by Ashraf (1974) as a supplement to study geochemistry and petrogenesis of acid minor bodies.

The Mansehra granitic complex and associated metasediments are found in the area west of Hazara-Kashmir Syntaxis of the North West Himalaya (Wadia, 1931) and east of Indus re-entrent. The metasediments are composed of pelites, psammitic pelites and pelitic-psammites with relatively pure bands of quartzites in Hazara and Tanol Formations. These metasediments are intruded by plutonic granitic rocks which are now porphyritic, granitoid to gneissic and with smaller outcrops of tourmaline granite. These granitic rocks have been grouped into the Hazara granitic complex by

Shams (1967, 1969) but most other workers like LeFort (1980) call these granitic rocks as Mansehra granitic complex. Henceforth, it will be called Mansehra granitic complex in this publication.

Six type groups of acid minor bodies were identified associated with Mansehra granitic complex and the surrounding metasediments. They are (i) albitites, (ii) albite - aplites / pegmatites (iii) albite-(microcline) aplites / pegmatites (iv) albite - microcline aplites / pegmatites (v) microcline - albite aplites / pegmatites and (vi) complex aplites / pegmatites. Consi-dering their internal structures and mineral compositions these acidic bodies have been further subdivided by Ashraf (1976, 1983). The type groups (i) to (iv) are found in interior - lateral zone upto 1525 m (5000 ft) contour (Ashraf 1974a, 1974b, 1975, 1976 modified after Heinrich 1953), the type groups (iv) and (v) are found in interior - marginal zone 1525 m - 2750 m (5000 - 9000 ft) and groups types (v) and (vi) to the exterior - marginal zone more than 2750 m (>9000 ft). The Bagarian pegmatite falls in the interior-marginal

Fig. 1 Geological Map of Mansehra and Batgram Area Hazara District showing Location and Distribution of Acid Minor Bodies.

zone. This ultra-acidic complex body occur in Mansehra district north of Oghi near village Bagarian at long. 70° 1′ 35″ and lat. 34° 34′ 45″ (Fig. 1).

GEOLOGY OF BAGARIAN PEGMATITE

There are numerous pegmatites in the area north-east of Bagarian which are simple unzoned to zoned and complex zoned (symmetrical and asymmetrical). The one near ridge top (NNE of Bagarian) is asymmetrically zoned and with rare minerals occurrence and is called Bagarian asymmetrical zoned complex pegmatite.

This pegmatite is the most interesting one in this respect that it is an asymmetrical body with zones developed on both sides of the quartz core (Fig. 2) having different mineral composition. On the eastern side are comparatively higher temperature zones and on the western side are lower temperature zones. On the eastern side zones are (vii) border+wall zone with oligoclase, muscovite, quartz and tourmaline, (vi) outer intermediate zone (eastern) - graphic granite, (v) inner intermediate zone-subgraphic albite, quartz, muscovite (iv) the core of quartz (iii) inner intermediate zone (western) microcline perthite with minor quartz, (ii) outer intermediate zone (western) microcline perthite, muscovite, (i) borber + wall zone western albite, tourmaline, quartz and muscovite. This pegmatite has also been replaced by pneumatolytic fluids near the inner intermediate zones on both side of core with the development of beryl, columbite, microcline perthite, samarskite muscovite and garnet. But the northern most end of the pegmatite on both sides has extensively been replaced.

This body is about 60 metres long and 25 metres wide in the middle and is pod like which is evident from its structural relation or the contact foliation with the granite gneiss. The foliation of the contacts on both sides of the body dip in opposite directions i.e., 192°E/50°E and 21°E/42°W and the pegmatite is completely enveloped by granite gneiss in the southern portion. The quartz core is developed throughout the body almost in the centre with variable thickness.

In the outer portion of outer intermediate zone near wall zone, pods of muscovite are developing in the form of books with haphazard orientation. Similar muscovite books are also developing in the inner intermediate zone near core. The size of muscovite books is 2 to 10 cm. The garnet bearing muscovite pods have muscovite around 3 to 10 cm. The modal composition of different zones is listed in Table - 1.

(i & vii) Border+Wall Zones

These zones are about 2 to 28 cm thick and with variation in thickness it is present all around the pegmatite body. The composition of the border and wall zone is essentially same except that the wall zone has much coarser grains about 3 to 12 mm. Therefore, for the sake of convenience the border and wall zones have been described here under the same heading.

These zones are rich in tourmaline, albite, quartz and muscovite in the western contact and tourmaline, oligoclase, quartz and muscovite in the eastern contact. In both cases tourmaline is replacing feldspar and quartz. The texture is clearly evident (alongwith the wall zone) on the western contact which is foliated and the grains are usually fine (0.2 to 1 mm) and occasionally upto 1.5 mm. The details of minerals in these zones are:

Albite is in the form of 0.5 to 1.5 mm euhedra and subhedra. It is twinned according to albite law and sometimes on carlsbad, baveno and pericline laws. Composition is An_6. It is quite fresh, fractured and contains inclusions of muscovite. It is present in the rocks of western border and wall zone.

Oligoclase occurs as 1 to 9 mm euhedra and subhedra twinned on albite and pericline laws. Composition is An_{12}. It alters to sericite and being replaced by muscovite and tourmaline.

Quartz is generally 1 to 4 mm anhedra with finer grains around 0.4 to 1 mm. Its interlocking aggregates occur at places. It is being replaced by tourmaline and sometimes have inclusions of very fine muscovite tablets.

Muscovite is usually 1 to 1.5 mm needles and occasionally as tabular flakes upto 2 mm. Sometimes it exsolves biotite along cleavage traces. It is abundantly present in the eastern wall zone and less common in the western wall zone.

Biotite is present as very fine flakes alongwith muscovite flakes and show pleochroism from light brown to yellowish colours.

Tourmaline is a light green to bottle green pleochroic mineral replacing quartz, albite, and muscovite. In the western wall zone it is usually anhedral and coarser upto 10 mm in thin section while in the border zone tourmaline is 0.2 to 0.5 mm in size and is light green, brownish green to dirty green

Legend:

- [+] Susalgali granite gneiss
- [/] Border & wall zones
- Outer intermediate zone (eastern)
- [△] Inner " " "
- Intermediate zone (western)
- The core
- [C] Columbite
- [S] S̱marskite
- Muscovite pod
- [▲] Tourmaline
- [△] Beryl
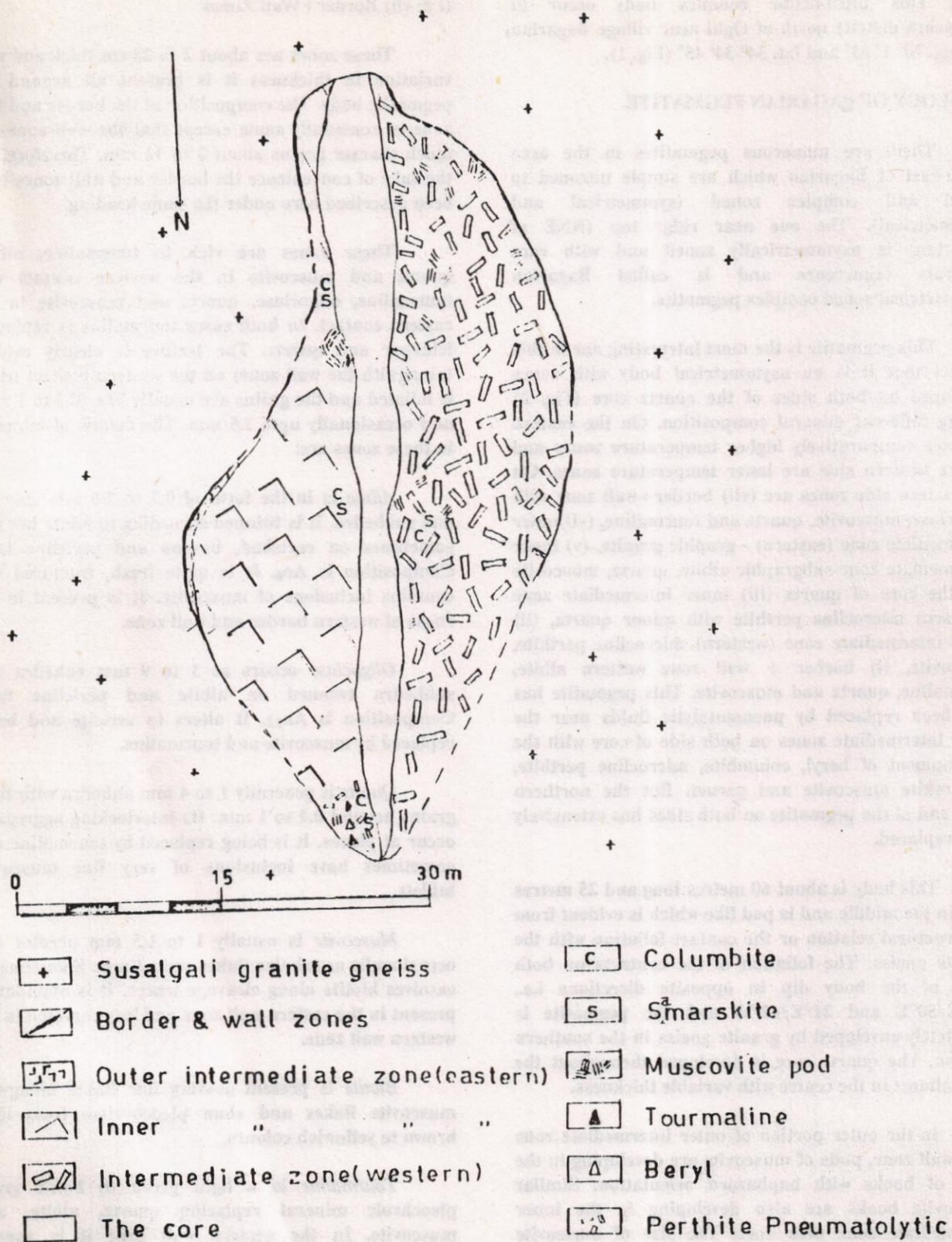- Perthite Pneumatolytic

0   15   30 m

N

Fig. 2 Complex pegmatite zoned asymmetrical near Bagarian.

pleochroic in both zones.

Garnet is present as 0.3 to 1 mm skeletal grains in the eastern wall zone. It is altering to limonitic material along cracks and on the surface.

Apatite is present in all the rocks of this zone from 0.2 to 1.2 mm subhedra and anhedra being replaced by muscovite and tourmaline.

Sphene occurs as very fine 0.1 to 0.2 mm brownish grains.

(vi) Outer Intermediate Zone (Eastern)

It is irregularly developed along the wall zone in the form of graphic granite. The structure is megascopic and subgraphic. Near the wall zone intergrowth is on finer scale and perfect while inward it is coarser and subgraphic. The zone is about 0.75 to 1.25 metres thick.

To find out the graphic relationship fine to medium-grained strings and rods bearing samples were cut for microscopic studies. It is found that the growth of quartz is graphic and subgraphic, and the latter type is dominantly present. The microcline - perthite is usually very coarse and the whole section is covered by it, the quartz forms aggregate of angular to subangular strings and rods which makes subgraphic to graphic intergrowth with microcline. Sometimes the microcline grains recrystallize near quartz rods and give rise 0.3 to 0.8 mm non-perthitic grains. The whole section is otherwise perthitic microcline.

Microcline normally covers the whole thin sections and has graphic to subgraphic intergrowth with quartz. Sometimes a few 0.3 to 0.8 mm grains are also found. The finer grains of microcline might be secondary possibly due to crushing and recrystallization along the weak zones. Twinning is well developed. Perthitic lamellae are widely forming at some places and comparatively less at other places. It alters to very fine grains of sericite and kaolinite.

Quartz occurs as angular to subangular rods forming a sort of graphic to subgraphic structure with microcline perthite. The rods are 3 to 6 mm long in one direction and these rods consist of interlocking quartz grains 0.5 to 3 mm in size. The quartz is mostly strained.

Albite occurs as perthitic lamellae and tablets twinned on albite and carlsbad laws. They occur in the form of very fine to about 0.5x2 mm stringlets and tablets subhedral and euhedral in shape respectively.

Muscovite is present as less than 0.1 to 0.5 mm tablets and flakes associated with microcline.

Sericite is an alteration product of microcline and rarely of albite.

Apatite forms very fine anhedral grains 0.1 mm occurring in the interstices of quartz and micricline in the sheared zone.

(v) Inner Intermediate Zone (Eastern)

This is the thickest (15 metres) zone of the pegmatite under study. It mainly consists of albite and quartz with minor muscovite. This zone gradually pinches out in the southern direction and is covered by granite gneiss. In the northern side the zone is being terminated and is modified by pneumatolytic replacement forming translucent microcline, beryl, columbite, samarskite, tourmaline and muscovite. The intergrowth of albite and quartz is subgraphic. The intergrowth of minerals was studied in the case of only those rock types which were medium grained. The coarsest grains were studied at their contacts and individually. However, it is seen that albite and quartz have subgraphic intergrowth where the former is a minor mineral from 8 to 25% in this zone near core.

Albite occurs as anhedral to subhedral 1 to 5 mm aggregate with finer grains in the range of 0.35 mm. The twin lamellae are wavy, curved and twinned according to albite law, moreover the twin lamellae are broken as they do not run along the entire length of the grains. Muscovite tablets about 0.1 to 0.3 mm are enclosed in it. Composition of albite is An$_7$.

Quartz grains are mostly of uniform size (3 to 5 mm) and shape, with occasional grains about 0.5 to 0.8 mm. The finer as well as coarser grains show wavy extinction and crenulated boundaries. Quartz grains contain small inclusions of muscovite tablets.

Muscovite is present as fine 0.1 to 0.3 mm fine inclusions and tablets (about 0.5 to 3 mm) associated with albite and quartz. Sericite occurs as an alteration product of albite.

Apatite occurs as very fine anhedral grains.

(ii)   **Outer Intermediate Zone (Western)**

This zone is about 8 metres thick in the middle. It pinches out in the northern direction while in the southern direction its width is slightly variable. The major constituting mineral is microcline - perthite with books of muscovite at places. The crystals of perthite are generally 8 to 20 cm long. In addition, tourmaline crystals (4 to 8 mm) are also developing in the outer portion of this zone.

In thin section the rocks consist of dominantly one grain of microcline perthite and some minor grains of muscovite, sericite and apatite.

Microcline is present as the sole mineral of the rock with occasional secondary finer grains of microcline. It shows gridiron twinning. Microcline exsolves albite patches and tablets. It shows a little alteration to sericite and kaolinite.

Albite occurs as veinlets, perthitic patches and as scattered tablets with albite and carlsbad twinning. The composition of albite in the veinlets is An_2 and that of perthtic lamellae is An_7. It also alters a little to sericite and kaolinite.

Muscovite is present in the form of fine tablets around 0.1 to 0.2 mm.

Sericite is an alteration product of microcline and rarely of albite.

(iii)   **Inner Intermediate Zone (Western)**

This zone is about 1 to 5 metres thick consisting mainly of microcline perthite with some muscovite books and rarely tourmaline and quartz. In the area near the core quartz pods are sometimes present in this zone. This zone is also replaced by columbite, samarskite, beryl, translucent microcline perthite and muscovite. The crystal size is about the same as that in the outer intermediate zone, but a few larger crystals are also present.

Under the microscope, the rocks of this zone are like the outer intermediate zone as regards size, texture etc. and also the mineralogy of the zone is almost same.

(iv)   **The Core**

It consists of only quartz (Fig. 2) with minor impurities like muscovite and ore at a few places throughout the zone. The thickness of the zone is slightly variable throughout its length and this zone is straight and occurs in the central region of the body. There is very divergent composition of the zones on both sides of it as mentioned earlier i.e., the eastern zone is composed of quartz and albite and the western zone consists of microcline.

Quartz: In thin sections the rocks of this zone are composed of an aggregate of fine to medium grains (0.3 to 1.5 mm) and rarely coarser upto 4 mm. The grains are thoroughly welded together to form medium grains aggregate. Sometimes fine inclusions of muscovite are present alongwith very fine inclusions of ores.

REPLACEMENT UNITS IN THE BAGARIAN PEGMATITES

As already mentioned there are columbite, samarskite, beryl, microcline, muscovite and tourmaline as replacement minerals. They have been emplaced on both sides of the core irrespective of the mineralogical composition of the zones.

Beryl is present in the northern most replacement unit in the eastern inner intermediate zone of the body. It is anhedral and sometimes subhedral to euhedral and almost white or sometimes with greenish tinge. Muscovite flakes about 1 to 2 mm envelope the crystals in almost all the cases as thin film around beryl. Under the microscope the beryl is colourless with low birefringence about that of quartz. Sometimes fine muscovite tablets occur as inclusions in it. Muscovite is euhedral needle like and as tablets (0.1 nm). Microcline occurs on the boundary and being replaced by beryl.

Columbite and samarskite both of them are closely associated together but **as** separate phases in lenticular to branching **type** ore bodies about 10 to 30 mm in thickness and about 10 to 15 cm long. They occur close to quartz core but definitely in the inner intermediate zone. Columbite (10 to 50 mm in size) is black to jet black with veinlets of muscovite. The samarskite is always jet black glassy looking material, the crystals (3 to 20 mm) of which are not traversed by any material except the outer surface is being enveloped by fine muscovite flakes. Columbite in thin section is dark red to brownish red coloured traversed by fractures which are sometimes filled by muscovite flakes (about 0.5 to 1 mm in size). The veinlets of muscovite are about 0.2 to 0.8 mm thick.

Table - 1 Petrographic composition of various zones of complex asymmetrical pegmatite from Bagarian

	A-85 Border+wall zone (eastern)	A-367 Outer intermediate zone (eastern)	A-365 Inner Intermediate zone (eastern)	A-98 Quartz Core	A-86 Muscovite pod in intermediate zone (western)
Albite	0.00	13.65	68.40	0.00	0.00
Oligoclase	18.04	0.00	0.00	0.00	0.00
Microcline	0.00	73.98	0.00	0.00	0.00
Quartz	26.04	10.08	24.58	98.11	0.00
Muscovite	31.81	1.08	6.37	1.89	100.00
Sericite	0.00	1.23	0.55	0.00	0.00
Biotite	0.26	0.00	0.00	0.00	0.00
Apatite	1.33	0.08	0.09	0.00	0.00
Tourmaline	21.91	0.00	0.00	0.00	0.00
Garnet	0.22	0.00	0.00	0.00	0.00
Epidote	0.04	0.00	0.00	0.00	0.00
Sphene	0.00	0.00	0.00	0.00	0.00
Ore	0.34	0.00	0.00	0.00	0.00

	A-89 Inner intermediate zone (western)	A-203 Outer intermediate zone (western)	A-291 Replacement unit of microcline perthite	A-358 Border+wall zone (western)
Albite	20.35	9.50	4.67	55.99
Oligoclase	0.00	0.00	0.00	0.00
Microcline	76.37	89.70	93.86	0.00
Quartz	0.00	0.00	0.00	23.08
Muscovite	0.00	0.79	0.20	6.90
Sericite	3.03	0.00	1.27	0.00
Biotite	0.00	0.00	0.00	0.00
Apatite	0.25	0.00	0.00	0.10
Tourmaline	0.00	0.00	0.00	13.54
Garnet	0.00	0.00	0.00	0.00
Sphene	0.00	0.00	0.00	0.10
Ore	0.00	0.00	0.00	0.29

Table - 2 Chemical composition of various zones of Bagarian complex pegmatite

	A-85 Border+ wall zones (eastern)	A-367 Outer intermediate zone (eastern)	A-365 Inner intermediate zone (eastern)	A-93 Quartz Core	A-86 Muscovite pod in intermediate zone (western)	A-89 Inner intermediate zone (western)	A-203 Outer intermediate zone (western)	A-291 Replacement unit of microcline perthite	A-358 Border+ wall zone (western)
SiO_2	61.38	67.40	75.56	97.57	46.62	61.97	61.81	62.87	70.01
TiO_2	0.63	0.17	0.08	0.04	0.08	0.06	0.09	0.00	0.45
Al_2O_3	19.78	17.80	14.72	0.00	34.82	20.11	20.56	20.96	17.34
Fe_2O_3	2.88	1.81	0.41	1.10	0.98	0.50	0.33	0.20	0.86
FeO	2.97	0.05	0.08	0.63	0.71	0.45	0.07	0.02	0.65
MnO	0.00	0.00	0.00	0.00	0.12	0.00	0.00	0.00	0.06
MgO	1.21	0.10	0.10	0.00	0.91	0.00	0.03	0.00	0.96
CaO	1.40	0.42	0.28	0.00	0.66	0.42	0.24	0.12	1.33
Na_2O	3.25	1.88	7.24	0.35	0.67	2.93	2.61	0.81	5.02
K_2O	2.60	10.58	0.35	0.05	9.99	13.50	14.13	14.75	1.16
P_2O_5	0.22	0.11	0.04	0.02	0.03	0.07	0.05	0.00	0.11
B_2O_3	2.21	0.00	0.00	0.00	0.00	0.00	0.00	0.00	1.20
H_2O^+	1.62	0.10	0.63	0.08	3.66	0.17	0.00	0.02	0.68
H_2O^-	0.06	0.07	0.36	0.00	0.45	0.00	0.04	0.00	0.10
Total:	100.01	100.49	99.85	99.84	99.70	100.18	99.96	99.75	99.93

Table - 3 Trace elements (ppm) in various zone of Bagarian complex pegmatite

	A-354 Ab.mi. aplite	A-354M Ab.mi. pegmatite	A-354T Ab.mi pegmatite	A-334 Ab.mi pegmatite (near contract)	A-337 Ab.mi. pegmatite	A-85 Wall zone	A-367 Graphic granite	A-365 Ab. Qtz. zone	A-93 Qtz. core	A-89 Microcline pegmatitic	A-291 Microcline pod pneumatolytic	A-86 Muscovite pod pneumatolytic
	Simple pegmatites unzoned					Bagarian complex pegmatite zoned						
Cr	--	--	--	--	--	18	--	--	--	30	--	--
Sc	--	--	--	--	--	--	--	--	--	--	--	--
Co	--	--	--	--	--	--	--	--	--	--	--	--
Zr	5	5	-	18	5	370	--	--	--	--	--	--
Ni	--	--	--	--	--	--	--	--	--	--	--	--
Y	--	--	--	--	--	10	--	--	--	--	--	--
V	--	--	--	--	--	--	--	--	--	--	--	--
Ga	5	5	5	5	10	20	10	14	--	5	5	40
Sn	--	--	--	---	--	200	--	--	--	--	--	500
Pb	15	10	10	--	10	10	30	--	--	15	5	--
Ba	10	10	25	25	5	--	25	10	--	10	5	--
Sr	5	5	5	5	--	5	10	--	--	5	5	--
Rb	240	240	240	180	240	240	700	25	--	3000	4500	3000
Li	1	1	2	5	15	100	40	15	--	40	40	300
Cs	--	--	--	--	--	--	--	--	--	--	--	--
Cu	10	22	4	4	4	10	4	10	10	10	-	10
Mo	--	--	--	--	--	--	--	--	--	--	--	--

Microcline perthite, it occurs as 3 to 15 cm thick white opaque to translucent material in the northern replacement zone and as pods or lenses in the inner intermediate zone. It is less perthitic than normal microcline perthite of the intermediate zone (western). It slightly alters to sericite. The albite lamellae show well developed albite twinning.

Tourmaline occurs in the replacement units of northern end of the pegmatite as black crystals about 10 to 15 mm in size and are scattered in this zone. Under the microscope it is green to bottle green pleochroic.

Muscovite occurs as thin flakes to books (10 to 60 mm) light grey and transparent. In thin section muscovite is colourless and have some inclusions of ore. It alters to kaolinite sometimes.

CHEMISTRY

The Bagarian complex pegmatite is asymmetrically zoned with minerological composition of the zones entirely different on both sides of the quartz core. Like variations in mineralogical compositions its chemistry also varies considerably on both sides of the core.

The border + wall zones on eastern sides has SiO_2 61.38%, Al_2O_3 19.78%, Fe_2O_3 2.88%, FeO 2.97%, MgO 1.21%, CaO 1.40%, Na_2O 3.25, K_2O 2.6%, P_2O_5 0.22%, B_2O_3 2.21%. On the western side composition is SiO_2 70.01%, Al_2O_3 17.34%, Fe_2O_3 0.86%, FeO 0.65%, MnO 0.06%, MgO 0.96%, CaO 1.33%, Na_2O 5.02%, K_2O 1.16%, P_2O_5 0.11%, B_2O_3 1.20%, (Table 2). This shows that mineralogical compositional variation is considerable on both sides of the core as there is oligoclase (18.04%) on the eastern side instead of albite (55.99%) on the western side, muscovite 31.81% and 6.92%, tourmaline 21.91% and 13.54%, apatite 1.33% and 0.10%, quartz 26.04 and 23.08% respectively.

The outer intermediate zones have also lot of variations on both sides of the core. SiO_2 in the eastern zone is 67.40% and in the western zone is 61.81%, TiO_2 0.17 and 0.09%, Al_2O_3 17.80 and 20.56%, Fe_2O_3 1.81 and 0.33%, FeO 0.05 and 0.07%, MgO 0.10 and 0.03%, CaO 0.42 and 0.24%, Na_2O 1.88 and 2.61%, K_2O 10.58 and 14.13%, P_2O_5 0.11 and 0.05% respectively. The mineralogical composition is also contrasting (Table-1) as albite 13.55 and 9.50%, microcline 73.98 and 89.70%, quartz 10.08 and 0.00%, muscovite and sericite 2.31 and 0.79%, apatite 0.08 and 0.00%.

The inner intermediate zones on eastern and western sides of the quartz core have great contrasting composition with SiO_2 on eastern side is 75.56% and on western side is 61.97%, Al_2O_3 14.72 and 20.11%, Fe_2O_3 0.41 and 0.50%, FeO 0.08 and 0.45%, CaO 0.28 and 0.42%, Na_2O 7.24 and 2.93%, K_2O 0.35 and 13.50, P_2O_5 0.04 and 0.07% respectively. Similarly mineral compositions also vary on both sides greatly as albite 68.40 and 20.35% (the latter being perthitic albite and former intergrown as graphic granitic albite), microcline 0.00 and 76.37%, quartz 24.58 and 0.00%, muscoite 6.37 and 0.79%, sericite 0.55 and 0.00% apatite 0.09 and 0.00%.

The quartz core is quite pure having SiO_2 97.57%, TiO_2 0.04%, Fe_2O_3 1.10%, FeO 0.63%, Na_2O 0.35%, K_2O 0.05%, and P_2O_5 0.02%.

Two of miarolitic units which are present on the western side near quartz core were also analysed. These units were formed at pneumatolytic stage and are the most evolved in the development of pegmatite of Bagarian to a complex nature.

The muscovite pods are frequently present as small bodies 10 cm to 30 cm across while microcline units occur as aggregates of euhedral to subhedral translucent pods slightly perthitic and individual crystals. The muscovite pod compositionally has SiO_2 46.62%, TiO_2 0.08%, Al_2O_3 34.82%, Fe_2O_3 0.98%, FeO 0.71%, MnO 0.12%, MgO 0.91%, CaO 0.66%, Na_2O 0.67%, K_2O 9.99%, P_2O_5 0.03%, with anomolously high Li (300 ppm), Rb (3000 ppm) and Ga (40 ppm).

The microcline miarolitic unit has SiO_2 62.87%, TiO_2 0.0%, Al_2O_3 20.96%, Fe_2O_3 0.20%, FeO 0.02%, CaO 0.12%, Na_2O 0.81% and K_2O 14.75%. This analysis shows no TiO_2, MgO, MnO, P_2O_5, B_2O_3 etc. and minor amounts of Fe_2O_3 and FeO and minor amount of Na_2O is slightly perthitic in nature of microcline. Rb is 4500 ppm in this unit as compared to 3000 ppm in inner intermediate microcline zone. The anomaly is due to pneumatotic nature of unit.

DISCUSSION

The Bagarian asymmetrical complex pegmatite was evolved from Mansehra granite which formed as a result of partial melting of pelitic and pelitic-psammitic rocks of Hazara Formation and Tanol Formation. The Mansehra granite forms a complex structural and mineralogical mush room dome that was developed in Cambrian times (500 ma, LeFort 1969). It consists of

main granitoid to gneissic granites, tourmaline granites, aplitic granites etc. of peraluminous nature. During the formation of this granitic complex the water vapour started increasing and ultimately rose to more than 10 kbs where the trend of magmatic evolution was toward increase in albite rich solutions (as found by Luth et al. 1964, Hall 1972, 1973, Ashraf 1974).

Following the model of Shearer et al. (1992) and studies by Duke (1992) and Shearer et al. (1987) it is envisaged that partial melting of about 40% of the Hazara Formation pelites and Tanol Formation pelites and psammites produced Mansehra biotite granite (the main mass of Mansehra granitic complex). And with 60-75% fractional crystallization of primitive biotite granite evolved tourmaline granite (Hakle etc.). With more than 75 to 90% fractional crystallization aided by volatile component, changing partitioning behaviour, filter pressing mechanism, high water vapour pressure to release in water vapour pressure produced acid minor bodies from albitite to rare element pegmatites including Bagarian asymmetrical complex pegmatite (Ashraf 1974, 1975, 1983).

After the release in local water vapour pressure in the granitic complex which became possible due to upward and outward growth of the granitic complex fissures and master joint opening were formed. These fissures and joints were the sites for formation of acid minor bodies. Also due to local release in water vapour pressure the presence of albitic solutions resulted into albitites as individual bodies (Ashraf & Chaudhry 1976). Thereafter as the water vapour pressure decreased in the complex with upward movement of alkalic solutions or in the closed system gradual enrichment in K_2O started with the development of initially albite - (microcline) aplites / pegmatites, albite - microcline aplites / pegmatites, microcline - albite aplites / pegmatites and as composite acid minor bodies (Ashraf, 1975). In this system complex pegmatites evolved with well developed unzoned and zoned pegmatites in the marginal and marginal-exterior zones of Ashraf (1974). The Bagarian pegmatite was as a result of highly evolved magmatic, pneumatolytic and hydrothermal phases. The first two phases were developed in time and space whereas the last phase of hydrothermal activity was very minor forming minor sericite and kaolonite.

It is mentioned above in introduction that there are six types of acid minor bodies evolved associated with the Mansehra granitic complex. The first five types were derived from the poorly acqueous silicate melt and do not fully represent all the stages of development of the pegmatites including pneumatolytic and hydrothermal stages.

The most conspicuous features of the pegmatites is the development of sharply bounded internal mineralogical zones. This heterogeneous distribution of mineral assemblages which represent a form of anisotropy distinguishes pegmatites from typical granitic rocks (London 1992, 1987). Therefore, in the pegmatite closed system, the pegmatitic stage is the initiate zonal consolidation depending on mineral assemblages. Thus forming (a) the border zone, (b) the wall zone, (c) the outer intermediate and inner intermediate zones, (d) the core, which denote the sequence of consolidation from the wall inwards. From the mineral composition and chemistry of Bagarian pegmatite it is evident that the sequence of crystallization was from eastern side upto inner intermediate eastern zone being high temperature assemblages, as having oligoclase and graphic granitic textures in the border + wall zones and intermediate zones. The western border + wall zone crystallized at the time just after eastern border + wall zone has formed and before the development of intermediate zones. The western outer intermediate and inner intermediate zones developed later and the last of them is the quartz core followed by miarolitic units and pods developments of pneumatolytic stage.

The border + wall zones having aboundant tourmaline from 21.91 to 13.54 mode percent (Table - 1) show an aureole developed metasomatically at the expense of granite gneiss. This could be a later phenomenon that B-rich fluids were not present at the time when the pegmatite first began to crystallize. Thus B-rich fluid had ample time to react with host granite forming border zone. The tourmalization which proceeds rapidly, is localized at the site of mixing i.e., the wall - rocks forming comb-structured concentration of tourmaline. This sort of radiating structure of tourmaline has also been reported with basic host rocks (Morgan & London 1987, 1989). B-rich pegmatite fluid was also open to infiltration of Mansehra granitic rock rather than ferromagnesian wallrocks as reported by London (1992).The finer-grained texture of the wall zone is possibly due to higher nucleation maxima for sodic feldspar as compared to K-feldspar within the undercooling regions of maximum rate of crystal growth (Fenn, 1977). The same in true for quartz (Swanson & Fenn, 1986 and London et al. (1989). Thus the undercooled pegmatite forming melt with high nucleation densities of albite and quartz would promote fine-grained wall and border zones.

The intermediate zones were developed between

wall zone and the core. They were descernable into outer intermediate and inner intermediate zones with contrasting mineralogy and structure of mineral assemblages (Quensel, 1955). As we have oligoclase in the wall zone (eastern) and a graphic granite texture of intermediate (eastern), so they represent the higher temperature assemblages of minerals comparing to wall zone and intermediate zones western. The development of graphic to subgraphic growths by microcline and quartz is due to rapid accumulation of those minerals as a function to promote local saturation of a second phase at the margins of the growth front (Fenn, 1986). Therefore transition from fine grained albite/oligoclase - quartz to graphic K-feldspar - quartz intergrowth can be regarded as a change in feldspar-mineralogy caused by the depletion in Na and increase in K as the growth front proceeds inwards. The rising amount of fluxing components in the wall zone western aided in the diffusion of potash away frm the advancing front so that boundary layer saturation in K-feldspar was not attained until the melt adjacent to the crystallizing front is grossly oversaturated in K-feldspar. K-feldspar therefore, crystallized in the intermediate zones western as microcline. Next in sequence is almost pure quartz core in Bagarian pegmatite. London *et al.* (1989) in their experiments emphasized that the quartz rich central zones, including the formation of quartz - mica assemblages were developed by direct crystallization from melt in the absence of an aqueous vapour phase. Therefore, the experimental results helped explain the formation of quartz rich - zones and cores in closed magmatic systems of pegmatite, without any unreasonable requirements of vigorous convection, incongruent partitioning of elements and selective deposition from aqueous vapour, large aqueous vapour / melt ratios, or hydrothermal influx from external sources (London, 1992).

It is known that all pegmatitic systems evolve an aqueous vapour phase after complete crystallization and or zonal development. Similarly after all the zones of Bagarian pegmatite have developed asymmetrically an aqueous phase resulted from magmatic stage to form miarolitic cavities. Those were developed in most cases near the quartz core on both sides in graphic granite zone and western inner intermediate zone. These miarolites consists of dominantly, Rb-rich translucent microcline (Rb ≃ 4500 ppm), Rb-rich muscovite (Rb ≃ 3000 ppm) and Li-muscovite (Li ≃ 300 ppm), columbite, beryl, samarkite, garnet etc. These miarolitic cavities diminishes and become smaller away from quartz core. The saturation of aqueous phase was

not only found in microlitic cavities but also metasomatic replacement of pre-existing minerals by introduction of 3000 ppm Rb in microcline of inner intermediate zone (sample A-89, Table - 3). Such observations were also reported by London & Burt (1982), Burt & London (1982). 300 ppm of Sn in the miarolitic muscovite pod shows that this pegmatite is evolved by fractional crystallization upto about 90%. Trace elements distribution in simples pegmatites are also presented in Table - 3 which significantly show low amounts of elements which is due to minor available aqueous vapour phase.

CONCLUSIONS

1. The Bagarian asymmetricaly zoned complex pegmatite body is closely associated with Mansehra granitic complex.

2. The Mansehra granitic magma was formed after 40% partial melting of more or less uniform pelitic Hazara Formation and lower part of Tanol formaton which was also dominantly pelitic.

3. It is envisaged that 75-90% fractional crystallization of granitic rest magma was responsible for the zonal development and miarolitic mineral formation of the Bagarian pegmatite.

4. The petrographic and chemical compositions of western intermediate microcline zones and the quartz core show that they are excellent materials for ceramic and glass industries without any processing.

5. The miarolitic minerals are developed as a result of development of aqueous phase subsequent to zonal devleopment of Bagarian pegmatite. These minerals are beryl, columbite, samarskite, Rb-microcline, Li-muscovite etc. The former three are ores of Bi, Nb and U.

ACKNOWLEDGEMENTS

REFERENCES

Ashraf, M., (1974). Geochemistry and petrogenesis of acid minor bodies of Mansehra and Batgram area, Hazara district. *Ph.D. thesis, Punjab University Lahore.* 232 p.

Ashraf, M., (1974a). Geology and petrology of acid minor bodies form Mansehra and Batgram area, Hazara district, Pakistan. *Geol. Bull. Punjab Univ.,* Vol. 11, pp. 81-88.

Ashraf, M., (1984b). The geochemistry and petrogenesis of albitites from Mansehra and Batgram area, Hazara district, Pakistan. *Geol. Bull. Punjab, Univ.,* Vol. 11, p. 97.

Ashraf, M., (1975). Composite albitite-aplite and pegmatite form Mansehra and Batgram area, Hazara distict, Pakistan. Spec. Issue IMA papers, 9th Meeting, *Forschr. Miner.,* Vol. 52, pp. 329-344.

Ashraf, M., (1983). Geochemistry of the acid minor bodies associated with the Hazara granitic complex, Hazara Himalayas, northern Paksitan. In: Granites of Himalayas, Karakorum and Hindukush, F.A. Shams ed. *Inst. Geol. Punjab Univ. Lahore.* pp. 123-141.

Ashraf, M., and Chaudhry, M.N., (1976). Geology and classification of acid minor bodies of Mansehra and Batgram area, Hazra Division, Pakistan. *Geol. Bull. Punjab Univ.,* Vol. 12, pp. 1-16.

Burt, D.M., and London, D., (1982). Subsolidus equilibria. In: Granitic Pegmatites in Science and Industry (P. Cerny ed.). *Mineral Assoc. Canda, Short-Course Handbook,* Vol. 8, pp. 329-346.

Duke, E.F., Papike, J.J., and Laul, J.C., (1992). Geochemistry of born-rich peraluminous granite pluton: the Clamity Peak layered granite-pegmatite complex, Black Hills, south Dakota. *Canadian Mineral.* Vol. 30, pp. 811-834.

Fenn, P.M., (1986). On the origin of grpahic granite. *Amer. Mineral.,* Vol. 71, pp/ 325-300.

Heinrich, E.W., (1953). Zoning is pegmatite districts. *Amer. Mineral,* Vol. 38, pp. 68- .

Hall, A., (1972). New data on the composition of Caledonian granites. *Mineral. Mag.,* Vol. 39, pp. 847- .

Hall, A., (1973). Geochemical control of granitic compositions in the Variscan orogenic belt. *Nature Phy. Sci.,* Vol. 242, (118), pp. 72- .

LeFort, P., Debon, F., and Sonet, J., (1980). The lesser Himalayan cordierite granite belt typology and age of the pluton of Mansehra, Pakistan. *Geol. Bull. Univ. Peshawar,* Vol. 13, pp. 51-61.

London, D., (1987). Internal differentiatoin of rare-element pegmatites: effect of born, phosphorous and fluorine. *Geochem. Cosmochim. Acta,* Vol. 51, pp. 403-420.

London, D., (1992). The application of experimental petrology to the genesis and crystallization of granitic pegmatites. *Canadian Mineral.,* Vol. 30, 499-540.

London, D., Burt, D.M., (1982). Alleration of spodumene, montebrasite, and lithophyllite in pegmatites of the White Picacho district, Arizona. *Amer., Mineral.* Vol. 67, pp. 494-509.

London, D., Morgan, G.B., and Hervig, R.L., (1989). Vapour undersaturated experiments with Macusani glass + H_2O at 500 MPa, and internal differentiation of granitic pegmatites. *Contr. Mineral. Petrol.,* Vol. 102, pp. 1-17.

Luth, W.C., Jahns, R.H., and Tuttle, O.F., (1964). The granite system at pressure of 4 to 10 kbs. *Jour. Geophys. Res.,* Vol. 69, pp. 759- .

Margan, G.B., and London, D., (1987). Alteration of amphibolitic wallrocks around the Tanco rare-element pegmatite, Bernic Lake, Manitoba. *Amer. Mineral.,* Vol. 72, pp. 1097-1121.

Morgan, G.B., and London, D., (1989). Experimental reactions of amphibolite with boron-bearing aqueous fluids at 200 MPa: implication for tourmaline stability and partial melting in mafic rocks. *Contrl. Mineral. Petrol.,* Vol. 102, pp. 281-297.

Quensel, P., (1955). the paragenesis of the Varutrask pegmatite. *Arkiv. Mineralogy. Och. Geologi- Stockholm,* Vol. 2(2), pp. 9- .

Shams, F.A., (1967). Granites of the Mansehra-Amb state area and the associated metamorphic rocks. *Ph.D. thesis, Punjab University, Lahore.*

Shams, F.A., (1969). Geology of the Mansehra-Amb State area, northern west Pakistan. *Geol. Bull. Punjab Univ.,* Vol. 8, pp. 1- .

Shams, F.A., (1983). Granites of the northwest Himalays in Pakistan. In: Granites of Himalayas Karakorum and Hindukush. (F.A. Shams ed). *Inst. Geol. Punjab Univ., Lahore.* pp. 75-121.

Shearer, C.K., Papike, J.J., and Laul, J.C., (1987). Mineralogical and chemical evolution of a rare element granite pegmatite system: Hanery Peak granite, Black Hills, South Dakota. *Geochim. Cosmochim. Acta,* Vol. 51, pp. 473-486.

Shearer, C.K., Papike, J.J., and Jolliff, B.L., (1992). Petrogenetic links among granites and pegmatites in the Harney Peak rare-element granite-pegmatite system, Black Hills, South Dakota. *Candian Mineral.,* Vol. 30, pp. 785-810.

Swanson, S.E., out Fenn, P.M., (1986). Quartz crystallization in igneous rocks. *Amer. Mineral.,* Vol. 71, pp. 331-342.

Wadia, D.N., (1931). The syntaxis of the north west Himalaya, its rocks, tectonics and geology. *Rec. Geol. Surv. India,* Vol. 65(2), pp. 185-370.

^{40}Ar/^{39} Ar EVIDENCE FOR LATE CRETACEOUS FORMATION OF THE KOHISTAN ISLAND ARC, NW, PAKISTAN

By

SYED HAMIDULLAH* & TULLIS C. ONSTOT**

*National Centre of Execellence in Geology, University of Peshawar, Pakistan.
**Department of Geological and Geophysical Sciences, Princeton
University, Princeton, N.J. 08544, U.S.A.

ABSTRACT: *Hornblende, biotite and plagioclase separates from Kalam-Dir igneous complex, Kohistan Island Arc, N.W. Pakistan, have been analyzed by the ^{40}Ar/^{39}Ar technique. Hornblende from the volcanics and diorite plutons of Gabral (near Kalam) and Dir areas and biotite from tonalite at Matiltan yield dates ranging from 74 to 54 Ma, whereas other boitite and one of the plagioclase separates from the diorite plutons at Gabral yield 44 to 39 Ma plateau dates. Plagioclase from another diorite of Gabral and one from the ultramafic rock units of Mahodand are contaminated by excess argon.*

These data indicate that the Late Cretaceous to Early Eocene period was dominated by calc-alkaline plutonic magmatism (represented by diorites) accompanied by a short span of calc-alkaline volcanism (Kalam-Dir volcanics) at about 70 Ma, in the northern Swat and Dir areas. The ages increase progressively southward. Each major magmatism and/or volcanism has caused high-grade metamorphism of already crystalline rocks in the south. The culmination of magmatism in the Kalam-Dir area at 54 Ma probably resulted from the collision of the Kohistan Island Arc with India.

The 45-39 Ma dates of the biotite and plagioclase from the diorites of Gabral reflect a middle Miocene to Oligocene metamorphism followed by cooling due to uplift and erosion in the area, and may represent the after-effects (extensional environments) of collision of Kohistan Island Arc with India. Alternatively, they may reflect the collision of the combined Indian and Kohistan Island Arc plates with that of Eurasia (along the MKT).

INTRODUCTION

The Kohistan Island Arc (KIA) represents a 40 km thick pile of mafic, ultramafic and calc-alkaline plutonic and volcanic rocks and has been widely accepted as a vertical section through an intra-oceanic island arc. It separates the Eurasian and Indian plates in the Himalayan Range of northwestern Pakistan, where its northern and southern boundaries are demarcated by the Main Karakoram Thrust (MKT) and the Main Mantle Thrust (MMT) respectively (Fig. 1). Recent studies have proposed that this oceanic island arc formed in the Cretaceous time in response to northward subduction of a Paleo-Tethys oceanic plate and was later obducted onto the Indian plate before the collision of India with Eurasia (Tahirkheli, *et al.* 1979).

The Shangla blueschist zone and garnet granulite (the Jijal complex) outcrop along south-bounding MMT. From south to north the major rock units of the KIA are: the southern amphibolite belt ('A' in Fig. 1), the Chilas complex, the Kalam group (ocean metasedimentary series), the Utror volcanics (6-8 km thick; intruded by intermediate to felsic plutons), the Kohistan batholith including granitic rocks intruded by various dioritic bodies, the Rakaposhi volcanics and an upper detrital series including Cretaceous sediments and volcanics of Yasin group (see Bard *et al.*, 1980; Bard, 1983; Tahirkheli, 1982).

Previous workers have proposed various models to explain the nature and timing of various events

responsible for the evolution of KIA (Andrews-Speed and Brookfield, 1982; Windley, 1986). On the basis of published isotopic data, Jan and Asif (1981) suggested the following sequence of events occurred: (1) the northward subduction of the oceanic crust as recorded by plutonic and volcanic magmatism (Chalt volcanics, southern amphibolite belt, etc.) during the Early and Middle-Cretaceous (130-90 Ma), (2) the intrusion of Chilas and Jijal complexes and the development of the Shangla blueschist (Fig. 1) in the Late Cretaceous (90-65 Ma), (3) the collision of the island arc with the Indian plate and the concomittant obduction of the ophiolites and blueschist, causing regional matamorphism in the Paleocene to the very Early Eocene (65-50 Ma), and (4) the emplacement of the Utror volcanics and younger granitic rocks in Eocene to Early Miocene (50-18 Ma).

Patterson and Windley (1985) reported 40 to 56 Ma Rb-Sr isochron dates for Kohistan-arc granitoids between MMT and MKT in Trans-Himalayas of the northeastern part of KIA, and also correlated the calc-alkaline Utror volcanics in the northwestern part of KIA with these plutonic assemblages. Immediately to the south of MMT on the Indian Plate, Maluski and Matte (1984) detected two tectonometamorphic events from their $^{40}Ar/^{39}Ar$ study. The first is a 75-80 Ma blueschist facies metamorphism, which they interpreted as reflecting either intra-oceanic subduction or obduction of the oceanic/island arc crust over the continental Indian plate. The second is a 50-30 Ma metamorphism which they attributed to the main period of the Indian plate beneath Eurasian plate.

On the basis of fission track and $^{40}Ar/^{39}Ar$ data, Zeitler et al. (1982a, b) and Zeitler (1985) have delineated the unroofing history along MMT and the cooling history of the northwest Himalayas. These studies have revealed varied uplift rates, both spatially and temporally, in various parts of northern Pakistan. With exception of limited data of Zeitler (1985) on the calc-alkaline Utror volcanics and associated diorites and tonalites, referred to here as the Kalam-Dir igneous complex (Figs. 2), no detailed isotopic studies have been carried out to record the emplacement and post-emplacement history of such rocks in the northern Swat and Dir areas (Fig. 1). Zeitler (1985) obtained 36 to 39 Ma zircon fission track dates on one of the diorites (tonalite in Zeitler, 1985) from Gabral and on a rhyolite located in the Utror area (Figs. 12) which he interpreted as representing uplift ages. He also derived a 45 Ma $^{40}Ar/^{39}Ar$ date on biotite from one of the diorites from Gabral and suggested it recorded an emplacement date.

Applying the $^{40}Ar/^{39}Ar$ step-heating technique to hornblende, biotite and plagioclase separates, this study revealed the emplacement and post-emplacement history of the Kalam-Dir igneous complex in further detail in order to establish its role in the process of arc construction.

PETROGRAPHY

The calc-alkaline Utror volcanics occur in the form of a linear belt trending NE-SW between Kalam and Dir (Fig. 1). The field relationships, petrography and geochemistry of these volcanics have been described by Majid and Paracha (1979). Rock types include andesite, dacite, rhyodacite and rhyolite with plagioclase occurring as the principle phenocryst phase. During the present investigation pyroxene of [Ca, Mg]-rich augite composition (Hamidullah, unpubl. data) was discovered as the sole phenocryst phase in andesite north of Balogah (Fig. 2) whereas primary magmatic hornblende phenocrysts of pargasite composition were discovered in volcanics of Gira Khwar NNE of Dir (see Table-1; LR14HB, Fig. 1). The occurrence of secondary chlorite, epidote and calcite (Majid and Paracha, 1979) indicate that the Utror volcanics have undergone greenschist facies metamorphism.

Associated with Utror volcanics are diorites (and some tonalites) with calc-alkaline characteristics (Majid, 1979). On the basis of field relationship with Utror volcanics, two types of diorites have been distinguished at Gabral (Fig. 1). One is a pre-volcanic hornblende diorite which contains amphibole of magnesio-hornblende composition (Table 1; UT36HB) as the dominant ferromagnesium together with plagioclase (Table 1; UT36PL), orthoclase, magnetite and biotite in increasing order of model abundance as well as some secondary epidote and muscovite after plagioclase. The Utror volcanics have developed chilled margins against this diorite at Gabral.

The second is a post-volcanic hornblende-biotite diorite (Khalil and Afridi, 1973), which clearly intrudes both the hornblende diorite and the volcanic rocks and also contains xenoliths of both. Its principal mineral constituents are plagiocalse (An_{50-90}), primary biotite and primary hornblende in decreasing order of abundance. Hornblende and biotite (Table 1; UT31HB1, UT31HB2, UT30BI) are usually unaltered but plagioclase has partially altered to epidote. In the hornblende-biotite diorite, the modal abundance of hornblende varies locally from 1 to 35%, biotite from 7 to 18%, plagioclase from 50 to 70% and orthoclase from
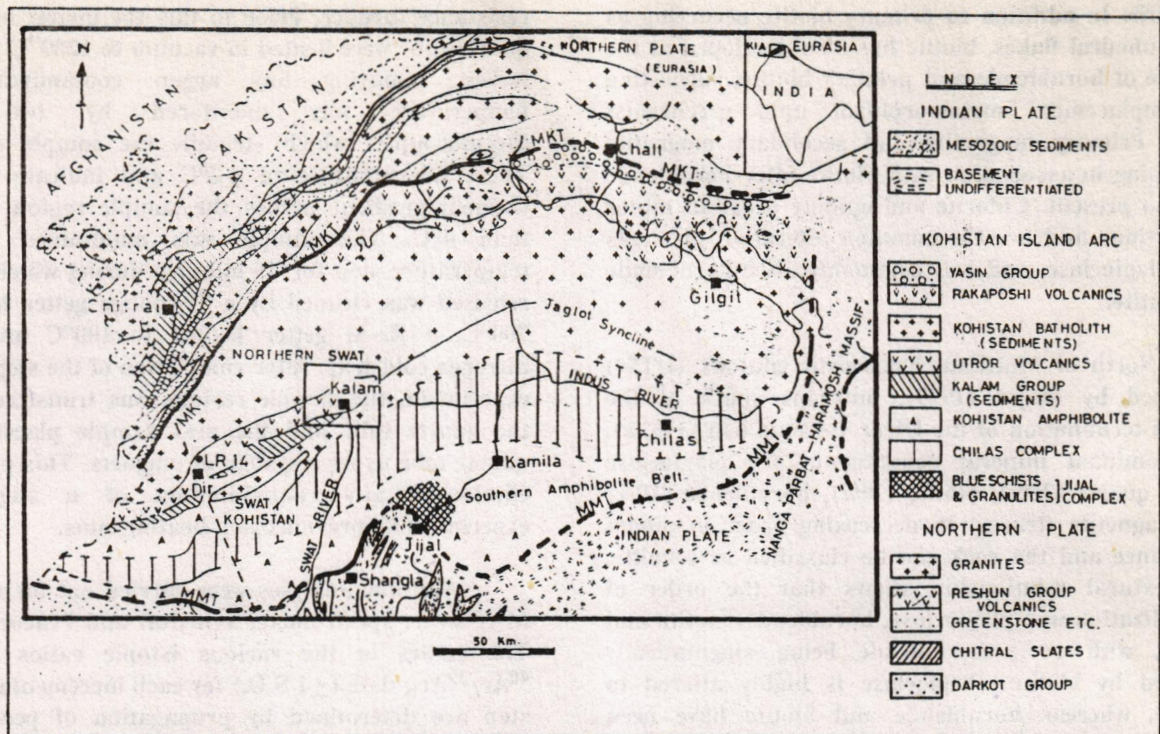
Fig. 1. Geological map of the Kohistan island arc (modified from Coward *et al.*, 1986). Inset box indicates the location of Fig. 2.
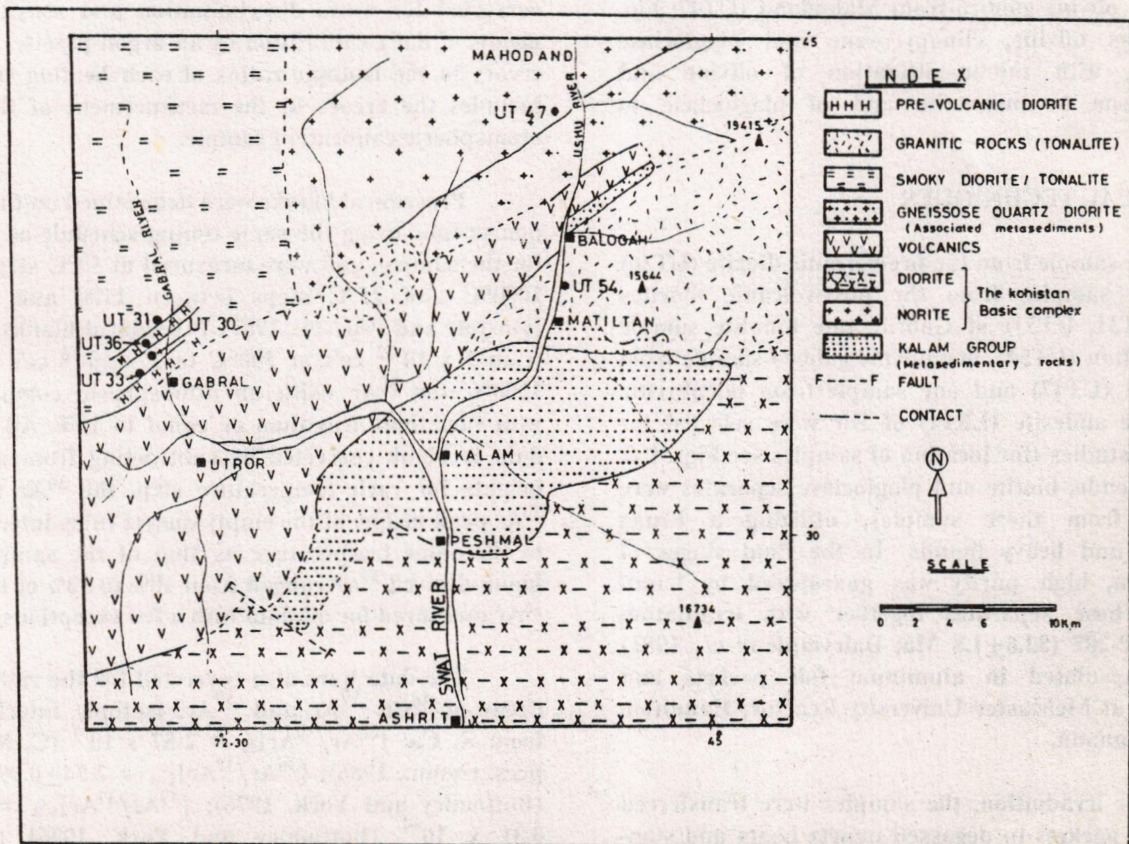

Fig. 2. Geological map of the eastern part of Kalam-Dir igneous complex (modified from Majid, 1979).

5 to 10%. In addition to primary biotite occurring as large euhedral flakes, biotite has also developed at the expense of hornblende and primary biotite, suggesting post-emplacement metamorphism upto greenschist facies. Primary magnetite and secondary magnetite developing in association with biotite after hornblende are also present. Chlorite and epidote occur in minor proportions and are the common alteration products after plagioclase, and less commonly after hornblende and biotite.

North of Matiltan, leucocratic plutons (UT54) described by Majid (1979), outcrops south of the eastern termination of the Utror volcanic belt (Fig. 2). The dominant mineral constituents are plagioclase (45%), quartz (25%), biotite (20%), hornblende (10%) and magnetite (traces) in decreasing order of modal abundance and the rock can be classified as tonalite. The textural relationship shows that the order of crystallization was plagioclase, hornblende, biotite and quartz, with some hornblende being magmatically replaced by biotite. Plagioclase is highly altered to sericite, whereas hornblende and biotite have been partially altered to chlorite, epidote and probably magnetite.

The olivine gabbro from Mahodand (UT47; Fig. 2) contains olivine, clinopyroxene and plagioclase ($An_{86-93\%}$), with minor alteration of olivine and clinopyroxene to magnetite and of plagioclase to sericite.

ANALYTICAL TECHNIQUES

One sample from the pre-volcanic diorite (UT36) and three samples from the post-volcanic diorites (UT30, UT31, UT33) of Gabral, one tonalite sample from Matiltan (UT54), one olivine gabbro sample from Mahodand (UT47) and one sample from porphyritic hornblende andesite (LR14) of Dir were selected for $^{40}Ar/^{39}Ar$ studies (for location of samples see Figs. 1 & 2). Hornblende, biotite and plagioclase separates were extracted from these samples, utilizing a Franz separator and heavy liquids. In the final stages of preparation, high purity was guaranteed by hand-picking. These separates together with irradiation standard P-207 (82.6$\pm$1.8 Ma; Dalrymple *et al.*, 1981) were encapsulated in aluminum foil packets and irradiated at McMaster University Reactor, Hamilton, Ontario, Canada.

After irradiation, the samples were transferred from their packets to degassed quartz boats and stepwise degassed in a quartz tube, using a Lindberg

resistance furnace. Prior to this the quartz boats and quartz tube were heated in vacuum to 1200°C for 10-12 hours, removing any argon contaminant. The temperature was monitored by two Pt-Rh thermocouples which straddle the sample chamber. These are accurate to $\pm$2°C and indicate that the thermal gradient across the sample region was less than 4°C. The sample was maintained at each temperature step for 45 minutes during which the gas released was cleaned by a Ti-sponge getter heated to 700°C, a Zr-Al getter heated to 100°C and liquid nitrogen cold trap. After completion of the step-heating experiment, the sample residue was transferred from the quartz tube and the next sample placed in the quartz tube using a system of magnets. This procedure eliminated any contamination of a step-heating experiment by previous step-heating runs.

Isotopic analyses were carried out on a Varian-MAT mass spectrometer (Onstott and Peacock, 1987). The errors in the various istopic ratios and the $^{40}Ar/^{39}Ar_K$ date ($\pm$1 S.D.) for each incremental heating step are determined by propagation of peak height errors derived from linear least squares regression on seven measurements of each peak height (^{36}Ar through ^{40}Ar-baseline corrected). The measurements are corrected for mass discrimination and sensitivity by means of daily calibration by an argon pipette, and the errors in the isotopic ratios of each heating step also includes the errors in the measurement of the daily atomspheric calibration sample.

Procedural blanks were determined on the empty quartz tube using the same timing schedule as utilized for the sample, and were measured at 50°C steps up to 1000°C and 25°C steps between 1100 and 1200°C (Onstott and Peacock, 1987) Procedural blanks ranged from 3 x 10^{-12} cc's at 500°C to 1 x 10^{-10} cc's STP at 1200°C for ^{36}Ar (with an atmospheric composition) with variations less than or equal to 10%. All sample data is blank corrected by subtracting from all peak heights for each temperature step, the ^{36}Ar through ^{40}Ar peak heighs of the empty quartz tube, interpolated to the same temperature as that of the sample. The blank-derived ^{36}Ar ranged from 10% to 50% of the total ^{36}Ar measured for all data with a few exceptions.

The data were also corrected for the radioactive decay of ^{36}Cl, ^{37}Ar and ^{39}Ar, isotopic interferences from K, Ca: $[^{40}Ar/^{39}Ar]_K$ = 2.87 x 10^{-2} (C. M. Hall, pers. comm., 1986); $[^{36}Ar/^{37}Ar]_{Ca}$ = 2.54$\pm$0.09 x 10^{-4}, (Bottomley and York, 1976); $[^{39}Ar/^{37}Ar]_{Ca}$ = 6.51$\pm$ 0.31 x 10^{-4} (Bottomley and York, 1976] and Cl (Roddick, 1983). Masliwec (1981) reported the following

interference values: $[^{36}Ar/^{37}Ar]_{Ca} = 2.55 \pm 0.28 \times 10^{-4}$ and $[^{39}Ar/^{37}Ar]_{Ca} = 6.50 \pm 0.47 \times 10^{-4}$, which are identical within erros of those presented by Bottomley and York (1976). Bottomley and York (1976) reported $[^{40}Ar/^{39}Ar]_K = 1.56 \pm .04 \times 10^{-2}$, however, which is significantly different from the value quoted above, suggesting that an approximately 60% error may exist in the determination of this correction factor.

The errors (± 1 S.D.) for the various isotopic ratios and the $^{40}Ar/^{39}Ar_K$ date for each incremental heating step does not include the systematic errors caused by the uncertainty in the J-value, the uncertainty in the interference corrections, and the uncertainty in the age of the standard.

The integrated dates are calculated from the sum total of the peak heights and the error from the square root of the sum square of the peak height errors for all the temperature steps. The integrated date and error correspond to the result one would obtain if the sample was degassed in a single temperature step, as would be the case with a conventional K-Ar determination (Tables - 2,3). The "plateau" dates are calculated by the same approach, but utilizing only those temperature steps yielding dates on the plateau. The "plateau" dates and errors correspond to the result one would obtain if the plateau portion of the sample's spectra had been released in one temperature step. If the dates for each plateau step fall within 2 S.D. of the average, then the error derived with this method is probably a conservative estimate because of sampling statistics (Berger and York, 1970). If, however, the variance in the dates on the "plateau" exceed 2 S.D. (i.e. it is not a good plateau) the error given by this procedure underestimates the true error.

Some of the variation in plateau step dates may be caused by real difference in the cooling ages within grains or between grains. For those samples where the range in dates for the plateau steps clearly exceeds the analytical uncertainty, the data were plotted on a $^{36}Ar/^{40}Ar$ versus $^{39}Ar/^{40}Ar$ plot (Roddick et al., 1980). In these cases the $^{40}Ar/^{39}Ar_K$ date and error were calculated from the intercept of the best-fit line (York, 1969) with the $^{39}Ar/^{40}Ar$ axis. The dates calculated in this manner are referred to as "intercept" dates (Table - 2). The error estimates (± 1 S.D. in Table-2) are multiplied by (SUMS/N-2)1/2 in order to incorporate the degree of scatter of the data points about the best-fit line (York, 1969).

The errors quoted for the integrated, plateau, and intercept dates also include the error in the determination of the J-value for the irradiation and the erros in the determination of the interference corrections, but does not include the error in the K-Ar age of the standard P-207, and hence should be considered "intralaboratory" errors. For McMaster Reactor, the relationship Ca/K = 1.82 (± 0.17) $^{37}Ar_{Ca}/^{39}Ar_K$ was used to derive the Ca/K (Onstott and Peacock, 1987).

Table -1. Mineral compositions from Kalam - Dir igneous complex.

Sample	UT36HB	LB14HB	UT31HB1	UT31HB2	UT30BI	UT36PG
SiO$_2$	48.17	42.83	44.72	47.80	36.62	57.20
TiO$_2$	1.30	1.39	.60	0.00	2.08	0.19
Al$_2$O$_3$	6.80	13.19	10.82	5.66	16.46	28.63
Cr$_2$O$_3$	0.05	0.06	0.02	0.03	0.02	0.01
FeO	16.00	11.92	18.12	18.52	20.42	0.13
MnO	0.35	0.22	0.00	0.38	0.47	0.00
CaO	11.28	11.74	11.66	11.57	0.15	9.75
Na$_2$O	0.63	1.92	1.20	0.76	0.00	6.45
K$_2$0	0.26	0.13	0.30	0.34	9.32	0.14
P$_2$O$_5$	0.00	0.04	0.00	0.00	0.14	0.00
Total	97.89	97.03	97.37	96.94	97.11	102.50

	U36HB	LR14HB	UT31HB1	UT31HB2	UT30BI	UT36PG
Si	7.084	6.306	6.701	7.210	5.518	2.511
Al	0.916	1.694	1.299	0.790	2.482	1.481
Al	0.265	0.590	0.613	0.197	0.442	0.000
Ti	0.144	0.154	0.068	0.000	0.235	0.006
Cr	0.005	0.007	0.002	0.004	0.003	0.000
Fe	1.969	1.473	2.271	2.336	2.573	0.005
Mn	0.044	0.028	0.000	0.049	0.061	0.000
Mg	2.858	2.990	2.218	2.695	2.500	0.000
Ca	1.778	1.854	1.872	1.870	0.025	0.458
Na	0.081	0.547	0.349	0.222	0.000	0.549
K	0.049	0.024	0.570	0.065	1.792	0.008
P	0.000	0.005	0.000	0.000	0.018	0.000
Ca/K	36.290	77.250	19.300	28.760	0.014	57.250

U36HB: Hornblende from the pre-volcanism diorite (UT36), Gabral.

LR14HB: Hornblende from hornblende andesite (LR14), Dir.

UT31HB1: Hornblende from the post-vocanism diorite (UT31), Gabral.

UT31HB2: High-silica marginal portion of certain hornblendes grains from UT31.

UT30BI: Biotite from post-volcanism diorite (UT30), Gabral.

UT36PG: Plagioclase from pre-volcanic diorite (UT36), Gabral.

Note: Mineral formulae have been calculated on the basis of 23 oxygens for all the amphibole analyses, on the basis of 20 oxygens for biotite and on the basis of 8 oxygens for plagioclase; For precise locations of samples see Figures 1 & 2.

Many of the mineral separates used for step heating were also analyzed by electron microporbe on ARL-EMX wavelength dispersive system (WDS) combined with TN-2000 Tracor Northern energy dispersive system (EDS) with operating conditions of 15 Kev, 0.2 microamps beam current and a beam diameter of about 7 microns. K and Ca were analyzed by WDS and other elements by EDS. The unit time for EDS spectra was 50-100 seconds combined with 10 seconds WDS analysis. All analyses were converted to weight percent using the Bence-Albee (1968) reduction scheme. Procedural details are presented in Hollister *et al.* (1984).

Representative average compositions are shown in Table - 1.

ANALYTICAL RESULTS

Hornblende

UT36HB: Hornblende (Tables - 2 & 3) from the pre-volcanic diorite near Gabral yields an integrated date of 55.6± 0.6 Ma. In the initial 26% of ^{39}Ar release (700-912ºC) the incremental heating dates decrease from 60 Ma to 30 Ma. At 937ºC the spectrum increase

to 56 Ma and yields on a minimum date of 57.3 ± 0.6 Ma for 45% of the ^{39}Ar release (937-974ºC). The spectrum at 987ºC records a stepwise increasing pattern attaining a maximum date of 70.25 ± 4.9 Ma for 1025-1074ºC temperature interval.

In the low temperature portion of the spectrum (Fig. 3), the ^{37}Ar$_{Ca}$/^{39}Ar$_K$ increases drastically from ≃2 to ~8 (700-937ºC). The ^{37}Ar/^{39}Ar (mean 19.64 = 35.8 (Ca/K) of the remaining high temperature steps exhibit a slight gradual increase, but the average agrees well with the average Ca/K value of 36.3 determined from the electron microprobe analyses of the hornblende.

When the 937-974ºC plateau steps of UT36HB are plotted on an ^{36}Ar/^{40}Ar versus ^{39}Ar/^{40}Ar plot (Roddick *et al.*, 1980) they form a linear array. The least square fit of the array yields an intercept date of 59.3 ± 2.6 Ma, which closely corresponds to the minimum date of 57.3 ± 0.6 Ma.

LR14HB: The age spectrum for hornblende (Fig. 3).from the andesite of dir is highly discordant for the initial 52% of ^{39}Ar release, with several steps yielding negative dates. A plateau is recovered from the remaining 48% of the release (1020-1150ºC), however,
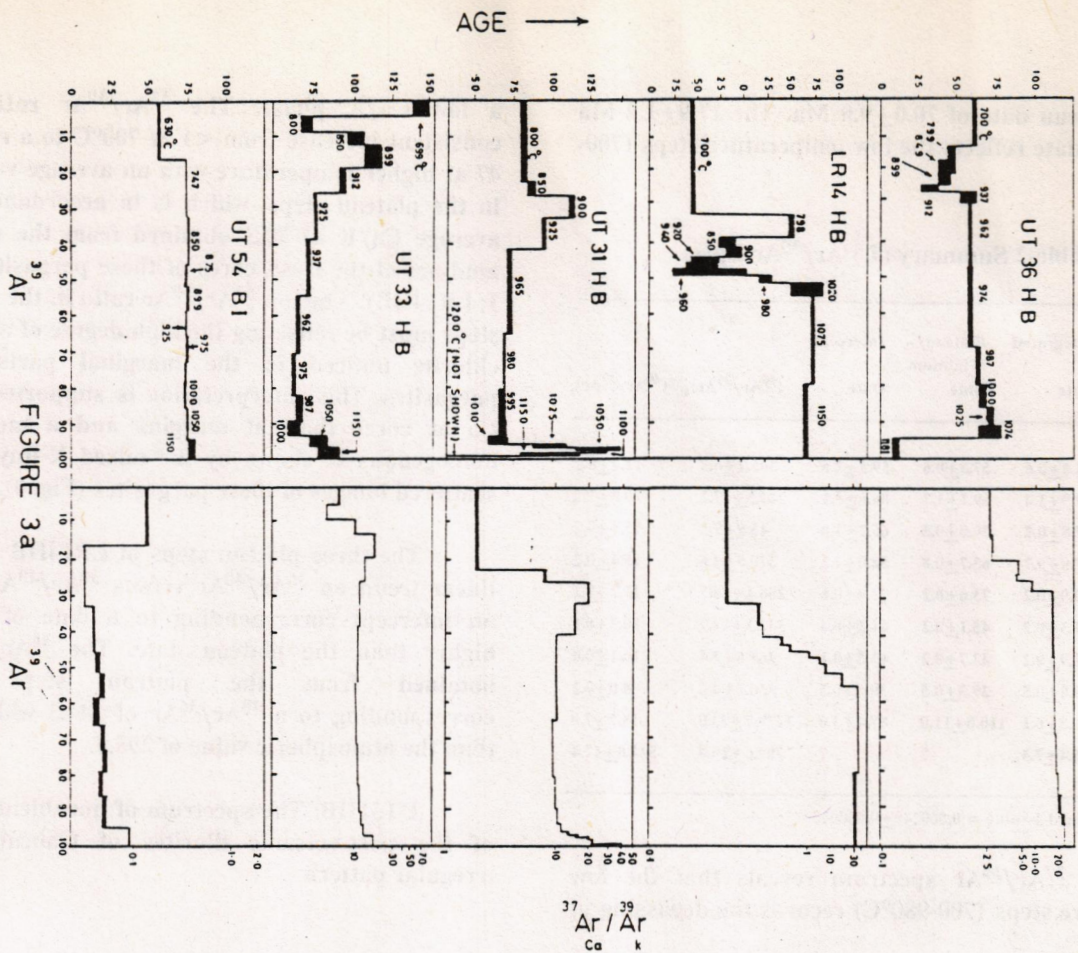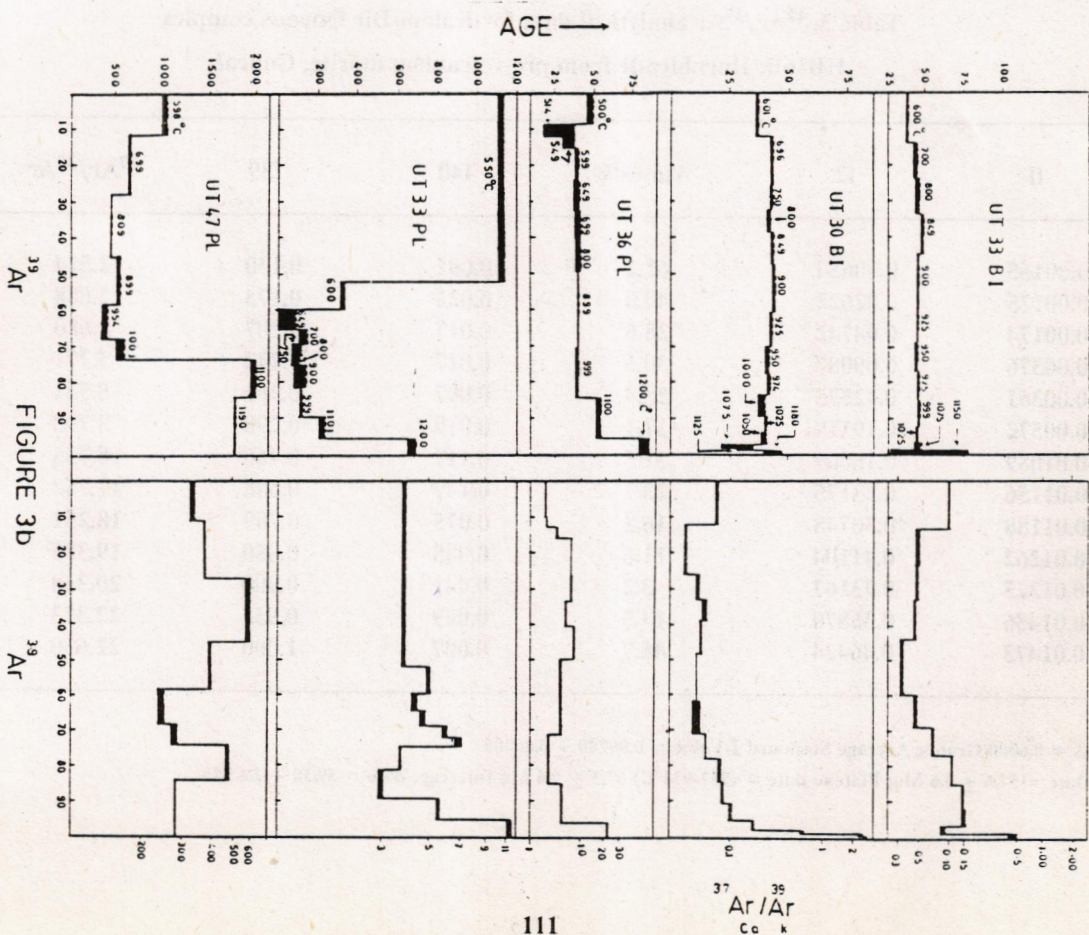
Fig. 3. Age and $^{37}Ar/^{39}Ar$ versus release ^{39}Ar spectra of minerals from the Kalam-Dir igneous complex.

FIGURE 3a

FIGURE 3b

111

with a plateau date of 70.0±9.0 Ma. The 17.9±1.4 Ma integrated date reflects the low temperature steps (700-980°C).

Table-2 Summary of $^{40}Ar/^{39}Ar$ Dates

Sample	Integrated Date	Plateau-/ Minimum Date	Intercept Date	$(^{40}Ar/^{36}Ar)_i$	$(^{40}Ar/^{39}Ar)$
UT36HB	54.6±0.6	57.3±0.6	59.3±2.6	365.2±6.9	11.7±0.2
LR14HB	17.9±1.4	69.7±1.7	86.6±5.1	244.5±17.2	20.3±1.2
UT31HB	77.8±0.7	70.0±0.5	66.7±1.8	45.5±7.2	15.1±0.2
UT33HB	77.8±0.7	63.7±0.8	54.0±2.3	370.5±4.6	15.4±0.2
UT54BI	70.9±0.2	73.6±0.2	73.9±0.6	286.4±18.7	17.2±0.1
UT33BI	44.3±0.2	45.1±0.2	44.2±0.4	342.3±19.7	10.2±0.1
UT30BI	41.9±0.2	42.7±0.2	43.5±0.1	265.6±2.4	10.1±0.0
UT36PL	42.8±0.5	39.3±0.5	39.6±0.5	336.2±4.2	8.0±0.2
UT33PL	756.8±6.1	110.0±11.0	87.4±3.0	1279.7±23.0	-18.7±7.8
UT47PL	996.4±7.3	?	?	799.6±10.4	-544.8±17.4

*Average Standard J-value = 0.000240±0.000005

The $^{37}Ar/^{39}Ar$ spectrum reveals that the low temperature steps (700-980°C) records the degassing of

a low Ca/K phase. The $^{37}Ar/^{39}Ar$ ratio show a consistent increase from <1 at 700°C to a range of 29-47 at higher temperature with an average value of 39.8 in the plateau steps, which is in accordance with the average Ca/K of 77.3 obtained from the microprobe analyses of the fresh cores of these pargasites (Table - 1; LR14HB). The low $^{37}Ar/^{39}Ar$ ratio in the nonplateau steps must be reflecting the high degree of alteration to chlorite noticed in the marginal parts of these pargasites. This interpretation is supported by higher Ca at cores than at margins and a more or less homogenous K shown by the mixed X-Ray and back-scattered images of these pargasites (Fig. 4).

The three plateau steps of LR14HB also yield a linear trend on $^{36}Ar/^{40}Ar$ versus $^{39}Ar/^{40}Ar$ plot, with an intercept corresponding to a date of 86±5 Ma, higher than the plateau date. The $^{36}Ar/^{40}Ar$ ratio obtained from the plateau steps (4.09E-3) corresponding to a $^{40}Ar/^{36}Ar$ of 244.5 which is lower than the atmospheric value of 295.5.

UT31HB: The spectrum of hornblende from one of the post-volcanic diorites of Gabral yields an irregular pattern

Table 3. $^{40}Ar/^{39}Ar$ analytical data for Kalam-Dir igneous complex
HB36B: Hornblende from pre-volcanism diorite, Gabral

T°C	f1	f2	Atmos%	f40	f39	$^{37}Ar/^{39}Ar$	Age (Ma)
700	-0.00165	0.00654	62.2	0.091	0.130	2.524	59.6 ± 1.4
799	-0.00175	0.02622	40.0	0.022	0.173	2.688	45.1 ± 2.6
849	-0.00174	0.04742	28.6	0.017	0.207	2.680	41.7 ± 5.2
899	-0.00376	0.09087	30.5	0.017	0.242	5.771	40.5 ± 4.3
912	-0.00361	0.12573	28.4	0.007	0.261	5.541	30.4 ± 5.2
937	-0.00572	0.19119	17.1	0.019	0.290	8.793	56.1 ± 5.0
962	-0.01089	0.16069	31.5	0.117	0.466	16.735	56.9 ± 0.9
974	-0.01156	0.23175	23.7	0.149	0.686	17.762	57.8 ± 0.7
987	-0.01188	0.30748	16.8	0.075	0.789	18.251	62.5 ± 1.6
1000	-0.01262	0.41104	11.6	0.048	0.850	19.386	65.5 ± 2.6
1025	-0.01325	0.73167	3.2	0.041	0.900	20.350	70.3 ± 2.2
1074	-0.01456	0.36870	14.3	0.029	0.935	22.373	70.2 ± 7.6
1181	-0.01473	0.46424	45.7	0.007	1.000	22.630	9.8 ± 2.1

Sample mass = 0.6000 Grams; Average Standard J-Value = 0.00240 ± 0.00005

Integrated Date = 54.6 ± 0.6 Ma; Plateau date = (937-974°C) 57.3 ± 0.6 Ma Intercept date = 59.30 ± 2.6 Ma.

LR14HB: Hornblende from andesite Dir area

T°C	f1	f2	Atmos%	f40	f39	$^{37}Ar/^{39}Ar$	Age (Ma)
700	-0.00065	0.00195	178.9	-0.092	0.324	0.997	-54.1 ± 1.5
798	-0.00167	0.00471	72.2	0.016	0.383	2.558	59.8 ± 3.2
850	-0.00191	0.00529	114.9	-0.003	0.413	2.935	-17.4 ± 8.3
900	-0.00330	0.00848	108.2	-0.001	0.439	5.063	-10.6 ± 9.1
920	-0.00418	0.00749	128.8	-0.004	0.456	6.417	-40.5 ± 14.6
940	-0.00771	0.00837	112.3	-0.003	0.470	11.845	-44.2 ± 17.7
960	-0.01006	0.01134	117.6	-0.004	0.489	15.451	-35.3 ± 39.7
980	-0.01168	0.02530	86.7	0.003	0.516	17.937	23.7 ± 6.9
1020	-0.01901	0.03367	72.1	0.013	0.553	29.201	66.7 ± 16.8
1075	-0.03101	0.13708	51.7	0.097	0.795	47.633	73.4 ± 1.1
1150	-0.02776	0.07911	64.2	0.074	1.000	42.641	66.0 ± 2.7

Sample mass = 0.6000 Grams; Average Standard J-Value = 0.00240 ± 0.00005

Integrated Date = -17.9 ± 1.4 Ma; Minimum date = (1020-1150°C) 70.0 ± 9.0 Ma

Intercept date = 86.6 ± 5.1 Ma.

Table 3. (Contd)

UT31HB: Hornblende from the post-volcanism diorite, Gabral

T°C	f1	f2	Atmos%	f40	f39	$^{37}Ar/^{39}Ar$	Age (Ma)
800	-0.00156	0.00660	53.4	0.297	0.230	2.400	81.1 ± 2.0
850	-0.00589	0.04249	39.8	0.047	0.264	9.050	85.9 ± 3.0
900	-0.01402	0.09544	33.3	0.108	0.324	21.534	112.3 ± 1.8
925	-0.01076	0.12320	26.7	0.133	0.413	16.533	94.1 ± 1.1
950	-0.00758	0.15696	21.0	0.270	0.650	11.641	71.5 ± 0.6
965	-0.00706	0.24380	13.0	0.169	0.804	10.842	69.5 ± 0.6
980	-0.00740	0.29607	11.0	0.095	0.891	11.368	68.4 ± 1.8
995	-0.00766	0.26579	12.8	0.48	0.935	11.769	68.7 ± 2.0
1010	-0.00834	0.13564	27.4	0.021	0.955	12.803	65.1 ± 6.1
1025	-0.00951	0.17166	17.6	0.015	0.965	14.614	99.0 ± 11.1
1050	-0.01114	0.10133	24.9	0.013	0.971	17.116	129.2 ± 14.2
1100	-0.01400	0.05590	40.9	0.018	0.980	21.506	131.7 ± 5.2
1150	-0.01527	0.04699	53.2	0.020	0.992	23.456	99.9 ± 18.8
1200	-0.02694	0.17100	-79.4	0.016	1.000	41.386	-132.0 ± 20.4

Sample mass = 0.6000 Grams; Average Standard J-Value = 0.00240 ± 0.00005

Integrated Date = 77.8 ± 0.7 Ma; Plateau date = (965-1010°C) 70.0 ± 0.5 Ma

Intercept date = 66.7 ± 1.8 Ma.

UT33HB: Hornblende from the post-volcantism dierite, Gabral

T°C	f1	f2	Atmos%	f40	f39	$^{37}Ar/^{39}Ar$	Age (Ma)
699	-0.00421	0.00132	72.1	8.32E6	0.046	6.471	141.4 ± 5.1
800	-0.00291	0.01281	56.3	3.84E6	0.089	4.470	69.4 ± 3.6
850	-0.00682	0.04779	36.3	4.56E6	0.125	10.483	101.3 ± 5.6
899	-0.01205	0.09426	30.8	9.35E6	0.190	18.518	111.8 ± 5.6
912	-0.00926	0.12612	23.9	827E6	0.260	14.224	92.7 ± 2.2
925	-0.00775	013369	23.7	1.15E7	0.382	11.908	74.9 ± 1.2
937	-0.00732	0.16655	19.5	1.46E7	0.545	11.241	70.8 ± 1.0
962	-0.00695	0.24341	13.8	1.30E7	0.705	10.683	64.5 ± 0.9
975	-0.00711	0.29348	11.7	9.24E6	0.823	10.916	62.2 ± 1.2
978	-0.00747	0.64705	2.9	5.85E6	0.893	11.478	65.6 ± 2.0
1000	-0.00759	0.47877	6.0	3.17E6	0.934	11.661	62.0 ± 3.9
1050	-0.00834	0.84754	0.9	3.26E6	0.967	12.208	78.1 ± 5.4
1150	-0.01131	0.65532	3.3	3.54E6	1.000	17.374	84.0 ± 7.1

Sample mass = 0.6000 Grams; Average Standard J-Value = 0.00240 ± 5E-6

Integrated Date = 77.8 ± 0.7 Ma; Minimum date = (962-1000°C) 64.0 ± 0.8 Ma

Intercept date = 54.0 ± 2.3 Ma.

UT54BI: Biotite from tonalite at Matiltan

T°C	f1	f2	Atmos%	f40	f39	$^{37}Ar/^{39}Ar$	Age (Ma)
630	-0.00009	0.00113	40.1	2.418	0.166	0.143	56.1 ± 0.4
747	-0.00002	0.00180	8.0	3.153	0.329	0.033	78.9 ± 0.3
850	-0.00003	0.00225	7.3	2.551	0.459	0.042	74.8 ± 0.5
875	-0.00003	0.00174	10.2	1.288	0.527	0.046	72.7 ± 0.5
899	-0.00003	0.00203	9.5	1.281	0.593	0.051	73.8 ± 0.5
925	-0.00003	0.00155	11.1	1.387	0.666	0.045	73.2 ± 0.4
950	-0.00003	0.00176	11.2	1.366	0.737	0.052	73.4 ± 0.4
975	-0.00004	0.00145	14.1	1.184	0.799	0.055	72.7 ± 0.5
1000	-0.00003	0.00121	15.2	1.263	0.666	0.050	72.1 ± 0.5
1050	-0.00004	0.00143	14.0	1.672	0.952	0.055	74.4 ± 0.3
1150	-0.00006	0.00067	35.8	0.970	1.000	0.098	77.2 ± 2.2

Sample mass = 0.0800 Grams; Average Standard J-Value = 0.00240 ± 0.00005

Integrated Date = 70.9 ± 0.2 Ma; Plateau date = (747-1050°C) 73.6 ± 0.2 Ma

Intercept date = 73.9 ± 0.6 Ma

UT33BI: Biotite from post-volcanism diorite, Gabral

T°C	f1	f2	Atmos%	f40	f39	$^{37}Ar/^{39}Ar$	Age (Ma)
600	-0.00007	0.00064	56.8	1.381	0.136	0.110	38.7 ± 0.5
699	-0.00003	0.00161	19.1	1.107	0.233	0.052	43.3 ± 0.9
798	-0.00003	0.00202	15.1	1.218	0.337	0.050	44.8 ± 0.7
849	-0.00003	0.00197	13.9	1.344	0.445	0.047	47.5 ± 0.5
900	-0.00002	0.00228	9.8	1.848	0.599	0.35	45.5 ± 0.3
925	-0.00003	0.00359	8.7	1.053	0.689	0.048	44.8 ± 0.3
950	-0.00005	0.00421	11.0	0.952	0.771	0.072	44.1 ± 0.3
975	-0.00007	0.00629	11.2	0.958	0.852	0.112	45.1 ± 0.3
999	-0.00010	0.00751	12.0	0.846	0.923	0.147	44.6 ± 0.4
1025	-0.00010	0.00498	17.7	0.553	0.970	0.151	44.6 ± 0.4
1075	-0.00006	0.00094	39.7	0.302	0.996	0.092	44.9 ± 2.5
1150	-0.00031	0.00023	84.4	0.062	1.000	0.473	52.8 ± 25.5

Sample mass = 0.0800 Grams; Average Standard J-Value = 0.00240 ± 0.00005
Integrated Date = 44.3 ± 0.2 Ma; Plateau date = (699-1075°C) 45.1 ± 0.2 Ma
Intercept date = 44.2 ± 0.4 Ma.

UT30BI: Biotite from the post-volcanism diorite, Gabral

T°C	f1	f2	Atmos%	f40	f39	$^{37}Ar/^{39}Ar$	Age (Ma)
601	-0.00005	0.00105	37.8	1.308	0.117	0.076	36.9 ± 0.3
696	-0.00002	0.00285	8.9	1.776	0.253	0.037	43.2 ± 0.3
750	-0.00003	0.01187	3.0	0.911	0.323	0.050	42.8 ± 0.3
800	-0.00004	0.02419	1.8	0.758	0.383	0.057	41.8 ± 0.6
849	-0.00003	0.00691	5.4	1.226	0.476	0.053	43.3 ± 0.3
900	-0.00003	0.00846	3.8	1.840	0.613	0.046	44.5 ± 0.2
925	-0.00003	0.00557	5.8	1.261	0.708	0.047	43.6 ± 0.2
950	-0.00004	0.00404	10.1	0.886	0.779	0.059	41.4 ± 0.9
974	-0.00005	0.00468	11.4	0.805	0.841	0.080	42.3 ± 0.5
1000	-0.00005	0.00292	18.7	0.678	0.898	0.084	39.6 ± 1.5
1025	-0.00007	0.00323	19.1	0.618	0.947	0.101	41.8 ± 0.5
1050	-0.00011	0.00286	31.4	0.369	0.976	0.101	41.8 ± 0.5
1075	-0.00036	0.00216	70.6	0.107	0.988	0.547	29.5 ± 7.1
1125	-0.00143	0.00289	83.4	0.063	0.995	2.197	32.7 ± 3.8
1180	-0.00163	0.00135	85.8	0.075	1.000	2.496	45.1 ± 4.0

Sample mass = 0.0800 Grams; Average Standard J-Value = 0.00240 ± 0.00005
Integrated Date = 41.9 ± 0.2 Ma; Plateau date = (696-1050°C) 42.7 ± 0.2 Ma
Intercept, date = 43.5 ± Ma.

UT36PL: Plagioclase from the pre-volcanism diorite, Gabral

T°C	f1	f2	Atmos%	f40	f39	$^{37}Ar/^{39}Ar$	Age (Ma)
500	-0.00230	0.00574	74.7	0.040	0.095	3.538	47.5 ± 1.7
514	-0.00238	0.02320	62.1	0.007	0.124	3.650	27.4 ± 10.4
549	-0.00318	0.02849	59.0	0.010	0.159	4.891	33.6 ± 4.3
599	-0.00496	0.02054	70.6	0.034	0.255	7.620	39.1 ± 1.2
649	-0.00497	0.05427	50.2	0.028	0.336	7.641	38.9 ± 2.0
699	-0.00420	0.08291	35.7	0.025	0.406	6.448	39.3 ± 1.9
800	-0.00542	0.12752	30.6	0.034	0.503	8.320	39.8 ± 1.5
899	-0.00366	0.04097	49.6	0.074	0.713	5.625	39.5 ± 0.6
999	-0.00256	0.02983	49.1	0.048	0.851	3.927	39.2 ± 0.7
1100	-0.00394	0.02099	58.8	0.053	0.963	6.045	53.3 ± 1.6
1200	-0.01495	0.04046	60.6	0.028	1.000	22.972	82.3 ± 3.1

Sample mass = 1.0000 Grams; Average Standard J-Value = 0.00240 ± 0.00005

Integrated Date = 42.8 ± 0.5 Ma; Plateau date (600-1000°C) = 39.3 ± 0.5 Ma

Intercept date = 39.6 ± 0.5 Ma.

UT33PL: Plagioclase from post-volcanism diorite, Gabral

T°C	f1	f2	Atmos%	f40	f39	$^{37}Ar/^{39}Ar$	Age (Ma)
550	-0.00250	0.00000	24.0	1.059	0.529	3.847	1133.8 ± 11.2
600	-0.00326	0.00543	34.1	0.033	0.601	5.002	327.7 ± 11.1
649	-0.00283	0.00331	93.7	0.001	0.652	4.341	15.4 ± 70.3
700	-0.00304	0.02376	29.7	0.007	0.692	4.670	126.5 ± 18.3
750	-0.00385	0.16840	8.3	0.004	0.725	5.910	99.3 ± 27.8
800	-0.00449	0.13795	13.1	0.003	0.752	6.903	88.1 ± 20.5
900	-0.00198	0.01134	38.4	0.012	0.899	3.043	115.9 ± 13.5
1101	-0.00363	0.01594	27.0	0.018	0.957	5.581	231.5 ± 13.1
1200	-0.00769	0.02326	12.8	0.046	1.000	11.812	682.0 ± 23.5

Sample mass = 1.0000 Grams; Average Standard J-Value = 0.00240 ± 0.00005

Integrated Date = 756.8 ± 6.1 Ma; Plateau date (700-1000°C) = 110 ± 11 Ma

Intercept date = 87.4 ± 30.0 Ma.

UT47PL: Plagioclase from ultramafic rock, Mahodand

T°C	f1	f2	Atmos%	f40	f39	$^{37}Ar/^{39}Ar$	Age (Ma)
598	-0.21748	-0.17378	68.4	0.052	0.118	334.066	1013.2 ± 27.7
699	-0.24721	-0.18045	74.1	0.040	0.278	379.742	640.7 ± 15.1
809	-0.38122	-0.24092	77.5	0.028	0.453	585.594	435.0 ± 10.5
899	-0.26140	-0.14868	69.4	0.027	0.595	401.530	512.6 ± 18.5
954	-0.16067	-0.08783	75.7	0.012	0.691	246.803	351.9 ± 26.2
1003	-0.18335	-0.11090	70.1	0.011	0.748	281.640	521.0 ± 37.2
1100	-0.30934	-0.25800	52.0	0.114	0.848	475.178	1950.4 ± 28.0
1190	-0.18549	-0.14823	49.2	0.148	1.000	284.929	1758.3 ± 9.8

Sample mass = 1.0000 Grams; Average Standard J-Value = 0.00240 ± 0.00005

Integrated Date = 996.4 ± 7.3 Ma; Plateau date = (?); Intercept Date = (?)

Explanation of Table-3 is as follows:

$f1 = 1/[1-(37/39)Ca/(37/39)M]$

and $f2 = [1-(36/39)Ca/(36/39)M]$, where OCa = isotope ratio of argon extracted from irradiated calcium salts,

OM = isotope ratio of argon extracted from irradiated unknown.

$f40 = {}^{40}Ar$ (x10^{-6} cc STP)

f(39) = cumulative fraction of ^{39}Ar released in each step.

Age 9Ma) = the constraints used for date calculation are:

lambda/epsilon = 0.581E-10/year; lambda/beta = 4.961E-10/year; $^{40}K/K$ = 0.01167 atom % (Steiger and Jager, 1977).

The quoted error is one standard deviation and does not include the error in the J-value or the standard error.

Integrated Date = date and error calculated from the sum total from all steps; the error includes the error in the J-value.

Plateau Date = date and error calculated from the sum total from those steps, the dates of which fall within 2 S.D. of each other; the error includes the error in the J-value.

Intercept Date = date and error calculated from the intercept of the best-fit line (York, 1969) with the $^{39}Ar/^{40}Ar$ axis on a $^{36}Ar/^{40}Ar$ versus $^{39}Ar/^{40}Ar$ plot.

Turn of dates ranging from 8.1 to 112.3 Ma for the initial 41% of the gas released (800-925°C). For temperature steps between 950-1010°C, a well-defined plateau with a date of 70.0±0.5 Ma is obtained. The spectra for the remaining 5% of the ^{39}Ar release pattern is highly irregular with dates ranging from 131.7 to -12.2 Ma. An integrated date of 77.8±0.7 Ma is higher than the plateau date, and is interpreted to reflect excess argon contamination as revealed by the low and high temperature steps of the spectrum. Except for the temperature step 1010°C, the remainder of the plateau steps form a linear array on $^{36}Ar/^{40}Ar$ versus $^{39}Ar/^{40}Ar$ plot, with an intercept date of 66.7±1.8 Ma.

A close correspondence is also shown by the $^{37}Ar/^{39}Ar$ spectrum with the age spectrum. The average $^{37}Ar/^{39}Ar$ of 11.5 of the plateau steps is in accordance with the overall average Ca/K of 19.3, obtained from microprobe data of these magnesio-hornblende grains (Table-1; UT31HB1).

UT33HB: This sample of post-volcanic diorite was collected closer to the diorite-volcanic contact. The spectrum for the initial 55% of the ^{39}Ar release (699-937°C) indicates decreasing age with increasing temperature, suggesting excess argon contamination (Lanphere and Dalrymple, 1976; Harrison and McDougall, 1980, 1981). The spectrum from 55 to 93% ^{39}Ar (962-1000°C) yields a plateau (gas was lost at temperature step 950°C is not included in the plateau date calculation) with a date of 64.0±0.8 Ma, which is less than the 70.0±0.5 plateau date of UT31HB. The position of the 950°C temperature step lost during step heating in relation to other plateau steps indicate that its absence has most probably not affected the plateau date. The remaining spectrum records an increase in dates with ^{39}Ar released, with a maximum age of 84.0 Ma for 1150°C temperature step. An integrated date of 77.8±0.7 Ma is given by the overall spectrum which is higher than the plateau date and reflect mostly excess argon in this particular hornblende. A linear array is obtained from temperature steps, 899-1150°C, on a

117

$^{36}Ar/^{40}Ar$ versus $^{39}Ar/^{40}Ar$ plot, with an intercept date of 54.0 ± 2.3 Ma, which is lower than the plateau date obtained for UT33HB.

The $^{37}Ar/^{39}Ar$ spectrum generally corresponds to the age versus ^{39}Ar spectrum and is very similar to that of UT31HB.

Biotite

UT54BI: Except for the initial 630°C step, the spectrum for UT54BI exhibits a well-defined plateau for 78% of the ^{39}Ar release (747-1150°C) with a date of 73.6 ± 0.2 Ma. The integrated date of 70.9 ± 0.2 Ma reflects the relatively lower date of the 630°C temperature step. A well defined linear array on a $^{36}Ar/^{40}Ar$ versus $^{39}Ar/^{40}Ar$ plot of all the temperature steps for UT54BI yields an intercept date of 73.9 ± 0.6 in good agreement with the plateau date.

Except for the 630°C step, the $^{37}Ar/^{39}Ar$ spectrum yields very low (<0.1) values. The higher $^{37}Ar/^{39}Ar$ ratio shown by the 630°C step probably reflects the contamination of the biotite by a calcium bearing alteration phase.

UT33BI and UT30BI: Except for the initial low temperature step, the spectra for biotite from both UT33BI and UT30BI show well-defined plateau for approximately 80% of the ^{39}Ar release with plateau dates of 45.1 ± 0.2 Ma and 42.7 ± 0.2 Ma respectively. Intercept dates obtained for both samples of biotite are 44.22 ± 0.4 Ma and 43.5 ± 0.1 Ma respectively, very similar to their corresponding plateau dates (Tables-2 & 3).

The pattern revealed by the $^{37}Ar/^{39}Ar$ spectra of these biotites are highly irregular; a saddle-shaped spectrum is shown by UT33BI and a more or less similar spectrum for UT30BI. Such patterns can be interpreted as representing the mixing of the two types of biotites mentioned earlier in the post-volcanic hornblende diorite or the inhomogeneous distribution of Ca in these biotites. This interpretation is supported by the average $^{37}Ar/^{39}Ar$ ratio of 0.07 (Ca/K = 0.12) for the plateau steps of UT30BI which is considerably higher than the Ca/K ratio of 0.014 obtained from microprobe data of the same sample (see Tables-1 & 3).

UT36PL: The initial 15% of ^{39}Ar release of the $^{40}Ar/^{39}Ar$ spectrum for the plagioclase from the pre-volcanic diorite yields an irregular profile. This is followed, however, by a plateau between 17-85% of the ^{39}Ar release with a date of 39.3 ± 0.5 Ma. Above 85% the

spectra show increasing age with a maximum date of 82.3 Ma for 1200°C temperature step. An intercept date of 39.6 ± 0.5 Ma is obtained for this separate, which closely corresponds with the plateau date. The $^{37}Ar/^{39}Ar$ spectrum does not yield a similar plateau. This feature is also reflected by the incompatibility of Ca/K ratio (plateau step = 12, overall average 13.35) obtained from the argon data with that obtained from microprobe data (57.25, Tables - 1 & 3). The reasons for this is not understood, but may be attributable to partial epidotization or sericitization of the plagioclase. The higher Ca/K ratio of epidote (142) then that of plagioclase (10) support the latter possibility.

UT33PL: Plagioclase from the post-volcanic diorite near Gabral yields a highly discordant saddle-shaped spectrum. Fifty three percent of the ^{39}Ar that was released in the first tempertaure step (550°C) yields a very high date of 1134 ± 11 Ma. The age decreases with increasing temperature, between 60 and 65% of the ^{39}Ar release (600 and 649°C), attaining a plateau (25% of the ^{39}Ar release) at intermediate temperature steps with a plateau date of 110.0 ± 11.0 Ma. The remaining spectra record an increase in incremental heating date, with a maximum date of 682 ± 23 Ma at 1200°C. The integrated date is 756.8 ± 6.1 Ma. All these features are indicative of the presence of a considerable amount of excess radiogenic-enriched argon in this sample (Lanphere and Dalrymple, 1981; Harrison and McDougall, 1981).

UT47PL: A considerably discordant $^{40}Ar/^{39}Ar$ spectrum with dates varying from 435 ± 10 Ma to 1950 ± 28 Ma are given by the data obtained from UT47PL. These ages are considerably higher than the accepted age of rocks of the KIA and indicate the presence of a high proportion of radiogenic-enriched excess argon in this plagioclase. The $^{37}Ar/^{39}Ar$ values are extremely high, varying from 250 to 580.

DISCUSSION

The 57 Ma minimum date obtained from hornblende of the pre-volcanism diorite (UT36HB) at Gabral is younger than the corresponding dates (70 and 64 Ma) obtained from hornblende from the post-volcanic diorites (UT31HB, UT33-Hb) at the same locality (except the intercept date of 54 Ma for UT33-Hb; see Table-2). Similarly, hornblende from the andesite at Dir (LR14HB) also yields a higher plateau date, 70 Ma, than obtained for hornblende from the prevolcanic diorite. Such data disagrees with the age relationships established on the basis of field observations. This shows that the K-Ar system for the

118

hornblende from the pre-volcanic diorite (UT36HB) must have been partially reset. This is supported by shape of age spectrum of UT36HB, particularly the high temperature steps (1025-1074 °C) which do attain ≃70 Ma.

Biotites from the post-volcanism diorites of Gabral (UT33BI, UT30BI) reflect plateau dates of 45 to 43 Ma, whereas plagioclase from the pre-volcanic diorite (UT36PL) yields a plateau date of 39 Ma (Tables - 2 & 3). As hornblendes from all these rocks have shown higher dates, the biotite and plagioclase dates must record a thermal overprint at this time. On the other hand biotite from the tonalite at Matiltan (UT54BI) yields a highly concordant 74 Ma plateau which is within error of the 70 Ma dates obtained for hornblendes from the diorites and volcanics of Gabral and Dir (Tables - 2&3). Except for minor chloritization at margins (reflected by the 630°C temperature step in Fig. 3), the Matiltan biotite is generally fresh and undeformed, suggesting that the 74 Ma date is probably an emplacement age. Petrographically, the Matiltan tonalite (UT54) is similar to the pre-volcanic diorite at Gabral (UT36). The reason why it apparently escaped the middle Eocene thermal event which completely reset the biotite at Gabral is not clear. A more detailed study is required to investigate this problem.

The record of the 45-39 Ma event reflected in biotites and plagioclase from the pre- and post-volcanic diorites of Gabral analyzed during the present study (Fig. 3; Tables - 2&3) indicates that the temperature exceeded the blocking temperature of biotite and plagioclase at this particular locality. Zeitler (1985) obtained a 44.9 ± 0.4 $^{40}Ar/^{39}Ar$ integrated date for biotite from a diorite (Zeitler's tonalite, SW10) at Gabral and a 45.2 ± 0.4 Ma $^{40}Ar/^{39}Ar$ integrated date for hornblende from a diorite (Zeitler's 1985; altered tonalite; 80D3) at Dir and considered these dates as "concordant" and reprsenting an emplacement age for diorites. The present study has shown that the K-Ar system in biotite from Gabral has been reset at 45-42 Ma and thus the dates obtained for these biotites do not represent an intrusion age. In view of Zeitler's (1985) Middle Eocene Ar date for hornblende from Dir, the temperature must have passed above the blocking temperature of hornblende (~500°C) in this region and between the blocking temperature of hornblende and biotite (~300°C) in the east at Gabral, but did not attain the latter limit and sur-passed the blocking temperature of plagioclase (~200°C), further east at Matiltan. This westward increase in the peak metamorphic temperatures attained during the Middle Eocene is consistent with the greater deformation of the

diorites and even of certain volcanics at Dir relative to those near Gabral and Matiltan.

The present study shows that the emplacement of diorites in Swat, Kohistan and Dir areas began at or before 74 Ma and continued till 54 Ma (intercept date for UT33HB) and was interrupted by a span of volcanism at about 70 Ma. Previous studies have shown that the collision between the Eurasian plate and KIA along MKT occurred around 102 Ma whereas collision between the Indian plate and KIA along MMT occurred around 55 Ma (Patterson & Windley, 1985; Treloar *et al.*, 1989; see also Patriot & Achache, 1984; Searle *et al.*, 1987; Zeitler *et al.*, 1987). A Sm-Nd mineral isochron age of 103 ± 4 Ma has been reported for the garnet granulite of the Jijal complex (Fig. 1), a date considered as representing high pressure island-arc subduction related metamorphism by Searle *et al.* (1987). An $^{40}Ar/^{39}Ar$ date of 75 Ma has been reported for the southern amphibolite belt rocks (Kamila amphibolite) by these workers. Jan and Asif (1981) have mentioned an age range of 90 to 65 Ma for the emplacement of the Chilas complex. On the basis oof structural data, however, the Jaglot syncline (cf. Fig. 1) which has deformed the Chilas complex has been correlated to collision along MKT, indicating that the age of the Chilas complex is at least 102 Ma (age of the collision along MKT) and can be correlated with the date obtained for the high grade metamorphism of the Jijal complex (Patterson and Windley, 1985; see also Coward *et al.*, 1986). Such interpretations show that the 90-65 Ma date of the Chilas complex (cf. Jan and Asif, 1981) and most probably the 75 Ma date of the southern amphibolite belt rocks (cf. Searle *et al.*, 1987) are metamorphic overprinting dates. These interpretations also show that the production of the parent magma(s) for the Chilas complex occurred as a result of an island arc subduction related phenomenon, a conclusion supported by the petrochemistry of the Chilas complex (Hamidullah and Jan, 1987). All these features indicate that a considerable magmatic and metamorphic activity has occurred between the two colision dates (102 Ma and 55 Ma) throughout KIA (see also Treloar *et. al.*, 1989), and that the arc has been generally younging from south (Jijal) towards north (Kalam-Dir) areas (cf. Fig. 1). These features also show that magmatism in the north had a parallel metamorphism in the south (e.g. magmatism at Chilas with metamorphism at Jijal, and magmatism at Kalam-Dir with metamorphism at Chilas).

The rock sequence of the KIA has been subdivided into northern and southern intrusive belts or northern and southern arcs. Rocks north of Kalam in the Swat valley and Dir area have been classified as

part of the northern arc, with those south of Kalam being part of the southern arc (Zeitler, 1985; Honnegar *et al.*, 1982). This classification is based on previously obtained isotopic dates of 120-65 Ma for rocks of the southern arc and 65-40 Ma for rock of the northern arc (Zeitler, 1980, 1985; Brookfield and Reynold, 1981). Patterson and Windley (1985) have however, reported plutonic activity of the Kohistan-arc-batholith in Gilgit area at 102 ± 12 Ma (Matum Das), 54 ± 4 Ma (Gilgit proper), 40 ± 6 Ma (Shirot) and 34 ± 4 Ma (Indus confluence). Therefore, the classification of KIA into two arcs on the basis of radiometric data seems premature and requires further investigation.

The results of this study indicates that a Middle Eocene-Oligocene metamorphism was followed by cooling due to uplift and erosion in the Swat Kohistan and Dir areas. This metamorphic event can be related to collision along MMT or underthrusting of India below KIA (and below Eurasia in the east) following collision along MMT (see Maluski and Matte, 1984). Another possibility is that the Middle Eocene-Oligocene metamorphism resulted from the collision along MKT at about 40 Ma, after the collision along MMT, as suggested by Klootwijk *et al.*, (1979). No major magmatic activity however, has been reported during the Oligocene from the northern part of KIA except the intrusion of aplite-pegmatite sheets at Indus confluence and Pari, Gilgit area, mentioned earlier. Therefore the occurrence of a 40 Ma collision along the MKT and the relation of the Middle Eocene to Oligocene metamorphism to this collision seems unlikely (see also Patterson & Windley, 1985; Coward *et al.*, 1986), The intrusion of the post-Oligocene aplite pegmatite sheets in Gilgit area can be also related to post-collisional environment of MMT and seem to have played no major role in the process of arc construction.

The source region for the calc-alkaline igneous activity in Kalam-Dir areas is not yet specifically known but Cr of >1000 ppm has been detected in clinopyroxene from the Utror lavas (Hamidullah, unpubl. data) which points to a source at least more basic than the continental crust. The melting of the oceanic crust and/or mantle and/or the base of the Chilas complex at greater depth can be suggested as the possible source region.

CONCLUSIONS

Hornblendes from the volcanics and the various diorites of Dir and Gabral areas and biotite from the tonalite of the Matiltan area record $^{40}Ar/^{39}Ar$ dates of 74 to 54 Ma, which are interpreted as emplacement or post-emplacement cooling dates. It is suggested that the Late Cretaceous to Early Eocene period was dominated by plutonism (diorites and tonalite) with a short span of volcanism at 70 Ma in Kalam-Dir areas of the KIA. The 54 Ma date indicates the minimum age for the culmination of active plutonism, and may reflect the collision of the KIA with India.

Plagioclase and biotite from the postvolcanic diorite of Gabral yield 45-39 Ma $^{40}Ar/^{39}Ar$ dates, interpreted as recording a Middle Eocene metamorphism followed by cooling possibly related to uplift in the area.

Plagioclase from the post-volcanic diorite of Gabral and from the olivine gabbro of Mahodand yield unreasonably old ages, reflecting the presence of a high proportion of excess argon.

The accretion of KIA may have occurred from south to north (at least in the study area and south of it) as each plutonic and volcanic activity in the north appears to be contemporaneous with a high grade metamorphism in the south.

At least on the basis of isotopic age data, the present study does not support the division of KIA into northern and southern arcs as suggested by the previous workers.

REFERENCES

Andrews-Speed, C.P., and Brookfield, M.E., (1982). Middle Paleozoic to Cenozoic tectonic evolution of the northwestern Himalaya. *Tectonophysics,*

Vol. 82, pp. 253-275.

Bard, J.P., Maluski, H., Matte, Ph., and Proust, F., (1980). The Kohistan sequence: Crust and mantle of an obducted island arc. *Geol. Bull. Univ. Peshawar,* Vol. 13, pp. 87-94.

Bard, J.P., (1983). Metamorphism of an obducted island arc: Example of the Kohistan sequence (Pakistan) in the Himalaya collided range. *Earth Planet. Sci. Lett.,* Vol. 65, pp. 133-144.

Bence, A.E., and Albee, A.L., (1968). Empirical correction factors from the electron microanalyses of silicates and oxides. *Jour. Geol.,* Vol. 76, pp. 383-402.

Berger, G.W., and York, D., (1970). Precision of the $^{40}Ar/^{39}Ar$ dating technique. *Earth Planet. Sci. Lett.,* Vol. 9, pp. 39-44.

Bottomley, R.J., and York, D., (1981). $^{40}Ar/^{39}Ar$ determinations on the Owyhee basalt of the Columbia plateau. *Earth Planet. Sci. Lett.,* Vol. 31, pp. 75-84.

Brookfield, M.E., and Reynolds, P.H., (1981). Late Cretaceous emplacement of the Indus Suture Zone ophiolitic melanges and an Eocene-Oligocene magmatic arc on the northern edge of the India plate. *Earth Planet, Sci. Lett.,* Vol. 55, pp. 157-162.

Coward, M.P., Windley, B.F., Broughton, B., Luff, L.W., Patterson, M.G., Pudsey, C., Rex, D., and Khan, M.A., (1986). Collision tectonics in N.W. Himalyas. In: Collision Tectonics (Eds. M.P. Coward and A. Bies). *Geol. Soc. Lond. Spec. Publ.,* Vol. 19, pp. 203-219.

Dalrymple, G.B., Alexander, E.C., Jr., Lanphere, M.A., and Kraker, G.P., (1981). Irradiation of samples for $^{40}Ar/^{39}Ar$ dating using the Geological Survey TRIGA Reactor. *U.S. Geol. Surv. Prof. Pap.,* 1176, 55 P.

Harrison, T.M., (1981), Diffusion of ^{40}Ar in hornblende. *Contr. Min. Pet.,* Vol. 70, pp. 324-331.

Harrison, T.M., and McDougall, I., (1980). Investigation of an intrusive contact, northwest Nelson, New Zealand. II, Diffusion of radiogenic and excess ^{40}Ar in hornblende revealed by $^{40}Ar/^{39}Ar$ age spectrum analysis, *Geochim. Cosmochim. Acta,* Vol. 44, pp. 2005-2020.

Harrison, T.M., and McDougall, I., (1981). Excess ^{40}Ar in metamorphic rocks from Broken Hill, New South Wales. Implications for $^{40}Ar/^{39}Ar$ age spectrum and the thermal history of the region. *Earth Planet. Sci. Lett.,* Vol. 55, pp. 123-149.

Harrison, T.M. and McDougall, I., (1982). The thermal significance of potassium feldspar K-Ar ages inferred from $^{40}Ar/^{39}Ar$ age spectrum results. *Geochim. Cosmochim. Acta,* Vol. 46, pp. 1811-1820.

Hollister, L.S., Crisp. J., Kullick, C.G., Maze, W., and Sission, V.B., (1984). Quantitative energy dispersive analyses of rock-forming silicates. Proc. 19th *Ann. Microbeam Analysis Soc. Mtg.,* pp. 143-144.

Honneger, K., Dietrich, V., Frank, W., Gansser, A., Thoni, M., and Trommsdorff, V., (1982). Magmatism and metamorphism in the Laddakh Himalaya (the Indus-Tsangpo suture zone). *Earth Planet. Sci. Lett.,* Vol. 60, pp. 253-292.

Jan, M.Q., and Asif, M., (1981). A speculative tectonic model for the evolution of N.W. Himalaya and Karakoram. *Geol. Bull, Univ. Peshawar,* Vol. 14, pp. 199-201.

Khalil, M.A., and Afridi, A. G., (1973). Geology of the Deshail Diwangar area, Swat. Unpublished M.Sc. thesis, University of Peshawar.

Klootwijk, C.T., Sharma, M.L., Gergan, J., Tinkey, B., Shah, S.K., and Agarwal, V., (1979). The extent of greater India II. Palaeomagnetic data from the Laddakh intrusives of Kargil, N.W. Himalayas. *Earth Planet. Sci. Lett.,* Vol. 44, pp. 47-64.

Lanphere, M.A., and Dalrymple, G.B., (1976). Identification of excess ^{40}Ar by the $^{40}Ar/^{39}Ar$ age spectrum technique. *Earth Planet. Sci. Lett.,* Vol. 32, pp. 141-148.

Lanphere, M.A., and Dalrymple, G.B., (1971). A test of the $^{40}Ar/^{39}Ar$ spectrum technique on some terrestrial materials. *Earth Planet. Sci. Lett.,* Vol. 12, pp. 359-372.

Majid, M. and Paracha, F.A., (1979), Calcalkaline magmatism at destructive plate margin in Kohistan, northern Pakistan. *Geol. Bull. Univ. Peshawar,* Vol. 13, pp. 109-120.

Majid, M., (1979). Petrology of diorites from the "Kohistan Sequence", Swat, Northern Pakistan. A genetic interpretation at plate scale. *Geol. Bull. Univ. Peshawar,* Vol. 11, pp. 131-151.

Maluski, H., and Matte, P., (1984). Ages of Alpine tectonometamorphic events in the northwestern Himalaya (Northern Pakistan) by $^{40}Ar/^{39}Ar$ method. *Tectonics,* Vol. 3, pp. 1-18.

Masliwec, A., (1981). The direct dating of ore minerals. Unpublished M.Sc. thesis, University of Toronto, Canada.

Onstott, T.C., and Peacock, M.W., (1987). Argon reactivity of hornblendes: A field experiment in a slowly cooled metamorphic terrain. *Geochim. Cosmochim. Acta,* Vol. 51, pp. 2891-2903.

Patriat, P. and Achache, J., (1984). India-Eurasia collision chronology has implication for crustal shortening and driving mechanism of plates.

Nature, Vol. 311, pp. 615-621.

Patterson, M.G., and Windley, B.F., (1985). Rb-Sr dating of the Kohistan-arc-batholith in the Trans-Himalaya of north Pakistan and tectonic implications. *Earth Planet. Sci. Lett.,* Vol. 74, pp. 45-57.

Roddick, J., (1983). High precision intercalibration of $^{40}Ar/^{39}Ar$ standards. *Geochim. Cosmochim. Acta,* Vol. 47, pp. 887-898.

Roddick, J.C., Cliff, R.A., and Rex, D.C., (1980). The evolution of excess argon in Alpine biotites - An $^{40}Ar/^{39}Ar$ analysis. *Earth Planet. Sci. Lett.,* Vol. 48, pp. 185-208.

Searle, M.P., Windley, B.F., Coward, M.P., Cooper. D.J.W., Rex, D.C., Tingdong, L., Xuchang, X., Jan, M. Q., Thakur, V.C., and Kumar, S., (1987). The closing of Tethys and the tectonics of the Himalaya. *Geol. Soc. Amer. Bull.,* Vol. 98, pp. 678-701.

Snee, L.W., (1982). Emplacement and cooling of the Pioneer Batholith, southwestern Montana. Unpublished Ph.D. thesis, Ohio State University, Columbus, OH.

Tahirkheli, R.A.K., Mattauer, Proust, F., and Tapponnier, P., (1979). The Indian Eurasian suture zone in northern Pakistan. Synthesis and interpretation of recent data at plate scale. In: Geodynamics of Pakistan (Eds. Abdul Farah and Kees A. Dejong). *Spec. Publ. Geol. Surv. Pakistan Quetta,* pp. 125-131.

Tahirkheli, R.A.K., (1982). Geology of Himalaya, Karakorum and Hindu Kush. *Geol. Bull. Univ. Peshawar Spec. Iss.* Vol. 15, 54p.

Treloar, P.J., Rex, D.C., Guise, P.G., Coward, M.P.,

Searle, M.P., Windley, B.F., Patterson, M.G., Jan, M.Q., and Luff, I.W., (1989). K-Ar and Ar-Ar geochronology of the Himalayan collision in NW Pakistan: Constraints on the timing of suturing, deformation, metamorphism and uplift. *Tectonocs,* Vol. 8 , pp. 881-909.

Windley, B.F., (1986). The evolving continents. John Wiley & Sons, New York, (revised, 399p.

York, D., (1969), Least square fitting of a straight line with correlated errors. *Earth Planet. Sci. Lett.,* Vol. 5, pp. 320-324.

Zeitler, P.K., (1980). The tectonic interpretation of fission-track ages from the Himalayan ranges of northern Pakistan. Unpublished M.A. thesis, Dartmouth College, Hanvor, N.H.

Zeitler, P.K., (1985). Cooling history of the N.W. Himalaya, Pakistan. *Tectonics,* Vol. 4, pp. 127-151.

Zeitler, P.K., Tahirkheli, R.A.K., Naeser, W.C., and Johnson, N.M., (1982a). Unroofing history of a suture zone in the Himalaya of Pakistna by means of fission-track annealing ages. *Earth Planet. Sci. Lett.,* Vol. 57, pp. 227-240.

Zeitler, P.K., Johnson, N.M., Naeser, C.M., and Tahirkheli, R.A.K., (1982b). Fission-track evidence for Quaternary uplift of the Nanga Parbat region, Pakistan. *Nature,* Vol. 298, pp. 255-257.

Zeitler, P.K., Sutter, J.F., Williams, I.S., Zortman, R., and Tahirkheli, R.A.K., (1989). Chronology and temperature history of the Nanga Parbat-Haramosh Massif, Pakistan. *Geol. Soc. Amer, Spec. Pub.;* Vol. 232. pp. 1-22.

PETROCHEMISTRY OF AMPHIBOLITES FROM THE SHERGARH SAR AREA, ALLAI KOHISTAN, N. PAKISTAN

By

MOHAMMAD TAHIR SHAH[*], MOHAMMAD MAJID,[**]
SYED HAMIDULLAH[*] AND JOHN W. SHERVAIS[***]
[*]National Centre of Excellence in Geology University of Peshawar.
[**]Department of Geology University of Peshawar.
[***]Department of Geological Sciences, University of South Carolina, Columbia (USA).

ABSTRATCT: *Shergarh Sar area, a part of the Allai Kohistan is located at the closure of the Indo-Pakistan and Kohistan island arc block. Rocks of the area are distinguished into three petrotectonic units:[1] the Kohistan island arc sequence[2] the Indus melange zone and[3] the Indo-Pakistan subcontinent sequence. Amphibolites are the most abundant rocks exposed in the area and are considered to be a part of the southern amphibolite belt. These are occurring in both banded and non-banded form. The banded feature is attributed to the metamorphic segregation processes. Mineralogically these rocks are distinguished as epidote amphibolite and garnet epidote-amphibolites. Amphibole + epidote + clinopyroxene + plagioclase + actinolite + chlorite + quartz + opaque is the main mineral assemblage. Garnet occur sporadically in these rocks. The textural features are indicative of retrogression from epidote-amphibolite to green schist facies conditions. The major and trace element constraints of these amphibolites, suggest their derivation from basic igneous parent of tholeitic character developed in the island arc type of environment.*

INTRODUCTION

From stand point of the new global tectonic, evolution of the Himalayas has been interpreted through the continental collision process between Asia and Indo-Pakistan. In accordance with the proposed model, the Main Karakoram Thrust (MKT) in the north and the Main Mantle Thrust (MMT) in the south are regarded as the tectonic fingerprints of the past subduction zones. Both are characterized by the ophiolitic melanges, in addition the blueschist and high-P garnet granulites are also associated with MMT. These faults are the result of bifurcation of the Indus Zangbo Suture (IZS) in Ladakh and Kohistan. This suture is considered to be the northern limit of the Indian continent, both in the Pakistan and in Indian territories. Both the MMT and MKT enclose the Kohistan-Ladakh Island arc and are separating it from the Indian plate in the south and the Karakoram plate in the north. The Kohistan island arc from north to south, between MKT and MMT, is mainly comprises:

(1) metavolcano- clastics and detrital sediments of Mid Cretaceous (Yasin group), (2) Chalt volcanics of Cretaceous to late Jurassic, (3) Kohistan-Ladakh plutonic belt, (4) The Chilas complex, (5) The Southern (Kamila) amphibolite belt, (6) The Jijal-Patan complex. Each of the lithologic unit is stretching for several hundred of Kilometers (for detail see Tahirkheli and Jan 1979; Jan, 1979; Tahirkheli *et al.* 1979; Klootwijik *et al.* 1979; Gansser, 1980; Jan and Hawie, 1981; Andrews Speed and Brookfield, 1982; Coward *et al.* 1982, 1986; Jan and Asif, 1983; Bard, 1983; Patterson and Windley, 1985; Jan, 1988).

Shergardh Sar area a part of the Allai Kohistan (39km[2] between latitude 34° 50' 15" N to 34° 54' 15"N and longitude 73° 1" E to 73° 5' E, sheet No. 43F/1) marks an ideal section of the collision zone between the Kohistan island arc and Indo-Pakistan plate in Hazara division (Fig. 1). The area of study is situated east of Indus River and south of the Indus Kohistan and is bounded by the two main streams i.e., Allai Khwar and
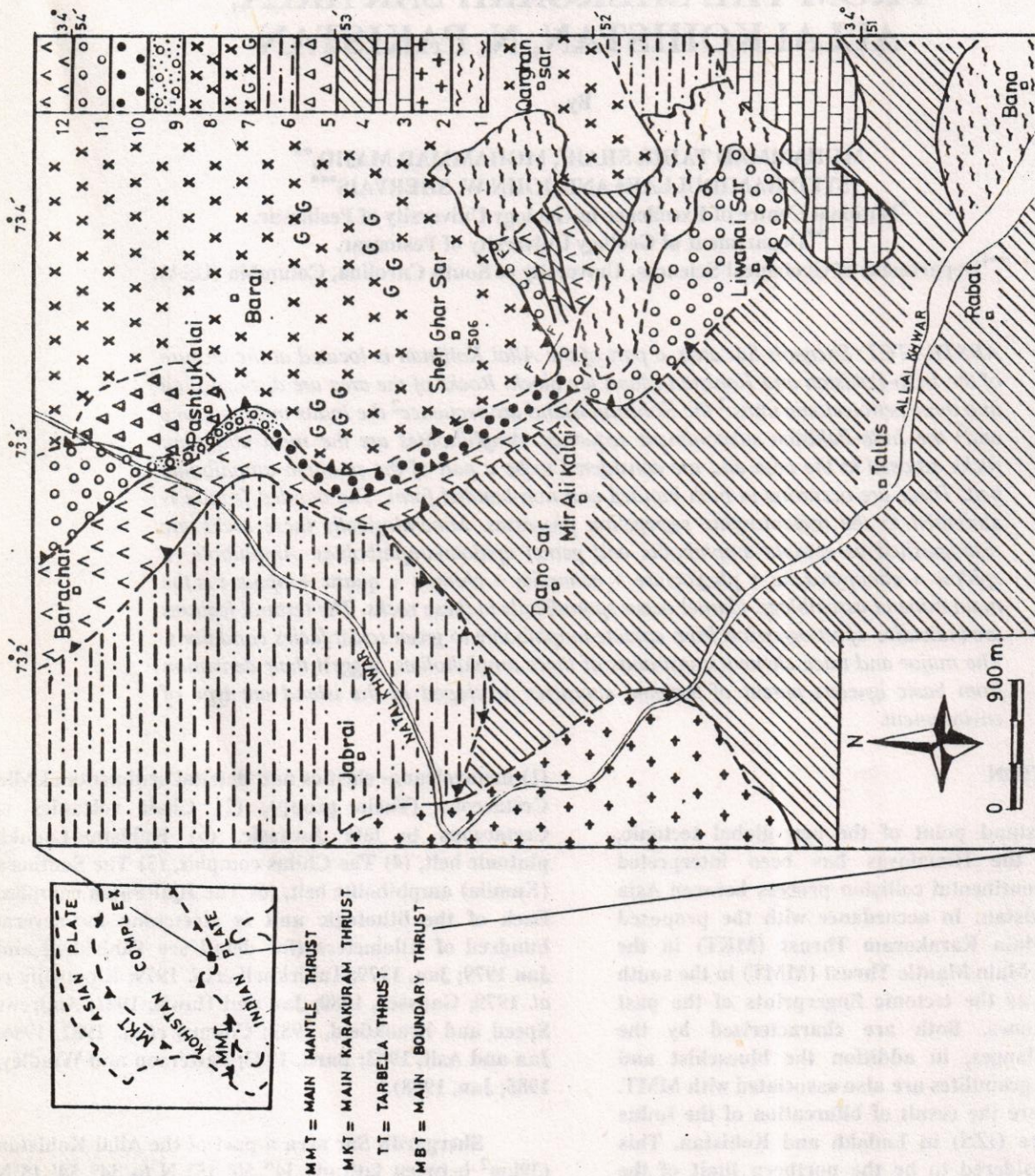
Fig. 1 Geological map of the Shergarh Sar area, Allai Kohistan, N. Pakistan. 1. Overburden; 2. Granite gneiss; 3. Limestone; 4. Schist; 5. Brecciated zone; 6. Greenschist; 7. Garnet-epidote-amphibolite; 8. Epidote-amphibolite; 9. Serpentinite; 10. Peridotite; 11. Clinopyroxenite; 12. Lavas. Thrusted contact, dashed where inferred.

MMT = MAIN MANTLE THRUST
MKT = MAIN KARAKURAM THRUST
TT = TARBELA THRUST
MBT = MAIN BOUNDARY THRUST

the Natal Khwar. The area is easily accessible from the Karakoram high way (KKH) by an unmetaled road from Thakot to Bana. The rocks of the area are predominantly composed of amphbibolites, ultramafics, lavas with associated metachert and limestone, greenschists, blueschist facies metagraywacke, schists, crystalline limestone and minor granite gneiss (Shah and Majid, 1985). These are group together in three petrotectonic units (Shah, 1986), which are described in a north to southward stratigraphic succession as (a) the Kohistan arc sequence (b) the Indus suture melange zone (c) Indo-Pakistan subcontinent sequence.

The amphibolites are the most voluminous rocks developed in the northern and north-eastern portion of the area, which delimits the southern exposure of the Kohistan arc sequence in the investigated area. Jan *et al.* (1984) and Jan (1988) considered these amphibolites as a part of the southern (Kamila) amphibolite belt. This belt is of late Jurassic to Cretaceous age and is mainly composed of volcanics, a variety of plutonic rocks, rare siliceous and calcareous metasediments (see Jan, 1979).

These amphibolites have not been extensively studied and their petrogenetic affinity remains undefined. This paper presents results of geochemical investigation of the Shergarh Sar amphibolites in order to ascertain the possible petrotectonic affinity.

FIELD FEATURES

Two types of amphibolites (a) epidote-amphibolite and (b) garnet epidote-amphibolite are identified in the studied area. The epidote-amphibolite type of rocks are widely exposed along north and north-eastern part of the area under discussion. These rocks overlies the ultramafic rocks in the area (Fig. 1) and are characterized by the dark green to light gray colour with white patches and linear fabrics of felsic and mafic minerals. These fabrics occasionally grade to schistosity. Occasionally felsic veins up to 4 cm thick containing large crystals (about 2cm long) of amphibole and cross cutting the epidote-amphibolite have been noticed, especially at the top of the Qarghan Sar. These veins are some time displaced by the later deformations. Minor faulting in these rocks is, however, not uncommon. The dark coloured patches containing very high proportion of hornblende are disseminated through out these rocks. These constitutes coarse-grained bodies of various shapes and sizes within the epidote-amphibolites.

No distinct horizon of the garnet epidote-amphibolites is present in the area but these occur as scattered patches within the epidote-amphibolite (Fig. 1). These patches are particularly confined to those places where later feldspathic veining is prominent. The development of garnet, at places in porphyroblast (up to 6cm in diameter) or in thin bands, is evident in a section at the base of Shergarh Sar where these rocks have a thrust contact with lower lying ultramafics. Here the heterogeneous banded or striped amphibolites clearly indicate the concentration of felsic and mafic minerals in alternate bands.

PETROGRAPHY

The Epidote-Amphibolites

In hand specimen the epidote-amphibolite appears as medium-to coarse-grained compact rock varying from dark green to light green colour. Hornblende, epidote and quartz are easily recongizable. The hornblende grains are dark gray in colour, usually less than 5mm in size, and have a well defined fabric. Their concentration form big clots which impart a dark colour to the rock. The epidote occur as elongated grains 1mm to 5mm long, generally following the fabric of the rock. Quartz along with other minerals is mostly concentrated in thin veins and lenses.

In thin sections, the epidote-amphibolites are medium to coarse-grained rocks having inequigranular porphyroblastic to subidioblastic texture. Majority of these rocks show a well developed fabric. In addition to the hornblende, epidote and quartz, as mentioned earlier, the other major constituents are chlorite, actinolite and ores. Clinopyroxene and plagioclase have also been noticed in few sections. Rutile, apatite and calcite occur as accessories.

Hornblende, homogeneously pleochroic, generally occur as green to dark green grains. Weakly developed zoning with a core of brownish green to green and a margin of light green to bluish green colour has also been noticed in certain sections. Hornblende in some thin sections show bluish green to green pleochroic colour and is usually found in association with actinolite and some time show alteration to actinolite along margins. Kink banding and pressure shadows are also common in some of the hornblende grains in these rocks.

Epidote occurs in two habits: (a) as long subhedral to anhedral crystal (max. size 4 x 2mm across) and (b) as small granular aggregates with highly birefringent interference colours. On the basis of

interference colours, zoning has been noticed in the type "a" epidote crystals, having cores displaying an anomalous bluish gray intereference colour and margins showing normal gray to yellow interference colour. In some cases an additional highly birefringent rim, surrounds the type "a" epidote. The type "a" epidote and hornblende both occur in close association and are intergrown with each other. Certain epidote-amphibolites are highly banded with the dark bands composed of type "a" epidote and hornblende and the white bands generally contain quartz and albite. Occasionally, the type "a" epidote occurs as "augen porphyroblast" surrounded by relatively finer grains of prismatic hornblende in such rocks.

Hornblende, in association with quartz, has been noticed in the core of some grains of type "a" epidote. The occurrence of type "a" epidote as core to hornblende crystals is, however, not uncommon. Some of the type "a" epidote and hornblende crystals poikelitically enclose quartz, ore (magnetite), rutile and apatite. Hornblende and quartz together also exhibit salt and pepper mesh type of intergrowth. Quartz also occurs interstitially as disseminated grains in the relatively less basic epidote amphibolites. These interstitial quartz grains are usually fractured and show undulose extinction due to deformation. Discontinuous microveins of quartz and carbonate have been noticed in certain thin sections. Clinopyroxene and plagioclase occur within the core of hornblende and type "a" epidote respectively. The plagioclase some time acquires dusty appearance. Clinopyroxene vary in proportion from trace to about 30% in different parts of the epidote-amphibolites. The amount of plagioclase also vary from trace amount to about 25%. In most part of the epidote-amphibolite, especially in the samples obtained from Qarghan Sar and Shergarh Sar, the plagioclase has been completely replaced probably by epidote and are/or hornblende. Actinolite along with chlorite and/or type "b" epidote occur as secondary alteration product of hornblende and type "a" epidote. The kink banding, indicating pressure shadows, are common in the actinolite flakes. A corona structure comprising a core of magnetite, a middle rim of chlorite and an outer rim of type "b" epidote has also been noticed in these rocks.

The Garnet Epidote-Amphibolites

These rocks are medium-to coarse-grained with granular mosaic to a banded texture in hand specimens. These are generally light green to dark-gray in colour and very commonly exhibit a reddish tint due to the development of garnet. The granular varieties clearly show amphiboles and elongated crystals of epidote, while the felsic material is randomly distributed. Garnet is concentrated in clusters but also occurs as porphyroblasts, with a maximum diameter of 6cm. Certain garnet epidote-amphibolites are locally banded with hornblende and epidote dominating the colour bands and felsic minerals dominating the light colour bands. Garnet is common to both the bands.

Mineralogically, the garnet epidote-amphibolites are similar to epidote-amphibolite except for the presence of garnet having lesser modal hornblende and epidote than the latter. In the non-banded amphibolites, garnet is found along the contact zones of epidote and hornblende and also form rim around them. The textural features clearly suggest the development of garnet at the expense of hornblende and epidote. A high proportion of quartz, surrounding garnet crystals and occupying microveins diverging from reaction spots, has been noticed. These features support the idea that SiO_2 was released during the formation of garnet in at least some cases.

GEOCHEMISTRY

Major and trace element analyses of 23 epidote-amphibolites and 6 garnet epidote-amphibolites are presented in Tables 1 and 2 along with C.I.P.W norms and Niggili's values. Major and trace elements have been determined by using pressed powder pellets on X-ray Fluorescence Spectrophotometer at the University of South Carolina, Columbia (USA). The FeO concentration was determined by titration, using ammonium metavenadate as described by Wilson (1960). The H_2O and CO_2 have been determined as loss on ignition by heating about one gram of powder sample at 1000^oC.

Table - 1 Major and trace element data along with C.I.P.W Norms and Niggli values for epidode-amphibolites from Shergarh Sar area.

SAMPLE NO.	ALK43A	ALK28	ALK10A	ALK139A	ALK47A	ALK1SA	ALK99A	ALK54A	ALK50A	ALK93A	ALK6A	ALK40	ALK46A	ALK53A	ALK33	ALK52A	ALK21	ALK8A	ALK37	ALK94A	ALK23	ALK46A	ALK9
SiO_2	52.88	57.29	42.51	46.06	50.97	42.68	54.38	49.79	44.15	47.09	49.80	48.18	53.65	52.97	46.60	49.93	47.24	45.17	47.47	50.05	46.97	52.32	52.63
TiO_2	0.72	0.71	1.06	1.33	0.62	0.94	0.75	0.98	0.77	0.55	0.36	0.68	0.70	0.50	1.34	0.59	0.74	0.73	0.69	0.67	0.85	0.67	0.85
Al_2O_3	14.58	14.79	14.81	12.88	14.55	13.66	14.23	14.19	14.81	15.79	14.12	15.49	14.38	15.26	15.43	14.44	14.49	14.48	14.23	15.30	14.92	14.48	14.92
Fe_2O_3	6.92	4.32	9.86	11.44	6.56	7.28	4.08	7.60	14.94	3.16	8.40	6.24	4.73	8.96	10.44	8.33	11.23	7.69	5.82	9.62	4.05	6.12	6.28
FeO	4.87	5.04	7.90	5.05	5.90	10.32	7.60	5.32	1.22	7.74	7.52	5.36	5.37	3.89	1.23	3.18	6.71	7.83	5.89	6.42	6.28	5.38	5.38
MnO	0.18	0.16	0.12	0.25	0.16	0.21	0.12	0.20	0.18	0.20	0.10	0.16	0.19	0.16	0.18	0.11	0.20	0.20	0.20	0.19	0.16	0.16	0.17
MgO	6.76	4.52	10.24	8.81	7.06	10.79	6.66	7.31	10.65	8.94	6.96	9.00	7.24	7.78	10.40	8.19	8.23	11.36	8.19	10.74	6.50	5.82	5.82
CaO	9.46	8.79	12.55	7.69	10.55	12.17	9.80	10.79	12.72	10.63	11.06	10.18	10.70	11.96	11.95	10.55	9.23	12.53	10.90	9.82	12.02	10.15	9.13
Na_2O	1.77	2.07	1.42	2.40	2.05	1.07	1.19	1.60	0.82	2.18	2.19	1.37	1.35	0.96	2.06	2.15	0.71	1.69	1.88	1.21	2.27	2.06	2.27
K_2O	0.03	0.57	0.04	0.93	0.04	0.03	0.03	0.06	0.03	0.06	0.10	0.03	0.05	0.03	0.03	0.06	0.13	0.02	0.04	0.03	0.02	0.06	0.07
P_2O_5	0.05	0.07	0.06	0.19	0.04	0.04	0.03	0.04	0.02	0.03	0.02	0.05	0.06	0.02	0.03	0.05	0.17	0.03	0.03	0.04	0.03	0.04	0.07
H_2O	0.10	0.00	0.10	0.12	0.10	0.06	0.10	0.00	0.10	0.00	0.05	0.03	0.03	0.10	0.09	0.00	0.00	0.09	0.00	0.06	0.09	0.04	0.09
I/L	2.18	1.82	1.20	2.32	1.78	1.25	2.36	1.97	0.56	1.45	1.49	2.03	1.94	1.65	1.89	1.75	1.65	2.57	2.89	1.30	2.90	1.81	1.81
TOTAL	100.50	100.15	101.59	99.47	100.40	101.09	98.35	100.73	100.89	100.63	99.28	100.90	99.14	100.98	99.94	99.70	99.71	100.06	99.67	100.53	99.73	99.73	99.35

Trace elements (ppm)

	ALK43A	ALK28	ALK10A	ALK139A	ALK47A	ALK1SA	ALK99A	ALK54A	ALK50A	ALK93A	ALK6A	ALK40	ALK46A	ALK53A	ALK33	ALK52A	ALK21	ALK8A	ALK37	ALK94A	ALK23	ALK46A	ALK9
Nb	6	10	6	21	3	5	4	3	7	3	8	2	5	3	12	3	11	5	9	7	9	5	6
Zr	30	52	1	83	22	26	47	22	38	59	42	21	49	75	43	11	41	10	41	22	49	66	41
Y	23	28	39	62	24	35	22	31	27	33	16	37	21	18	22	56	22	29	22	22	20	30	30
Sr	198	177	87	14	198	165	215	189	157	256	179	220	179	141	166	201	68	137	174	173	249	211	179
Rb	13	0	0	21	14	0	3	0	6	7	14	0	23	6	7	17	0	0	0	0	2	2	0
Ni	12	6	23	68	11	36	10	6	20	11	29	11	19	20	20	20	87	42	9	9	25	8	0
Cr	42	30	127	47	53	68	44	50	62	53	72	65	71	53	83	51	185	118	45	35	96	40	47
V	348	241	476	415	302	540	260	433	501	370	302	226	280	292	371	360	425	496	380	346	329	391	312
Sc	45	33	59	40	46	62	50	57	63	50	46	49	44	46	47	49	45	60	53	51	53	41	44
Ba	0	59	0	119	19	0	0	0	0	0	0	0	2	0	0	0	4	0	0	0	0	0	9
Zn	70	80	36	78	50	53	55	64	43	62	50	34	60	55	61	64	98	29	64	63	36	59	81
Cu	52	53	225	166	17	115	64	62	115	17	74	14	19	24	17	40	4	146	75	123	23	0	49
La	4	5	0	0	9	0	0	0	2	0	9	20	74	8	0	0	0	0	0	0	28	0	0
Ce	8	21	14	25	11	15	10	7	9	6	11	12	12	15	7	11	12	14	15	12	12	19	19

Table - 1 (Contd.)

C.I.P. Norms

Q	14.62	18.79	0.00	2.80	8.50	0.00	18.28	9.20	1.84	0.00	1.90	6.24	15.79	9.85	4.37	7.96	7.19	1.44	2.94	9.19	3.90	13.53	14.28
Or	0.18	3.43	0.24	5.67	0.24	0.18	0.19	0.18	0.12	0.12	0.60	0.31	0.30	7.03	0.36	0.48	0.79	0.12	0.12	0.18	0.00	0.12	0.43
Ab	15.23	17.79	9.44	20.91	17.59	9.07	10.49	13.69	6.91	18.58	18.93	12.03	11.54	11.17	8.19	17.76	18.72	6.13	14.67	16.42	10.31	11.36	17.40
An	32.29	29.84	35.12	22.26	30.80	33.96	33.17	31.81	36.52	30.76	33.67	37.34	32.66	30.39	37.73	32.76	21.21	36.86	32.68	32.01	33.64	37.02	32.41
Di	11.97	11.33	21.06	12.29	17.59	21.20	13.68	17.43	20.39	17.45	18.05	18.77	14.34	16.73	16.91	15.80	19.50	20.76	18.15	14.40	20.21	11.93	10.85
Wo	0.00	0.00	0.00	0.00	0.00	0.00	0.00	0.00	0.00	0.00	0.00	0.00	0.00	0.00	0.00	0.00	0.00	0.00	0.00	0.00	0.00	0.00	0.00
Hy	13.98	10.92	11.20	17.01	14.34	8.86	16.71	14.91	17.10	20.60	20.98	14.69	14.77	15.05	18.42	12.53	13.98	22.28	21.22	16.66	17.72	18.56	13.65
Ol	0.00	0.00	6.51	0.00	0.00	14.26	0.00	0.00	0.00	0.92	0.00	0.00	0.00	0.00	0.00	0.00	0.00	0.00	0.00	0.00	0.00	0.00	0.00
Mt	10.22	6.37	14.26	13.64	9.66	10.58	6.17	11.16	2.28	9.47	4.69	3.58	9.15	6.97	11.49	8.75	15.60	11.38	8.67	9.62	9.69	6.07	9.13
He	0.00	0.00	0.00	2.39	0.00	0.00	0.00	0.00	13.32	0.00	0.00	6.26	0.00	0.00	1.12	2.46	0.00	0.00	0.00	0.00	0.00	0.00	0.00
Il	1.93	1.37	2.05	2.60	1.20	1.79	1.15	1.44	1.46	1.88	1.07	0.71	1.31	0.77	1.15	1.36	2.62	0.97	1.44	1.43	1.39	1.32	1.66
Ap	0.11	0.16	0.13	0.43	0.09	0.09	0.16	0.18	0.07	0.22	0.11	0.07	0.13	0.04	0.07	0.11	0.38	0.07	0.11	0.09	0.18	0.09	0.20

Niggli Values

al	132.25	164.44	80.65	102.48	120.03	80.79	145.83	114.04	85.74	99.93	115.16	108.90	133.10	131.39	95.96	116.16	105.93	90.29	105.05	120.23	96.35	133.26	135.83
al	21.45	24.97	16.53	16.86	20.16	15.83	21.55	19.12	16.92	18.47	21.48	20.59	20.61	20.98	18.69	20.88	14.81	16.98	18.85	20.48	17.17	22.92	22.65
fm	48.87	41.20	55.86	58.32	48.49	57.52	47.16	50.81	55.05	52.85	46.02	47.37	49.01	47.17	52.95	48.06	58.16	54.79	51.66	49.83	54.01	46.14	46.32
c	25.35	27.03	25.51	18.33	26.62	24.66	28.16	26.48	26.47	24.17	27.45	28.96	27.06	28.42	26.37	26.30	22.18	26.83	25.84	25.28	26.42	27.70	25.25
alk	4.33	6.79	2.10	6.49	4.73	1.99	3.14	3.59	1.57	4.50	5.05	3.07	3.32	3.42	1.99	4.76	4.85	1.40	3.65	4.42	2.40	3.24	5.78
k	0.01	0.015	0.20	0.01	0.02	0.02	0.01	0.02	0.01	0.03	0.02	0.02	0.09	0.04	0.02	0.04	0.02	0.01	0.01	0.00	0.01	0.02	0.02
mg	0.52	0.47	0.52	0.50	0.52	0.53	0.57	0.49	0.56	0.54	0.56	0.64	0.53	0.47	0.61	0.56	0.48	0.62	0.53	0.52	0.61	0.54	0.49

Sample No. ALK43A, AIK139A, ALK54A, ALK40, ALK33, ALK58A, and ALK86A are the banded amphibolites.

Table 2 Major and Trace element data along with C.I.P.W Norms and Niggli values for garnet epidote-amphibolites from Shergarh sar area.

SAMPLE No.	ALK98A	ALK49A	ALK8	ALK97A	ALK92	ALK80	ALK88A
SiO_2	44.17	57.73	48.05	45.94	44.18	46.17	52.12
TiO_2	0.97	0.71	0.83	1.05	0.91	0.13	1.32
Al_2O_3	14.18	15.84	13.22	14.47	15.84	12.67	16.52
Fe_2O_3	5.27	1.42	5.81	5.33	6.04	4.54	3.82
FeO	10.37	6.35	11.11	9.35	7.37	7.89	7.86
MnO	0.25	0.25	0.30	0.21	0.25	0.16	0.21
MgO	10.13	3.43	9.30	8.72	11.57	16.88	6.32
CaO	12.13	8.69	9.60	11.32	11.26	10.08	8.94
Na_2O	0.81	2.95	1.11	1.47	0.74	0.85	0.77
K_2O	0.02	0.09	0.05	0.03	0.05	0.05	0.00
P_2O_5	0.05	0.25	0.07	0.16	0.03	0.03	0.06
H_2O	0.10	0.00	0.08	0.11	0.02	0.00	0.00
Ig Loss	1.84	1.86	1.69	2.77	1.78	0.88	1.80
TOTAL	100.29	99.57	101.22	100.93	100.04	100.31	99.79

Trace elements (ppm)

Nb	2	1	3	5	6	11	4
Zr	24	29	17	26	24	15	21
Y	40	17	41	37	29	30	34
Sr	133	243	64	203	180	23	210
Rb	5	4	12	4	0	2	3
Ni	18	11	24	11	13	201	16
Cr	98	37	64	71	66	116	48
V	493	136	409	292	413	85	389
Sc	64	31	60	46	50	29	58
Ba	31	0	0	0	0	0	0
Zn	45	78	56	55	28	0	46
Cu	114	36	32	67	8	26	38
La	0	0	0	0	0	31	0
Ce	11	10	15	15	6	10	11

C.I.P.W Norms

Q	0	15.67	3.92	0.05	0	0	15.66
Or	0.12	0.54	0.3	0.18	0.3	0.03	0
Ab	6.95	25.52	9.43	12.67	6.37	7.25	6.64
An	35.54	30.38	31.08	33.42	40.42	30.84	42.43
Di	20.54	10.06	13.34	18.50	12.96	15.45	2.21
Wo	0	0	0	0	0	0	0
Hy	20.57	13.77	31.72	24.91	24.98	23.43	24.71
Ol	6.51	0	0	0	4.24	15.77	0
Mt	7.77	2.11	8.47	7.88	8.91	6.64	5.65
He	0	0	0	0	0	0	0
Il	1.87	1.38	1.59	2.04	1.76	0.25	2.56
Ap	0.11	0.56	0.15	0.36	0.07	0.07	0.13

Niggli Values

si	88.54	173.61	102.17	98.17	87.71	84.91	133.25
al	16.72	28.02	16.60	18.19	18.50	13.71	24.84
fm	55.63	35.22	59.13	52.81	56.06	64.86	48.76
c	26.05	28.00	21.84	25.92	23.95	19.86	24.49
alk	1.60	8.76	2.43	3.08	1.49	1.57	1.91
k	0.02	0.02	0.05	0.01	0.04	0.04	0.00
mg	0.55	0.44	0.50	0.53	0.61	0.72	0.50

Table 3 Comparison of the average major and trace elements data of garnet free and garnet bearing epidote-amphibolites from Sharegarh Sar area.

	1	2
SiO_2	49.16	48.34
TiO_2	0.75	0.85
Al_2O_3	14.47	14.68
Fe_2O_3	7.37	4.60
FeO	5.53	8.61
MnO	0.17	0.23
MgO	8.20	9.48
CaO	10.67	10.43
Na_2O	1.60	1.24
K_2O	0.15	0.04
P_2O_5	0.06	0.09
Ig. Loss	1.88	1.80
Trace elements (ppm)		
Nb	7	5
Zr	38	22
Y	29	33
Sr	171	151
Rb	7	4
Ni	22	42
Cr	68	71
V	363	317
Sc	49	48
Ba	9	4
Zn	57	44
Cu	73	46
La	2	4
Ce	13	11
Fe_3+/Fe_2+	1.21	0.49

1. Average epidote amphibolites.
2. Average garnet epidote amphibolites.

Table 4- Average major and trace elements (ppm) of Shergarh Sar amphibolites and tholeitic basalt of various tectonic environment.

	1	2	3	4
SiO_2	48.97	51.57	50.59	50.45
TiO_2	0.77	0.80	1.05	3.73
A_2O_3	14.52	15.91	16.29	14.17
Fe_2O_3	7.02	2.74	3.66	0.00
FeO	5.95	7.04	5.08	11.55*
MnO	0.19	0.17	0.17	0.23
MgO	8.50	6.73	8.96	7.77
CaO	10.58	11.74	9.50	11.49
Na_2O	1.51	2.41	2.89	2.15
K_2O	0.09	0.44	1.07	0.06
P_2O_5	0.06	0.11	0.28	0.00
Trace elements (ppm)				
Zr	34	70	100	94
Sr	167	200	330	63
Rb	6	5	10	1
Ni	27	30	25	70
Cr	69	50	40	165
V	353	270	255	460
Ba	8	75	115	11

1. Average Shergarh Sar amphibolites.
2. Average island arc tholeities Jakes and White, 1971.
3. Average island arc calc-alkaline. basalt (Jakes and White, 1971).
4. Lavas of MORB (Prift and Fornari, 1983)

* Total iron as FeO.
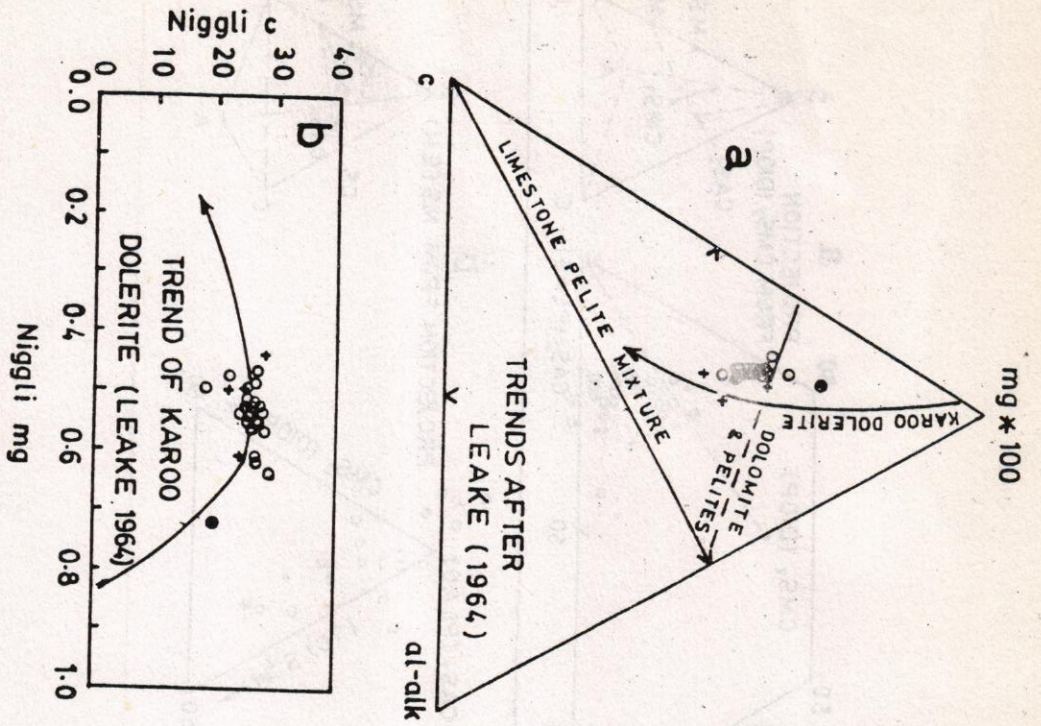
Fig.2 (a) Nigglic-mg100-(al-alk) plot of the Shergarh Sar amphibolites.

(b) Niggli c vs mg plot of the Shergarh Sar amphibolites. Various fields are after Leake, 1964. Samples shown by empty circles are epidote-amphibolite, while crosses and filled circle represent epidote-amphibolite and more basic garnet garnet epidote-amphibolite and more basic garnet epidote amphibolite (hornblendite) respectively.
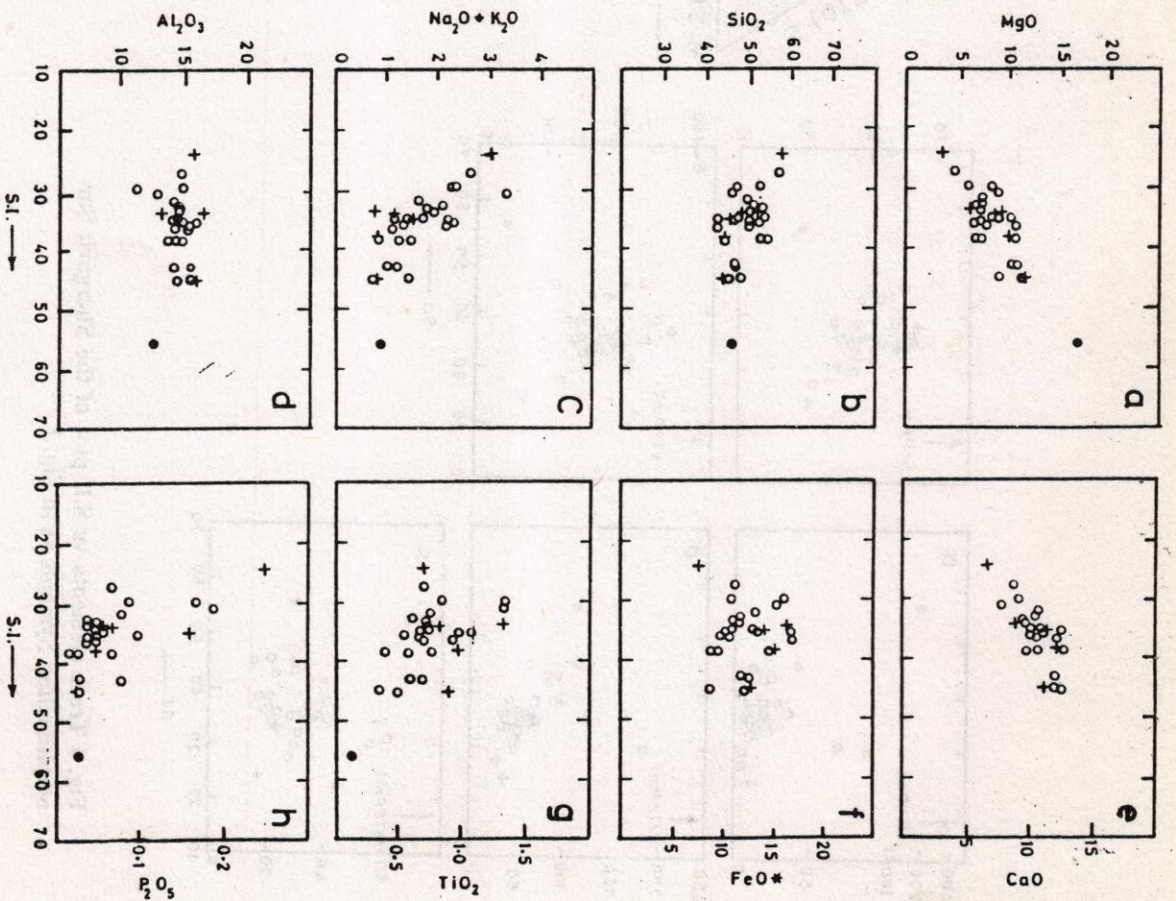
Fig. 3 Oxides vs S.I. plot of the Shergarh Sar amphibolites. Symbols as in Fig. 2.
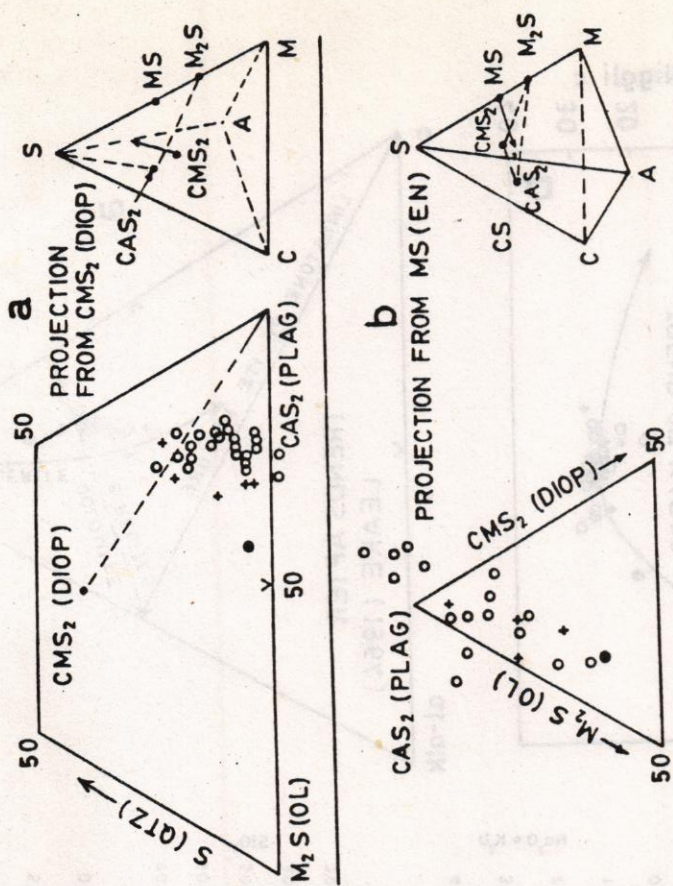
Fig. 5 Plots of Shergarh Sar amphibolites within CMAS projections. Symbols as in Fig. 2.
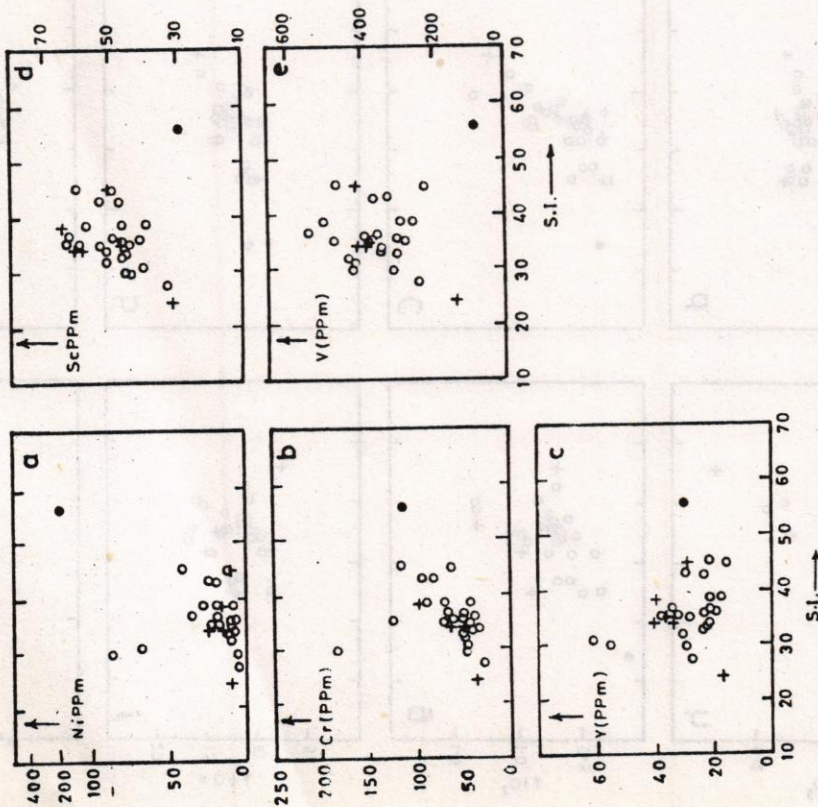
Fig. 4 Trace elements vs S.I. plot of the Shergarh Sar amphibolites. Symbols as in Fig. 2.

Amphibolite's Protolith

Evens and Leake (1960) and Leake (1964) used various major and trace elements to differentiate the igneous and sediments derived amphibolites. The Niggili's values listed in Tables 1 and 2 are, therefore, employed as genetic indicator on the diagrams of Evans and Leake (1960) and Leake (1964). Igneous nature of the parent material for both the banded and non-banded amphibolites from Shergarh Sar is indicated by the variation trends of their analyses on c-mg-(al-alk) and c vs mg diagrams in Fig. 2. In both these diagrams the studied amphibolites follow the magmatic trend represented by the middle stage differentiation of Karroo dolerites of South Africa. It further suggest that the clinopyroxene and calcic-plagioclase were probably the dominant phases during crystallization (see Leake, 1964). It is now clear from these diagrams that the banded and non-banded amphibolites of the Shergarh Sar area are following the igneous trend. Previously the banded structures and association of sedimentary rocks with the amphibolites were considered as evidence of sedimentary origin of certain amphibolites (Poldervaart, 1953). Later studies disprove these evidences to be conclusive. The banded appearance of the amphibolites under discussion can, however, be assigned to the process of metamorphic segregation or shearing (see Evans and Leake, 1960; Orville, 1969).

Major and Trace Elements Chemistry

The distinctive chemical features, of both the garnetiferous and non-garnetiferous amphibolites, are the small variations within the major and trace elements abundances. Some of the major elements have the following characteristics, wide range of SiO_2 (42-47%), low K_2O (0.15% on average) and low contents of TiO_2 (1.34%) and P_2O_5 (0.25 %). The average data of the epidote-amphibolites and garnet epidote-amphibolites are matching well (Table 3). There is, however, an average 1% decrease in SiO_2 and about 1% increase in MgO in the garnetiferous amphibolites. The average total iron remains approximately the same in both the amphibolites. A significant increase in FeO has, however, been noticed in garnet bearing amphibolites. Major elements variation plots in Fig. 3 display well defined variation trends with changes in the solidification index (S.I., 100 MgO/MgO + FeO + Fe_2O_3 + Na_2O; Kuno, 1959) and further confirm the magmatic character of the amphibolite protolith. The gap between S.I. 46 to 55 is probably due to incomplete sampling.

Among the major oxides, MgO (Fig. 3a) exhibit a well defined positive correlation while SiO_2 (Fig. 3b) and alkalies (Fig. 3c) show a negative correlation when plotted against S.I. This reflects the separation of ferromagnesian minerals from magma during crystallization. Al_2O_3 (Fig. 3d) remains more or less constant, indicating the separation of alumina-bearing and alumina free phases in a 1:1 ratio during fractionation. On the other hand, CaO (Fig. 3e) initially shows an increase in the S.I. range of 56-45, followed by a platue of 12% CaO in the S.I. range of 45-38 and a subsequent sharp decrease afterward with decreasing S.I. Assuming crystallization under low PH_2O (most probably volcanic), such Ca variation trends can be attributed to the control of olivine and/or orthopyroxene in the early stages of fractionation followed by a dominant control of clinopyroxene together with plagioclase in the later stages. FeO vs S.I. plots (Fig. 3f) are generally scattered but the overall trend reflects negative correlation in the early stages (S.I. 56-35) followed by a positive correlation. Similar behaviour is also indicated by the TiO_2 vs S.I. plot (Fig. 3g). An early build up of FeO^* and TiO_2 in magma followed by their fall due to crystallization of ilmenite and/or titanomagnetite at the late stage may be considered responsible for development of such trend. Like SiO_2, P_2O_5 (Fig. 3h) also exhibits a vague negative correlation, indicating that apatite did not play any significant role during the fractionation history of the suite.

The trace elements variations within amphibolites of Shergarh Sar, reflect magmatic differentiation and the control of ferromagnesian minerals in the early stages. Except for the three samples of epidote-amphibolites (indicating exceptionally variably high Ni, Cr and Y), Ni (Fig. 4a) and Cr (Fig. 4b) behave compatibly and show a positive correlation with S.I. analogous to MgO vs S.I. variation. This supports olivine/orthopyroxene and clinopyroxene fractionation in the early stages. Similarly Y (Fig. 4c) shows a limited range of variation analogous to that of Al_2O_3 (Fig. 3d) and signifies plagioclase fractionation. Sc and V vs S.I. plots (Figs. 4d, e) are generally similar to those of FeO^* and CaO vs S.I. (Figs. 3f, e). Sc is preferred by orthopyroxene than by olivine (Mason and Moor, 1982 p. 132) whereas V usually follows Fe_2O_3 distribution. Therefore, the less Sc in the most basic garnet epidote-amphibolites (Table 1, Alk 80) support the fractionation of olivine instead of orthopyroxene in the very initial stage whereas the general variation of both Sc and V confirm clinopyroxene as the major fractionating phase.

CMAS Plots

The data was also plotted into the CMAS tetrahedron model of O'Hara (1976) to confirm the magmatic fractionation history revealed by the oxide vs S.I. plots. In a projection from CMS_2 into $S-M_2S-CAS_2$ (Fig. 5a) the general trend of the studied amphibolites cross cut the $Diop-CAS_2$ join but is showing more affinity towards CAS_2. This indicates plagioclase and clinopyroxene fractionation with the former mineral dominating over the latter on liquidus. The greater affinity of the most basic garnet epidote-amphibolite/horblendite (sample Alk 80) towards ol-apex points to the fractionaiton (accumulation in this particular sample) of olivine in the earliest stage. Similarly in a projection from MS into $CAS_2-M_2S-CMS_2$ (Fig. 5b) plane, majority of the points lie close to the CAS_2 apex on a trend parallel to M_2S-CAS_2 join and confirm the interpretation obtained from the previous projection.

Magmatic Affinity and Tectonic Environment

Various established discrimination diagrams have been used for the studied rocks to know their magmatic affinity and tectonic environment. On alkalis and Ni vs SiO_2 diagrams majority of the rocks plot in the fields shown for tholeiitic rocks whereas on AFM diagram the data also follow the trend of the tholeiitic series (Figs. 6a, b, c). It is not sure whether Sr remained immobile during metamorphism in studied amphibolites but when plotted on Ti-Zr-Sr discrimination diagram, majority of the data of these amphibolites are still akin to the field of island arc basalts (Fig. 6d). On Ti vs Zr Plot, these data cluster within or near the overlapping field of arc lavas and mid-oceanic ridge basalts (MORB, Fig. 6e). Majority of the data points also occupy the field of ocean island rocks on the $FeO-MgO-Al_2O_3$ plot of Pearce (1977; Fig. 6j). The average major and trace elements data of the studied amphibolites is compared with basaltic composition from various environment in Table 4. These amphibolites show a greater correspondence to the island arc tholeiites than to calc-alkali basalts (CAB) or MORB. Any significant difference (relatively low SiO_2, K_2O, High FeO^* and MgO) can be related to the limited mobility of elements with larger ionic radii during metamorphism. On the basis of very low K_2O (generally less then 0.1%) these amphibolites can be classified as very low K-tholeiites.

DISCUSSION

Amphibolites cover a considerable horizon along

MMT in the KIA. Both the volcanic and plutonic features, including pillow structures and cumulate layering and texture have been noticed at several localities (pillow lavas at Mahak; M.Q. Jan Personal communication). The chemistry of the Allai amphibolites provide sufficient evidence for these being the product of an arc type tholeiitic parent liquid. It also suggests that the banding in these amphibolites is not a sedimentary feature but probably a product of volcanic layering or metamorphic segregation/shearing (Evans and Leake, 1960; orville, 1969). These features together with the development of green to dark green hornblende, and type "a" epidote indicate that epidote-amphibolite facies conditions prevailed for a considerable time. If the relics clinopyroxene and plagioclase are considered as the original igneous assemblage, then the parent rock for epidote-amphibolite was presumably of gabbroic to dioritic/andesitic composition and these two minerals were probably the dominant liquidus phases.

Opaque grains generally occurring in the core of hornblende may represent primary magnetite or its metamorphic equivalent, as epidote-amphibolites are considerably rich in normative magnetite. The rutile noticed in several epidote-amphibolites seems to be the metamorphic product, most probably developed at the expense of TiO_2, released by magnetite. This interpretation is supported by the close association of rutile with the opaque grains.

The occurrence of type "b" epidote in association with chlorite/actinolite and their development at the expense of type "a" epidote and hornblende, signify the establishment of greenschist facies environment after the prevalence of the epidote-amphibolite conditions. The presence of kink banding and the development of schistosity, indicate that these amphibolites have been subjected to great shear and stress conditions.

The evolutionary pattern, established on the basis of the study of mineral assemblages in epidote-amphibolites, show localized retrogressive metamorphic conditions. This interpretation is supported by the zoning observed in hornblende and type "a" epidote. Variations in colour of the large hornblende grains and type "a" epidote from core towards margin favour a decrease in metamorphic grade from high grade epidote-amphibolite facies to low grade epidote-amphibolite facies (Miyashiro, 1973, P-254 and 249). The highly birefringent outer most rim, noticed around certain type "a" epidote may correspond to type "b" epidote in order of development and thus related to greenschist facies. All these teatures exhibit
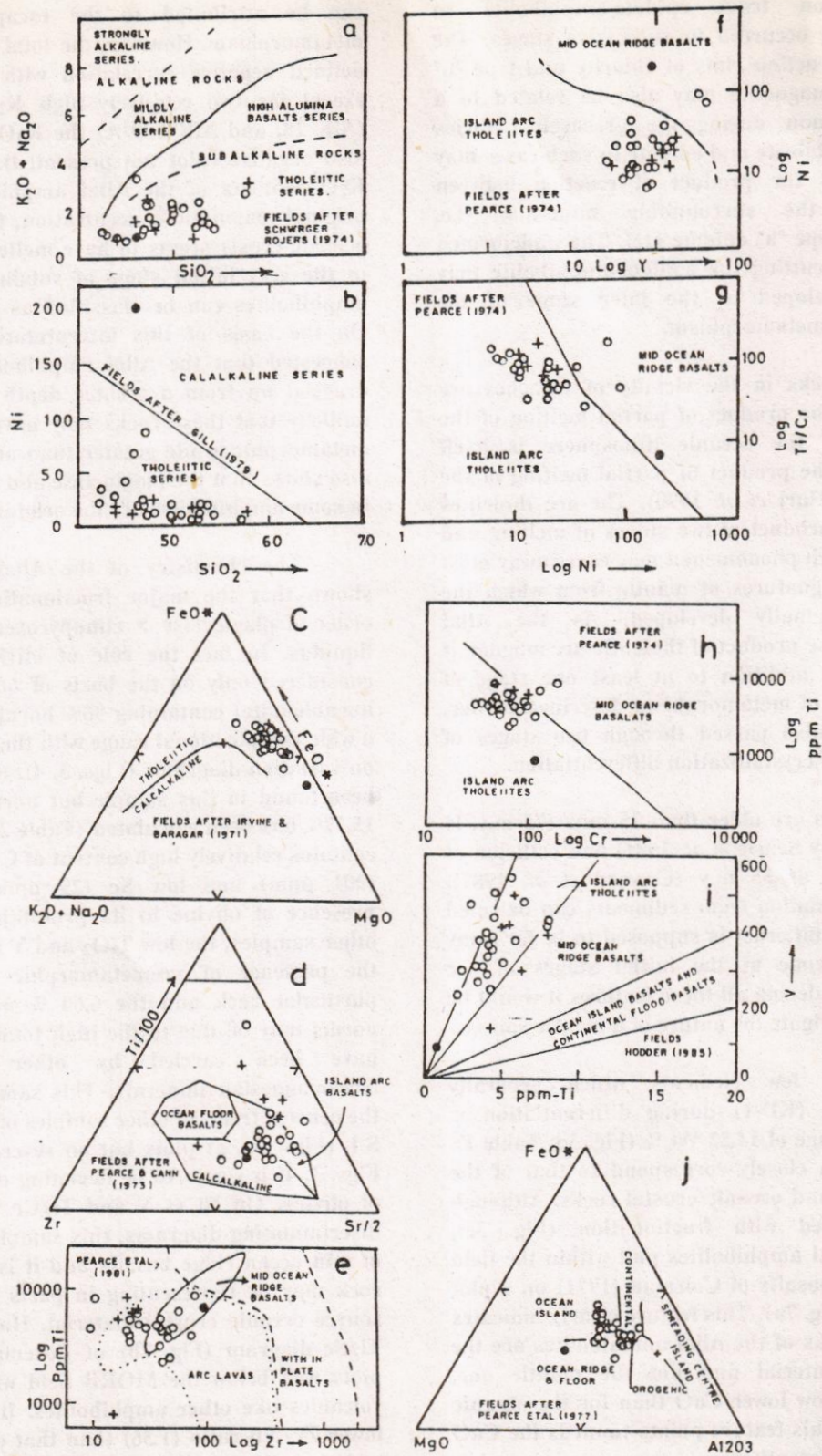
Fig. 6 Shergarh Sar amphibolite data within various discrimination diagrams:
a. Total alkalies vs SiO₂ b. Ni vs SiO₂ c. AFM d. Zr-Ti/100-Sr/2 e. Ti vs Zr f. Ni vs Y g. T/Cr vs Ni h. Ti vs Cr i. V Vs Ti j. FeO* - MgO - Al₂O₃ Symbols as in Fig. 2. * = total iron expressed as FeO.

that retrogression from epidote-amphibolite to greenschist facies occurred in successive stages. The development of reaction rims of chlorite and type "b" epidote around magnetite may also be related to a similar phenomenon during the greenschist facies metamorphism. Chlorite and epidote in such cases may be considered as the product of reaction between magnetite and the surrounding minerals, (i.e. hornblende and type "a" epidote etc). The undeformed microveins cross cutting the epidote-amphibolite may probably be developed at the later stage of the greenschist facies metamorphism.

Volcanic rocks in the vicinity of trenches are considered to be the product of partial melting of the upper portion of the oceanic lithosphere is itself considered to be the product of partial melting of the depleted mantle (Hart *et al.* 1970). The arc tholeiites are generally the product of two stages of melting and differentiation. Such phenomenon may carry away most of the chemical signatures of mantle from which the magma was originally developed. As the Allai amphibolites are the product of tholeiitic arc magma, it is obvious that in addition to at least one stage of amphibolite facies of metamorphism described earlier, these rocks have also passed through two stages of partial melting and crystallization differentiation.

Amphibolites are older than 75 m.y. (75 m.y. is metamorphic age by Searle *et al.* 1981) and collision of the KIA occurred at 55 m.y (Coward *et al.* 1987). Therefore, contamination from sediments can be ruled out as the continental crust is supposed to be far away from the suture zone at the initial stages of arc construction. Considering all these features it would be unrealistic to investigate the nature of a mantle source.

Among the few elements which generally remained constant (KD-1) during differentiation is Al_2O_3 with an average of 14.52 Wt % (Fig. 3d; Table 1). This average Al_2O_3 closely correspond to that of the ophiolitic, MORB and oceanic crustal rocks. Although CaO has decreased with fractionation (Fig. 3e), majority of the Allai amphibolites plot within the field of oceanic crustal basalts of Coleman (1971) on a plot of CaO vs Al_2O_3 (Fig. 7a). This feature clearly indicates that the source rocks of the Allai amphibolites are the oceanic crustal material and not the mantle one. Certain samples show lower CaO than for the oceanic basalts in Fig 7a. This feature points towards the CaO depletion due to differentiation.

The very low K_2O content of the Allai amphibolites (mean 0.09%; i.e less than low-K-tholeiite)

can be attributed to the escape of K_2O during metamorphism. However, the total alkali display a well defined negative correlation with S.I. (Fig. 3c) and except for two relatively high K_2O bearing samples (AlK 28, and AlK 139 A) the K_2O vs S.I. variation is also negative (plot not presented). If we consider the K_2O contents of the Allai amphibolites close to the original magmatic concentration, then the source (i.e. oceanic crust) seems to have melted at a shallow level in the very initial stage of subduction and the Allai amphibolites can be classified as early arc tholeiites. On the basis of this interpretation, it can also be suggested that the Allai amphibolites have not been dragged up from a greater depth and thus it seems unlikely that these rocks may have passed through a metamorphic grade greater than amphibolite facies. It also shows that the plagioclase and clinopyroxene relics in some amphibolites are the original igneous phases.

The chemistry of the Allai amphibolites has shown that the major fractionating phases were in order of plagioclase > clinopyroxene > olivine on the liquidus. In fact the role of olivine fractionation is considered only on the basis of one sample (AlK 80: hornblendite) containing 90% hornblende and showing a wide compositional range with the rest of the samples on variation diagrams (Figs. 3, 4). Relic olivine has not been found in this sample but normative olivine upto 15.77% has been calculated (Table 2). This sample also contains relatively high content of Cr (116 ppm) and Ni (201 ppm) and low Sc (29 ppm), supporting the presence of olivine in its protolith. As compared to other samples, the low TiO_2 and V in AlK 80 rules out the presence of premetamorphic magnetite in this particular rock and the 6.64 % magnetite shown in norms may be due to the high total iron which might have been carried by other pre-metamorphic ferromagnesian minerals. This sample is in line with the general trend of other samples on MgO and TiO_2 vs S.I. (Figs. 3a, g) plots but on several other plots (e.g. Figs. 3, 4) it seems to be deviating due to the presence of olivine. On Ni vs Y and Ti/Cr vs Ni (Figs. 6f, g) discriminating diagrams, this sample plots in the field of mid ocean ridge basalts and it is possible that this rock may be representing in parts or as a whole the source oceanic crustal material. However, on Ti/V vs Ti/Sc diagram (Fig. 7b) of Roseman *et al.* (1982) it plots well below the MORB field with boninite series volcanics like other amphibolites. It also shows much lower Zr/NB ratio (1.36) than that of the MORBS (37 ppm), corresponding to that of the mean Allai amphibolites (5.23). Therefore, the higher Ni concentration can be attributed merely to olivine accumulation due to crystallization differentiation and

this rock may be in parts representing a mixture of cumulate and residual or parent liquid. It also shows that the parent liquid for Allai amphibolites was at least less basic than this particular horblendite.

Ultramafic rocks and lavas have been reported from the contact zone of amphibolites and continental rocks in the Allai Area (Shah & Majid, 1985; Shah, 1986). Petrographic and geochemical data has shown that the lavas are of island arc tholeiitic type whereas the ultramafic rocks are considered to be of ophiolitic nature (Shah, 1986). Detailed isotopic/geochronological study is needed to be carried out for volcanic/ ultramafic rocks and Allai amphibolites for genetic comparison.
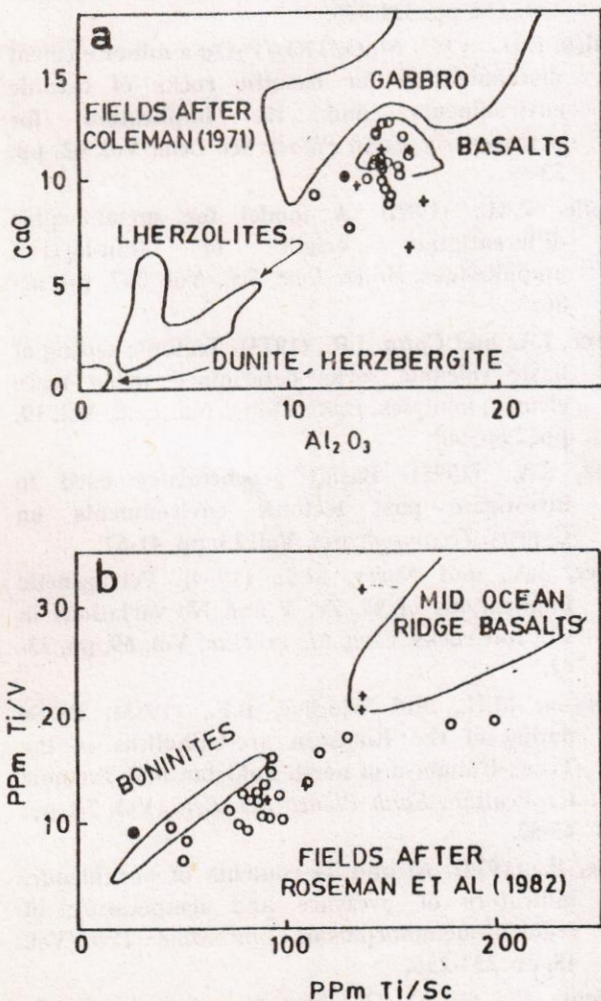
Fig. 7 Shergarh Sar amphibolite data within the discrimination diagrams of Coleman (1971) and Roseman et at. (1982). Symbols as in Fig. 2.

CONCLUSIONS

The Shergarh Sar amphibolites are derivatives from a basic parent produced by crystallization differentiation of an early low-K-tholeiitic magma. Plagioclase > clinopyroxene > olivine fractionation played a role in the evolution of igneous crystallization trend of these amphibolites. Magnetite also accompanied plagioclase and clinopyroxene. Amphibolite grade metamorphism prevailed for a considerable time to reorganize the petrographic and textural features of the suite which was followed by a greenschist facies metamorphism indicating limited retrogression. The source rock of the magma/lava from which amphibolites have been derived was probably of oceanic crustal composition.

REFERENCES

Andrew-Speed, C.P., and Brookfield, M.E., (1982). Middle Paleozoic to Cenozoic geology and tectonic evolution of the northwestern Himalaya. *Tectonophysics*, Vol. 82, pp. 253-275.

Bard, J.P., (1983). Metamorphic evolution of an obducted island arc: example of the Kohistan sequence (Pakistan) in the Himalayan collided range. *Geol. Bull. Univ. Peshawar, Pakistan*, Vol. 16, pp. 105-184.

Clark, M.D., (1979). Geology of the older Precambrian rocks of the Gran canyon, III. Petrology of mafic schists and amphibolites. *Precamb. Res.*, Vol. 8, pp. 277-302.

Coward, MP., Jan, M.Q., Rex, D., Tarney, J., Thirlwall, M., and Windley, B.F., (1982). Geotectonic framework of the Himalayas of N. Pakistan *Jour. Geol. Soc. London*, Vol. 139. pp. 299-308.

Coward, MP., Windley, B.F., Broughton, R., Luff, I.W., Patterson, M.G., Pudsey, C., Rex, D., and Khan M.A., (1986). Collision tectonics in N.W. Himalayas. In "Collision Tectonics" (Coward, M.P and Ries, A, ed.), *Geol. Soc. London*, Special Publication, Vol. 19, pp. 203-219.

Coward, MP., Butler, R.W.H., Khan, M.A., and Knip, R. J., (1987). The tectonic history of Kohistan and its implication for Himalayan structure *Jour.*

Geol. Soc. London, Vol. 144, pp. 377-391.

Coleman, R.G., (1971). Plate tectonic emplacement of upper mantle peridotite along continental edge. *Jour. Geophy. Res.,* Vol. 76, pp. 1212-1222.

Evans, B.K., and Leake, B.E., (1960). The composition and origin of the striped amphibolites of Connemara, Ireland. *Jour. Petrol.,* Vol. 1, pp. 337-363.

Floyd, P.A., and Winchester, J.A., (1978). Identification and discrimination of altered and metamorphosed volcanic rocks using immobile elements. *Chem. Geol.,* Vol. 21, pp. 291-306.

Gansser, A., (1980). The significance of the Himalayan suture zone. *Tectonophysics,* Vol. 62, pp. 37-52.

Hart, S.R., Brook, C., Krogh, T.E., Davis, G.H., and Nava, D., (1970). Ancient and modern volcanic rocks: A trace element model. *Earth Planet. Sci. Lett.,* Vol. 10, pp. 17-28.

Hodder, A.P.W., (1985). Depth of origin of basalts inferred from Ti/V ratios and a comparison with the K_2O depth relationship for island arc volcanics. *Chem. Geol.,* Vol. 48, pp. 3-16.

Irvine, T.N., and Baragar, W.R.A., (1971). A guide to the classification of the common volcanic rocks. *Canadian Jour. Earth. Sci.,* Vol. 8, pp. 523-549.

Jan, M.Q., (1979). Petrology of the obducted mafic and ultramafic metamorphites from the southern part of the Kohistan island arc sequence. *Geol. Bull. Univ. Peshawar, Pakistan,* Vol. 13, pp. 95-107.

Jan, M.Q., and Hawie, R.A., (1981). The mineralogy and geochemistry of the metamorphosed basic and ultrabasic rocks of the Jijal Complex, Kohistan, NW Pakistan. *Jour. Petrol.,* Vol. 22, pp. 85-126.

Jan, M.Q., and Khan Asif, M., (1983). Geochemistry of tonalites and (quartz) diorites of the Kohistan Ladakh (Transhimalayan) granite belt in Swat, N.W. Pakistan. In: "Granite of Himalaya, Karakoram and Hindukush" (F.A. Shams, ed.), *Inst. Geol. Punjab Univ. Lahore, Pakistan.*

Jan, M.Q., Khattak, M.U.K., Parvez, M.K., and Windley, B.F., (1984). The Chilas stratiform complex: Field and mineralogical aspects. *Geol. Bull. Univ. Peshawar, Pakistan,* Vol. 17, pp. 153-169.

Jan, M.Q., (1988). Geochemistry of amphibolites from the southern part of the Kohistan arc, N. Pakistan. *Mineral. Mag.* Vol. 52, pp. 147-159.

Jakes, P., and White. A.J.R., (1971). Composition of island arc and continental growth. *Earth Planet. Sci. Lett.,* Vol. 12 pp. 224-230.

Klootwijk, C., Sherma, M.L., Gergan, J., Tirkey, B.,

Shah, S.K., and Angrawal, V., (1979). The extent of greater India, II. Paleomagnetic data from the Ladakh intrusive at Kargil north western Himalayas. *Earth Planet. Sci. Lett.,* Vol. 44, pp. 47-46.

Kuno, H., (1959). Origin of Cenozoic petrogenic origin of Japan and surrounding areas. *Bull. Volcan. Series,* Vol. II, pp. 37-76.

Leake, (1964). The chemical distinction between ortho and para amphibolites. *Jour. Petrol.* Vol. 5, pp. 238-254.

Mason, B., And Moor, C.B., (1982) Principals of Geochemistry. John Wiley & Sons, New York.

Miyashiro, A., (1973). Metamorphism and metamorphic belts George Allen and Unwin Ltd., London, pp. 249 and 254.

Miyashiro, A., (1974). Volcanic rock series in island arc and active continental margin. *Amer. Jour. Sci.,* Vol. 274, pp. 321-355.

Mullen, E.D., (1983) $MnO/TiO_2/P_2O_5$: a minor element discrimination for basaltic rocks of oceanic environments and its implication for petrogenesis. *Earth Planet. Sci. Lett.,* Vol. 62, pp. 53-62.

Orville, P.M., (1969). A model for metamorphic differentiation origin of thin-layered amphibolites. *Amer. Jour. Sci.,* Vol. 267, pp. 62-86.

Pearce, J.A., and Cann, J.R., (1973). Tectonic setting of basic volcanic rocks determined using trace element analyses. *Earth Planet. Sci. Lett.,* Vol. 19, pp. 290-300.

Peace, J.A., (1975). Basalt geochemistry used to investigate past tectonic environments on Cyprus. *Tectonophysics,* Vol. 25, pp. 41-67.

Pearce, J.A., and Norry, M.J., (1979). Petrogenetic implications of Ti, Zr, Y and Nb variations in volcanic rocks. *Cont. Miner. Petr.,* Vol. 69, pp. 33-47.

Petterson, M.G., and Windley, B.F., (1985). Rb-Sr dating of the Kohistan arc-batholiths in the Trans-Himalaya of north Pakistan and Tectonic implication. *Earth Planet. Sci. Lett.,* Vol. 74, pp. 45-57.

Raase, P., (1974). Al and Ti contents of hornblende, indicators of pressure and temperature of regional metamorphism. *Contr. Miner. Petr.,* Vol. 45, pp. 231-236.

Rivalenti, G., (1976). Geochemistry of metavolcanic amphibolites from the south-west Greenland, Inc: B.F. Windley (ed), The Early History of the Earth. Proceedings of a Nato Advanced Study

Institute, John Wiley, New York, N.Y, pp. 213-223.

Roseman, L.K., and Frederick, A.F., (1982) Geochemical characteristics of boninites series volcanics: implications for their source. *Geochemica et Cosmochemica Acta,* Vol. 46, pp. 2099-2115.

Sheraton, J.W., (1984). Chemical changes associated with high-grade metamorphism of mafic rocks in the east Antarctic Shield. *Chem. Geol.* Vol. 47, pp. 135-157.

Sighinolfi, G.P., and Goroni, C., (1978). Chemical evolution of high- grade metamorphic rocks-anatexis and remotion of material from granulite terrane. *Chem. Geol.* Vol. 22, pp. 157-176.

Searle, M.P., Windley, B.F., Coward, M.P., Cooper, D. J. W., Rex, D.C., Tingdong, L., Xuchang, X., Jan. M.Q., Thakur, V.C., and Kumar, S., (1987). The closing of Tethys and the tectonics of the Himalaya. *Geol. Soci. Amer. Bull.,* Vol. 98, pp. 678-701.

Shah, M.T., (1986). Petrochemistry of the rocks from Shergarh Sar area, Allai Kohistan, Northern Pakistan (M. Phil thesis) *Univ. Peshawar, Pakistan,* p. 5.

Shah, M.T., and Majid M., (1985). Major and trace element variations in the lavas of Shergarh Sar area and their significance with respect to the Kohistan tectonic anomaly. *Geol. Univ. Peshawar, Pakistan,* Vol. 18, pp. 163-188.

Tahirkheli, R.A.K., and Jan, M.Q., (1979) Geology of Kohistan, Karakorum, Himalaya, northern Pakistan. *Geol. Bull. Univ. Peshawar, Pakistan.* Special issue, Vol. 11, pp. 1-187.

Tahirkheli, R.A.K., Mattauer, M., Proust, F., and Tapponnier, P., (1979). The India Eurasia suture zone in northern Pakistan some new data for an interpretation at plate scale. *Geodynam. Pakistan. G.S.P. Quetta* pp. 25.

Wilson, A.F., (1960). Coexisting pyroxene: some causes of variation and anomalies in optically derived compositional tie-lines, with particular reference to charnockitic rocks. *Geol. Mag.* Vol. 97, pp. 1-17.

Winchester, J.A., and Floyd, P.A., (1976). Geochemical magma type discrimination: application to altered and metamorphosed basic igneous rocks. *Earth Planet. Scie. Lett.,* Vol. 28, pp. 259-469.

REVIEW OF GEOTECHNICAL CHARACTERISTICS OF NEELUM GRANITES, NEELUM VALLEY, AZAD KASHMIR

By

M. ARSHAD KHAN, AND M. SHOAIB QURESHI

Institute of Geology, University of Azad Jammu & Kashmir Muzaffarabad.

ABSTRACT: *The Neelum granite of Neelum Valley Azad Kashmir, has been investigated to evaluate its geotechnical properties. The geotechnical properties like compressive strength, shear strength, soundness, porosity, water absorption and slake durability of the granite show their potential to be used as construction raw material. The compressive strength value ranges from 100-350 MPa. The shear strength varies from 150-950 MPa, soundness 0.1%-2.0%, water absorption 14-20%, slake durability 99.5-99.8%, porosity 0.2%-15% and degree of polish good - excellent.*

An evaluation of geotechnical properties of different granites suggest the rational use of the raw material, considering the deformability characters of the rocks.

INTRODUCTION

The use of granite as construction raw material is well known in the territory of Azad Kashmir (Wadia, 1920). The granites are present in different parts of the Neelum Valley (Fig. 1, Ghazanfar *et al.*, 1983).

In other parts of the world granites have been used as commercial decorative stones (Dale, 1923; Bowles, 1956, Eisenberg and Milton, 1973). The granites of the Neelum Valley differ in colour, texture and structure. During the geotechnical study of granite, considerations have been given to the accessibility, geographic location, manpower, and engineering geological properties (Table 1). Presently, the granites of the Neelum Valley are randomly quarried and no proper considerations have been given to the quarry sites (Fig 1). The present investigation was under-taken to explore the geotechnical properties of granite. The granite localities at Jura (Fig. 1), have been investigated to classify the granite as building material. Total fifty samples have been taken from Jura, Islampura, Mori and Karen quarries for the engineering geological studies. The representative sample tests are given in the Tables 1-2. The deformability characters of the granites were also determined.

ENGINEERING GEOLOGICAL PROPERTIES

The determination of compressive strength, shear strength, soundness, porosity, abrasion, slake durability index, water absorption and sieve analysis help in the study of geotechnical properties of granites.

Shear Strength

The Jura granite is foliated whereas the granite at Islampura, Mori and Karen is porphyritic in nature. These show variation in shear strength from 150-950 MPa (Table-1). The shear strength for the granites of Neelum Valley is within the recommended range (90-100 MPa) of American Standards for Testing Materials (ASTM). The rock samples from less foliated Jura granite at Mori show shear strength of 260-950 MPa as compared to shear strength of 150-630 MPa fractured to unfractured porphyritic granite at Karen. The porphyritic fresh granite at Islampura show shear strength of 380-650 MPa whereas, the foliated and tectonized granite at Jura yields shear strength of 250-850 MPa. The change in shear strength is due to the mineralogical composition, and microcracks, joints, foliation and locally toctonized nature of the granite. These factors decrease the durability and strength of the granite in general.

Scale 1:50000 or 1 inch to 0·789 miles

Terrace

Authmugam biotite chlorites phyllites and schist

Kundalshahi garnet mica schist

Keran granite

Tithwal garnetiferous chlorite schist

Porphyritic Issampura granite

Foliated Jura granite gneiss

Sample location
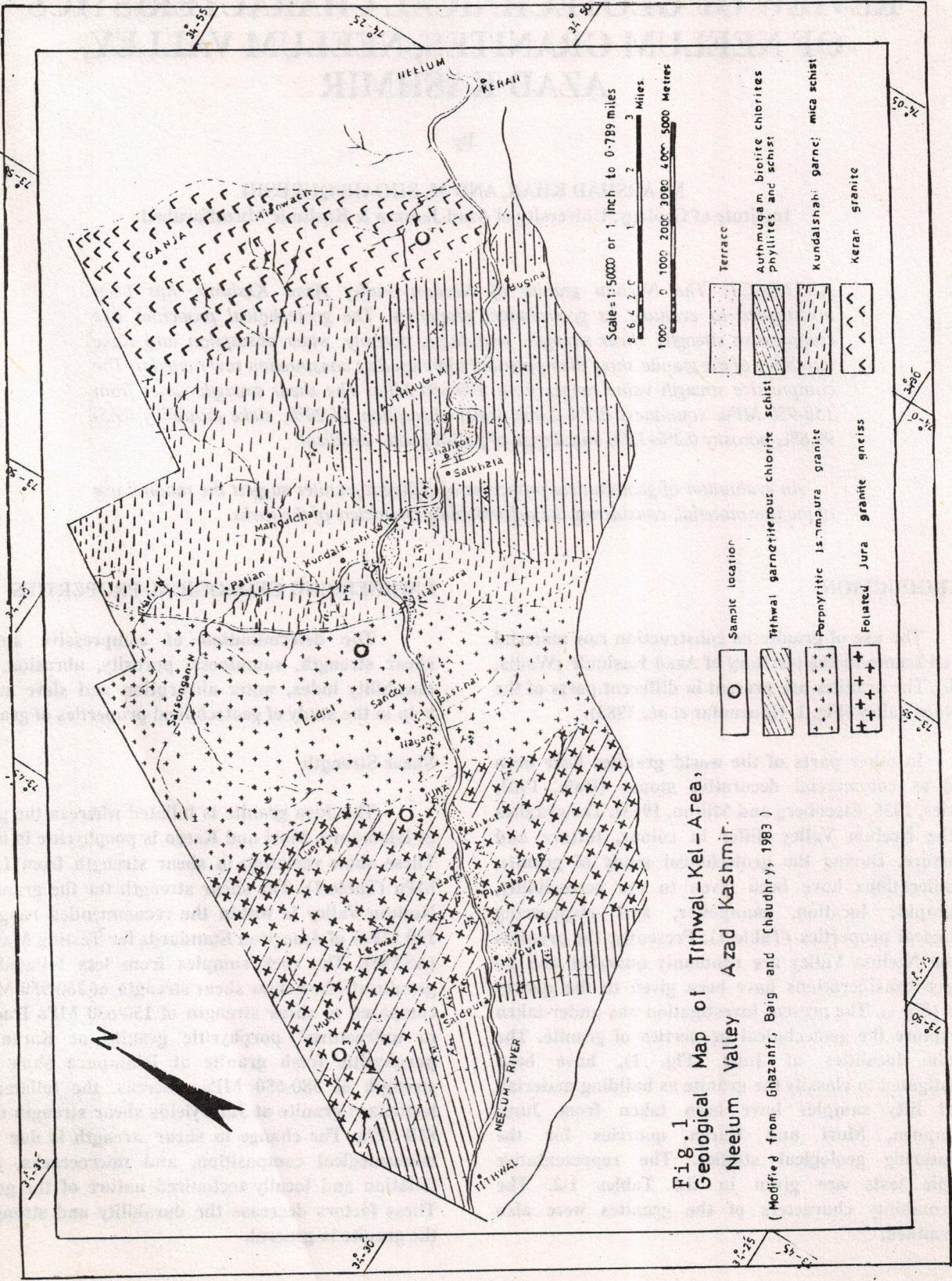
Fig. 1
Geological Map of Tithwal-Kel-Area,
Neelum Valley Azad Kashmir.
(Modified from Ghazanfr, Baig and Chaudhry, 1983)

Compressive Strength

The unconfined compressive strength were carried out on 2x2x2 inches (125 cm) granite blocks with ASTM (1986) standards. The samples were oven dried at 110°C. The samples were loaded to failure in an uniaxial compression machine. The compressive strength of foliated Jura granite is 350 MPa which is highest in this locality. This is probably due to recrystallization of the rocks. The porphyritic Islampura granite has a decrease due to microcracks present in these rocks. The less foliated Mori granite is very hard with a maximum compressive strength of 380 MPa (Table 1, Fig. 3). The compressive strength of the granite again decreases at Karen (300 MPa). This decrease in compressive strength is probably due to mineralogical composition of the rocks. High porosity (12%) also effect the compressive strength of the rocks. The deformability characteristics are more as compared to Mori granite which is the extension of Jura granite.

Grading, Abrasion and Slake Durability

To find out the behaviour of rocks as crushed stone, the granites from Jura, Islampura, Mori and Karen have been crushed separately. It was jaw type small unit crusher and small pieces of rocks size ranging from 12 x 14 cm to 15x 20 cm were used for crushing. The product got after one revolution was mechanically analysed to see the granite samples, were retained on sieve No. 4. All granites show excellent aggregate grading while crushing (Table 2). The abrasion values range from 14% to 20% and slake durability index values range from 98.6% to 99.8% (Table 2). Abrasion and slake durability values are high and are within the limit of ASTM specifications.

Water Absorption

To find water absorption and the behaviour of rocks 2x2x2 sq inches (125 cm) oven dried granite samples were tested using ASTM C-170 (1986) method. The water absorption values range from 0.54% to 9% (Table 2). The difference in the values is due to structural weaknesses like microporosity produced by tectonic deformation and the amount of clayey material in the cracks affect the rocks in contact with water (Table 2).

Porosity

The total porosity of granites are within the recommended limits (10%) of ASTM. However, the granites at Mori and Karen show higher values (Table 2). The granites can be identified by textural characteristics and micaceous composition. The granite at Mori show higher percentage of total porosity (15%) and can be used as building material in arid regions, because of their higher strength. Alternatively, the granites of Karen which show higher porosity (12%) can be utilized in the manufacture of decoration pieces. The Jura granite has less porosity (5%) and can be used for exterior decoration.

Deformability of rocks:

The stress-strain character of the Neelum granites have shown that the rocks are not always clastic in nature. During uniaxial compression test, the elastic behaviour was limited (300-380 MPa). The deformation of the granites has been divided into three stages. 1). Preexisting microcracks. This is an initial stage at low stress level with significant strain in samples. 2) Elastic behaviour. This region is not always well defined. In most cases axial stress-strain curve do not contain a straight line. Segment repesenting linear elastic behaviour. The new microcracks propagate at low velocity and are relatively stable. The increase in stress resulted the failure of the sample. At intermediate level, granites exhibits a hardening behaviour as cracking increases, a closure of the cracks resulting in an increase in area of the rock. As the stress increases intragranular cracking result in linear behaviour. This represents a balance between strain, microcracking and hardening or decrease in volume of the spcimen.

DISCUSSION

The comparison of the data with the compressive strength of building stones (US Bureau of Standards, 1970) for granites reveals higher values for Jura and Mori granites. In some cases the granites of Jura (350 MPa) and Islampura (300 MPa) exceed the upper recommended limit (200 MPa). Most probably this increase in values of compressive strength is due to compact texture of the granites. Likewise, some of the samples from Mori show a maximum of 380 MPa compressive strength (Table - 1) which may be attributed to their origin and higher degree of recrystallization and interlocking of grains. The micaceous Jura granite do not show such a higher value (Table-1).
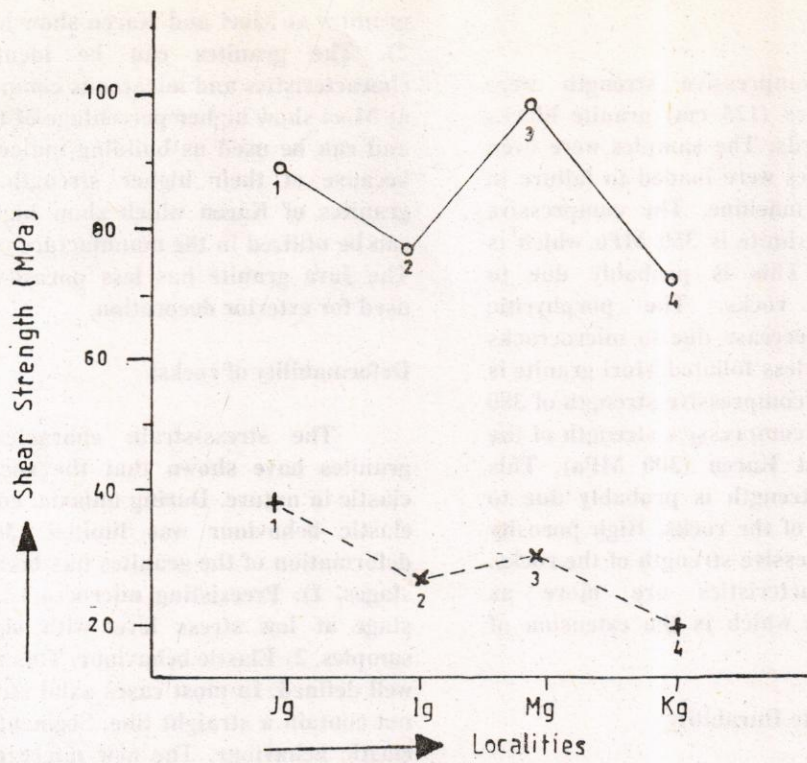
Fig·2   Maximum and Minimum Shear Strength of Neelum Valley granites
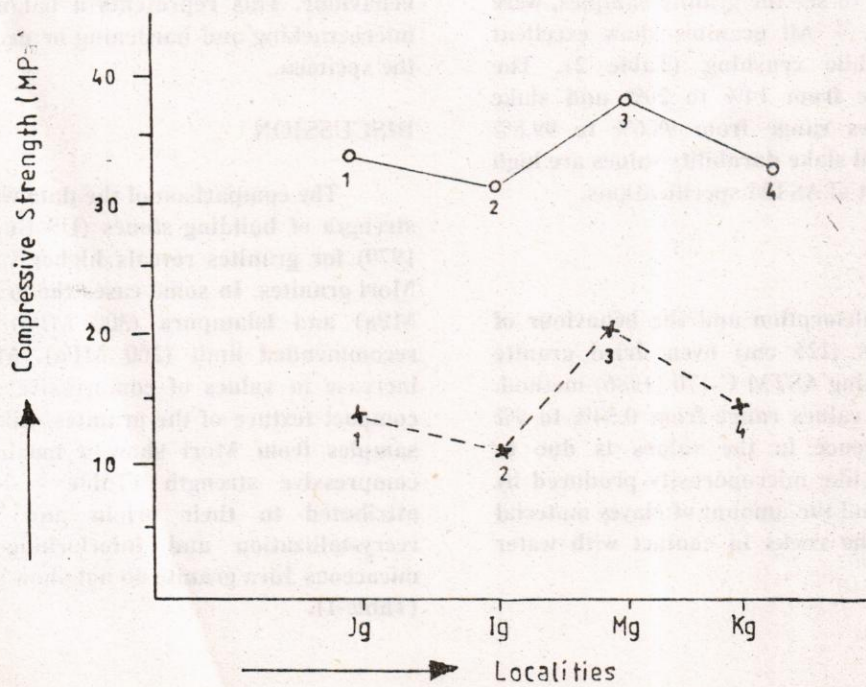
Fig·3   Maximum and Minimum Compressive Strength of Neelum Valley granites

Table-1 Geotechnical Properties of Neelum granites.

S. No.	Locality/Rock Type	Shear Strength (MPa)	Comprosive Strength (MPa)	Water Absorption %	Porosity %
1.	Foliated Jura Granite (Jg)	850	350	0.51	5.0
2.	Porphyritic Islampura granite (Ig)	850	300	3.0	10.0
3.	Less Foliated Mori granite (Mg)	950	380	8.0	15.0
4.	Karen granite (Kg)	630	300	9.0	12.0

Table-2 Abrasion, Salke Durability and Aggregate Grading properties for the Granites of the Neelum Valley.

S. No.	Locality/Rock Type	Abrasion %	Salke Durability Index (5 cycles) %	Retained on sleve 4 after creasing %
1.	Foliated Jura Granite (Jg)	15	99.8	75
2.	Porphyritic Islampura granite (Ig)	18	99.5	75
3.	Less Foliated Mori granite (Mg)	20	98.6	75
4.	Karen granite (Kg)	14	99.6	70

The granite rock samples from Islampura show recommended range of values for compressive strength (150-380 MPa), Hence, it appears reasonable to consider that the building material of the Jura, Islampura, Mori and Karen are of fairly high quality with respect to their compressive strength. However, some of the samples from Islampura and Mori localities show compressive strength values less than the lower limit of recommended values (150 MPa) but such granites are few and can be identified in the field by their micaous nature. The shear strength values are not of much importance and are not described.

The water absorption in the granites is well within the recommended range of water absorption percentage (0.54-9%) with few exceptions (Table-2). Hence, the absorption of water will not cause any problem or effect the quality in the exploitation of the rock material. A definite correspondence could not be established from the present study.

The porosity in the granites are mostly within the recommended range (10%) however, there are some samples from Jura, Islampura Mori and Karen which show 5%, 10%, 15% and 12% porosities respectively. Most probably these variations in porosity percentage are related to the textural and geological conditions prevailing at the time of crystallization of these rocks and the cavities developed through geological times.

The rational exploitation of these rocks require the consideration of climatological factors and bearing capacity of subsoil conditions of the locality selected for the use of these rocks. The abrasion percentage for granites (20%) is within the recommended values of ASTM (1986). Thus rocks from the area under study can be used for road surfacing.

Mining techniques in use are old and unscientific due to lack of practical and scientific information. The explosives mainly used are gilatinous, powdered, wabocard and detonators. The above

mentioned explosives produce shock waves which travel with very high velocity and disturb the bonding between particles and also break the internal structure resulting small and large cracks. The rocks with discontinuities more than 20 per meter are not suitable raw material for decorative stones.

During mining, safety measures such as ohmmeter, leakage testers lightening detectors, short firing cables and crispers should be used to reduce the wastage and risk assessment. Such purpose can be achieved by providing training facilities blasting and cutting services.

CONCLUSIONS

The reserves of good quality decorative stones are huge and transport charges would not be very high due to easy approach to the sites, cheap labour and proximity to the city of Muzaffarabad.

The rocks having compressive strength more than 200 MPa from Jura and other localities can be used for important buildings and external surfacing in addition to their use in special engineering works.

The soundness values of rocks are within recommended limits with few exceptions. Hence the effects of tectonism appear to affect the engineering properties of the rocks of different localities.

The rocks with discontinuities more than 20 per meter are not suitable raw material for decorative stones.

The degree of recrystallization and diagenesis appear to have affected the porosity of the rocks.

The exploitation of the stones can be done by open quarry mining and the waste material can be used for filling purposes. The exploitation of the granites can be economical.

REFERENCES

American Standards for Testing Materials (1986). Natural building stones Vol. 22, pp. 10-32.

American Society for Testing Materials (1970). Standard Method of Testing for Weathering Resistance of Natural Slates. ASTM C-217-58, pp. 26-50.

Bowles, O., (1956). Granites as a dimension stone. *US Bur. Min. Inf. Circ.* 7753, p. 76-80.

Dales, T.N., (1923). Commercial granites of New England. *US Geol. Sur. Bull.,* 12348, pp. 1-685.

Eisenberg, N.K.S., and Milton M.C., (1973). Case history of a structural granite cleaning problem. *First Int. Sympos.,* pp. 1236-1309.

Ghazanfar, M., Baig M.S., and Choudhary, M.N., (1983). Geology of Tithwal Kel area Neelum Valley Azad Kashmir. *Kashmir Jour., Geol.,* Vol. 1, No. 1, pp. 1-10.

Wadia, D.N., (1929). Age of gypsum and origin of gypsum associated with salt deposit of Kohat. *Trans. Min. Geol. Inst. Ind.,* Vol. 21, pp. 202-222.

SUBDIVISIONS OF THE KAMILA AMPHIBOLITE BELT IN SOUTHERN KOHISTAN ISLAND ARC COMPLEX, PAKISTAN

By

ROBERT R. LOUCKS[*], MOHAMMAD ASHRAF[**],
M. AMJAD AWAN[**], M. SABIR KHAN[**] & D. JAY MILLER[***]

[*]Research School of Earth Sciences, Australian National University, Canberra, ACT, 2601 Australia.
[**]Institute of Geology, Azad Jammu & Kashmir University, Muzaffarabad, Pakistan.
[***]Department of Earth and Atmospheric Sciences, Purdue University West Lafayette, IN 47907, U.S.A.

ABSTRACT: *Previously know Kamila Amphibolite Belt has been studied further now in details and found to consist of three principal subdivisions. They are Dasu, Kayal and Patan complexes underplated successively. They are composite of several mafic-ultramafic cumulate intrusions that vary in degree of metamorphic hydration and deformation. The Dasu Complex in Indus Valley consists of extremely deformed, polymetamorphosed, epidote-garnet amphibolite banded gneisses. These record metamorphic P-T conditions averaging 5.5-6.5 kb and 520-580°C. The Kayal Complex consists chiefly of garnet-epidote amphibolites with strong foliation but only rare gneissic segregation banding, with igneous hornblende and layering. Metamorphic assemblages record P-T conditions of about 7 kb and 620°C near base. The Patan Complex is massive to modally layered and locally crossbedded gabbronorite at base to hornblende-gabbronorite and diorite in the upper part with magmatic-epidote tonalite adjacent to its roof. Mineral geobarometry yeilds a pressure of 7.5 kb near roof. The stacking thus formed by a process whereby a thick crust of continent-like thickness and composition developed by repeated episodes of igneous intrusion along Moho.*

INTRODUCTION

Principal lithologic units and structural features have been mapped of southern Kohistan along a succession of north-south traverses in the valleys of the Panjkora River (Dir), Swat River, Indus River (Besham northward), and another north and south from Chilas. Each traverse extends from the Main Mantle Thrust northward to the southern part of the Kohistan batholith. We have found that the region previously referred to as the "Southern Amphibolite Belt" or "Kamila Amphibolites" (Fig. 1) is in fact a composite of several mafic-ultramafic cumulate intrusions that vary in degree of metamorphic hydration and deformation, and can be correlated east-west from one traverse to another to develop a consistent "stratigraphy" of layered cumulate complexes in the lower crust of the Kohistan arc. From the deepest level upward, the four principal cumulate intrusions are the Jijal Complex, which is overlain by the Patan Complex, that is in turn overlain by the Kayal-Chilas Complex, which is overlain

by the Dasu Complex. The contact of the Jijal Complex with the Patan Complex is a thrust fault contact in the northwest and strike slip in the north extending to south east. Ashraf *et al.* (1991), (Fig. 2). The contact of the Patan Complex with the Kayal-Chilas Complex is an igneous intrusive contact where exposed in the village of Khawazakhela in Swat and along the Karakoram Highway (KKH) 9 km north of Patan village. The roof of the Kayal-Chilas Complex intrudes the gneissic Dasu Complex in upper Swat 18 km north of Bahrain, and along the Karakoram Highway 31 km north of Patan, and in Kiner Gah 5 km north of Chilas town.

The principal structural features in southern Kohistan have been described by Coward *et al.* (1986) and consist of (1) and east-west trending, large, tight anticline within the Chilas Complex, of which the north limb dips ~ 50° to the north, and the overturned south limb also dips to the north; and (2) the Kamila Syncline, which lies on the south side of, and parallel to
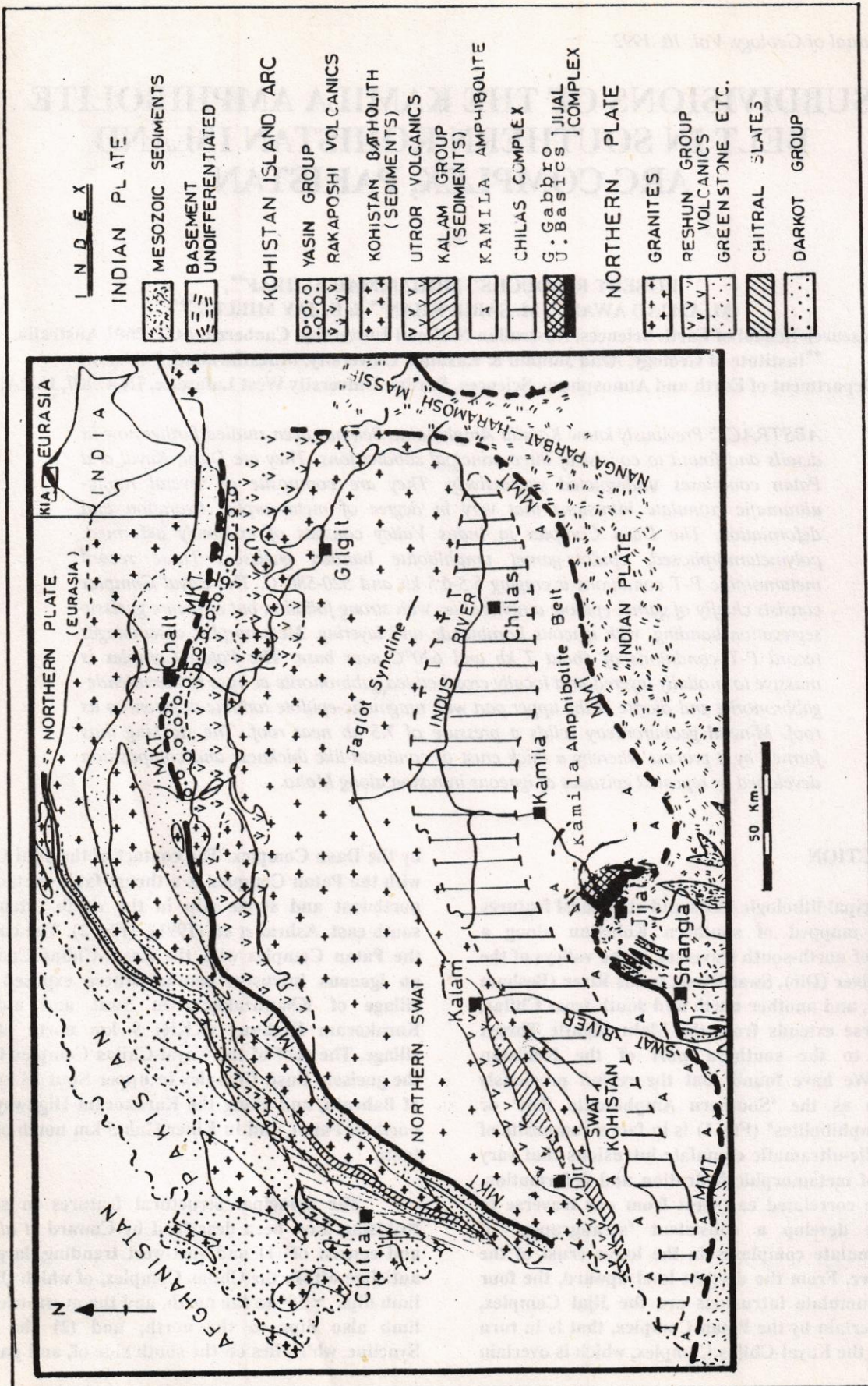
Fig.1 Geological map of Kohistan Island Arc Complex showing occurrence of Kamila Amphibolite Belt in Indus, Swat & Dir Valleys(modified after S.Hamidullah,1992)

INDEX

INDIAN PLATE
- MESOZOIC SEDIMENTS
- BASEMENT UNDIFFERENTIATED

KOHISTAN ISLAND ARC
- YASIN GROUP
- RAKAPOSHI VOLCANICS
- KOHISTAN BATHOLITH (SEDIMENTS)
- UTROR VOLCANICS
- KALAM GROUP (SEDIMENTS)
- KAMILA AMPHIBOLITE
- CHILAS COMPLEX
- G. Gabbro U. Basics / JIJAL COMPLEX

NORTHERN PLATE
- GRANITES
- RESHUN GROUP VOLCANICS
- GREENSTONE ETC.
- CHITRAL SLATES
- DARKOT GROUP

50 Km.

the Chilas Anticline. The axis of the Kamila Syncline appears to plunge gently to the east, causing the Chilas-Kayal Complex to have a map outcrop pattern in the form of <. We have previously (Miller et al., 1990) termed the south limb of the < pattern the "Kayal Complex"; The north limb is the previously recognized Chilas Complex. The southern Kayal and northern Chilas limbs of the < map pattern seem to merge between the Indus and Swat valleys to form a single broad mafic intrusion in the Swat valley that we call the Chilas-Kayal Complex, but was previously called just the Chilas Complex in Swat by Jan *et al.* (1984 a, 1984 b).

DASU COMPLEX

In the Indus valley, the core of the < is occupied by the Dasu Complex, which consists of extremely deformed, poly-metamorphosed epidote-garnet amphibolite banded gneisses that crop out extensively at Kamila and have previously been called the Kamila Amphibolites. These record metamorphic P-T conditions averaging 5.5-6.5 kb and 520-580°C. South of Kamila, the Dasu gneiss complex is split by a young unmetamorphosed, sheet-like intrusion 1.5-2 km thick that grades from diorite on the south (bottom) to tonalite at its top. The Dasu Amphibolite gneiss is the roof of the Chilas Complex on both the north and south limbs of the Chilas Anticline and is the roof of the "Kayal Complex" along the interior south limb of the Kamila Syncline. The Dasu gneisses record similar metamorphic pressures (~ 5.5-6 kb) at all three roof contacts. Primary igneous differentiation within the Dasu Complex is represented by gradation from basal

mela-amphibolites along its southern border to meta-quartz-diorite at its top, with prolific boudinaged and folded quartz-hornblende-plagioclase pegmatite dikes that represent the roof zone of the Dasu intrusion, located ~ 14 km along the KKH south of Kamila town.

KAYAL COMPLEX

On the south side of the Kamila Syncline, the south (Kayal) limb of the Kayal-Chilas Complex consists chiefly of garnet-epidote amphibolites with generally strong foliation but only rare gneissic segregation banding. Relict igneous layering and igneous pyroxenes and hornblende are preserved locally in weakly deformed outcrops. Metamorphic assemblages record P-T conditions of ~ 7 kb and 620°C near the base of the Kayal sequence.

The Kayal amphibolite / metagabbro sequence is much less intensely deformed than the Dasu gneisses, but in both garnet is locally absent and locally conspicuous. The disappearance - reappearance - disappearance - reappearance of garnet along the KKH north and south of Kamila was misinterpreted by Treloar *et al.* (1990) as due to tectonic juxtaposition of amphibolite slices of contrasting grade in the broad amphibolite sequence they called the "Kamila Shear Zone" and which we call the Dasu and Kayal Complexes. We find no evidence to support the existence of large-scale displacements associated with the off-and-on distribution of garnet. Rather, minor local variations in shear-induced permeability and H_2O fugacity cause garnet abundance to vary in response to the equilibria:

garnet $\qquad$ plagioclase $\qquad\qquad$ epidote $\qquad\qquad$ quartz

(1) $\quad Ca_3Al_2Si_3O_{12} + CaAl_2Si_2O_8 + 2H_2O = 4Ca_2Al_3Si_3O_{12}(OH) + SiO_2$

garnet $\qquad\qquad$ garnet $\qquad\qquad$ hornblende $\qquad\qquad$ quartz

(2) $\quad 8\,Ca_3Al_2Si_3O_{12} + 13Mg_3Al_2Si_3O_{12} + 9Ca_2Mg_5Si_8O_{22}(OH) + 12\,SiO_2 + 12H_2O$

hornblende
$= 21Ca_2Mg_4Al_2Si_7O_{22}(OH)_2$

PATAN COMPLEX

The Patan Complex consists chiefly of massive to modally layered and locally crossbedded gabbronorite in its lower part, grading to hornblende-gabbornorite and diorite in the upper part, with magmatic-epidote-bearing tonalite adjacent to its roof. Its upper part is only weakly and locally amphibolitized, but becomes increasingly amphibolitized and foliated southward toward its basal boundary faults - the Patan fault in the

village of Patan, and the MMT near Tigak Banda in Swat. The basal ultramafic cumulate sequence is faulted out along the KKH at Patan, but a sequence of serpentinized, layered chromite dunite, wehrlite, and clinopyroxenite about 1.5 km thick is exposed in the bazaar of Dubair village ~ 11 km north of the MMT along the Dubair stream road, Ultramafics possibly representing the same unit at the base of the Patan Complex are exposed along the MMT at Tighak Banda village Swat. The MMT cuts upward to higher levels of

the crust westward toward Dir, so that in the Panjgora River valley, the MMT cuts the Chilas (-Kayal) Complex at the deepest crustal level exposed there.

Mineral geobarmetry yields a pressure of ~ 7.5 kbar (~ 26 km depth) for igneous crystallization in the tonalitic roof zone of the Patan Complex. An estimated stratigraphic thickness of ~ 5-7 km implies crystallization of the Patan basal ultramafic cumulates at ~ 9-10 kbar (31-33 km depth). These pressures are in satisfactory agreement with P = 7 ± 0.5 kbar obtained for the conformably overlying basal part of the Kayal Complex, and stratigraphically correlative unmetamorphosed green-spinel + olivine gabbro in the Chilas Complex (i.e., north outcrop limb of the Kayal-Chilas Complex) which yield P = 7 kbar by mineral geobarometry. Various garnet-based geobarometers yield pressures of 5.5-6 kbar for the roof contact of the Kayal-Chilas Complex with the Dasu gneiss, which is consistent with the mapped stratigraphic thickness of the Chilas Complex north limb.

DISCUSSION

We thus conclude on the basis of mineral geobarometry and mapped igneous intrusive contacts that the "Southern Amphibolite Belt" is a structurally coherent stack of three principal mafic intrusions. Each is internally differentiated along a calc-alkalic trend from a tonalitic top downward through diorite to hornblende gabbronorite to ultramafic cumulates in the case of the Patan and Chilas Complexes. The Dasu complex is the uppermost and is the oldest and most deformed. Its missing ultramafic cumulates were presumably displaced downward into the mantle when the next intrusion, the Chilas-Kayal Complex, developed as a sheet-like magma chamber along the density trap corresponding to the ultramafic-mafic cumulate contact within the Dasu Complex, ultramafic cumulates are also missing and presumably were peeled from the base of the Kayal sequence during emplacement of the Patan magma chamber. However, the Chilas limb contains dunite and wehrlite along the base of major cyclic units within the sequence.

The Patan Complex is missing its ultramafic cumulates over most of its mapped strike length (>110 km), but a portion is preserved in the section along Dubair Stream and possibly at Tighak Banda.

Each intrusion underwent compressive deformation and metamorphism before emplacement of the next one downward in the stack. The regime of intra-arc-horizontal compression acts to keep "pinched

shut" the dike conduits that could carry magma to shallower levels. Only after the mafic magmas had differentiated to more siliceous and hydrous quartz-diorite or tonalite composition did the residual liquid acquire sufficient buoyancy to resume ascent to shallower levels to form the Kohistan batholith and volcanic sequence.

We envision a process whereby a thick crust of continent-like thickness and composition developed by repeated episodes of igneous intrusion along the Moho which corresponds to the mafic-ultramafic cumulate contact of the most recent intrusion at the bottom of the arc crust. As the pre-existing ultramafic cumulates were peeled off and displaced downward into the mantle, a new Moho developed (deeper than the previous one) at the ultramafic-mafic cumulate contact of the new intrusion. By repetition of this process of delamination of ultramafic cumulates and upward segregation of differentiated residual magmas, a continent-like crust of dioritic bulk composition was developed from mantle-derived primitive, Mg-rich tholeiitic basaltic magmas. It has been a longstanding question why the worldwide continental crust appears to have an average composition of diorite (andesite), whereas the magmas that issued from the mantle to make the crust are primitive basalts. The answer to the question is evident by inspection of magmatic intrusion processes in southern Kohistan.

The intra-arc compression that deformed the cumulate complexes during and after their crystallization ~ 115-95 Ma ago and ultimately led to collision of the arc with Asia is suspected to be a response to low-angle, fast subduction of the northern Neotethys oceanic plate.

During the Permian, Triassic, and Jurassic, several episodes of rifting in Northern Gondwanaland developed into spreading ocean ridges that transported Gondwana fragments north to be accreted to Asia (much like the more recent fragmentation of Africa has split off the Indian and Arabian plates by spreading ocean ridges). The available information suggests that the opening of the Neotethys basin in late Triassic-early Jurassic transported the Gondwana fragments Central Afghanistan and South Tibet and Burma-Malaya northward to be accreted to the southern Asia margin in the late Jurassic. The approximately east-west-trending spreading ocean ridge responsible for their transport also migrated northward, with the result that the Neotethys oceanic lithosphere entering the Trans Himalayan subduction zone became progressively younger and hotter and less dense during the early

Cretaceous. The increasing buoyancy of the younger, hotter oceanic lithosphere caused the angle of subduction to become shallower and to drag against the over-riding Kohistan-Ladakh microplate in the west, and against the Asian margin farther east in Tibet-Burma-Malaya where a major episode of compressive deformation and concomitant surge in arc magmatic activity dates to ~ 100 ± 10 Ma age (Audley-Charles et al., 1988).

The inferred shallowing of subduction, broadening of the magmatic arc to $\geq$ 120 km in Kohistan, and compressive deformation accompanying a major episode of plutonic intrusion and relatively minor volcanism are similar to events that immediately preceded the late Cretaceous approach of the NW Pacific spreading ridge toward western North America, causing subduction angle to flatten, the magmatic arc to broaden from California eastward more than 400 km, and major thrust deformation (Laramide Orogeny) to >1000 km inland from the subduction zone.

Similar effects are presently accompanying the present-day subduction of the young hot Nazca plate at a shallow angle (~35°) under Chile, as the East Pacific Rise approaches the Chile Trench.

REFERENCES

Ashraf, M., Awan, M.A., Yasir, A., Warraich, M.Y., Khan, A., and Awan, M.S., (1991). Geology and petrsology of Jijal and Pattan Layerad ultramafic-mafic complexes in the vicinity of Jijal, Duber and Pashto, NWFP, Pakistan. *Kashmir, Jour. Geol.* Vol. 8 & 9, pp. 193-195.

Coward, M.P., Windley, B.F., Broughton, R.D., Luft, I.W., Peterson, M.G., Pusdey, G.J., Rex, D.C., and Khan, M.A., (1986). Collision tetconics in the NW Himalaya. In: Collision Tectonics (M.P. Coward and A.C. Rex oditors). *Sp. Pub. Geol. Soc. Lond,* Vol. 19, pp. 203-219.

Jan, M.Q., Parvez, M.K., and Khaltak, M.U.K., (1984 a). Coronites from the Chilas and Jijal - Patan complexes of Kohistan. *Geol. Bull. Peshwar. Univ.,* Vol. 17, pp. 75-85.

Jan, M.Q., Khaltah, M.U.K., Parvez, M.K., and Windley, B.F., (1984 b). The Chilas stratiform complex: Field and mineralogical aspects. *Geol. Bull. Peshwarn. Univ.,* Vol. 17, pp. 153-169.

Miller, D.J., Loucks, R.R., and Ashraf, M., (1990). Platinum group elements mineralization in the Jijal ultramafic-mafic complex, Pakistan, Himalayas. *Econ. Geol.,* Vol. 86, pp.

REVISED STRATIGRAPHY OF THE SOUTHERN TANAWAL AREA, NORTH OF HARIPUR, N.W.F.P. PAKISTAN

By

SAJJAD AHMAD*, IMTIAZ AHMAD*, ARIF ALI KHAN GHAURI** & MOHAMMAD RIAZ**

*Department of Geology, University of Peshawar
**National Centre of Excellence in Geology, University of Peshawar

ABSTRACT: *The southern Tanawal area exposes a suite of metasedimentary rocks comprising quartzite, dolomite, argillite and conglomerate. The oldest rocks belong to the Tanawal Formation of Precambrian age. The Tanawal Formation is unconformably overlain by a thick sequence of quartzite, dolomite, argillite and conglomerate, previously named as Abbottabad Formation. Baig and Lawrence (1987) renamed this sequence as Sherwan Formation and considered it to be of Cambrian age. The stratigraphy of the area is revised in order to differenciate between the dolomite-quartzite sequence exposed north and south of the Panjal fault in the southern Hazara region.*

INTRODUCTION

The study area encompasses approximately 60 sq. km of the southern Tanawal region and lies in the Survey of Pakistan topographic sheet No. 43 B/16 between latitudes 34° 4' 20" N to 38° 8' 6" N and longitudes 72° 53' 30" E to 73° 0' 0" E (Fig. 1).

Two formations are identified in the study area; the Precambrian Tanawal Formation and the unconformably overlying Cambrian Sherwan formation. The dominant lithologies in the area are quartzite and dolomite. The revised stratigraphic sequence is proposed as under in Table-1.

Sherwan	Dolomite member	
Formation	Quartzite member	Cambrian ?
	Argillite member	
_____ Unconformity _____		
Tanawal		
Formation		Precambrian ?

HISTORICAL REVIEW

The earliest attempt to establish the stratigraphy of Hazara was made by Waagen and Wynne (1872). They described a series of unfossiliferous, partly metamorphosed slates, conglomerate, schist and quartzite under the name "Tanol Series", overlain by a thick succession of carbonates which they called "Below the Trias". Middlemiss (1896) renamed the "Tanol Series" as "Tanol Quartzites" and described them as feldspathic schistose quartzites. He also changed the name "Below the Trias" to "Infra Trias".

Ali (1962) in a paper about southern Tanawal area, named the carbonate sequence of the area as "Abbottabad Formation", unconformably underlain by the "Tanol Formation".

Calkins *et al.* (1975) while working in southern Himalayas described the geology of southern Tanawal area. They renamed the Abbottabad Formation as Kingriali Formation.

Baig and Lawrence (1987) proposed the name "Sherwan formation" for the dolomite-quartzite sequence exposed in the Tanawal area.

PROBLEMS WITH THE EXISTING STRATIGRAPHY

The revised and previous stratigraphic schemes proposed for the southern Tanawal area are shown in Table 1. The reasons which convinced the authors to revise the stratigraphy of the area are based on the following observations:
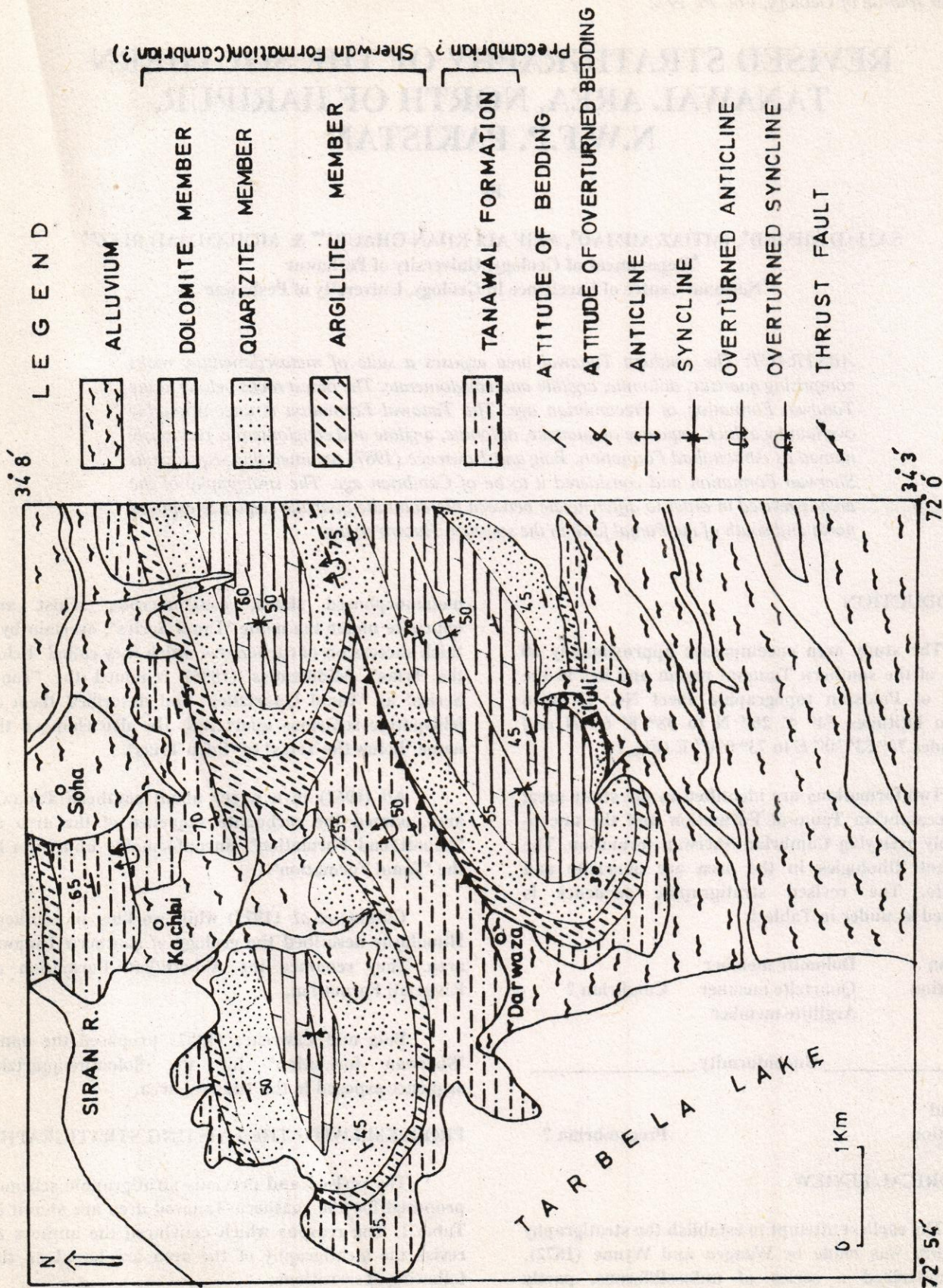
Fig. 1 Geological map of the Southern Tanawal area, north of Haripur, N.W.F.P; Pakistan.

Fig. 2 Geological sketch map of the Tanawal and Abbottabad Zones (modified and interpreted after Calkins *et al.*, 1975; G. Fuchs, 1975; and Baig and Lawrence (1987).
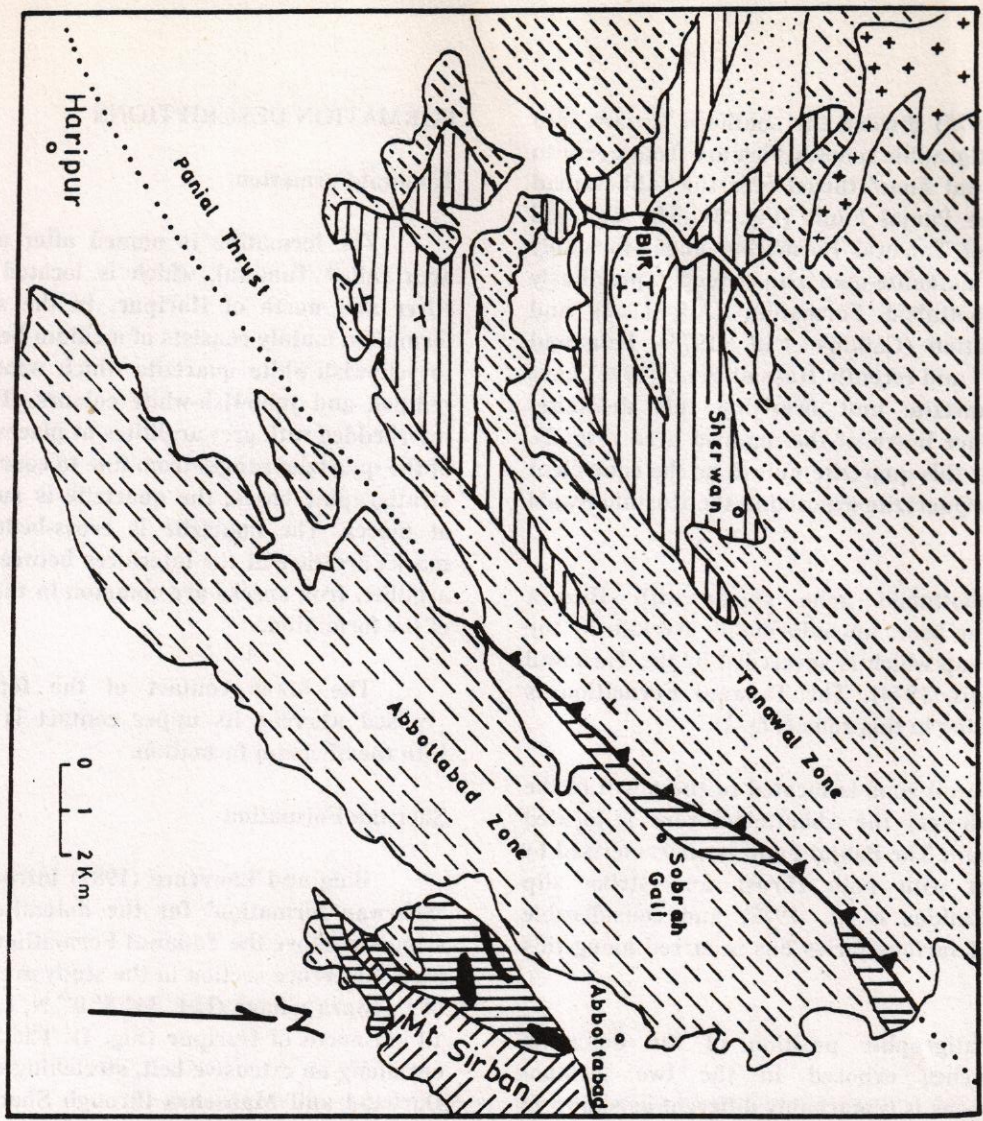
LEGEND
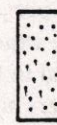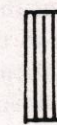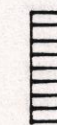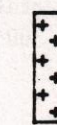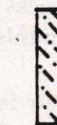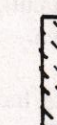
- QUATERNARY ALLUVIUM
- JURASIC UNITS
- HAZIRA FORMATION
- MISRI BANDA QUARTZITE
- SHERWAN FORMATION
- ABBOTTABAD FORMATION
- TANAWAL FORMATION
- MANSEHRA GRANITE
- HAZARA FORMATION
- ATTITUDE OF BEDDING
- THRUST FAULT

Fuchs (1975) divided the southern Hazara into two tectonostratigraphic zones, which are from north to south as "Tanawal Zone" thrust over the "Abbottabad Zone" along the Panjal Fault (Fig. 2). The Tanawal Zone consists of Tanawal Formation uncon-formably overlain by the dolomite-quartzite sequence previously named as Abbottabad Formation (Ali, 1962) and Kingriali formation (Calkins *et al.* (1975). Baig and Lawrence (1987) and recently Hussain *et al.* (1990) have reported a quartzite unit overlying this dolomite-quartzite sequence north of the mapped area (Fig. 2). They considered this quartzite unit to be the equivalent of Misri Banda Quartzite exposed in the Rustam-Swabi area.

The Abbottabad zone starts with Hazara Formation at the base, unconformably overlain by the Abbottabad Group which is succeeded by the Tarnawai Formation (Latif, 1974). The Tanawal Formation is completely missing in this zone (Fig. 2).

The Tanawal zone is located to the north of the Panjal Fault whereas the Abbottabad zone is located south of this fault. The Panjal Fault is characterised by a displacement with both thrust and strike slip components (Calkins *et al.*, 1975) and considerable displacement of various facies has occurred along this fault.

The stratigraphic position of the dolomite-quartzite sequence exposed in the two tectono-stratigraphic zones is remarkably different as shown in the Table-2.

A thick conglomerate bed is present at the base of the dolomite - quartzite sequence exposed in the two zones. The conglomerate bed exposed in the Abbottabad zone consists of pebbles and boulders upto m-size and are rounded to angular in form with glacial striations (Fig. 3). The clasts are embedded in green, dark grey and purple shaley or silty matrix and are poorly sorted.

In contrast, the conglomerate bed of the Tanawal zone comprises clasts of quartzite and argillite embedded in argilliceous and sandy matrix. The clasts range in size from one cm upto 40 cm in diameter and are commonly elongated parallel to the bedding with no glacial striations (Fig. 4).

On the basis of the above mentioned observations the stratigraphy of the Tanawal area is revised to seperate the same kind of rocks exposed in the Tanawal and Abbottabad Zones.

FORMATION DESCRIPTIONS

Tanawal Formation

The formation is named after a former tribal area called Tanawal, which is located east of Indus River and north of Haripur. In the study area, the formation mainly consists of medium-bedded, light grey to yellowish-white quartzite which weathers to faintly reddish and yellowish-white colours. The quartzite is interbedded with grey argillites at places. The grain size of the quartzite ranges from fine to coarse. In the upper stratigraphic levels, the quartzite is subconglomeratic at places. The quartzite is cross-bedded and ripple marks are rare at the interfaces between quartzite and argillite. Iron specks are common in the quartzite beds of the formation.

The lower contact of the formation is not exposed whereas its upper contact is unconformable with the Sherwan formation.

Sherwan Formation

Baig and Lawrence (1987) introduced the name "Sherwan formation" for the dolomite and quartzite sequence above the Tanawal Formation in the Tanawal area. Reference section in the study area is located east of Darwaza village (Lat. 34° 5′ 0″ N, Long 72° 57′ 0″), 10 km north of Haripur (Fig. 1). The formation crops out along an extensive belt, stretching from Haripur to Darband and Mansehra through Sherwan area which forms the Tanawal territory of Hazara. The formation is intensely folded and faulted making the measurement of thickness difficult. The estimated thickness is about 300 m in this area.

No fossils have been reported so far from the formation. The age assigned by the previous workers is mainly based on its stratigraphic position and lithological similarities with other rocks in Hazara and adjoining areas. In northern Hazara, the Mansehra granite intrudes the Tanawal Formation. Le Fort *et al.*, (1980) have reported a whole rock Rb/Sr age of about 516 ± 16 Ma for the granite body, thus restricting the Tanawal Formation to Precambrian age.

Lithologically the formation is divided into three members from bottom to top; an argillite member, a quartzite member and a dolomite member.

The basal part of the argillite member at several localities consists of conglomerate which has poorly

Table - 1.   Stratigraphic schemes for the Southern Tanawal area as proposed by various authors.

Middlemiss (1896)	M. Ali (1965)	Calkins et al. (1975)	Baig et al. (1987)	Suggested by author
Infra-Triass	*Abbottabad Formation — Cambrian:* Dolomite member; Quartzite member; Quartz mica schist member; Basal conglomerate member	*Kingriali Formation (Triassic):* Dolomite unit; Lower Quartzite unit; Phyllite unit	Sherwan Formation	*Sherwan Formation — Cambrian:* Dolomite member; Quartzite member; Argillite member
———————————————————————— Unconformity ————————————————————————				
Tanol Quartzites	Tanol Formation	Tanawal Formation	Tanawal Formation	Tanawal Formation — Pre-cambrian

Table - 2.   Stratigraphic position of the Sherwan and Abbottabad Formations in the Tanawal and Abbottabad Zones.

TANAWAL ZONE (PRESENT REPORT)	ABBOTTABAD ZONE (LATIF, 1974)
Misri Banda Quartzite	Hazira Formation
———————————— Unconformity ————————————	
Sherwan Formation	Abbottabad Formation
———————————— Unconformity ————————————	
Tanawal Formation	Hazara Formation

Table - 3   Stratigraphic column for the Southern Tanawal area, north of Haripur.

AGE	FORMATION	MEMBER	
CAMBRIAN	SHERWAN	DOLOMITE	
		QUARTZITE	
		ARGILLITE	
PRE-CAMBRIAN	TANWAL		

LEGEND

DOLOMITE
QUARTZITE
CONGLOMERATE
ARGILLITE
CROSS BEDDED
SANDY
ARGILLICEOUS

SCALE
100 m.
0
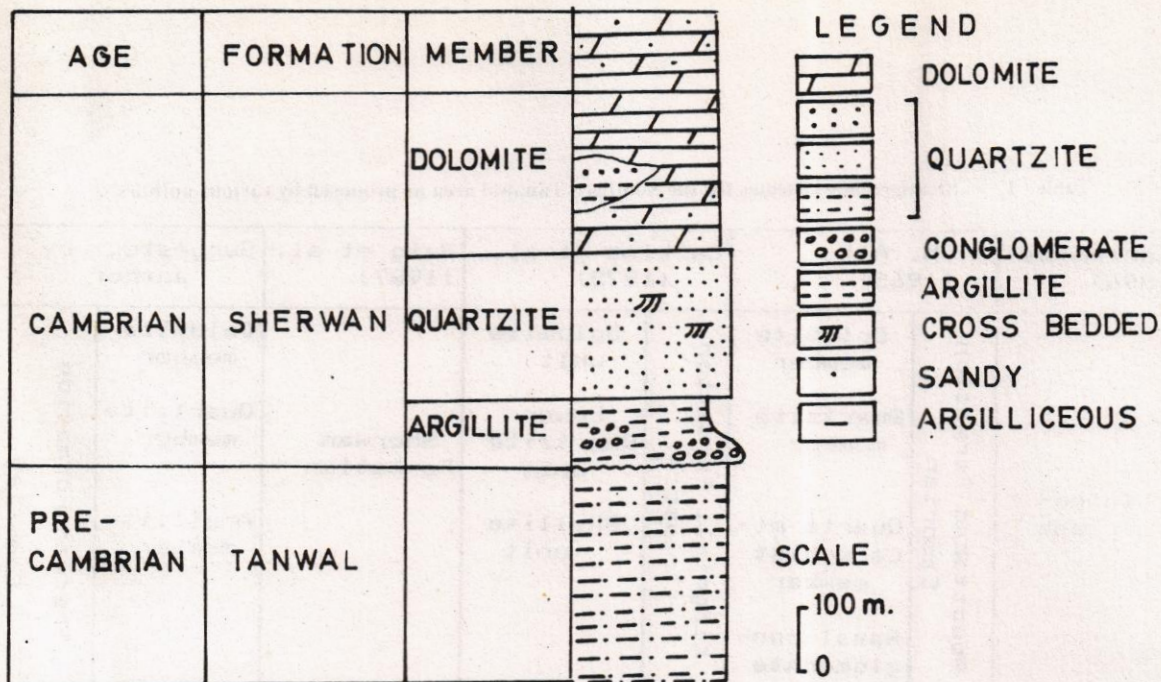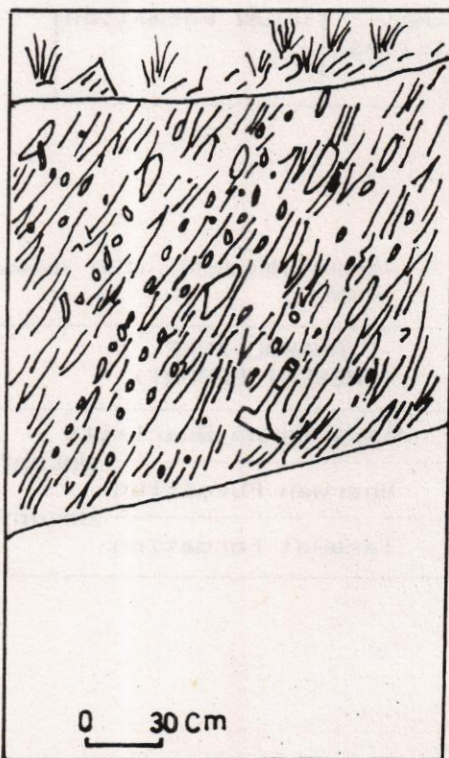
Fig. 3 Tannaki Boulder Bed at the base of Abbottabad Formation, West of Mount Sirban, Khoti-di Qabar; sketch drawn from a colour slide.

Fig. 4 The conglomerate bed exposed at the base of the Sherwan formation along the Bir-Chappar road, south of Kachi, Hazara; sketch drawn from a colour slide.

158

sorted clasts. However, it is not restricted to the base of the member at places. The clasts mainly consist of white to grey quartzites and grey argillites embedded in argilliceous and sandy matrix. The clasts range in size from a few cm to about 40 cm in diameter and are commonly elongated parallel to the bedding. The conglomerate bed is about 30 m thick in places and gradually passes upwards into the quartzite member.

The quartzite member mainly consists of medium to thick-bedded quartzites. At its lower contact it is a light grey fine-grained quartzite, followed by greenish-grey quartzite and at the top it grades into coarse-grained yellowish-white quartzite. The grain size ranges from fine to coarse. The upper yellowish - white quartzite is very coarse-grained and on weathering produces rubbly material. The quartzite is cross-bedded and argilliceous laminations are common. The thickness of this unit is variable and ranges from 150 to 210 m. It attains maximum thickness south of village Chanjaliala (Fig. 1). Its upper contact with the overlying dolomite member is sharp and has a bed of about one meter thick dolomitic quartzite at places.

The dolomite member at the base is greyish-brown, weathers to brown, coarse-grained, recrystallized and medium bedded dolomite. It is sandy and has chert nodules and lenses. This grades upwards into thin to medium-bedded white, grey and pinkish dolomite. Which is fine-grained, recrystallized and has argilliceous laminations, resembling stromatolites. At about 60 meter above the base, the dolomite member has a quite persistent bed of quartzite-argillite in the form of lenses. Above the quartzite unit, the dolomite is medium-grained, grey in colour on fresh surfaces and weathers to brownish-grey colour. The weathered surfaces typically displays butcher's chopping board pattern.

In the upper horizon of the member cherty and argilliceous layers are common. Also dark grey limestone beds are found at few places. Its thickness is estimated about 400 meters. The lower contact with the quartzite member is sharp. Its upper contact is not exposed in the study area. However, a 60 meter thick lense of conglomerate is seen in the core of the largest syncline of the area, north of village Aluli (Fig. 1). The conglomerate consist of 80% argillite, 10% quartzite and 5% dolomite clasts. The quartzite clasts are grey to white, well rounded, embedded in coarse-grained quartzitic or argilliceous quartzitic matrix. The quartzite clasts are sometimes so densely packed that it gives a clast supported texture.

The dolomite member has thick and quite persistent lenses of quartzite-argillite at an approximate statigraphic height of 70 to 80 meters at various places (Table-3). These lenses have about 20 meters thick argillite at the base followed gradationally upward by a 30 meter thick grey coloured quartzite. The quartzite is medium-bedded, fine-grained and occasionally cross-bedded. Pyrite cubes are occasionally present.

The Sherwan formation is widely distributed in the lower and upper Tanawal region. Its thickness is estimated to be 750 meters in this area.

Baig and Lawrence (1987) and Hussain et al. (1990) have reported Ordovician quartzite (Misri Banda quartzite) overlying the Sherwan formation, north of the study area in the core of Sherwan syncline (Fig. 2). Baig and Lawrence (1987) have assigned Cambrian age to the formation on the basis of "Hyolithids" fossils reported from Sherwan area.

REMARKS

It is very difficult to differentiate between the Tanawal quartzite and the quartzite member of the Sherwan formation in outcrop. They are nearly identical in colour, grain size and bedding. The only difference is that the argillite interbeds are very regular in Tanawal quartzites and iron specks are quite prominent but lack in the Sherwan Formation.

CONCLUSIONS

Previously it was believed that the dolomite-quartzite sequence exposed north and south of the Panjal fault in southern Hazara is similar and was named as Abbottabad Formation. But the present investigation and the literature study of the recent research, led to the conclusion that the dolomite-quartzite sequence exposed in the two tectonic blocks is remarkably dissimilar and must be differentiated from each other. This conclusion is based upon the stratigraphic position, tectonic setting and lithologic comparision of the dolomite - quartzite sequence present in the two zones.

REFERENCES

Ali, C. M., (1962). The stratigraphy of the south western Tanol area, Hazara, west Pakistan. *Geol. Bull. Punjab. Univ.*, Vol. 2, pp. 31-38.

Baig, M. S., and Lawrence, R. D., (1987). Precambrian to Early Paleozoic orogenesis in the Himalaya. *Kashmir Jour. Geol.*, Vol. 5, pp. 1-2..

Calkins, J. A., Offield, T. W., Abdullah, S. K. M., and Ali, S. T., (1975). Geology of the southern Himalaya in Hazara, Pakistan, and adjacent areas. *U. S. Geol. Surv. Prof. Paper 716-C*, pp. 1-20.

Fuchs, G., (1975). Contribution to the geology of north western Himalaya. *Abh. Geol. Bund. Wein 23*, pp. 40-46

Hussain, A., Pogue, K., Khan, S. R., and Ahamd, I., (1990). Working paper on the stratigraphy of Nowshera area, Pakistan. *Geol. Bull Univ. Peshawar*, Vol. 23, *In Press.*

Latif, M. A., (1974). A Cambrian age for the Abbottabad group of Hazara, Pakistan. *Geol. Bull. Punj. Univ.*, Vol. 10, pp. 1-20.

Middlemiss, S. S., (1896). Geology of the Hazara and Black Mountain. *Mem. Geol. Surv. India.*, Vol. 26, pp. 1-302.

Waagen, W., and Wynne, A. B., (1872). The geology of Mount Sirban in Upper Punjab. *Mem. Ged. Surv. India.*, Vol. 9, pp. 331-350.

THE FACIES CONTROL OF MINERALIZATION OF THE HANGU FORMATION IN HAZARA, ISLAMABAD AND AZAD KASHMIR

By

M.A. LATIF* M.H. MUNIR**, M. ANWER QURESHI**
NAZIR AHMED* AND M. S. TAREEN*
*Institute of Geology, University of the Punjab, Lahore.
**Institute of Geology, Azad Jammu & Kashmir University, Muzaffarabad, Azad Kashmir.

ABSTRACT: The Hangu Formation (Paleocene) reveals a range of lithologies in Hazara - Islamabad, northern Rawalpindi District and Azad Kashmir areas. Five lithologies comprise, the Hangu Formation i.e., bauxite facies (Azad Kashmir), laterite facies (Southeastern Hazara), haematite facies (central regions of Hazara), laterite cum arenaceous facies (mid northwestern Hazara region) and arenaceous/quartzitic facies (northwestern Hazara region). The five facies are delimited by thrusts and have been recognized as the members of the Hangu Formation.

INTRODUCTION

The first mention of the rocks now recognized as the Hangu Formation was made as a passing reference by Waagen and Wynne (1872) while describing the geology of Mount Sirban in the south of Abbottabad. The said unit was sandwitched between the underlying bedded grey limestones with minute unrecognized microfossils and overlying nummulites bearing massive limestones. For lack of definite proof of age, the grey limestone lying below the Hangu Formation was treated as the basal part of the Paleogene sequence by Middlemiss (1896).

For convenience of the field recognition Middlemiss (1896) preferred to select a 2 to 3 m thick bright-orange to chrome orange coloured sandy fossiliferous limestone, resting over sandstone sequence, now known as the Lumshiwal Formation, as a marker bed below the Paleogene rocks.

The coal indicated at number 2 was the first to be investigated, Middlemiss (1890) in the Dor Valley near abbottabad. He later attempted to bring an order to the accumulated geological information and unfinished geological investigations carried out by Wynne. Middlemiss (1896) further recognized "carbonaceous clays, powdery sand and coarse-grained grit" in Hazara. Beyond the limits of Hazara he recognized a "variegated sandstone overlying a coarsely pisolitic ferruginous band" at Hassanabdal similar to

rocks at the base of nummulitic series at Sabathu and in the western British Garhwal. He also recognized this horizon as homotaxial with the Basal Paleocene coal horizon of the Salt Range.

During the 1960's investigations by the University of the Punjab, microfossils of the Late Cretaceous age were discovered in the grey limestone, Latif, (1962) which is now called the Kawagarh Formation. Top of this formation marks the Cretaceous-Tertiary boundary. Midway between the two areas, i.e., Abbottabad in the north and Changlagali in the south, Khan and Ahmad, (1966) described oolitic haematite marking the Cretaceous-Tertiary boundary. Facies variations in the Hangu Formation were described by Latif (1969). Bauxite at Muzaffarabad was investigated by Malick *et al.*, (1971). Further southeast in Azad Kashmir, bauxite was reported to occur at the base of Paleogene deposits, Ashraf and Chaudhry, (1978; Ashraf *et al.*, 1982).

Keeping in view the variations in rock types at the base of Paleogene it was found necessary to investigate the occurrences of the Hangu Formation to bring an order to the lithologic chaos. The systematic studies involved, detailed measurements of the Hangu Formation both vertically and laterally which studies are being carried out separately. It was decided to restrict this study to preliminary investigations of the unit to bring a general order to a variety of the rocks constituting the unit. The detail of lithofacies study is

not presented in this paper. The bed to bed vertical variations have been ignored for the general dominating lithology to enable us to have a general view of the changes. For this purpose variations in composition of SiO_2, Al_2O_3 and Fe_2O_3 only, have been considered.

MESOZOIC - CAENOZOIC STRATIGRAPHIC SEQUENCE OF SOUTH EAST HAZARA &/OR AZAD KASHMIR

Group	Formation	
	Murree Formation	
	Kuldana Formation	
	Lora Formation	
	Margala Hill Limestone	
Galis	Patala Formation	Paleogene
	Lockhart Limestone	
	Hangu Formation	
	Kawagarh Formation	Cretaceous
Hothla	Lumshiwal Formation	Jurassic
	Chichali Formation	
	Samana Suk Formation	Jurassic
Thandiani	Shinawari Formation	
	Datta Formation	
	Tarnawai Formation	Ammended after Latif (1976).

STRUCTURAL AND LITHOSTRATIGRAPHIC SETTING

The area immediately south of the Hazara-Kashmir Syntaxis is structurally complex. There are two major thrusts, i.e, Panjal and Murree heading from Indian held Kashmir into Azad Kashmir in a northwestern direction, Wadia, (1928). Both these thrusts run almost parallel with few exceptions, like for instance near the Neelum river where they merge into one. Westwards the two end up sharply against the Jhelum Fault, heading from north of Balakot southwards passing by the eastern end of the Salt Rang. Another major thrust is the Himalayan Frontal Thrust, which heads towards Kotli, Azad Kashmir and Balakot from the Indian held Kashmir and sharply truncates against the Jhelum Fault (Fig. 1, Baig and Lawrence, 1987).

Across the Jhelum Fault from north of Balakot to the eastern end of the Salt Range, a number of major and minor thrusts truncate against the Jhelum Fault (Baig and Lawrence, 1987). It is however, an enigma to pinpoint with certainty the equivalents of the Himalayan Frontal Thrust of Azad Kashmir with those

on the west of Jhelum Fault. Southeast of the Panjal Thrust the major thrusts are Sangargali, Chitragali, Phalkot, Nathiagali, Ayubia, Murree and Khair-i-Murat (Fig. 1). The Precambrian to Caenozoic rocks of Hazara have been imbricated by northwest dipping thrust faults. Due to imbrication the different facies of the Hangu Formation have been juxtaposed.

STRATIGRAPHIC RELATIONSHIP OF THE HANGU FORMATION

Against the absence of Cretaceous rocks in the Salt Range and the Potwar, due to unconformity, the Hangu Formation in Hazara, is resting over the eroded surface of the Kawagarh Formation. In the bordering region of the Islamabad and the Rawalpindi districts, the Hangu Formation either rests over the reduced Kawagarh Formation as at Saidpur or over Lumshiwal Formation as at Sangjani. This is due to the down cutting of underlying beds by the Paleocene unconformity which is more pronounced southeast & southwards. Lockhart Limestone is invariably overlying the Hangu Formation in all the areas the Hazara, Islamabad/Rawalpindi and Muzaffarabad.

The contact relationship of the Hangu Formation with the underlying and overlying formations in Kotli District, Azad Kashmir is, somewhat different and has its own regional aspect. The beds underlying the so called Hangu Formation belong to the Cambrian, Sirban Formation (Ashraf et al., 1983). The disconformity in Azad Kashmir both at Kotli and Muzaffarabad districts seems to merge various planes of Toarcian, Oxfordian and Danian unconformities of Hazara. The upper contact also shows a regional aspect different from Hazara. The so called Hangu Formations in Kotli area is overlian by the Patala Formation followed by thin Margala Hill Limestone with Lockhart Limestone missing.

REGIONAL DISTRIBUTION OF VARIOUS FACIES OF THE HANGU FORMATION

Bauxite Facies: This facies is predominantly developed in Azad Kashmir, though, due to local effects it may also be present in southeastern Hazara. The facies is mainly composed of pisolitic bauxite. It is a compact, massive and greyish, greenish bauxite with high specific gravity. The percentage of alumina increases as compared to iron.

In Muzaffarabad area, it occurs at Khilla and Batoming and in Kotli area, at Bangong, Batla Khajari, Balmi, Barmoch, Dhanwan, Dandili, Goi, Janjora,
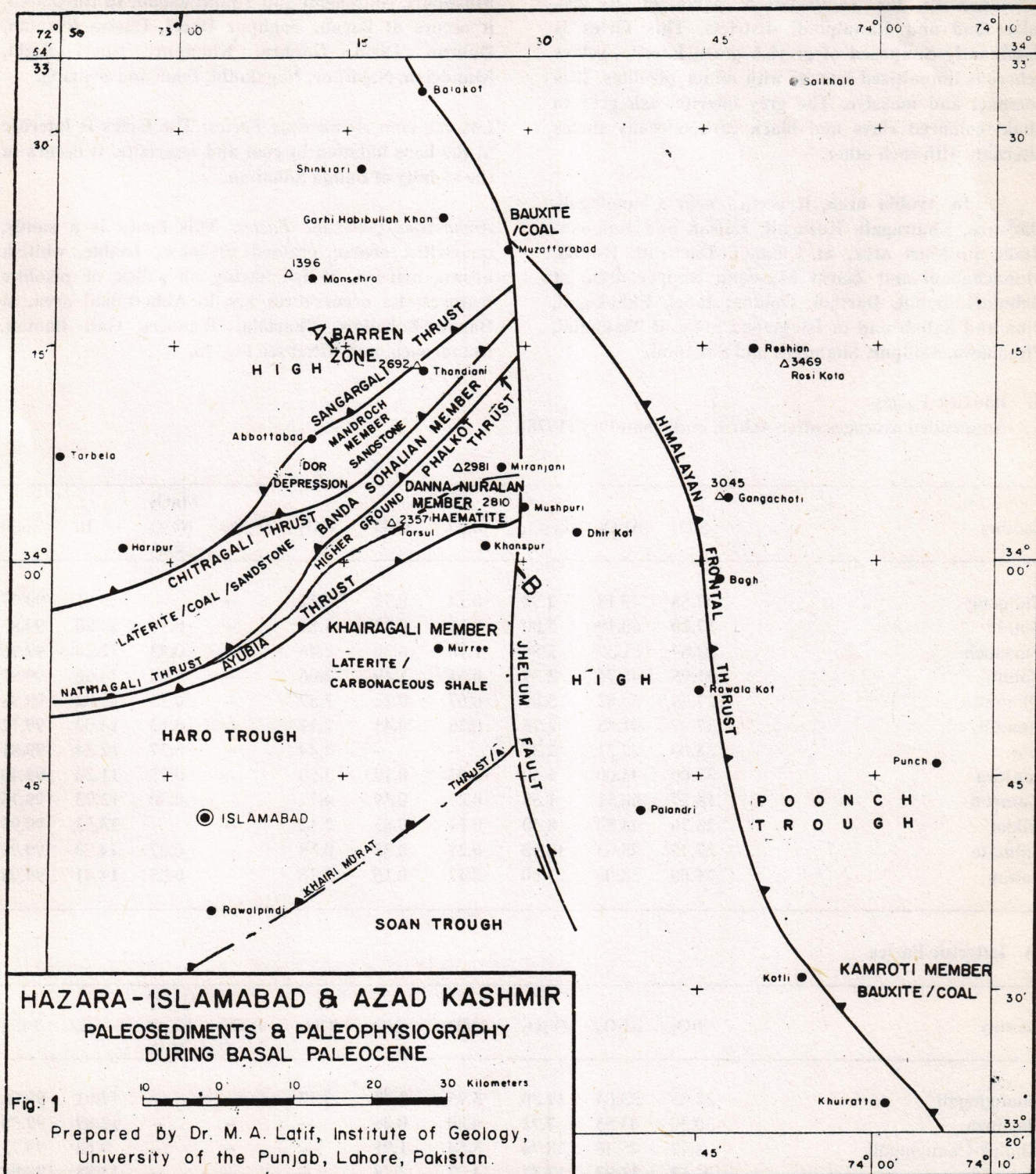
Fig. 1 Geological map of the Southern Tanawal area, north of Haripur, N.W.F.P; Pakistan.

Kamroti, Khandar, Nikial, Selhun, Salmote, Sawar, Gunimalni and Tattapani.

Lateritic Facies: This facies is predominantly developed in the southeastern parts of Hazara, Islamabad and Rawalpindi districts. This facies is dominantly composed of greyish green laterite, yellow ocherous limonitized laterite with minor pisolites. It is compact and massive. The grey laterite, ash grey to khaki coloured clays and black carbonaceous shales alternate with each other.

In Ayubia area, it occurs near Changlagali, Darwaza, Khairagali, Kuzagali, Kalsan and Kalaban-Riala; in Mari area, at Chanali, Darband, Hothla, Mandehabani and Ziarat Masoom; Rupper area, at Babutari, Bandi, Dartian, Gokina, Jabri, Kohalagali, Pina and Sahab and in Islamabad area, at Makhnial, Pirsohawa, Saidpur, Shahdara and Sangjani.

Haematitic Facies: It is dominantly an oolitic haematite with high specific gravity. It is black, brown, red, and maroon in colour. This facies is reported at Dungagali pipeline road, Dungagali - Ayubia ridge top, Kundla, Moshpuri, Nathiagali and Tauheedabad. In Nara area, it occurs at Bagan, Baghpur Dheri, Danna Nuralan, Dubran, Disal, Gauhra, Khanpur, Kheri Rajki, Mundrian, Najafpur, Nagakothi, Pona and Sribang.

Lateritic cum Arenaceous Facies: The facies is lateritic at the base followed by coal and quartzite. It occurs in the vicinity of Banda Sohalion.

Arenaceous/Quartzitic Facies: This facies is a sandy, quartzitic, coarse grained to loose, friable, whitish brown, maroon, redish having no oolitic or pisolitic features. Its occurrences are in Abbottabad area, at Banda Sohalian, Chariala, Jhanseri, Gali Banian, Mandroach, and Kihal see Fig. 10.

a) Bauxitic Facies
Ammended averages after Ashraf and Chaudhry (1978).

Locality	SiO_2	Al_2O_3	Fe_2O_3	MgO	CaO	TiO_2	P_2O_5	MnO_2 Na_2O K_2O	IL	Total
Bangong	37.58	43.18	2.92	0.14	0.72	0.22	--	--	15.21	99.97
Botala	17.20	60.19	5.00	0.21	0.32	1.81	--	0.30	14.80	99.83
Barmoch	22.64	51.39	2.86	1.78	6.20	2.46	--	0.43	12.20	99.96
Balmi	31.05	46.76	3.39	0.31	1.49	2.06	--	0.30	14.56	99.92
Dhanwan	27.34	50.82	5.09	0.07	0.12	2.59	--	0.13	13.82	99.98
Dandili	37.97	41.48	2.75	0.25	0.43	2.71	--	0.13	14.00	99.72
Goi	35.03	47.31	2.37	--	--	2.44	--	0.37	12.34	99.81
Janjora	37.00	46.00	1.50	0.05	0.10	3.50	--	0.95	11.20	99.40
Kamroti	18.27	60.51	1.58	0.27	0.39	4.71	--	0.30	13.73	99.76
Nikial	26.26	48.80	8.30	0.11	0.83	2.12	--	--	13.53	99.95
Salmote	27.75	45.63	10.90	0.21	0.75	0.38	--	0.07	14.30	99.99
Sawar	25.00	54.00	3.00	0.12	0.15	3.25	--	0.05	14.41	99.98

b) Lateritic Facies

Locality	SiO_2	Al_2O_3	Fe_2O_3	MgO	CaO	TiO_2	P_2O_5	MnO_2 Na_2O K_2O	IL	Total
Changlagali	22.43	33.64	19.80	5.95	2.47	2.77	--	--	12.01	99.66
Darwaza	30.30	43.53	7.72	4.80	0.26	--	--	--	12.89	99.50
Khaira-Changlagali	8.42	45.46	28.74	5.54	1.91	--	--	--	9.68	99.75
Kuzagali	24.52	38.87	13.77	4.03	2.58	--	--	--	13.88	98.94

c) Haematitic Facies.

164

Locality	SiO₂	Al₂O₃	Fe₂O₃	FeO	MgO	CaO	P₂O₅	TiO₂	S	IL	Total
Mundrian	16.60	13.8	48.97	3.60	2.07	3.97	1.6	0.63	.11	9.0	100.35
Durban	8.20	7.90	67.37	1.37	2.10	2.57	1.03	0.47	.11	8.47	99.59
Nagakothi	18.40	14.90	40.40	7.00	3.00	4.23	1.37	.63	.06	9.63	99.62
NW Durban	14.75	13.30	51.10	3.60	1.60	5.15	1.00	.45	.04	9.30	100.29
NNW Pona	24.63	16.60	39.45	4.25	2.15	2.83	1.48	.30	.07	8.75	100.51
Bagan	17.40	15.55	37.30	11.55	3.30	3.80	--	.22	--	8.25	97.37
Bagnotar	21.15	13.93	28.35	14.55	2.90	4.53	--	.24	--	9.45	95.10
Gauhra	30.28	15.63	39.08	3.90	1.25	1.70	1.25	.26	.04	6.98	100.72
Danna Nuralan	11.60	10.57	64.00	2.43	1.53	2.10	1.26	.35	.50	5.73	100.07
Majuhan	16.43	12.25	40.93	4.00	1.85	9.2	1.18	.33	.03	14.00	100.20

d) **Arenaceous Facies.**

Locality	SiO₂	Al₂O₃	Fe₂O₃	MgO	CaO	TiO₂	P₂O₅	S	IL	Total
Banda	45.90	9.40	33.40	--	--	--	--	--	11.10	99.80
Kathwal	54.93	4.80	22.50	--	--	--	--	--	17.31	99.54
Mandaroch	75.80	6.20	10.60	--	--	--	--	--	7.23	99.83
Kihal	76.00	3.20	9.00	--	--	--	--	--	11.20	99.40

SUBDIVISIONS OF THE HANGU FORMATION

As the Hangu Formation is represented in Hazara, Islamabad and Azad Kashmir by five distinct facies identifiable and mappable in separate regions, it is suggested that each facies may be recognized as a member and named after the localities where the relevant facies are better exposed.

Kamroti Member: After Kamroti (Long, 74°01′ 40″N. Lat. 33°59′ 30″E) Azad Kashmir, where bauxite facies is ideally exposed.

Khairagali Member: After Khairagali (Long 73°11′ 25″N, Lat. 33°59′ 30″E) where lateritic facies is ideally exposed.

Danna Nuralan Member: After Danna Nuralan (Long. 73°11′ 25″N, Lat. 33°56′ 25″E) Hazara where haematitic facies is ideally exposed.

Banda Sohalian Member: After Banda Sohalian (Long. 73°.16′.40″, Lat. 30°.07′.00″) Hazara, where lateritic cum arenaceous facies is ideally exposed.

Mandroch Member: After Mandroch (Long. 73°17′ 26″N, Lat. 34°11′ 30″E) Hazara where arenaceous facies is ideally exposed.

DISCUSSION

The top of the Kawagarh Formation (Late Cretaceous) in Hazara was subjected to erosion during early Danian (Paleocene). The erosion is more pronounced in the south-southeast than in the west-northwest. In the south at Juri, near Sangjani Rawalpindi District, complete removal of the Kawagarh Formation occurred due to erosion and the Hangu Formation rests directly over the Lumshiwal Formation. There is a gradual increase in the thickness of the Kawagarh Formation from Saidpur in the south to Abbottabad in the north.

In Azad Kashmir, however, the situation is quite different. In Muzaffarabad and Kotali, the hiatus extends from Middle Cambrian to Late Cretaceous and as a result, the Hangu Formation rests over Early Cambrian, Sirban Formation (Ashraf *et al.,* 1983). Pisolitic bauxite is exposed in most of the Azad

Fig. 2 TIRANA(HAZARA)-MINHAS(MURREE) CROSS SECTION SHOWING THRUST AND FACIES RELATIONSHIP OF HANGU FORMATION

Fig. 3 LITHOFACIES OF HANGU FORMATION & PALEOENVIRONMENT RELATIONSHIP (DIAGRAMATIC)

Fig. 3 Prepared by Dr. M. A. Latif.

Kashmir (Ashraf and Chaudhry, 1982). The alumina rich clays and bauxites may be due either to nearness of crystalline rocks or to the long exposure from Middle Cambrian to Late Cretaceous or both (Ashraf and Chaudhry, 1982).

In the first belt, in Hazara the Hangu Formation found at various localities between Juri-Sangjani-Saidpur, Islamabad district, extending towards Khairagali-Kuzagali in a southwest-northeast strike direction is composed of laterite (Fig. 1) with rocks relatively richer in alumina content exposed south-eastwards. The second belt, situated northwest-north of Kuzagali and south-southeast of Bagnotar and Abbottabad-Thandiani is composed of sandstone/orthoquartzite. The Al_2O_3, which is high at Khairagali in south-southeast is reduced to almost nil at Kihal in north-northwest near Abbottabad (Fig. 2). The Fe_2O_3 content is reduced from almost nil at Khairagali in southeast to 9% near Abbottabad in northwest and SiO_2 content increases from 3.28% in southeast to 79% in northwest. The central block is dominated by Fe_2O_3 content (Fig. 2). There is generally a sharp division between various sets of compositions. It appears that laterite is produced as a product of weathering in the southern block. The iron content was transported in colloidal form to shallower conditions where it transformed into oolitic haematite. Beyond the oolitic environments sandstone was deposited with iron traces. It may not be strange to record the absence altogether of Hangu Formation in areas close to Thandiani in the northwest, though a separate block has not been indicated. All the present blocks show abrupt appearance of various facies of the Hangu Formation. All the facies are to be separated by various thrusts (Fig. 3). The lateritic facies appears to be bounded by Murree Thrust in the southeast and Ayubia Thrust in the northwest. The haematitic facies is bounded by Ayubia Thrust in the southeast and Phalkot Thrust in the northwest. The lateritic cum arenaceous facies is bounded by Phalkot Thrust in the southeast and Chitragali Thrust in the northwest. The sandstone/orthoquartzite facies is bounded by Chitragali Thrust in the southeast and Sangargali Thrust in the northwest if not further southwest by Salhad Thrust. The nearness of various facies and absence of the passage beds is explained only by the relevant thrusts which have brought the far apart facies close together, see Figs. 1 and 3.

As far as the Azad Kashmir exposures are concerned these are also enclosed in the Himalayan Frontel Thrust and the Main Boundary Thrust/Murree Thrust.

CONCLUSIONS

The contact between rocks of Paleogene and older is an unconformity. Hiatus is widespread in Azad Kashmir where Hangu Formation rests over the Cambrian rocks. In southeastern parts of Hazara and Rawalpindi districts, the Hangu Formation rests over variously eroded surfaces of the rocks of Cretaceous age. In the central and northwestern parts of Hazara the Hangu Formation rests over the more completer sequence of Late Cretaceous age. The Hangu Formation in the first two blocks is of lateritized nature and in the later three blocks of the depositional nature.

The first phase of the splitting of the mighty Tethys is conspicuous during the deposition of the Hangu Formation as displayed by its varied lithology. Five different lithological sequences are recorded in various adjacent regions and are identified as Kamroti Member (Bauxite and coal); Khairagali Member (Laterite and carbonaceous sahle); Danna Nuralan Member (oolititic haematite); Banda Sohalian Member (laterite, coal and sandstone) and Mandroch Meber, (sandstone and quartzite). A belt unrepresented by the Hangu Formation is identified as the Barren Zone and represents a high further northwest of the Dor Depression see Figs. 1 & 4. The variations in the chemical composition of the lower non carbonaceous materials clearly separates Al_2O_3, Fe_2O_3 and SiO_2 rich belts, Figs. 1 & 2, situated in south east, centre and northwest respectively, specifying the variety of environments, see Fig. 4.

The above evidence proves the presence of highs in the southeast and northwest with a central depression receiving sediments from both sides see Fig. 1 & 4. The various facies have sharp contacts, as each facies in northwest is thrusted over the adjacent are in the southeast. The various lithofacies - thrust distribution from northwest to southeast is as fallows. Barren Zone-Sangargali Thrust-Mandroch Member-Chitragali Thrust-Banda Sohalian Member-Phalkot Thrust-Danna Nuralan Member-Ayubia Thrust-Khairagali Member, see Figs 1 & 3, Kamroti Member, not shown in the figure is thrusted southwest wards along Himalayan Frontal Thrust. It may not be out of place to mention that the Danna Nuralan Member was formed in northwest of the Haro Trough and southeast of Dor Depression, receiving deposits from both sides with central regions tough relatively evlevated, marking a line of division between Haro Trough & Dor Depression. The north western deposits of Danna Nuralan Member exposed near Bagnotar, appears to be separatead from southeastern deposits of Danna

Nuralan Member by Nathiagali Thrust Figs. 1 & 3. The final position of basinal set up at basal Paleocene indicates presence of Poonch Trough in Azad Kashmir, separated by a high in the east from rest of the troughs, Soan Trough in southeast, Haro Trough in middle and Dor & Neelum depression in the northwest, in line with Paleophysiographic model during Early Eocene, Latif *et al.*, (in press).

ACKNOWLEDGEMENTS

REFERENCES

Ashraf, M. and Chaudry, M N., 1978. Preliminary Mineral Survey in Kotli & Poonch districts of Azad Kashmir Vol. 1, Kotli E.C.L. Report (unpublished) pp 54-56

Ashraf, M,, and Chaudhry, M.N., (1982). Clayey bauxite and clay deposits of Kotli district of Kashmir. *Contr Geol Pakistan* Vol. 1, pp. 87-108.

Ashraf, M., Chaudhry, M.N., and Qureshi, K.A., (1983). Stratigraphy of Kotli area of Azad Kashmir and its correlation with standard type areas of Pakistan. *Kashmir Jour. Geol.*, Vol. 1, pp. 19-30.

Baig, M.S., and Lawrence, R.D., (1987). Precambrian to Early Palaeozoic Orogenesis in the Himalaya. *Kashmir Jour. Geol.*, Vol. 5, pp. 1-22.

Khan, S.N., and Ahmad, W., (1966). Iron deposits of Langrial district Hazara, West Pakistan *Geol. Surv. Pakistan Pre. Publ.*, Vol. 25, pp. 1-15.

Latif, M.A., (1962). An Upper Cretaceous limestone in Hazara district. *Geol. Bull. Punjab University*, Vol. 2, pp. 57.

Latif, M.A., (1969). Stratigraphy of South Eastern Hazara and parts of Rawalpindi and Muzaffarabad districts. Unpublished Ph.D thesis Univ. London pp. 169-171, Fig. $^8/_2$.

Latif, M.A., (1976). Stratigraphy and Micropalaeontology of Galis Group of Hazara, Pakistan. *Geol. Bull. Punjab University*, Vol. 13, pp. 1-64.

Latif, M.A., Iqbal, H. & Yasin A.R. A model of the Early Eocene sediments in upper Indus Basin, Northern Pakistan. Ideas for effective exploration. *Pakistan Journal of Petroleum Technology* (in press).

Middlemiss C.S. (1890). A preliminary note on the coal seam of the Dor River Hazara. *Rec. Geol. Survy. India*, Vol. 123, part 4.

Middlemiss, C.S. (1896). The Geology of the Hazara and the Black Mountains. *Mem. Geol. Surv. India*, Vol 26, pp. 38-41.

Shah, S M.I., (1977) Stratigraphy of Pakistan. *Mem. Geol. Surv., Pakistan*, Vol. 12, pp. 64-65.

Waagen, W., and Wynne, A.B., (1872). The Geology of the Mount Sirban in the Upper Punjab. *Rec. Geol. Surv. India*, Vol. 9, pp. 331-350.

Wadia, D.N., (1928). The Geology of Poonch State (Kashmir) and adjacent portions of the Punjab. *Mem. Geol. Surv. India*, Vol. 51, pp. 185-370.

STRATIGRAPHICAL PALYNOLOGY, VEGETATIONAL HISTORY AND PALAEOECOLOGY OF PERMIAN OUTCROP (AMB FORMATION) FROM WARCHHA GORGE, WESTERN SALT RANGE, PAKISTAN

By

KHAN RASS MASOOD*, KALEEM A. QURESHI**, M. JAVAID IQBAL*,
HUSSAIN R. SHARF*, AND ZAHID HUSSAIN***
*Department of Botany, Punjab University, Lahore.
**Geological Survey of Pakistan, Lahore.
***Department of Biology, F. G. College, Islamabad.

ABSTRACT: *Stratigraphic analysis of palynological data of the selected outcrop of Amb Formation from the Western Salt Range, Pakistan, has led to the recognition of three palynostratigraphic zones, viz;* Todisporites minor *Assemblage zone,* Acanthotriletes spinosus *Assemblage zone, and* Potoniesporites elegans *Assemblage zone, 23 species representing 16 genera of pollen and spores were recovered. Late Permian age is confirmed for the Amb Formation on the basis of palynomorph composition. Vegetational history, palaeoecology and depositional environment of the Amb Formation are suggested based upon miospore analysis.*

INTRODUCTION

Paleozoic palynology of the Salt Range began in late-1930's with the publication by Virkki (1937, 1946) on miospore genus *Nuskoisporites* Potonie and Klaus, and many other striated and non-striated vesiculate palynomorphs from the Talchir beds (Tobra Formation), Central Salt Range, Pakistan. Between then and now several series of publications have appeared (Gosh & Bose, 1951; Venkatachala & Kar, 1968; Balme 1970; Masood and Qureshi, 1991 (a); 1991 (b)). mainly dealing with descriptive palynology, with very little emphasis on regional biostratigraphy or palynostratigraphy. The palynostratigraphical determinations and correlations which are helpful in resolving detailed stratigraphical questions concerning depositional history, paleoecology, paleoclimatology and age confirmation have never been worked out. The present investigation presents new data towards a better understanding of the above mentioned aspects. It is a technical addition to the previous work based on the palynological analysis of 21 rock samples obtained from a selected upper Permian outcrop (Amb Formation) from the Western Salt Range, Pakistan.

GEOLOGY AND STRATIGRAPHY

A brief summary of the geology of the sampling site (Lat. 32°29' 12", Long 71°58' 45", Fig. 1) is given below. Readers are referred to P.J. Group (1981) for more detailed information. Amb Formation falls in the basal part of rocks of the "Zaluch Group" of Salt Range, Pakistan. The formation is mainly composed of sandstone, limestone and shale. Sandstone is grey, medium grained, calcareous and medium to thick bedded. These sandstone beds occupy the lower part of the formation. The calcareous bed associated with the sandstone contains abundant fusulinids. Upwards in the sequence, limestone with some shale appears. The limestone is sandy, and brownish grey, medium bedded and richly fossiliferous.

The shale is light to dark grey. The formation is well developed in the Western Salt Range and thins out eastwards.

PREPARATION METHODS

Maceration of the sediments involved common techniques such as those described by Phipps and

Buri Khel

Lake Nammal

Toroppi N.

Gotoi N.

Musa Khel

Chhidru

Sakesar

Uchhali

Bhocha Wahan

Amb

Lundi N.

Warcha Gorge

Study Area

Warcha

45' 72' 70° 28° 32°30'

AFGHANISTAN

PAKISTAN

INDIA

Jammu & Kashmir

Salt Range

500 Km

Scale
Metres 5000   0   5   10 Kilometres
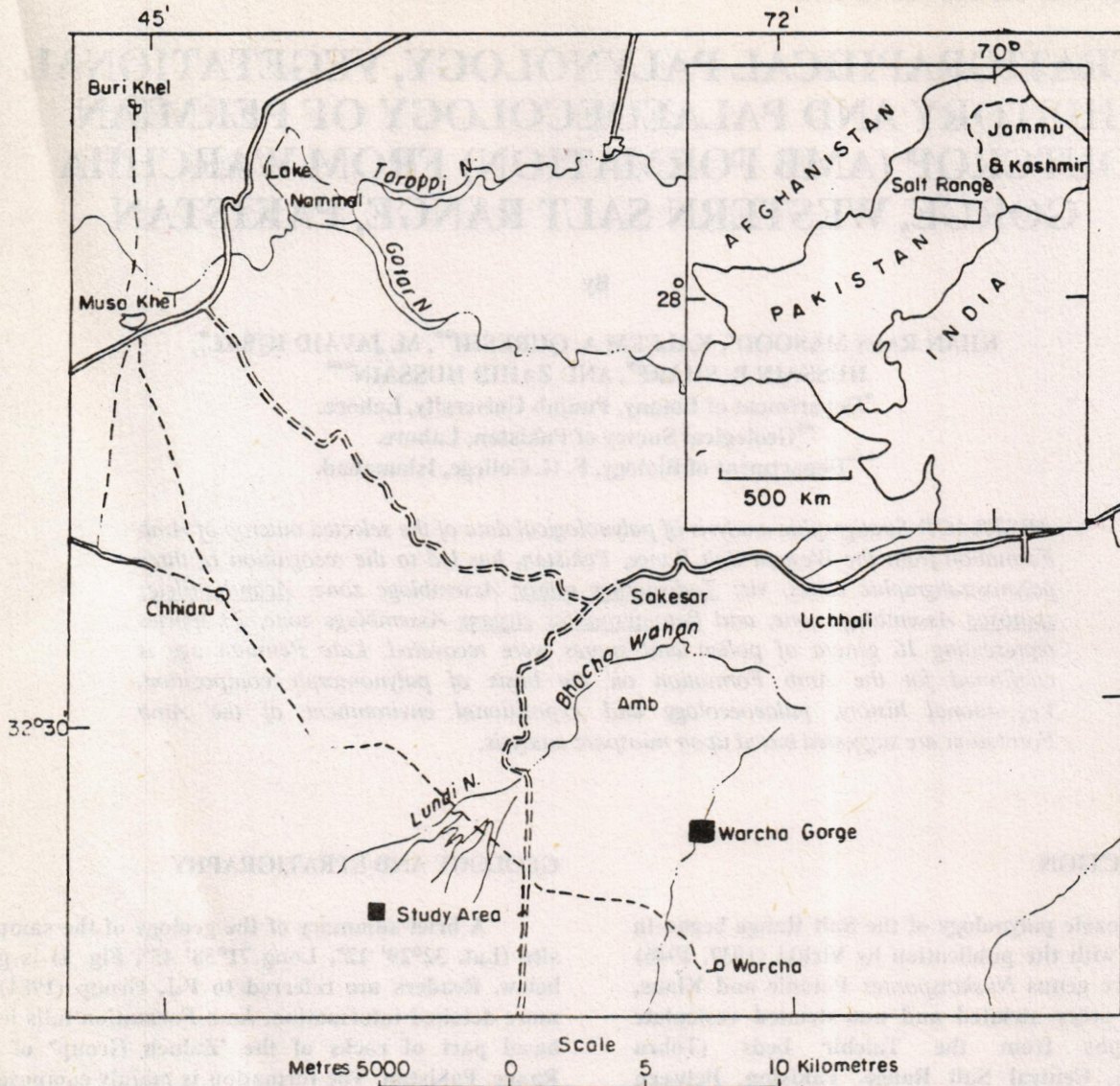
FIG. 1   LOCATION MAP

Fig.2 : LITHOSTRATIGRAPHIC SECTION OF AMB FORMATION SHOWING SAMPLING SPOTS AND PALYNOSTRATIGRAPHIC ZONES.

Locality: Lat. 32° 29' 12"
Long. 71° 58' 45"
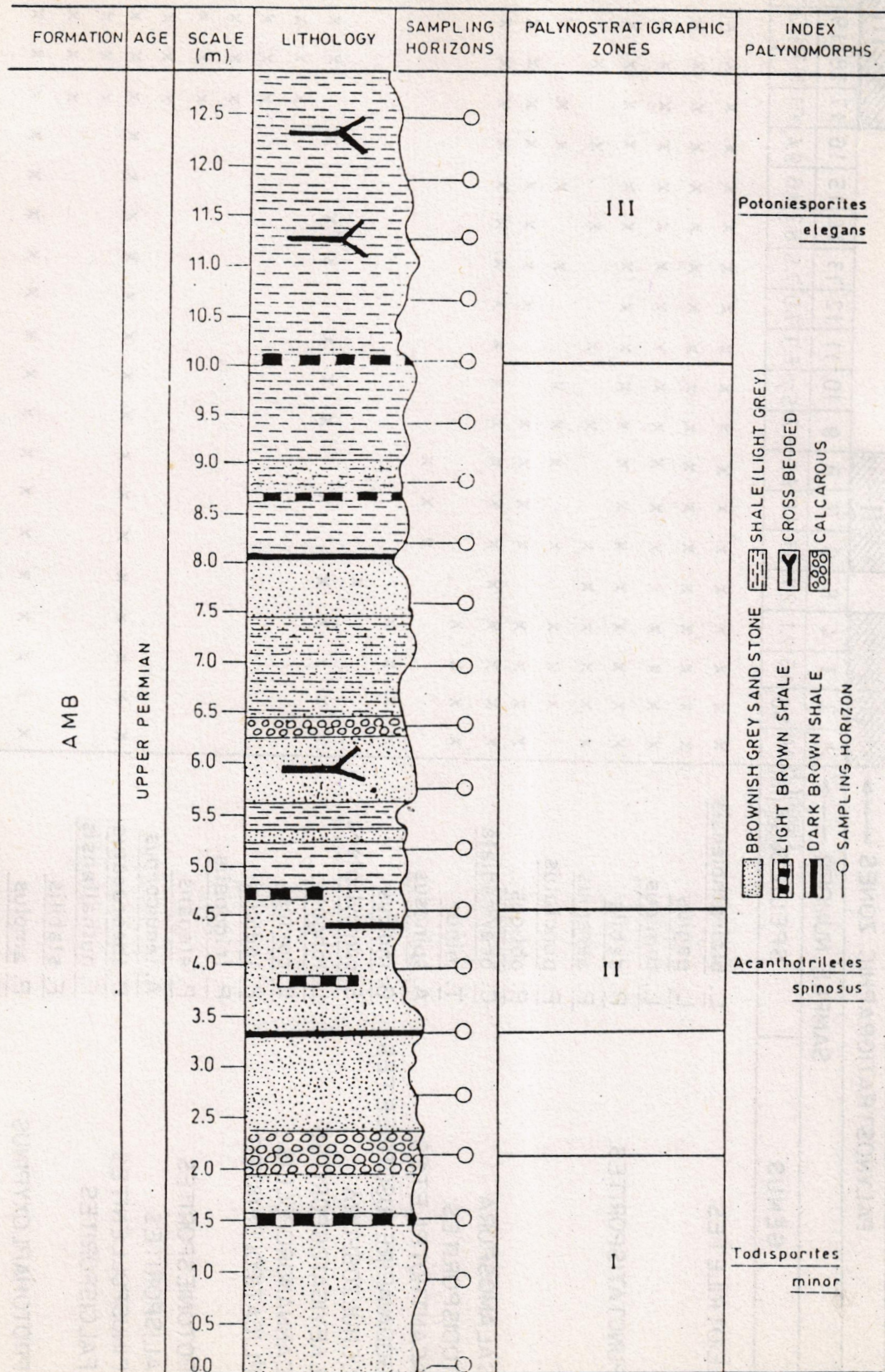
TABLE 1

QUANTITATIVE DISTRIBUTION OF PALYNOMORPHS IN DIFFERENT SAMPLES

PALYNOSTRATIGRAPHIC ZONES →	I							II									III				
SAMPLE NUMBER →	1	2	3	4	5	6	7	8	9	10	11	12	13	14	15	16	17	18	19	20	21
Height From Base (m)	0.0	1.0	1.5	2.1	2.7	3.4	4.0	4.6	5.2	5.7	6.3	7.0	7.6	8.2	8.8	9.4	10.1	10.7	11.3	11.9	12.5
GENUS / SPECIES																					
LEIOTRILETES L. blairatholensis	x	x	x	x	x	x	x	x	x	x	x	x	x	x	x	x	x	x	x	x	x
L. pagius	x	x	x	x	x	x	x	x	x	x	x	x	x	x	x	x	x	x	x	x	x
L. tumidus	x	x	x	x	x	x	x	x	x	x	x	x	x	x	x	x	x	x	x	x	x
PUNCTATISPORITES P. deblis	x	x	x	x	x	x	x	x	x	x	x	x	x	x	x	x	x	x	x	x	x
P. aerarius	x	x	x	x	x	x	x	x	x	x	x	x	x	x	x	x					
P. punctatus		x	x	x	x	x	x	x	x	x	x	x	x	x	x	x					
P. obliqus	x	x	x	x	x	x	x	x	x	x	x	x	x	x	x	x					
CALAMOSPORA C. breviradiata	x	x	x	x	x	x	x		x	x	x	x	x	x	x	x					
TODISPORITES T. minor	x	x		x		x	x				x										
ACANTHOTRILETES A. spinosus				x		x	x	x													
GODAVARIRETUSOTRILETES G. indicus	x	x	x	x	x	x	x	x	x	x	x	x	x	x	x	x	x	x	x	x	x
SCHULZOSPORA S. campyloptera					x				x					x							
LAEVIGATOSPORITES L. longus	x	x	x	x	x	x	x		x	x	x	x	x	x		x				x	
CANNANOROPOLLIS C. corius						x		x													
PLICATIPOLLENITES P. indicus																					
P. trigonalis												x	x	x	x	x	x	x	x	x	x
POTONIESPORITES P. elegans												x	x	x	x	x	x	x	x	x	x
ALISPORITES A. tenuicorpus	x	x	x	x	x	x	x	x	x	x	x	x	x	x	x	x	x	x	x	x	x
PINUSPOLLENITES P. theoracatus	x	x	x	x	x	x	x	x	x	x	x	x	x	x	x	x	x	x	x	x	x
FALCISPORITES F. nuthallensis																		x		x	
F. stabilis																					
PROTOHAPLOXYPINUS P. amplus	x	x	x	x	x	x	x	x	x	x	x	x	x	x	x	x	x	x	x	x	x
PLATYSACCUS P. goraiensis	x	x	x	x	x	x	x	x	x	x	x	x	x	x	x	x	x	x	x	x	x
P. queenslandi																	x	x	x	x	x

172

EXPLANATION OF PLATE I
Index Palynomorphs of Assemblage Zones

FIGURE.

1.   *Potoniesporites elegans* Bharadwaj 1966, Sample 20, Slide A 20387, Maceration A-HF, X 400

2.   *Plicatipollenites trigonalis* Lele 1964, Sample 17, Slide A 17387, Maceration A-HF, X 400.

3.   *Plicatipollenities indicus* Lele 1964, Sample 19, Slide A 19387, Maceration A-HCL, X 250.

4.   *Godavariretusotriletes indicus* (Tiwari and Moiz) Masood and Bhutta 1986, Sample 02, Slide A02387, Maceration A-HF, X 1000.

5.   *Cannanaropollis corius* (Bose and Kar) Chandra, Kar and Lacy, 1975, Sample 19, Slide A 19387, Maceration A-HF, X 400.

6.   *Falcisporites nuthalensis* Balme 1970, Sample 17, Slide A 18387, Maceration A-HF, X 400.

7-9.   *Acanthotriletes spinosus* Kosanke, Sample 06, Slide D 06387, Maceration A-HNO$_3$, X 1000.

10.   *Todisporites minor* Couper 1958, Sample 02, Slide E 02387, Maceration A-HF, X 1000.

11-12. *Falcisporites stabilis* Balme 1970, Sample 21, Slide B 21387, Maceration A-HCL, X 400.

13.   *Platysaccus queenslandi* de-Jersy 1962, Sample 21, Slide C 21387, Maceration A-HCL, X 400.

PLATE 1
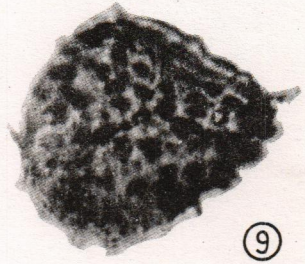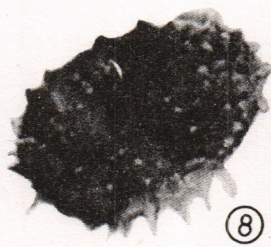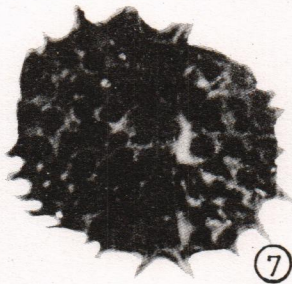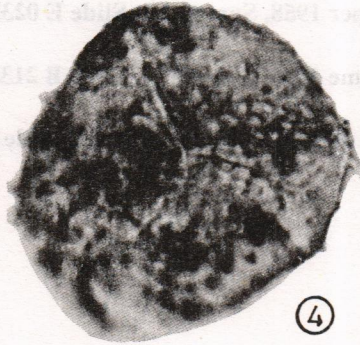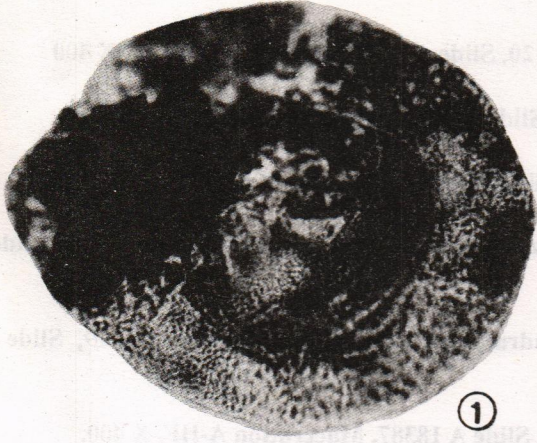
Playford (1984). Each sample was treated individually. The various lithologies encountered offered changes to apply a variety of techniques. "Barren" samples or those yielding only small number of microfossils were processed as many as three times. Samples (50 gram each) were subjected to bulk maceration in a mixture of 20 percent hydrofluoric acid and 80 percent nitric acid for twenty four hours for maceration. Acid was neutralized after several decantations allowing to settle for 12 hours between each decantation through natural sedimentation. Centrifugation was not employed. Completely neutralized and macerated material was treated with 2 percent potassium hydroxide solution to remove humic acids. Most samples yielded identifiable poorly to moderately preserved miospores. All slides were mounted in Canada balsam and were sealed with varnish.

PALYNOMORPH DISTRIBUTION

Palynomorph assemblage varied considerably vertically as regard the species diversity and frequency. This is illustrated in Table 1. Fig. 2, illustrates exact sampling horizons and other relevant details of the Amb Formation.

SYSTEMATIC LIST OF PALYNOMORPHS

Following is a systematic list of palynomorphs recovered from Amb Formation:

Anteturma SPORITES H. Potonie, 1893.
Turma TRILETES Reinsch Emend Dettmann, 1963.
Suprasubturma ACAVATITRILETES Dettmann, 1963.
Infraturma LAEVIGATI (Bennie and Kidston) Potonie, 1956.

GENUS LEIOTRILETES Naumova ex Potonie and Kremp, 1954.
L. blairatholensis Foster, 1975.
L. pagius Allen, 1965.
L. tumidus Butterworth and Williams, 1958.

GENUS PUNCTATISPORITES (Ibrahim) Potonie & Kremp, 1954.
P. debilis Hacquebard, 1957.
P. aerarus Butterworth & Williams, 1958.
P. punctatus Ibrahim, 1933.
P. obliques Kosanke, 1950.

GENUS CALAMOSPORA Schopf, Wilson and Bentall, 1944.
C. breviradiata Kosanke, 1950.

GENUS TODISPORITES Couper, 1958.
T. minor Couper, 1958.

Infraturma APICULATI (Bennie & Kidston) Potonie, 1956.

Subinfraturma NODATI Dybova and Jachovicz, 1957a.

GENUS ACANTHOTRILETES (Naumova) Potonie & Kremp, 1954.
A. spinosus (Kosanke) Masood & Bhutta, 1986.

GENUS GODAVARIRETUSOTRILETES (Tiwari & Moiz) Masood and Bhutta, 1986.
G. indicus (Tiwari & Moiz) Masood and Bhutta, 1986.

Suprasubturma PSEUDOSACCITRILETES Richardson, 1965.
Infraturma MONOPSEUDOSACCITI Smith and Butterworth, 1967.

GENUS SCHULZOSPORA Kosanke, 1950.
S. campyloptera (Waltz) Hoffmeister, Staplin and Mollay, 1955.

Turma MONOLETES Ibrahim, 1933.
Supraturma ACAVATOMONOLETES Dettmann, 1963.
Subturma AZONOMONOLETES Luber, 1935.
Infraturma LAEVIGATOMONOLETI Dybova and Jach, 1957.

GENUS LAEVIGATOSPORITES Ibrahim, 1933.
L. longus Chandra, Kar & Lacey, 1975.

Anteturma POLLENITES Potonie, 1931.
Turma SACCITES Erdtman, 1947.
Subturma MONOSACCITES (Chitaley) Potonie and Kremp, 1954.
Infraturma TRILETISACCITI Leschik, 1955.

GENUS CANNANOROPOLLIS Potonie and Sah, 1960.
C. corius (Bose & Kar) Chandra, Kar & Lacey, 1975.

GENUS PLICATIPOLLENITES Lele, 1964.
P. indicus Lele, 1964.
P. trigonalis Lele, 1964.

Infraturma VESICULOMONORADITI (Pant)

Bharadwaj, 1955.
GENUS POTONIESPORITES (Bharadwaj)
Bharadwaj, 1964.
P. elegans Bharadwaj, 1966.

Subturma DISACCITES Cookson, 1947.
Infraturma DISACCIATRILETI (Leschik) Potonie, 1958.

GENUS ALISPORITES (Wilson ex Daugherty)
Jansonius, 1971.
A. tenuicorpus Balme, 1970.

GENUS FALCISPORITES Leschik emend
Klaus, 1963.
F. nuthallensis Balme, 1970.
F. stabilis Balme, 1970.

GENUS PINUSPOLLENITES (Potonie) Raatz, 1938.
P. theoracatus Balme, 1970.

Infraturma STRIATITI Pant, 1954.

GENUS PROTOHAPLOXYPINUS Samoilovich
emend Hart, 1964.
P. amplus (Balme & Hennelly) Hart, 1964.

Infraturma PODOCARPOIDITI Potonie, Thomson and
Thiergart, 1950.

GENUS PLATYSACCUS Naumova ex Potonie &
Klaus, 1956.
P. queenslandi de-Jersy, 1962.

DISCUSSION

23 miospore species belonging to 16 genera were recovered from the Amb Formation. Of these 11 belong to trilete, 1 to monolete, 4 to monosaccate, 6 to bisaccate and 1 to pseudosaccate.

Tentative botanical affinities are assigned to the various groups of palynomorphs by considering that:- Trilete and monolete spores represent Cryptogams, monosulcate Cycadoginkops, striated bisaccate Glossopteroids, non striated bisaccate Conifers, trilete monosaccate Gangamopteroids and alete monosaccate Cordaitales (Bharadwaj, 1966).

Most samples were productive containing poorly or moderately to well preserved miospores. Mostly the qualitative and quantitative fluctuation in the miospore population at different stratigraphic levels did not bear any relationship with the varying lithology. Table 1 summarizes the quantitative range of occurrence of various miospore species at various stratigraphic horizons. Of the sixteen isolated genera, only six were long ranging (they occurred in all samples) viz: *Leiotriletes, Punctatisporites, Cala-mospora, Laevigatosporites, Protohaploxypinus,* and *Pinuspollenites*. Others exhibited highly variable range of occurrence at different stratigraphic levels. The availability, absence and relative frequency of occurrence of each miospore species at each stratigraphic level was carefully noted. It was, however, observed that some palynomorphs occurred strictly at certain fixed horizon and were totally absent at others. All such lithological pockets were recognized as major palynostratigraphic zones and were named after their most abundantly available marker palynomorph(s).

Stratigraphical Palynology

On the basis of trend of occurrence of various miospore species at different stratigraphic levels, the Amb Formation is classified into three basic palynostratigraphic zones (in ascending order).

1. *Todisporites minor* Assemblage Zone.
2. *Acanthotriletes spinosus* Assemblage Zone.
3. *Potoniesporites elegans* Assemblage Zone.

Palynostratigraphic Zone-I: Todisporites minor Assemblage Zone.

The lower 2.13 m thick section of Amb Formation constitute this zone, identified by the relative abundance of two miospore species (marker or index species) *Todisporites minor* and *Godavariretusotriletes indicus*. Other commonly occurring miospores are *Leiotriletes balairatholensis, L. pagius, L. tumidus, Puncatatisporites deblis, P. aerarius, P. punctatus, P. Obliqus, Calamospora breviradiata, Laevigatosporites longus, Pinuspollenites theoracatus* and *Protohaploxypinus ampuls*. Lithologically, brownish grey medium grained sandstone dominate this zone with occasional light brown calcareous shales.

Palynostratigraphic Zone-II: Acanthotriletes spinosus Assemblage Zone.

This is indicated by the sudden appearance of the members of the genus *Acanthotriletes*, constituting quantitatively about seventy per-cent of the entire palynomorph population of this zone. This zone begins at about 1.3 m above the zone I and exterminate after 1.2 meters i.e., at approximately 4.6 meters from the
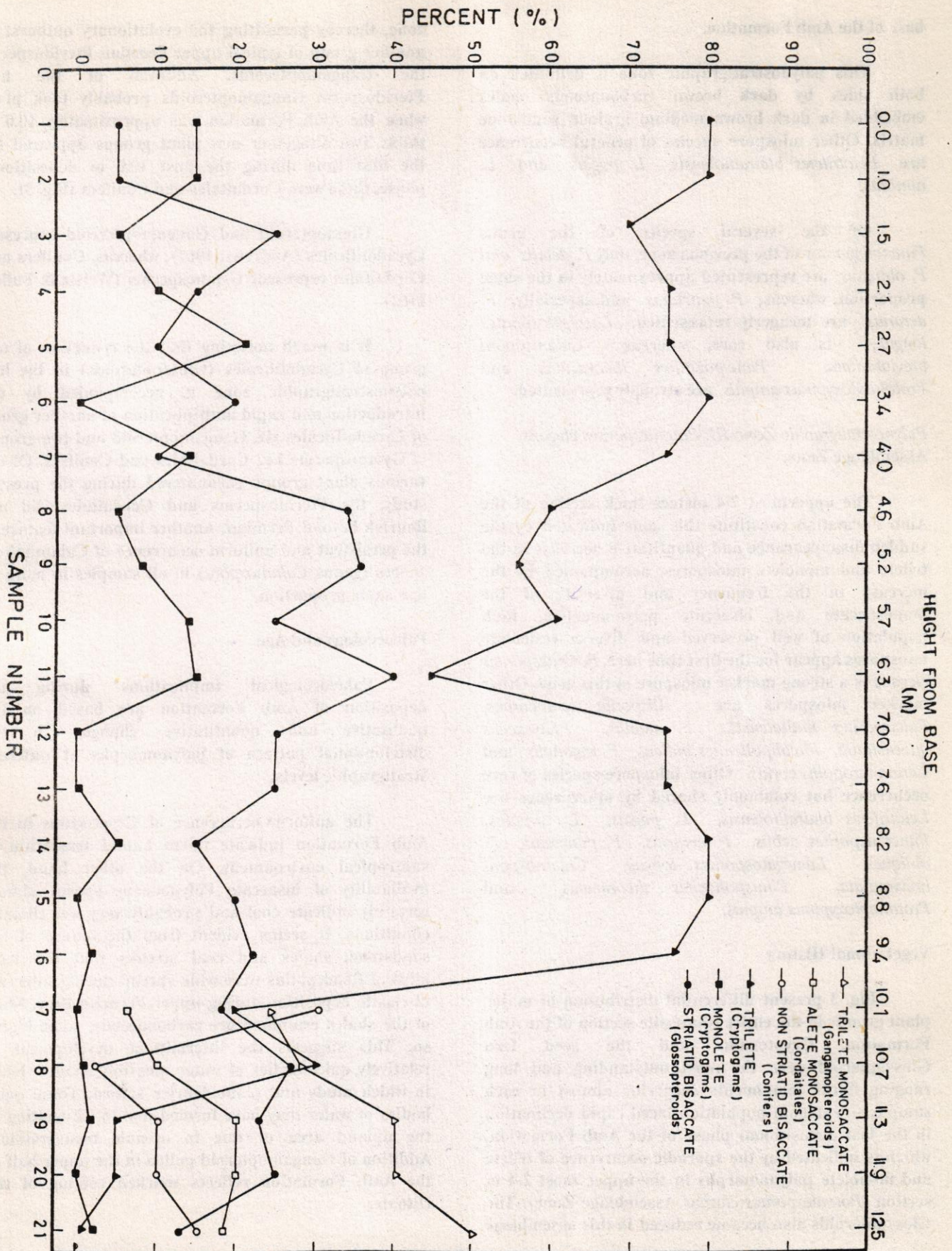
Fig. 3 : RISE AND FALL OF VARIOUS PLANT GROUPS AT DIFFERENT STRATIGRAPHIC LEVELS ACROSS THE ENTIRE AMB FORMATION.

base of the Amb Formation.

This palynostratigraphic zone is delimited on both sides by dark brown carbonaceous shales embedded in dark brown medium grained sandstone matrix. Other miospore species of general occurrence are *Leiotriletes blairatholensis*, *L. pagius* and *L. tumidus*.

Of the several species of the genus *Punctatisporites* of the previous zone, only *P. debilis* and *P. obliques* are represented approximately in the same proportion, whereas, *P. punctatus* and especially, *P. aerarius* are meagerly represented. *Laevigatosporites longus*, is also rare, whereas *Calamospora breviaradiata*, *Pinuspollinites theoracatus* and *Protohaploxypinus ampuls* are strongly represented.

Palynostratigraphic Zone-III: Potoniesporites elegans Assemblage Zone.

The uppermost 2.4 meters thick section of the Amb Formation constitute this zone indicated by the sudden disappearance and quantitative decrease in the trilete and monolete miospores, accompanied by the increase in the frequency and diversity of the monosaccate and bisaccate palynomorphs. Rich population of well preserved and diverse vesiculate miospores appear for the first time here. *Potoniesporites elegans* is a strong marker miospore of this zone. Other marker miospores are *Alisporite tenuicorpus*, *Falcisporites nuthalensis*, *F. stabilis*, *Platysaccus queenslandi*, *Plicatipollenites indicus*, *P. trigonalis* and *Cannanaropollis corius*. Other miospore species of rare occurrence but commonly shared by other zones are *Leiotriletes blairatholensis*, *L. pagius*, *L. tumidus*, *Punctatisporites deblis*, *P. aerarius*, *P. punctatus*, *P. obliques*, *Laevigatosporites longus*, *Calamospora breviaradiata*, *Pinuspollenites theoracatus* and *Protohaploxypinus ampuls*.

Vegetational History

Fig. 3 present differential distribution of major plant groups in the entire composite section of the Amb Formation. Cryptogams and the seed fern Glossopteroid were the most outstanding and long ranging floral components occurring almost in each sample. Cryptogam population faced rapid declination in the last depositional phase of the Amb Formation, which is indicated by the sporadic occurrence of trilete and monolete palynomorphs in the upper most 2.4 m section (*Potoniesporites elegans* Assemblage Zone). The Glossopteroids also became reduced in this assemblage

zone, thereby permitting the evolutionary outburst of another group of typical upper Permian Pteridosperm, the Gangamopteroids. Addition of the new Pteridosperm Gangamopteroids probably took place when the Amb Formation was approximately 10.0 m thick. Two altogether new plant groups appeared for the first time during the post 10.0 m depositional phase, these were Cordaitales and Conifers (Fig. 3).

Glossopteroid and Gangamopterroid represent Cycadofilicales (Andrews, 1967), whereas, Conifers and Cordaitales represent Gymnosperms (Weisiz & Fuller, 1962).

It is worth noticeing that the reduction of one group of Cycadofilicales (Glossopteroids) in the last palynostratigraphic zone is accompanied by the introduction and rapid multiplication of another group of Cycadofilicales viz, Gangamopteroid and two groups of Gymnosperms i.e., Cordaitales and Conifers. Of the various plant groups encountered during the present study, the Pteridosperms and Cordaitales did not flourish beyond Permian. Another important feature is the persistent and uniform occurrence of Calamitalean spores (genus *Calamospora*) in all samples in more or less same proportion.

Paleoecology and Age

Palaeocological implications during the deposition of Amb Formation are based on the qualitative and quantitative changes in the distributional pattern of palynomorphs at different stratigraphic levels.

The uniform occurrence of Cryptogams in the Amb Formation indicate warm humid temperate to subtropical environment. On the other hand, the availability of bisaccate Polypodeous spores almost certainly indicate cool and probably very wet climatic conditions. It seems evident from the nature of the sandstone, shales and coal streaks that low land alluvial flood plains were wide spread during intervals of clastic deposition during upper Permian time. Most of the shales examined are carbonaceous, some highly so. This suggests the intermittent development of relatively quiet bodies of water, possibly shallow lakes in which muds and plant debries settled. These quiet bodies of water may have formed due to ice melting in the upland area or due to oceanic transgression. Addition of Gangamopteroid pollen in the upper half of the Amb Formation reflects marked cooling of the climate.

Amb Formation has been designated Artinskian age (P. J. Groups, 1981). Palynological assemblages recorded during the present investigation strongly support this age. Striated haploxylonoid and diploxylonoid bisaccate palynomorphs, the cosmopolition markers of upper Permian strata (Balme, 1970), were of sporadic occurrence in Amb Formation. On the other hand, the monosaccate miospores found usually in abundance in early Permian sediments were also scarce. The 12.8 meters thick section of the Amb Formation due to the low frequency of bisaccate striated palynomorphs seems to be of middle Permian age. The upper most 2.4 m thick outcrop (*Potoniesporites elegans* Assemblage zone) exhibit a marked increase in the diversity of palynomorph composition, especially bisaccate palynomorphs outnumbering all other types. On this basis it can tentatively be considered as being slightly younger in age. Middle Permian age is also supported by the availability of Gangamopteriod pollen, which are cosmopoliton markers of early late or late Permian strata.

Comparison with other Permian Assemblages

Published literature on stratigraphical palynology of the Salt Range, Pakistan, is very meagre. Only Chiddru and Amb Formations have previously been palynologically investigated with very little emphasis on stratigraphical palynology (Balme, 1970).

Presently investigated section of Amb Formation differs markedly form Chiddru Formation as well as previously investigated sections of the Amb Formation due to the sporadic occurrence of bisaccate palynomorphs. However, some of the genera are commonly shared, these are *Leiotrileters*, *Punctatisporites* and *Calamospora*.

Most of the upper and lower Permian assemblages of Australia contain well preserved and diverse populations of bisaccate and monosacate palynomorphs (Foster, 1975; Balme, 1970), in contrast to this only the upper 2.4 m thick section of Amb Formation exhibited this composition. Some of the genera, eg; *Granulatisporites* Ibrahim emend Potonie and Kremp, 1954, *Microbaculispora* Bharadwaj, 1974, *Verrucosisporites* Ibrahim emend Smith and Butterworth, 1967, *Diatomozonotriletes* Naumova emend Playford, 1963, *Lophotriletes* Naumova emend Potonie and Kremp, 1954, which are characteristic for Australian Permian strata (Foster, 1975; Segroves, 1970) were totally extinct here. Genera commonly

shared by the Australian Permian assemblages and the presently investigated Amb Formation are *Potoniesporites*, *Protohaploxypinus* and *Alisporites*. Absence of the cosmopolition Permian marker species *Praecolpatites sinonicus* widely distributed in India and Australia (Bharadwaj, 1972; 1974) is noteworthy.

South African palynomorph population are dominated by *Praecolpatites sinonicus* and striated and non striated bisaccate miospores (Hart 1966; Foster 1975) which is certainly not true for Amb Formation. Simultaneous occurrence of genera *Plicatipollenites* and *Potoniesporites* in the third and uppermost palynobiostratigraphic zone permit very close comparison with lower Karharbari and Talchir stages of India, where these genera are index associations (Bharadwaj, 1966).

CONCLUSION

Amb Formation at Warchha Gorge, Western Salt Range, Pakistan, contain rich assemblage of palynomorphs including trilete, monolete and vesiculate miospores. Palynomorph composition and distribution is highly variable at different stratigraphic levels. Triletes are mostly long ranging where as bisaccates and monosaccates are more strongly represented in the upper part of the formation.

Three palynostratigraphic zones are recognized in the Amb Formation at Warchha Gorge (in ascending order) i.e. *Todisporites minor* Assemblage zone, *Acanthotirletes spinosus* Assemblage zone and *Potoniesporites elegans* Assemblage zone. As indicated by the affinites of different groups of palynomorphs, existence of six plant groups i.e; Cryptogams, Cycadoginkops, Glossopteroids, Gangamopteroids, Cordaitales and Conifers is suggested during the deposition of Amb Formation. As inferred from palynological data, the climate was warm humid temperate to subtropical during the early depositional phase, becoming slightly cool and wet at the end. Amb Formation at Warchha Gorge, Western Salt Range, is distinct palynologically as compared to its other counterparts in the Salt Range. Palynomorph assemblage reflect Artinskian age for Amb Formation.

ACKNOWLEDGEMENTS

REFERENCES

Andrews, H. N. Jr., (1967). Studies in Palaeobotany. *John Wiley & Sons Inc. New York,*. 487 p.

Balme, B.E., (1970). Palynology of Permian and Triassic Strata in the Salt Range and Surghar Range, W. Pakistan; in stratigraphic boundary problems: Permian and Triassic of West Pakistan (Ed. B. Kummel, and C. Teichert). *Univ. Kansas. Geol. Deptt. sp. pub. 4* pp. 305-453.

Bharadwaj, D.C., (1966). Distribution of spores and pollen grains dispersed in the Lower Gondwana formations of India. Symposium on Floristics and Stratigraphy of Gondwanaland. *Proc. Symp. Spec. Session,* pp. 69-84

Bharadwaj, D.C., (1972). Lower Gondwana microfloristics. In: Seminar on Paleopalynology and Indian Stratigraphy (1971), *Univ. Calcutta, Deptt. Botany,* pp. 42-50.

Bharadwaj, D.C., (1974). Permian palynostratigraphy in India. *proc. 3rd Intern. Palynol. Confr. Moscow,* pp. 125-129.

Foster, C.B., (1975). Permian plant microfossils from the Bliar Athol Coal Measures. Central Queensland, Australia. *Palaeontographica abt. B.* 1654- (5-6), pp. 121-171.

Gosh, A.K., and Bose, A., (1951). Permo-triassic microflora in the Punjab Salt Range. (Abst.), *Proc. Indian 38th Sci. Congr. Banglore* Vol. (3), pp. 126-127.

Hart, F.G., (1966). *Vittatina africana,* a new miospore from the Lower Permian of South Africa: *Micropaleontology,* Vol. 12, pp. 37-42.

Lele, K.M., (1976). Palaeooclimatic implications of Gondwana floras, *Geophytology,* 6(2), pp. 207-

229.

Masood, K.R., and Qureshi, K.A., (in press), Miospore assemblage from the Late Permian Warchha Sandstone of Salt Range, Pakistan, *Sind, Univ. Res. Jour.* Vol. 23, 1991 a.

Masood, K.R., and Qureshi, K.A., (in press), Disaccate pollen from the Permian of Pakistan *Sind Univ. Res. Jour.* Vol. 23.

Pakistan-Japanes Research Group, (P.J. Group)., (1981). Stratigraphy and correlation of Marine Permian-Lower Triassic in the Surghar Range and the Salt Range, Pakistan. *Kyoto Univ.* P. 25.

Phipps, D., and Playford, G., (1984). Laboratory techniques for extraction of palynomorphs from sediments, *Pub. Dep. Geol. Univ. W. Aust,* pp. 118-148.

Segroves, K.L., (1970). Permian spores and pollen grains from the Perth Basin, Western Australia, *Grana,* Vol. 10, No. 1, pp. 43-73.

Venkatachala, B.S., and Kar, R.K., (1968). Palynology of the Kathwai Shales, Salt Range, West Pakistan. I. Shales 25 ft. above the Talchir Boulder Bed. *Paleobotanist* Vol. 16 (2), pp. 156-166.

Virkki, C., (1937). On the occurrence of winged spores in the Lower Gondwana rocks of India and Australia. *Proc. nat. Acad. Sci. India,* Vol. 6, pp. 428-431.

Virkki, C., (1946). Spores from the Lower Gondwana of India and Australia. *Proc. nat. Acad. Sci. India,* Vol. 15 (4, 5). pp. 93-176 (1945).

Weisz, P., and Fuller, M., (1962). The science of botany. *McGraw Hill Book Company, inc.* Copyright, 1962.

STRATIGRAPHICALLY SIGNIFICANT MIOSPORES IN THE TREDIAN FORMATION (TRIASSIC) AT NAMMAL GORGE, WESTERN SALT RANGE, PAKISTAN

By

*KHAN RASS MASOOD, **KALEEM A. QURESHI, *SAJIDA N. SABRI
***ZAHID HUSSAIN AND *M. JAVAID IQBAL
*Department of Botany, University of the Punjab, Lahore.
**Geological Survey of Pakistan, Lahore.
***Department of Biology, F. G. College, Islamabad.

ABSTRACT: *The results of the palynostratigraphic analysis of the 16 samples of Middle Triassic origin (Tredian Formation) from the Western Salt Range, Pakistan, are discussed. Excellent chronologic control is obtained from the occurrence of several stratigraphically significant miospores viz,* Cyclogranisporites aureus, Limitisporites plicatus, Granulatisporites trisinus, Verrucosisporites triassicus, Alisporites grandis, Protohaploxypinus amplus, Kingiacolpites elongatus, Ginkgocycadophytus cymbatus, Rugulatisporites permixtus, Calamospora breviradiata, Lophotriletes buhiniae, Chasmatosporites major, Goubinispora morandavensis, Valiasaccites validus, Lunatisporites novialensis, Retusotriletes simplex, Acanthotriletes spinosus, Platysaccus queenslandi, *and* Lueckisporites diploxylonoidii.

Fossil pollen/spores assemblages indicate change in vegetation and climate during the deposition of the Tredian Formation.

INTRODUCTION

Triassic system of the Salt Range, Pakistan, has never been thoroughly explored palynologically. Only two publications are available (Sitholay, 1943; Balme 1970) mainly dealing with systematic and descriptive palynology. The purpose and scope of the present investigation is to carry out a more detailed and comprehensive palynological characterization of the Middle Triassic strata (Tredian Formation) of the Western Salt Range, Pakistan, indicating stratigraphically significant miospores.

The earlier name of Tredian Formation was Kingriali Sandstone (Gee; 1945).

Its type locality is Tredian Hills (lat 32° 43' N; long 71° 46' E) Mianwali district, Punjab.

The Formation consists of two divisions: an upper Khatkiara Member and a lower Landa Member. The name Landa Member was introduced by Kummel (1966) after Landa Nala (Lat. 32° 57' N; long. 71° 12' 30" E) in the Surghar Range. It consists of sandstone, claystone and shale. Sandstone is ferruginous, having red, maroon, brown, grey to black colours. It is crossbedded, with ripple marks and splintery structure. Danilchik and Shah (1967) introduced the name Khatkiara Member after Khatkiara Nala (Lat. 32° 56' N; long. 71° 11' E) in the Surghar Range. The member consists of massive, cross bedded, ferruginous, friable to hard sandstone and shale. The colour varies from white, cream, yellow, brown, grey to black. The total thickness of the Tredian Formation measured at Nammal Gorge (Lat. 32° 39' 30" Long 71° 48' E) was about 72.10 metres Fig. 1. Lithologic and other relevant details are presented in Fig. 2.

RESEARCH METHODOLOGY

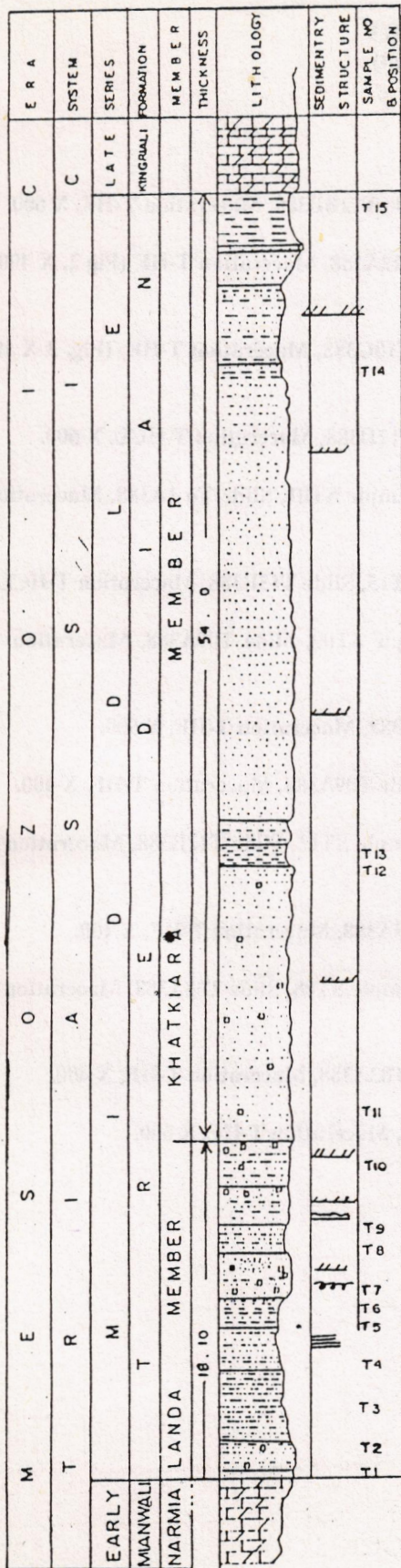Standard techniques for sample processing were applied (Phipps & Playford; 1984).

1. 30 g representative portion of the rock sample was crushed to 0.5 cm size.
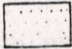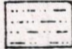
2. Conventional processing:-
   a. HF - 10 days.

LOCATION MAP
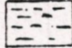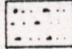
72°

Chakrala

Namal

Taroppi N.

Lake Namal

NAMMAL GORGE

Buri Khel

Musa Khel

45'

MIANWALI

■ Study Area

Scale

Metres 5000 0 5 10 Kilometres

32 30

FIG. 1

Jammu & Kashmir

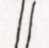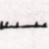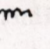Salt Range

INDIA

PAKISTAN

AFGHANISTAN

500 Km

70°

71°30'

28°
45'
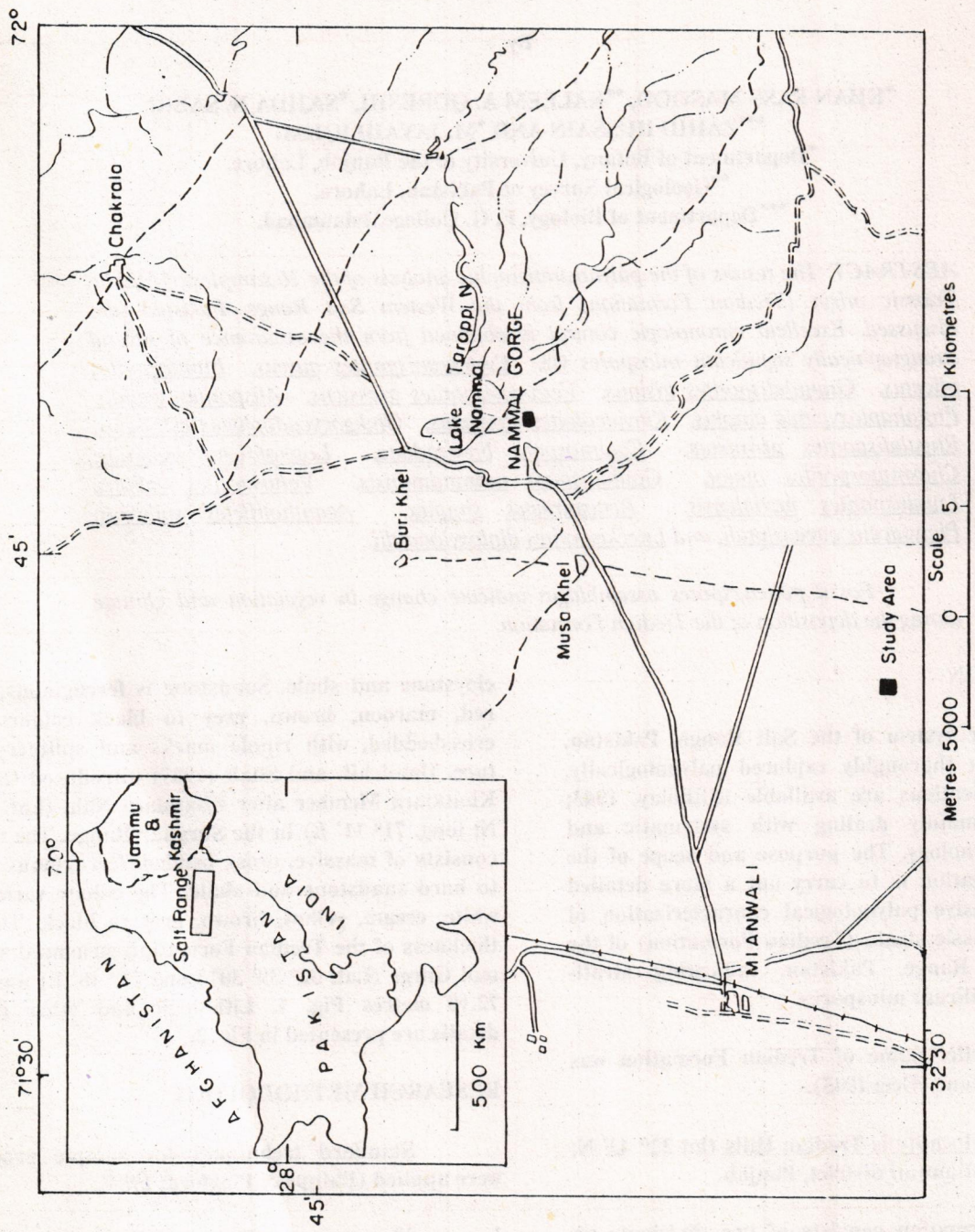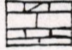
TREDIAN FORMATION
NAMMAL GORGE SECTION.

LEGEND

- ▨ Sandstone
- ▨ Sandy shale
- ▨ Shale
- ▨ Sandstone ferruginous
- ▨ Calc. Dolomite Dolomite Lst.
- ╱╱ Parallal Laminated
- ⌣ Crossbedded
- ⌢ Convolute bedding

MEASURED SECTION OF TREDIAN FORMATION
AT NAMMAL GORGE MIANWALI DISTRICT
SALT RANGE — PAKISTAN.

Scale 1cm= 2·5m.   Location: Lat. 32 39 30 On Long. 71 48E
Measured by:– Sajdda , R. Masood & Kaleem. Q.

5 Meters

0

Vertical Scale

FIG. 2

183
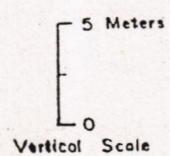
EXPLANATION OF PLATE I
(Stratigraphically significant)
miospores

FIGURE

1. *Lueckisporites dipoloxylonoidii* Masood 1983, Sample ST12, Slide T12BB388, Maceration T-HF, X 600.

2 & 10. *Valiasaccites validus* Bose and Kar 1966, Sample ST12, Slide T12A388, Maceration T-HF (Fig 2, X 400, Fig 10, X 600).

3 & 17. *Rugulatisporites permixtus* Playford 1982, Sample ST10, Slide T10C388, Maceration T-HF, (Fig. 3 X 1000, Fig. 17, X 600).

4. *Calamospora breviradiata* Kosanke 1950, Sample, ST12, Slide T12D388, Maceration T-HCL, X 600.

5. *Cyclogranisporites auraus* (Loose) Potonie and Kremp 1955, Sample ST01, Slide To 1A388, Maceration T-HF, X 1000.

6. *Goubinospora morandavensis* Tiwari and Rana 1981, Sample ST15, Slide T15B388, Maceration T-HCL, X 400.

7. *Ginkocycadophytus cymbatus* Balme and Hennelly 1955, Sample ST09, Slide T09A388, Maceration T-HF, X 400.

8. *Chasmatosporites majus* Nilson 1958, Sample ST12, Slide T12E388, Maceration T-HF, X 600.

9. *Kingiacolpites elongatus* Tiwari and Moiz 1970, Sample T09, Slide T09A388, Maceration T-HF, X 400.

11 & 15. *Lunatisporites novialensis* (Leschik) Tiwari and Rana 1980, Sample ST12, Slide T12B388, Maceration T-HF, X 400.

12 *Platysaccus queenslandii* de jersey 1962, Sample ST13, Slide T13A388, Maceration T-HF, X 400.

13. *Protohaploxypinus ampuls* (Balme and Hennelly) Hart 1964, Sample ST08, Slide T08A388, Maceration T-HF, X 400.

14. *Limitisporites plicatus* Bose and Kar 1966, Sample ST03, Slide T03A388, Maceration T-HF, X 400.

16. *Acanthotriletes spinosus* Kosanke, Sample ST12, Slide T12B388, Maceration T-HF, X 600.

PLATE 1
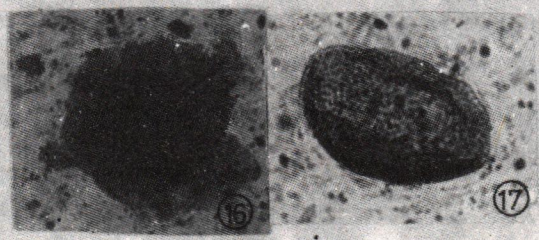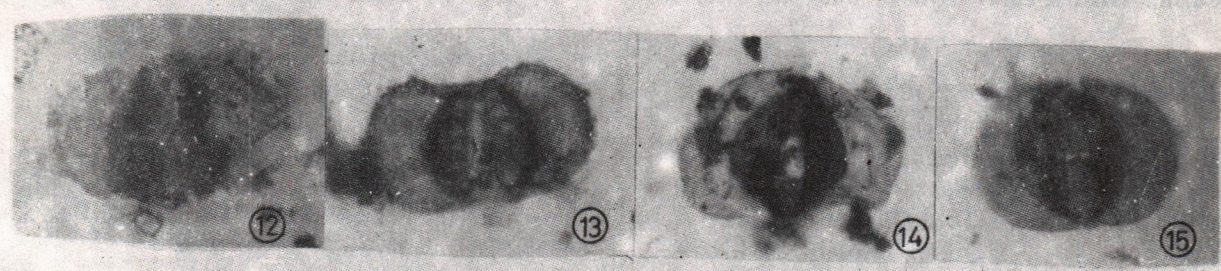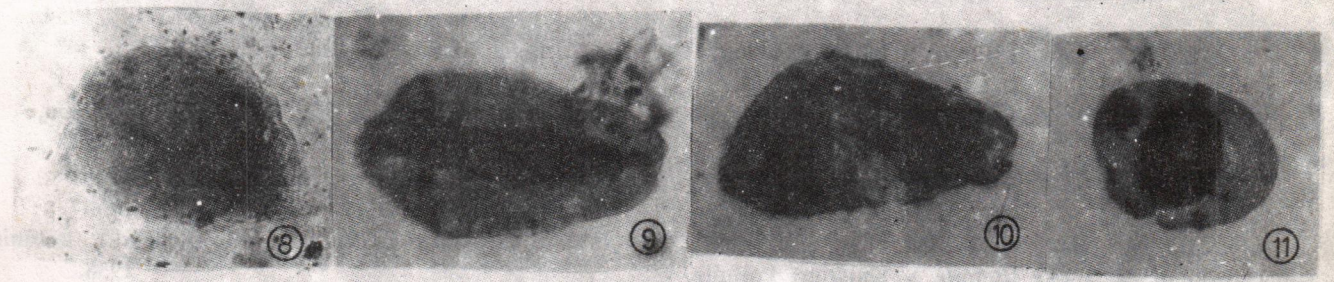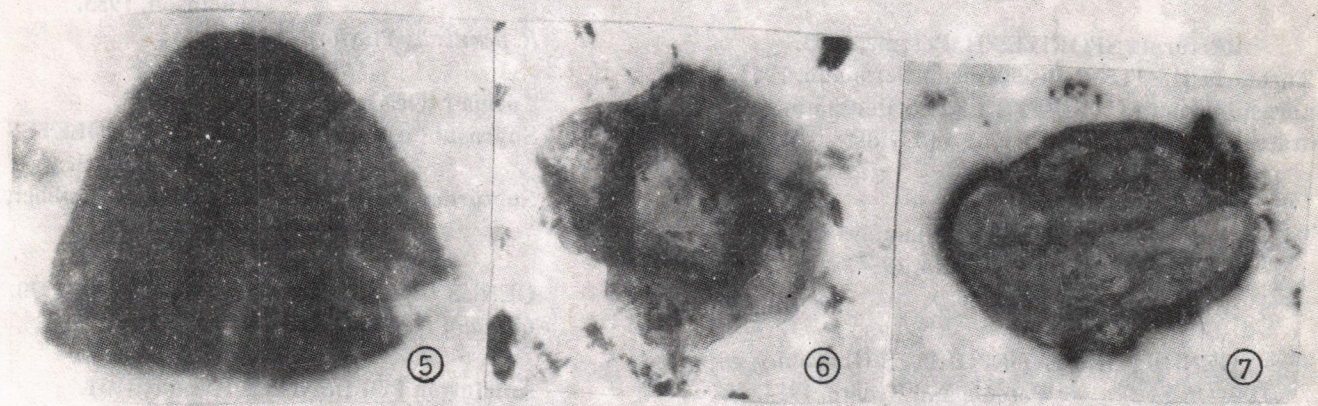
Several decantations allowing to settle, three hours between each decantation (no centrifugation).

b.   HCl   -- 48 hrs.   Decantation.
c.   HNO$_3$ -- 48 hrs.   Decantation.
d.   KOH 2%   -- $^1/_2$ hour. Decantation.

Slides were prepared in glycerine jelly for microscopic examination.

SYSTEMATIC LIST OF PALYNOMORPHS

Anteturma SPORITES H. Potonie, 1893.
Turma TRILETES Reinsch emend Dettmann, 1963.
Suprasubturma ACAVATITRILETES Dettmann, 1963.
Infraturma LAEVIGATI (Bennie and Kidston) Potonie, 1956.

GENUS LEIOTRILETES Naumova ex Potonie and Kremp, 1954.
L. ornatus Ischenko, 1956.

GENUS PUNCTATISPORITES (Ibrahim) Potonie and Kremp, 1954.
P. solidus Hacquebard, 1957.
P. irrasus Hacquebard, 1967.

GENUS CALAMOSPORA Schopf, Wilson and Bentall, 1944.
C. breviradiata Kosanke, 1950.

GENUS RETUSOTRILETES (Naumova) Richardson ex Streel, 1964.
R. simplex Naumova, 1953.
Infraturma APICULATI (Bennie & Kidston) Potonie, 1956.
Subinfraturma GRANULATI Dybova and Jachovicz, 1957.

GENUS GRANULATISPORITES (Ibrahim) Potonie & Kremp, 1954.
G. trisinus Balme and Hennelly, 1956.

GENUS CYCLOGRANISPORITES Potonie and Kremp, 1954.
C. aureus (Loose) Potonie and Kremp, 1955.
Subinfraturma NODATI Dybova and Jachovicz, 1957 a.

GENUS ACANTHOTRILETES (Naumova) Potonie & Kremp, 1954.
A. spinosus Kosanke.

GENUS LOPHOTRILETES Naumova ex Potonie & Kremp, 1954.
L. buhiniae de Jersey and Hamilton, 1967.
Subinfraturma VERRUCATI Dybova & Jachovicz, 1957.

GENUS VERRUCOSISPORITES Ibrahim emend. Smith & Butterworth, 1967.
V. triassicus Bharad. & Tiwari, 1977.
Infraturma MURONATI Potonie and Kremp, 1958.

GENUS RUGULATISPORITES Pflug & Thomson, 1953.
R. permixtus Playford, 1982.

Turma MONOLETES Ibrahim, 1933.
Suprasubturma ACAVATOMONOLETES Dettmann, 1963.
Subturma AZONOMONOLETES Lubber, 1935.

GENUS CHASMATOSPORITES Tiwari, 1970.
C. major Nilsoon, 1958.

Anteturma POLLENITES Potonie, 1931.
Turma SACCITES Erdtman, 1947.
Subturma MONOSACCITES (Chitaley) Potonie and Kremp, 1954.
Infraturma ALETISACCITI Leschik, 1955.

GENUS GOUBINISPORA Tiwari & Rana, 1986.
G. morandavensis Tiwari & Rana, 1980.
Subturma DISACCITES Cookson, 1947.
Infraturma DISACCIATRILETI (Leschik) Potonie, 1958.

GENUS ALISPORITES (Wilson ex Daugherty) Jansonius, 1971.
A. teunicorpus Balme, 1970.
A. thomasii (Couper) Pocock, 1962.
A. grandis (Cookson) Dettmann, 1963.
A. australis de Jersey, 1962.

GENUS VITREISPORITES Leschik, 1956 a.
Vitreisporites sp.

GENUS FALCISPORITES Leschik emend. Klaus, 1963.
F. nuthallensis Balme, 1970.
F. stabilis Balme, 1970.

GENUS ABIETINAEPOLLENITES Potonie 1951 ex Delcourt & Sprumont, 1955.

Abietinaepollenites sp.

GENUS PITYOSPORITES Seward emend Jansonius.
P. granulatus (Grrebe) Tschudy and Kosanke, 1966.

GENUS SULCATISPORITES Leschik emend Nilson, 1958.
S. ovatus Balme and Hennelly, 1955.
S. microsulcus Bharadwaj, 1970.
Infraturma DISACCIMONOLETI Klaus, 1963.

GENUS LIMITISPORITES Leschik, 1956 a.
L. plicatus Bose and Kar, 1966.

GENUS LUECKISPORITES Potonie and Klaus emend Klaus, 1963.
L. diploxylonoidii Masood, 1983.

GENUS CORISACCITES Venkatachala and Kar, 1966.
C. alutas Venkatachala and Kar, 1966.

GENUS LUNATISPORITES Leschik, 1956 a.
L. novialensis (Leschik) Tiwari & Rana, 1980.
Infraturma STRIATITI Pant, 1954.

GENUS PROTOHAPLOXYPINUS Samoilovich emend Hart, 1964.
P. ampuls (Balme and Hennelly) Hart, 1964.

GENUS STRIATOPODOCARPITES Samoilovich emend Hart, 1964.
Striatopodocarpites. sp. cf *cancellatus* (Balme and Hennelly) Hart, 1956.
Infraturma PODOCARPOIDITI Potonie, Thomson and Thiergart, 1950.

GENUS PLATYSACCUS Naumova ex Potonie and Klaus, 1956.
P. queenslandi de Jersey, 1962.
P. pakistanicus Masood and Qureshi, 1990.

GENUS PODOCARPITES (Cookson) Potonie, 1958.
Podocarpites sp.

GENUS VALIASACCITES Bose and Kar 1966.
V. validus Bose and Kar, 1966.
Subtruma MONOCOLPATES (Iverson and Troels) Smith, 1950.

GENUS GINKGOCYCADOPHYTUS Samoilovich 1953.
G. cymbatus Balme and Hennelly 1955.
Infraturma INTORTES (Naum) Potonie, 1958.

GENUS KINGIACOLPITES Tiwari and Moiz 1970.
K. elongatus Tiwari and Moiz, 1970.

DISCUSSION

36 palynomorph species belonging to 29 genera were recovered. Of these species, 11·belong to trilete, 1 to monolete, 1 to monosaccate and 23 to bisaccate palynomorphs. Each sample is characterized by the presence of different miospore genera.

Palynological Characterization of Different Stratigraphic Horizons

Following is a brief account of the palynological characterization of each stratigraphic horizon in ascending order i.e., from base to top. Each sampling level is treated as a stratigraphic horizon (T) (Table 1).

Horizon T1: It is characterized by the presence of only one stratigraphically significant miospore viz, *Cyclogranisporites aureus*.

Horizon T2: Fairly non productive, except few cor-roded unidentifiable bisaccate palynomorphs.

Horizon T3: Limitisporites plicatus is stratigraphically significant here. Other commonly occurring palynomorphs are:

Pityosporites granulatus, Sulcatisporites microsulcus and *Striatopodocarpites* sp. cf *cancellatus.*

Monoletes and triletes were 5%, striated bisaccate 22% and non striated bisaccate 73%.

Horizon T4: Stratigraphically significant miospore for this level is *Granulatisporites trisinus*. Other miospores of general occurrence are:-
Punctatisporites solidus and *Falcisporites nuthallensis.*

Among these monoletes and triletes were 22%, non striated bisaccate 60%, Alete monosaccates which were rare at other levels constitute 18% of the total population here.

Horizon T5: Only one miospore of sporadic occurrence i.e. *Alisporites thomasii* was recorded here, Fig 5 include

Table -1 Quantitative Distribution of Palynomorphs at Different Stratigraphic Horizons

Sample number		T1	T2	T3	T4	T5	T6	T7	T8	T9	T10	T11	T12	T13	T14	T15	T16
Height from base(m)		.15	2.1	4	6	8.5	9	10	12.5	14	16	18	33	34.5	62.5	66.5	72.1
Genus	**sp.**																
LEIOTRILETES	*L. ornatus*								+								
PUNCTATISPORITES	*P. solidus*				+												
	P. irrasus												O				
CALAMOSPORA	*C. breviradiata*												O				
RETUSOTRILETES	*R. simplex*												O				
GRANULATISPORITES	*G. trisinus*			O													
CYCLOGRANISPORITES	*C. aureus*	O															
ACANTHOTRILETES	*A. spinous*												O				
LOPHOTRILETES	*L. buhiniae*												O				
REGULATISPORITES	*R. permixtus*										O						
CHASMATOSPORITES	*C. major*												O				
VERRUCOSISPORITES	*V. triassicus*													O			
GOUBINISPORA	*G. morandavensis*															O	
ALISPORITES	*A. teunicorpus*							+						+			
	A. thomassii			+													
	A. grandis				O												
	A. australis							+									
FALCISPORITES	*F. stabilis*												O				
	F. nuthallensis		+	+			+	+									
ABIETINAEPOLLENITES	*A. sp.*							+									
PITYOSPORITES	*P. granulatus*		+														
SULCATISPORITES	*S. ovatus*		+														
	S. microsulcus		+														
LIMITISPORITES	*L. plicatus*		O														
LUECKISPORITES	*L. diploxylonoidii*												O				
CORISACCITES	*C. alutas*												+				
PROTOHAPLOXYPINUS	*P. amplus*							O									
STRIATOPODOCARPITES	*S. sp. cf. S. cancellatus*	+															
PODOCARPITES	*P. sp.*												+				
VALIASACCITES	*V. validus*												O				
PLATYSACCUS	*P. queenslandi*														O		
	P. pakkistanicus				+												
GINKGOCYCADOPHYTUS	*G. cymbatus*							O									
KINGIACOLIPTES	*K. elongatus*							O									
LUNATISPORITES	*L. novialensis*												O				
VITREISPORITES	*V. sp.*						+										

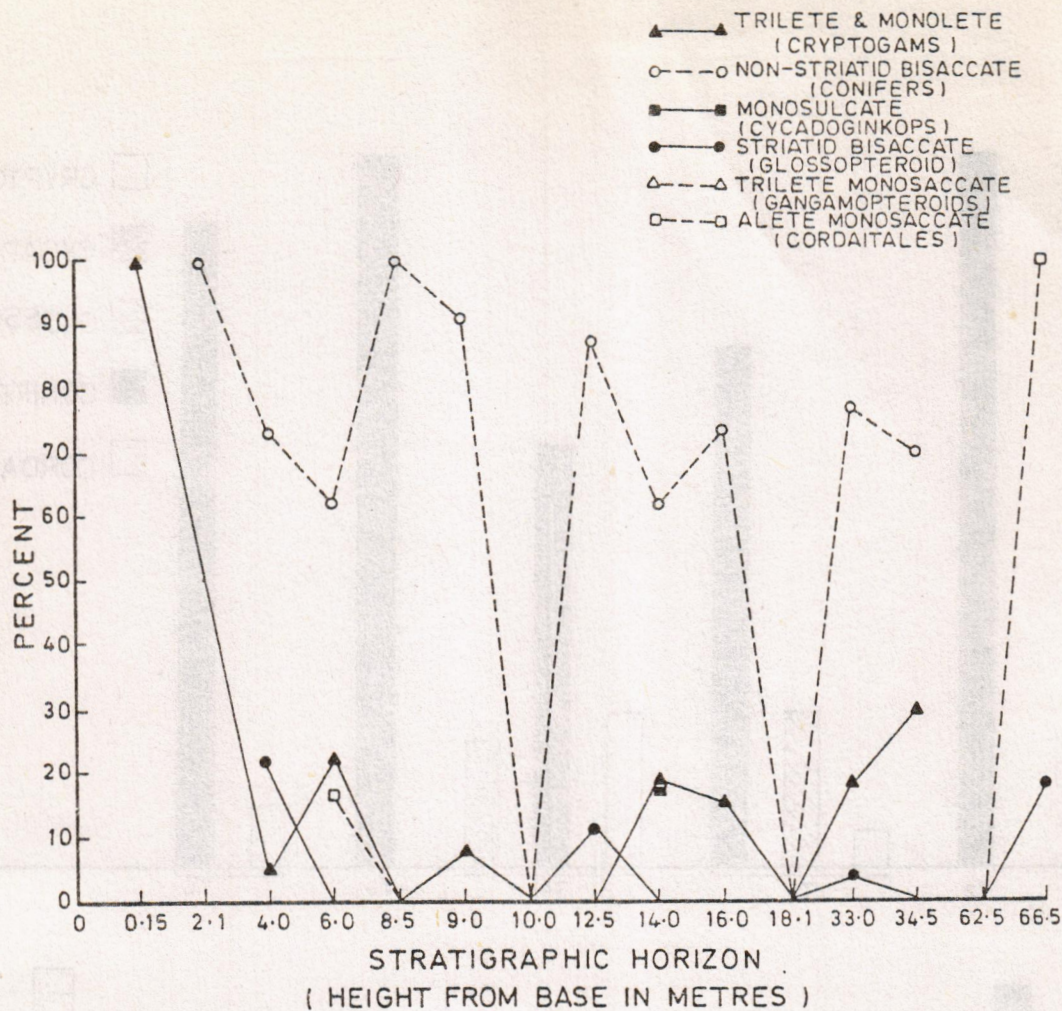**STRATIGRAPHICALLY SIGNIFICANT MIOSPORE : O**

FIG. 3: PHYTOSTRATIGRAPHIC FLUCTUATIONS THROUGH THE COMPOSITE
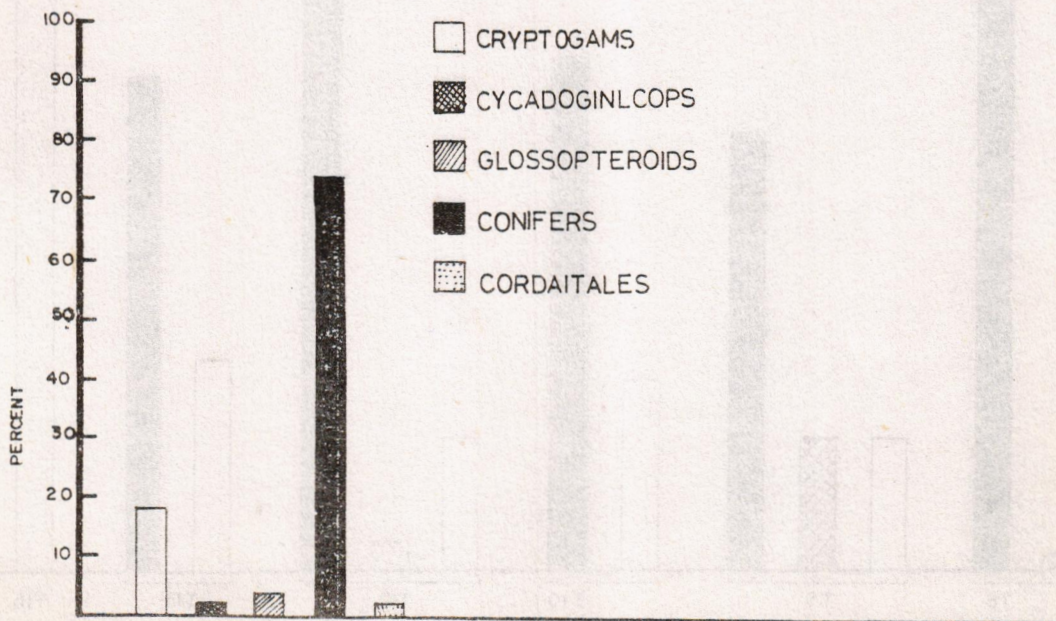TREDIAN FORMATION.

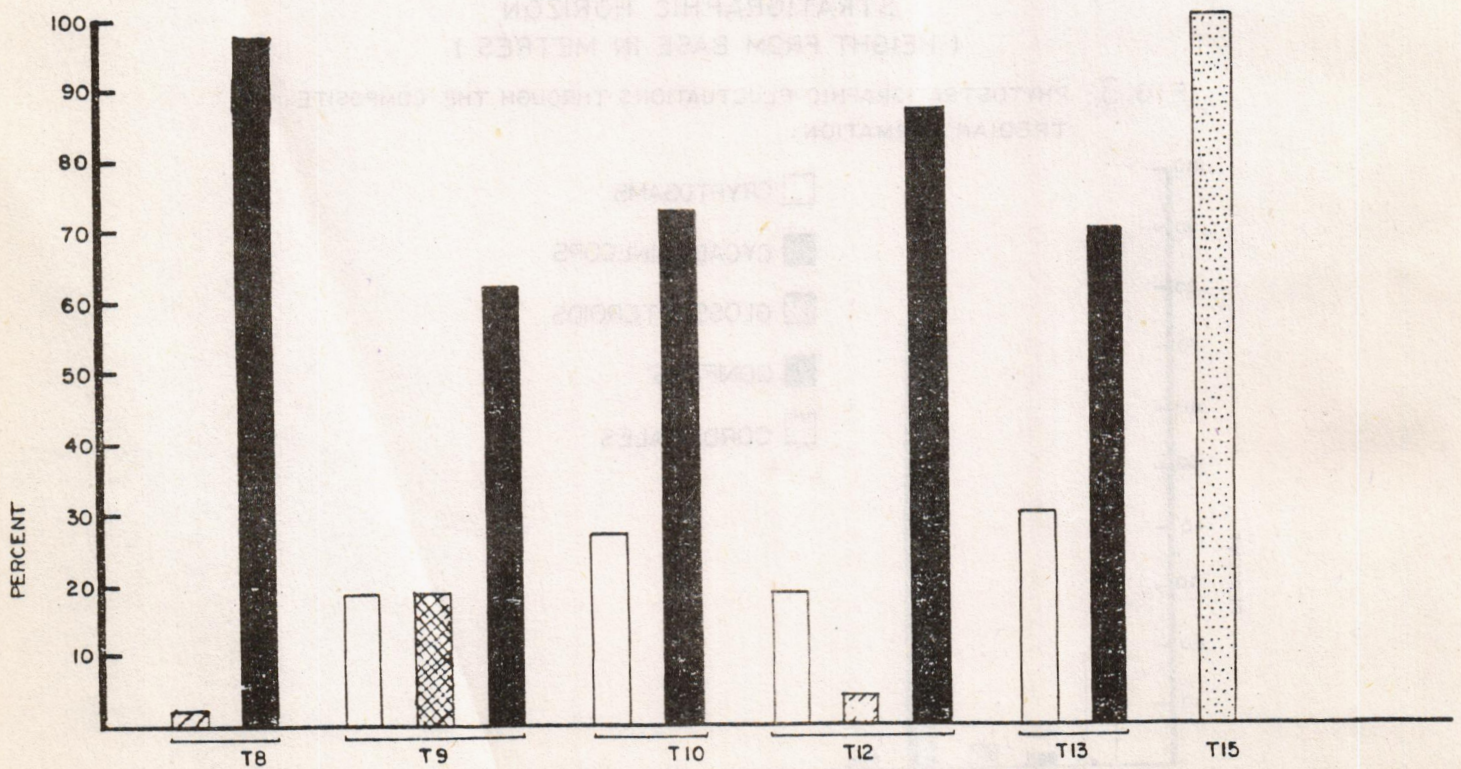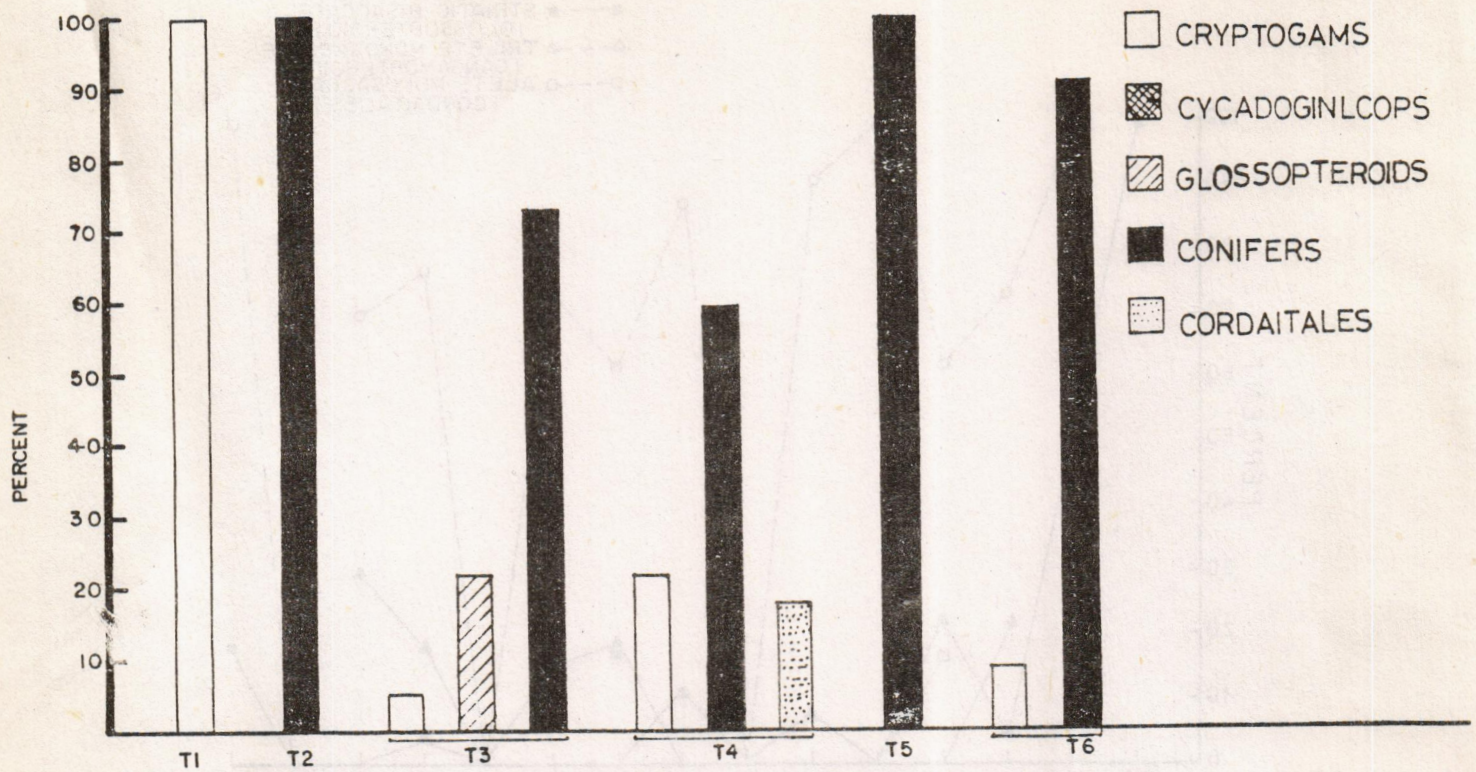FIG. 4. COMPOSITE FREQUENCY OF MAJOR PLANT GROUPS IN
THE TREDIAN FORMATION.

189

FIG 5 PALAEOPHYTIC COMPOSITION OF DIFFERENT ROCK SAMPLES(T) OF THE TREDIAN FORMATION.

190

palaeophytic composition of this horizon.

Horizon T6: *Alisporites grandis* is stratigraphically significant. Others are *Platysaccus pakistanicus*, *Falcisporites nuthallensis* and *Vitreisporites* sp. Percentage occurrence of palynomorphs are as follows: Monolete & trilete 9%, non striated bisaccate 91% .

Horizon T7: Non Productive.

Horizon T8: *Protohaploxypinus ampuls* is stratigraphically significant here whereas *Alisporites teunicorpus* is also frequent. Percentage occurrence of striated bisaccate is 2% and non striated bisaccate 98%.

Horizon T9: Monosulcate miospores viz, *Kingiacolpites elongatus* and *Ginkgocycadophytus cymbatus* are stratigraphically significant here. Among others *Alisporites australis* is noteworthy, as it is a cosmopolitan marker for middle Triassic strata. Other notable miospores are: *Falcisporites nuthallensis*, *Leiotriletes ornatus* and *Abietinaepollenites* sp. Percentage occurrence of others are: Monolete and trilete 19%, monosulcate 19% and non striated bisaccate 62%.

Horizon T10: *Rugulatisporites permixtus* is stratigraphically significant here. *Falcisporites nuthallensis* is also abundant.

Horizon T11: Non Productive.

Horizon T12: This is the most productive horizon containing diversified palynomorph population. Following palynomorphs are designated stratigraphically significant: *Calamospora breviradiata*, *Retusotriletes simplex*, *Acanthotriletes spinosus*, *Lophotriletes buhiniae*, *Chasmatosporites major*, *Lueckisporites diploxylonoidii*, *Valiasaccites validus* and *Lunatisporites novialenses*. Other miospors are: *Punctatisporites irrasus*, *Falcisporites stabilis*, *Sulcatisporites ovatus*, *Corisaccites alutas* and *Podocarpites* sp. Other groups are monolete and trilete 19%, Non striated bisaccate 77% and striated bisaccate 4%.

Horizon T13: *Platysaccus queenslandi* and *Verrucosisporites trissicus* are stratigraphically significant here. *Alisporites teunicorpus* was also observed. percentage occurrence is as follows; monolete and triletes 30%, non striated bisaccates 70%.

Horizon T14: Non Productive.

Horizon T15: Only one palynomorph species viz, *Goubinispora morandavensis* exists here indicating

prevalence of Cordaitales. Some other corroded unidentifiable bisaccate palynomorphs were also observed.

Horizon T16: Non Productive.

Interpretation of the present palynological data to reconstruct past vegetational history and climatic changes has recently been separately published (Masood *et al.*, 1991).

Most horizons are palaeophylitically distinct including one or more stratigraphically distinct miospores. Nineteen (19) such miospore species were recovered (Table 1). Rich assemblage of cuticular fragments were observed, especially at horizon twelve (12).

As proposed by Masood *et al.* (1991), climate was hot humid tropical at the early depositional phase of the Tredian Formation (indicated by the high percentage of Cryptogamic spores) becoming hot humid tropical to cool temperate thereafter, but again reverting to hot humid tropical at the mid depositional phase (horizon 9). Temperature slightly dropped at horizon 12, becoming ultimately cool temperate at the last depositional phase (horizon 14), this is evidenced by the rapid development of Glossopteroid and Cordaitales at that level. Fig. 3 depicts rise and fall of major plant groups across Tredian Formation, where as Fig. 4 represent composite frequency of occurrence of five major plant groups in the Tredian Formation. Fig. 5 summarises relative frequency of occurrence of different plant groups in each individual rock sample.

CONCLUSION

Tredian Formation of Middle Triassic age at Nammal Gorge, Western Salt Range, Pakistan, contain well preserved diversified palynomorph assemblage reflecting characteristic Triassic composition. Apart from others, nineteen stratigraphically significant miospores were identified viz, *Cyclogranisporites aureus*, *Limitisporites plicatus*, *Granulatisporites trisinus*, *Verrucosisporites triassicus*, *Alisporites grandis*, *Protohaploxypinus amplus*, *Kingiacolpites elongatus*, *Ginkgocycadophytus cymbatus*, *Rugulatisporites permixuts*, *Calamospora breviradiata*, *Retusotriletes simplex*, *Acanthotriletes spinosus*, *Lophotriletes buhiniae*, *Chasmatosporites major*, *Lueckisporites diploxylonoidii* *Valiasaccites validus*, *Lunatisporites novialensis*, *Platysaccus queenslandi* and *Goubinispora morandavensis*. *Goubinispora morandavensis* and *Alisporites grandis* are middle Triassic markers.

As inferred from palynological data, existence of five major plant groups i.e. Cryptogams, Gangamopteroids, Glossopteroids, Conifers and Cycadoginkops is predicted during middle Triassic period in the Salt Range, Pakistan (see Masood *et al.*, 1991). Further interpretation of palynological data indicate climatic changes during the deposition of Tredian Formation. Climate was hot humid tropical in the beginning, becoming humid tropical to cool temperate in the middle, finally becoming cool temperate.

ACKNOWLEDGEMENTS

## REFERENCES

Balme, B.E., (1970). Palynology of Permian and Triassic strata in the Salt Range and Surghar Range, W. Pakistan, In: Stratigraphic Boundry Problems: Permian and Triassic of West Pakistan. (Ed B. Kummel, and C. Teichert). *Univ. Kansas. Geol. Deptt. sp. Pub.* Vol. 4. pp. 305-453

Bharadwaj, D.C., (1966). Distribution of spores and pollen grains dispersed in the lower Gondwana Formations of India. Symposium on Floristics and Stratigraphy of Gondwana- land. *Proc. Symp. Spec. Session*. pp. 69-84.

Danilchik, M., and Shah, S.M.I. (1967). Stratigraphic nomenclature of formations in Trans Indus Mountains, Mianwali District, West Pakistan, *U.S. Geol. Surv., Project report (IR)* PK-33, 45 P.

Gee, E.R., (1945). The age of the saline series of the Punjab and of Kohat: *India Natl. Acad. Sci. proc.,* Sec B., Vol. 14, Pt. 6, pp. 269-310.

Kummel, B., (1966). The lower Triassic formations of the Salt Range and Trans-Indus ranges, West Pakistan. *Mus. Comp, Zoology Bull.,* Vol. 134, No. 10, pp. 361-429.

Masood, K.R., Qureshi, K.A. and Sabri, S.N., (in press) Middle Triassic flora and climatic changes in the Western Salt Range, Pakistan. *Acta. Scientia* Vol. 1(2), 1991.

Phipps, D., and Playford, G., (1984). Laboratory techniques for extraction of palynomorphs from sediments. *Dep. Geol. Univ. W. Aust.* pp. 118-148.

Sitholey, R.V., (1943). On *Psygmophyllum haydeni* Seward. jour. *Indian Bot. Sci.* Vol. 22, pp. 183-190.

INSTRUCTIONS TO THE CONTRIBUTORS OF THE KASHMIR JOURNAL OF GEOLOGY

The Kashmir Journal of Geology is devoted to the publication of original research in the field of geology including structure, tectonics, geophysics, petrology, mineralogy, geochronology, geochemistry, economic geology, engineering geology, geohydrology, petroleum geology, neotectonics, geomorphology, quaternary geology, stratigraphy and paleontology. The articles should deal with aspects of the geology of Pakistan or other parts of the world. Review articles, short communications and abstracts are also welcomed.

The article should be written in English accompanied with an abstract (not more than 300 words), text, conclusions, acknowledgements, references and figure captions. All text, references and figure captions should be double-spaced and on one side of the 21.5 x 28 cm paper. Either use a good typewriter or suitable computer printer to produce your manuscript. Do all mathematical and Greek characters by typewriter (or other printer) if possible; alternatively, write them by hand clearly. Give all measurements in metric units. The International System of Units (SI) is recommended except where other units are clearly preferable. Condense the manuscript as much as possible without sacrificing substance or clarity. All tables, illustrations and photographs should be self-explanatory. Photographs should be in black and white glossy prints, however, colour photo prints can by published on payment. The illustrations (figures, diagrams and maps) should be done in black ink on tracing paper or on computer with laser writer out put. In case of tracing paper, hand lettering is not acceptable. The lettering should be done with stencil. For 2 to 3 times final reduction of figures, diagrams, maps and tables preferable letter size should be used. The maximum length of the article including text, references and illustrations should not exceed 25 pages. The contributor will be charged for extra pages. The Institute of Geology requests voluntary contributions of about Rs. 300 per page for printing of articles in Kashmir Journal of Geology. The acceptance of a manuscript for publication is not contingent upon the payment of contributions. In order to save your time and trouble, ask for a copy of information to contributors of the Kashmir Journal of Geology before you prepare an article to submit for publication in the Journal. For review, please send three copies of your article to the Editor of the Kashmir Journal of Geology.
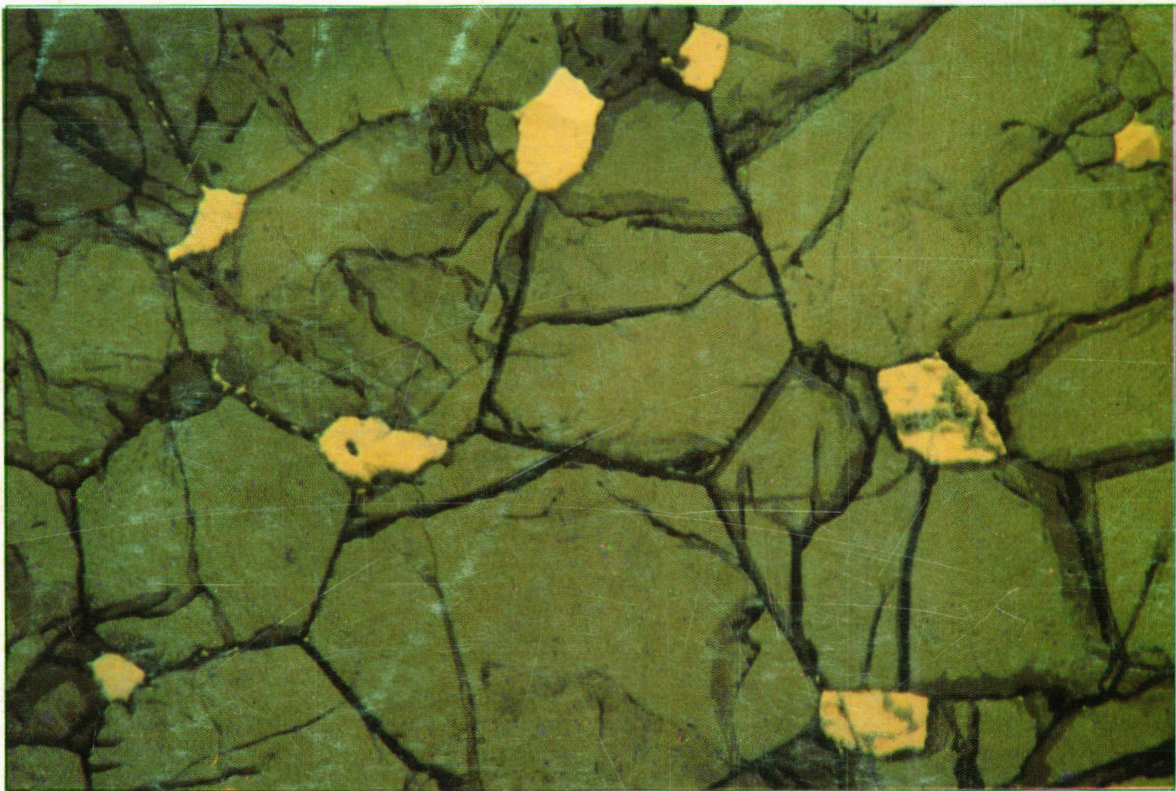
CHALCOPYRITE & PENTLANDITE AT TRIPLE JUNCTION OF OLIVINE GRAINS
IN CHILAS DUNITE
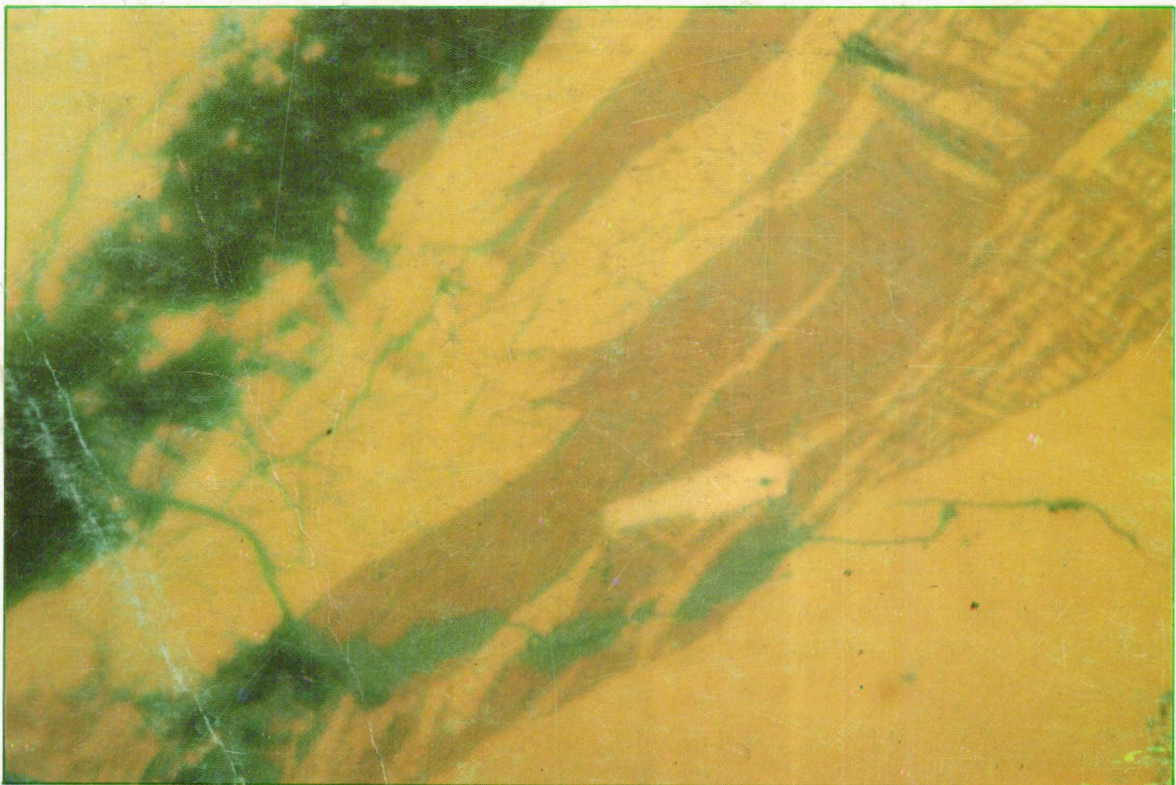
PGM MERENSKYITE (WHITE) & MICHENERITE (PALE GRAY) ENCLOSED IN BORNITE &
CHALCOPYRITE WITH BLUE COVELLITE VEINLETS (IN CHILAS DUNITE).